universidad de león

Doctoral Thesis

Prognosis and acquired resistance to sorafenib in hepatocellular carcinoma: role of hypoxia-mediated response

---

Pronóstico y resistencia adquirida a sorafenib en el carcinoma hepatocelular: papel de la respuesta mediada por hipoxia

Memoria presentada por la Graduada Carolina Méndez Blanco para la obtención del título de Doctor por la Universidad de León

Directores: Dr. Javier González Gallego y Dr. José Luis Mauriz Gutiérrez

Carolina Méndez Blanco
Departamento de Ciencias Biomédicas
Instituto de Biomedicina (IBIOMED)
León, 2021

Los resultados de la presente memoria han sido objeto de las siguientes publicaciones:

- **Sorafenib resistance in hepatocarcinoma: Role of hypoxia-inducible factors**.
  Méndez-Blanco C, Fondevila F, García-Palomo A, González-Gallego J, Mauriz JL.
  Exp Mol Med. 2018;50(10):1-9.
  JCR Impact Factor: 4.743
  Rank in Biochemistry & Molecular Biology: 53/299 (Q1)
  Rank in Medicine, research & Experimental: 27/136 (Q1)

- **Stabilization of hypoxia-inducible factors and BNIP3 promoter methylation contribute to acquired sorafenib resistance in human hepatocarcinoma cells**.
  Méndez-Blanco C, Fondevila F, Fernández-Palanca P, García-Palomo A, Pelt JV, Verslype C, González-Gallego J, Mauriz JL.
  Cancers (Basel). 2019;11(12):1984.
  JCR Impact Factor: 6.126
  Rank in Oncology: 37/244 (Q1)

- **Prognostic and clinicopathological significance of hypoxia-inducible factors 1α and 2α in hepatocellular carcinoma: A systematic review with meta-analysis.**
  Méndez-Blanco C, Fernández-Palanca P, Fondevila F, González-Gallego J, Mauriz JL.
  Ther Adv Med Oncol. 2021;13:1758835920987071.
  JCR Impact Factor: 6.852
  Rank in Oncology: 34/244 (Q1)

Asimismo, durante la realización de la presente Tesis Doctoral también se han llevado a cabo las siguientes publicaciones:

- **Melatonin-induced increase in sensitivity of human hepatocellular carcinoma cells to sorafenib is associated with reactive oxygen species production and mitophagy**.
  Prieto-Domínguez N, Ordóñez R, Fernández A, Méndez-Blanco C, Baulies A, Garcia-Ruiz C, Fernández-Checa JC, Mauriz JL, González-Gallego J.
  J Pineal Res. 2016;61(3):396-407.
  JCR Impact Factor: 10.391
  Rank in Endocrinology & Metabolism: 7/138 (Q1)
  Rank in Physiology: 3/84 (Q1)

- **Melatonin enhances sorafenib actions in human hepatocarcinoma cells by inhibiting mTORC1/p70S6K/HIF-1α and hypoxia-mediated mitophagy**.
  Prieto-Domínguez N, Méndez-Blanco C, Carbajo-Pescador S, Fondevila F, García-Palomo A, González-Gallego J, Mauriz JL.
  Oncotarget. 2017;8(53):91402-14.
  JCR Impact Factor: 5.168
  Rank in Oncology: 44/217 (Q1)

- **Anti-tumoral activity of single and combined regorafenib treatments in pre-clinical models of liver and gastrointestinal cancers**.
  Fondevila F, Méndez-Blanco C, Fernández-Palanca P, González-Gallego J, Mauriz JL.
  Exp Mol Med. 2019;51(9):1-15.
  JCR Impact Factor: 5.418
  Rank in Biochemistry & Molecular Biology: 46/297 (Q1)
  Rank in Medicine, research & Experimental: 21/139 (Q1)

- **Antitumor effects of quercetin in hepatocarcinoma *in vitro* and *in vivo* models: A systematic review**.
  Fernández-Palanca P, Fondevila F, Méndez-Blanco C, Tuñón MJ, González-Gallego J, Mauriz JL.
  Nutrients. 2019;11(12):2875.
  JCR Impact Factor: 4.546
  Rank in Nutrition & Dietetics: 17/89 (Q1)

- **Melatonin as an antitumor agent against liver cancer: An updated systematic review.**
  Fernández-Palanca P, Méndez-Blanco C, Fondevila F, Tuñón MJ, Reiter RJ, Mauriz JL, González-Gallego J.
  Antioxidants (Basel). 2021;10(1):103.
  JCR Impact Factor: 5.014
  Rank in Biochemistry & Molecular Biology: 56/297 (Q1)

Parte de los resultados obtenidos durante este periodo pre-doctoral han sido objeto de las siguientes comunicaciones a congreso:

- **XLI Congreso Anual de la Asociación Española para el Estudio del Hígado (AEEH)**. Madrid (España), 17-19/02/2016.
  La combinación de melatonina y sorafenib incrementa la mitofagia e induce procesos de muerte celular en líneas tumorales hepáticas humanas. Fernández A, Ordóñez R, Prieto-Domínguez N, Méndez-Blanco C, García-Palomo A, Mauriz JL, González-Gallego J. Gastroenterología y Hepatología. 2016;39(S1):41.

- **XXXVIII Congreso de la Sociedad Española de Ciencias Fisiológicas (SECF)**. Zaragoza (España), 13-16/09/2016.
  Melatonin increases sorafenib sensitivity in Hep3B liver cancer cells through mitophagy induction. Ordóñez R, Fernández A, Prieto-Domínguez N, Méndez-Blanco C, García-Palomo A, Baulies A, García-Ruíz C, Fernández-Checa JC, Mauriz JL, González-Gallego J. J Physiol Biochem. 2016;72(S1):S106.

- **XLII Congreso Anual de la Asociación Española para el Estudio del Hígado (AEEH)**. Madrid (España), 15-17/02/2017.
  La modulación de la vía de HIF-1α y de la mitofagia por acción de la melatonina reduce la resistencia al sorafenib en células de hepatocarcinoma en hipoxia. Prieto-Domínguez N, Méndez-Blanco C, Ordóñez R, Fondevila F, Fernández A, García-Palomo A, Mauriz JL, González-Gallego J. Gastroenterología y Hepatología. 2017;40(S1):45.

- **11th Annual Biotechnology Congress (BAC)- Congress of the Spanish Federation of Biotechnologists (FEBiotec)**. León (España), 12-14/07/2017.
  Melatonin downregulates hypoxia-inducible factor-1α through inhibition of the mTOR/p70S6K signaling pathway in human hepatocarcinoma cells. Méndez-Blanco C, Prieto-Domínguez N, Fondevila F, Carbajo-Pescador S, Mauriz JL, González-Gallego J.

- **XLIII Congreso Anual de la Asociación Española para el Estudio del Hígado (AEEH)**. Madrid (España), 21-23/02/2018.
  La inhibición de los factores HIF-1α y HIF-2α por el tratamiento con melatonina incrementa la sensibilidad al sorafenib en células de hepatocarcinoma humano en hipoxia. Méndez-Blanco C, Fondevila F, Prieto-Domínguez N, Carbajo-Pescador S, Fernández-Palanca P, Mauriz JL, González-Gallego J. Gastroenterología y Hepatología. 2018;41(S1):52.

- **12th Annual Biotechnology Congress (BAC)- Congress of the Spanish Federation of Biotechnologists (FEBiotec)**. Girona (España), 11-13/02/2018.
  Inhibition of HIF-1α/BNIP3 axis and hypoxia-mediated mitophagy by melatonin addition enhances human hepatocellular carcinoma cells sensitivity to sorafenib treatment. Fondevila F, Méndez-Blanco C, Prieto-Domínguez N, Fernández-Palanca P, García-Palomo A, González-Gallego J, Mauriz JL.

- **XXXIX Congreso de la Sociedad Española de Ciencias Fisiológicas (SECF)**. Cádiz (España), 18-21/09/2018.
  Role of hypoxia in a hepatocellular carcinoma *in vitro* model of acquired resistance to sorafenib. Méndez-Blanco C, Fondevila F, Fernández-Palanca P, García-Palomo A, González-Gallego J, Mauriz JL. J Physiol Biochem. 2018;74(S1):S91.

- **XLIV Congreso Anual de la Asociación Española para el Estudio del Hígado (AEEH)**. Madrid (España), 20-22/02/2019.
  La estabilización de los factores inducibles por hipoxia contribuye al desarrollo de resistencia a sorafenib en células de hepatocarcinoma humano. Fondevila F, Méndez-Blanco C, Fernández-Palanca P, García-Palomo A, González-Gallego J, Mauriz JL. Gastroenterología y Hepatología. 2019;42(S1):42.

- **13th Annual Biotechnology Congress (BAC)- Congress of the Spanish Federation of Biotechnologists (FEBiotec)**. Madrid (España), 10-12/07/2019.
  Study of acquired resistance to sorafenib in an *in vitro* HCC model: effect of regorafenib on AKT/mTOR and ERK signaling. Martín-Álvarez C, Fernández-Palanca P, Fondevila F, Méndez-Blanco C, García-Palomo A, González-Gallego J, Mauriz JL.

- **XLV Congreso Anual de la Asociación Española para el Estudio del Hígado (AEEH)**. Madrid (España), 12-14/02/2020.
  La hipermetilación del promotor de BNIP3 contribuye a la adquisición de resistencia a sorafenib en hepatocarcinoma humano. Fernández-Palanca P, Fondevila F, Méndez-Blanco C, González-Gallego J, Mauriz JL. Gastroenterología y Hepatología. 2020;43(S1):47.

- **I Congreso Anual de Estudiantes de Doctorado (CAED)**. Congreso virtual. 02/02/2021.
  Identification of a new mechanism involved in sorafenib resistance acquisition in hepatocarcinoma: epigenetic silencing of BNIP3. Fernández-Palanca P, Méndez-Blanco C, Fondevila F, van Pelt J, Verslype C, García-Palomo A, González-Gallego J, Mauriz JL.

- **I Congreso Anual de Estudiantes de Doctorado (CAED)**. Congreso virtual. 02/02/2021.
  Double-edge autophagy in sorafenib resistant and sensitive human hepatocarcinoma cells: dual role of regorafenib. Fondevila F, Fernández-Palanca P, Méndez-Blanco C, González-Gallego J, Mauriz JL.

- **I Congreso Anual de Estudiantes de Doctorado (CAED)**. Congreso virtual. 02/02/2021.
  Prognostic value of hypoxia-inducible factors 1α and 2α expression in hepatocarcinoma patients. Méndez-Blanco C, Fondevila F, Fernández-Palanca P, González-Gallego J, Mauriz JL.

- **27th Congress of the European Association for Cancer Research (EACR)**. Virtual congress. 09-12/06/2021.
  Identification of prognostic value of HIF-2α and a potential role in sorafenib resistance development in hepatocarcinoma. Fernández-Palanca P, Méndez-Blanco C, Fondevila F, González-Gallego J, Mauriz JL.

- **27th Congress of the European Association for Cancer Research (EACR)**. Virtual congress. 09-12/06/2021.
  Role of HIF-1α on prognosis value and acquisition of sorafenib chemoresistance in hepatocarcinoma. Méndez-Blanco C, Fondevila F, Fernández-Palanca P, González-Gallego J, Mauriz JL.

- **27th Congress of the European Association for Cancer Research (EACR)**. Virtual congress. 09-12/06/2021.
  Induction of a cytoprotective FOXO3-mediated autophagy as a novel mechanism of sorafenib acquired resistance in human advanced hepatocarcinoma. Fondevila F, Fernández-Palanca P, Méndez-Blanco C, González-Gallego J, Mauriz JL.

- **XLVI Congreso Anual de la Asociación Española para el Estudio del Hígado (AEEH)**. Madrid (España), 14-16/06/2021.
  Papel del factor inducible por hipoxia 1α sobre el pronóstico y las características clinicopatológicas de pacientes con hepatocarcinoma sometidos a resección quirúrgica. Méndez-Blanco C, Fondevila F, Fernández-Palanca P, González-Gallego J, Mauriz JL.

- **XLVI Congreso Anual de la Asociación Española para el Estudio del Hígado (AEEH)**. Madrid (España), 14-16/06/2021.

Identificación del potencial valor pronóstico del factor inducible por hipoxia 2α en pacientes con hepatocarcinoma. Fernández-Palanca P, Méndez-Blanco C, Fondevila F, González-Gallego J, Mauriz JL.

- **XLVI Congreso Anual de la Asociación Española para el Estudio del Hígado (AEEH)**. Madrid (España), 14-16/06/2021.
  Inducción de autofagia citoprotectora asociada a FOXO3 en hepatocarcinoma humano: Potencial mecanismo de resistencia a sorafenib. Fondevila F, Fernández-Palanca P, Méndez-Blanco C, Payo-Serafín T, van Pelt J, Verslype C, González-Gallego J, Mauriz JL.

- **XLVI Congreso Anual de la Asociación Española para el Estudio del Hígado (AEEH)**. Madrid (España), 14-16/06/2021.
  FOXO3 en cáncer hepático primario: Nuevo biomarcador con potencial diagnóstico y pronóstico. Fondevila F, Méndez-Blanco C, Fernández-Palanca P, Payo-Serafín T, González-Gallego J, Mauriz JL.

- **The International Liver Congress (ILC) by the European Association for the Study of the Liver (EASL)**. Virtual Congress. 23-26/06/2021.
  Resistance to sorafenib in hepatocarcinoma: role of BCL2 interacting protein 3 promoter hypermethylation. Fernández-Palanca P, Méndez-Blanco C, Fondevila F, van Pelt J, Verslype C, González-Gallego J, Mauriz JL.

- **The International Liver Congress (ILC) by the European Association for the Study of the Liver (EASL)**. Virtual Congress. 23-26/06/2021.
  Role of hypoxia-inducible factors 1α and 2α in prognosis and sorafenib chemoresistance in hepatocarcinoma. Méndez-Blanco C, Fondevila F, Fernández-Palanca P, van Pelt J, Verslype C, González-Gallego J, Mauriz JL.

Carolina Méndez Blanco ha sido beneficiaria de una Ayuda Predoctoral en Oncología (APRO-Convocatoria 2016) concedida por la Asociación Española Contra el Cáncer (AECC)-Junta Provincial de León para la realización de su proyecto de Tesis Doctoral.

Dicho proyecto se ha llevado a cabo en el Instituto de Biomedicina (IBIOMED) de la Universidad de León, bajo la dirección del Prof. Javier González Gallego y del Dr. José Luis Mauriz Gutiérrez.

La financiación ha estado a cargo de los siguientes proyectos:

- Estudio del efecto de inhibidores de tirosín quinasas en la modulación de la supervivencia y muerte celular en diferentes tipos de cáncer (Z367). Fundación Investigación Sanitaria en León. 29/01/2018-29/01/2019.
- Estudio de la modulación de autofagia y apoptosis en hepatocarcinoma tras la administración de inhibidores de tirosina quinasa (Z390). Universidad de León. 19/11/2019-18/11/2020 2019.
- Análisis de la contribución de los factores inducibles por hipoxia en la resistencia al tratamiento del hepatocarcinoma (Z403). Fundación Investigación Sanitaria en León. 02/12/2020-01/12/2022.

"A scientist in his laboratory is not a mere technician: he is also a child confronting natural phenomena that impress him as though they were fairy tales"

"Un científico en su laboratorio no es un mero técnico: es también un niño enfrentándose a fenómenos naturales que le impresionan como si fueran cuentos de hadas"

Marie Curie

Nobel Prize in Physics 1903 and Chemistry 1911

A mi familia

AGRADECIMIENTOS

Aquí terminan mis casi 5 años de etapa pre-doctoral, y ha llegado el momento de dar las gracias a todas aquellas personas que habéis estado ahí y me habéis ayudado a hacerlo posible.

En primer lugar, quiero dar las gracias a mis directores de tesis, **José** y **Javier**. Gracias por recibirme con los brazos abiertos en el grupo del HCC, y por haberme dado la oportunidad de realizar esta Tesis. Durante estos casi 7 años me habéis permitido investigar y crecer personal y profesionalmente.

Por supuesto, muchísimas gracias a la **Asociación Española Contra el Cáncer (AECC)**, y en especial a la **Junta Provincial de León**, por concederme la ayuda pre-doctoral que ha hecho que todo esto sea posible. También ha sido un placer que me hayáis permitido compartir nuestros avances en investigación y participar en talleres para acercar la ciencia a los más pequeños. ¡Gracias por contar conmigo y por la labor tan importante que hacéis!

A todos mis compañeros del **área de Fisiología Animal del Departamento de Ciencias Biomédicas**. Gracias por vuestro apoyo y vuestros consejos durante estos años. He aprendido mucho de vosotros, sobre todo cuando compartíamos prácticas.

A todos los que han pasado por el **IBIOMED** durante estos años: técnicos, doctorandos, post-docs... Hemos compartido charlas en los pasillos y durante las comidas, reactivos, protocolos, palabras de ánimo… me llevo muy buen recuerdo de vosotros. Sobre todo, gracias a todas las personas con quienes he compartido el despacho 25. En especial a **Brisa**, por las charlas y masajes reparadores; a **Diana, Irene y Bárbara**, las locas de las compras; y a **Rebe**, porque siempre estás para echar una mano.

Gracias a todos los que formáis o habéis formado parte del equipo HCC. **Néstor**, sin ti esta experiencia no hubiese sido lo mismo. **Flavia y Paula**, ¡qué decir de vosotras! No hubiese imaginado nunca unas compañeras mejores, la verdad es que he tenido mucha suerte. Tras miles de horas con nuestras celulillas, entre pipeteo y pipeteo,

cientos de miles de WB… quiero agradeceros todo vuestro esfuerzo para conseguir que esta Tesis sea posible. Porque es cierto que lleva mi nombre, pero también es vuestra. Habéis estado siempre en los buenos momentos, pero también para levantarme el ánimo y tranquilizarme cuando lo necesitaba. Hoy soy yo la que está a punto de defender mi Tesis, pero vosotras sois las siguientes y, aunque parezca imposible, sé que podéis con esto y más. **Tania**, tú acabas de llegar con esas ganas inmensas por aprender, esa energía y esa predisposición para enfrentarte a cualquier reto. Estoy segura de que tienes un gran futuro por delante.

Por último, y no por ello menos importante, quiero dar las gracias a mi familia y amigos por ser un pilar fundamental para superar todos los obstáculos. A **mi madre**, por apoyarme siempre en cada paso que he dado hasta llegar aquí. A **Jairo**, por estar siempre ahí, por aguantarme en los buenos y en los malos momentos, y por darme la fuerza necesaria para seguir. A **Emma**, por estar todas las tardes viendo cómo escribía "mi libro" y alegrarme con esa sonrisa. Y a **mi abuela**, porque una abuela es el mejor tesoro y el mejor ejemplo a seguir. Sé que en el siguiente capítulo de mi vida, sea cual sea, seguiré contando con vosotros.

universidad de león

Doctoral Thesis

Prognosis and acquired resistance to sorafenib in hepatocellular carcinoma: role of hypoxia-mediated response

Carolina Méndez Blanco
Department of Biomedical Sciences
Institute of Biomedicine (IBIOMED)
León, 2021

TABLE OF CONTENTS

LIST OF FIGURES

LIST OF TABLES

LIST OF ABBREVIATIONS

4E-BP1	eIF4E binding protein 1
5-Aza	5-aza-2'-deoxycytidine
5-FU	5-fluorouracil
a.u.	Arbitrary units
ABC	ATP-binding cassette
ADP	Adenosine diphosphate
ADRB2	β-2 adrenergic receptor
AFB1	Aflatoxin B1
AFP	α-fetoprotein
AFP-L3	Fucosylated fraction of α-fetoprotein
AIF	Apoptosis-inducing factor
AKT	Protein kinase B
ALT	Alanine aminotransferase
ANG-2	Angiopoietin 2
ANOVA	Analysis of variance
APAF-1	Apoptotic protease-activating factor 1
APS	Ammonium persulfate
AR	Androgen receptor
ARID1A	Adenine/Thymine-rich interaction domain 1A
ARID2	Adenine/Thymine-rich interaction domain 2
ARNT	Aryl hydrocarbon receptor nuclear translocator
ATCC	American Type Culture Collection
ATG	Autophagy-related gene
ATP	Adenosine triphosphate
AURKA	Aurora kinase A
Bad	Bcl-2-associated agonist of cell death
Bak	Bcl-2 homologous antagonist/killer
Bax	Bcl-2-associated X protein
BAX	BCL2 associated X apoptosis regulator
BCL2	BCL2 apoptosis regulator
Bcl-2	B-cell lymphoma 2
BCL2L1/BCL-X	BCL2 like 1
BCLC	Barcelona Clinic Liver Cancer
Bcl-w	Bcl-2-like protein 2
Bcl-x_L	Bcl-2-like protein 1
BCRP	Breast cancer resistance protein
BH	Bcl-2 homology
BH3	Bcl-2 homology 3

bHLH	Basic helix-loop-helix
Bid	BH3-interacting domain death agonist
Bik	Bcl-2-interacting killer
Bim	Bcl-2-like protein 11
BIRC3	Baculoviral IAP repeat containing 3
Bmf	Bcl-2-modifying factor
BMP4	Bone morphogenetic protein 4
BNIP3	Bcl-2/adenovirus E1B 19 kDa-interacting protein 3
bp	Base pair
BSA	Bovine serum albumin
CASP10	Caspase-10
CASP2	Caspase-2
CASP3	Caspase-3
CASP8	Caspase-8
CASP9	Caspase-9
CBP	CREB-binding protein
CCA	Cholangiocarcinoma
CD	Conserved domain
CDCP1	CUB domain-containing protein 1
cDNA	Complementary DNA
CEUS	Contrast-enhanced ultrasonography
CHX	Cycloheximide
CI	Confidence interval
CLIP	Cancer of the Liver Italian Program
$CoCl_2$	Cobalt chloride
CREB	cAMP response element-binding
CS	Cumulative survival
CSC	Cancer stem cell
CT	Computed tomography
C-TAD	COOH-terminal TAD
CTCF	Corrected total cell fluorescence
CTLA4	Cytotoxic T-lymphocyte-associated antigen 4
CUPI	Chinese University Prognostic Index
CXCL12	C-X-C motif chemokine 12
CXCL6	C-X-C motif chemokine 6
CXCR4	C-X-C chemokine receptor type 4
CXCR7	C-X-C chemokine receptor type 7
CYP3A4	Cytochrome P450 3A4
CYP450	Cytochrome P450
DAPI	4’6-diamidino-2-phenylindole
dATP	Deoxy ATP

DCP	Des-γ-carboxyprothrombin
DFS	Disease-free survival
DIABLO	Direct inhibitor of apoptosis-binding protein with low pI
diH_2O	Deionized H_2O
DISC	Death-inducing signaling complex
DMEM	Dulbecco's Modified Eagle's Medium
DMSO	Dimethyl sulfoxide
DNase	Deoxyribonuclease
DNMT	DNA methyltransferase
E2F1	E2F transcription factor 1
E-cadherin	Epithelial cadherin
ECL	Enhanced chemiluminescence
ECM	Extracellular matrix
ECOG-PS	Eastern Cooperative Oncology Group Performance Status
EDTA	Ethylenediaminetetraacetic acid
EGFR	Epidermal growth factor receptor
eIF3e	Eukaryotic translation initiation factor 3 subunit E
eIF4E	Eukaryotic translation initiation factor 4E
EMA	European Medicines Agency
EMT	Epithelial-mesenchymal transition
ENO1	Enolase 1
EPAS-1	Endothelial PAS domain-containing protein 1
EPO	Erythropoietin
ERK	Extracellular signal-regulated kinase
ER-SR	Endoplasmic reticulum-sarcoplasmic reticulum
EZH2	Enhancer of zeste homologue 2
FADD	Fas-associated death domain
FAF-BSA	Fatty acid-free BSA
Fas	First apoptosis signal
FasL	Fas ligand
FBS	Fetal bovine serum
FC	Fold change
FDA	Food and Drug Administration
FIH	Factor inhibiting HIF
FLT-3	FMS-like tyrosine kinase 3
FOXM1	Forkhead box protein M1
FOXO3	Forkhead box protein O3
GAPDH	Glyceraldehyde-3-phosphate dehydrogenase
GIDEON	Global Investigation of therapeutic DEcisions in hepatocellular carcinoma and Of its treatment with sorafeNib
GLUT1	Glucose transporter 1

GLUT3	Glucose transporter 3
GP73	Golgi protein 73
GPC-3	Glypican 3
GRETCH	*Groupe d'Etude et de Traitement du Carcinome Hépatocellulaire*
GS	Glutamine synthetase
HAF	Hypoxia-associated factor
HBV	Hepatitis B virus
HBx	Hepatitis B virus protein X
HCC	Hepatocellular carcinoma
HCV	Hepatitis C virus
HDAC	Histone deacetylase
HDV	Hepatitis D virus
HFSR	Hand-foot skin reaction
HIF	Hypoxia-inducible factor
HIV	Human immunodeficiency virus
HK1	Hexokinase 1
HK2	Hexokinase 2
HKLC	Hong Kong Liver Cancer
HPPCn	Hepatopoietin Cn
HR	Hazard ratio
HRE	Hypoxia-response element
HRK	Harakiri BCL2 interacting protein
HRP	Horseradish peroxidase
HSC	Hepatic stellate cell
Hsp70	Heat shock protein 70
Hsp90	Heat shock protein 90
IAP	Inhibitor of apoptosis
IBIOMED	Institute of Biomedicine
IC_{50}	Half maximal inhibitory concentration
ICC	Immunocytochemistry
IF	Immunofluorescence
IGF-1	Insulin-like growth factor 1
IGF-2	Insulin-like growth factor 2
IgG	Immunoglobulin G
IHC	Immunohistochemistry
IL-6	Interleukin-6
IL-8	Interleukin-8
IPAS	Inhibitory PAS domain protein
IV	Inverse Variance
JAK	Janus kinase

JIS	Japan Integrated Staging
JNK	c-Jun NH_2-terminal kinase
KEGG	Kyoto Encyclopedia of Genes and Genomes
LC3	Microtubule-associated protein 1A/1B-light chain 3
LDHA	L-lactate dehydrogenase A chain
LIR	LC3-interacting region
lncRNA	Long non-coding RNA
MAPK	Mitogen-activated protein kinase
Mcl-1	Myeloid cell leukemia-1
MDCT	Multi-detector computed tomography
Mdm2	Murine double minute 2
MDR1	Multidrug resistance protein 1
MEK	Mitogen-activated protein kinase kinase
miRNA	MicroRNA
MMP	Metalloproteinase
MNK	MAPK-interacting protein kinase
MOMP	OMM permeabilization
MPTP	Mitochondrial permeability transition pore
MRI	Magnetic resonance imaging
mRNA	Messenger RNA
MSP	Methylation-specific PCR
mTOR	Mammalian target of rapamycin
mTORC1	Mammalian target of rapamycin complex 1
mTORC2	Mammalian target of rapamycin complex 2
MTT	Thiazolyl blue tetrazolium bromide
MWA	Microwave ablation
NAFLD	Non-alcoholic fatty liver disease
NASH	Non-alcoholic steatohepatitis
N-cadherin	Neural cadherin
NCBI	National Center for Biotechnology Information
ncRNA	Non-coding RNA
NF-κB	Nuclear factor kappa B
NIH	National Institutes of Health
NIHR	National Institute for Health Research
NIX	BNIP3-like protein X
NLS	Nuclear localization signal
NOS	Newcastle-Ottawa scale
Noxa	Phorbol-12-myristate-13-acetate-induced protein 1
NS3	Non-structural protein 3
NS5A	Non-structural protein 5A
N-TAD	NH_2-terminal TAD

ODDD	Oxygen-dependent degradation domain
Omi/HtrA2	High-temperature requirement protein A2
OMM	Outer mitochondrial membrane
Opa1	Optic atrophy protein 1
OPN	Osteopontin
OR	Odds ratio
OS	Overall survival
p70S6K	Ribosomal protein S6 kinase beta-1
PAI-1	Plasminogen activator inhibitor-1
PARP	poly (ADP-ribose) polymerase
PAS	Per-ARNT-Sim
PBS	Phosphate buffered saline
PBS-T	PBS-Tween 20
PCD	Programmed cell death
PCNA	Proliferating cell nuclear antigen
PCR	Polymerase chain reaction
PD1	Programmed cell death 1
PDGF	Platelet-derived growth factor
PDGFR-β	Platelet-derived growth factor receptor β
PDK1	Pyruvate dehydrogenase kinase 1
PDL1	Programmed cell death 1 ligand 1
PEI	Percutaneous ethanol injection
p-ERK	Phosphorylated ERK
PEST	Proline, glutamic acid, serine, threonine
PFK	Phosphofructokinase
PGK1	Phosphoglycerate kinase 1
PHD	Prolyl hydroxylase domain protein
PI	Propidium iodide
PI3K	Phosphatidylinositol 3-kinase
PLAGL2	Pleiomorphic adenoma-like protein 2
PMAIP1	Phorbol-12-myristate-13-acetate-induced protein 1
pRb	Retinoblastoma
PRISMA	Preferred Reporting Items for Systematic Reviews and Meta-Analyses
PROSPERO	International Prospective Register of Systematic Reviews
PTEN	Phosphatase and tensin homolog
PTPN13	Protein tyrosine phosphatase non-receptor type 13
Puma	p53-upregulated-modulator of apoptosis
PVDF	Polyvinylidene difluoride
pVHL	von Hippel-Lindau disease tumor suppressor
qRT-PCR	Real-time quantitative RT-PCR

Rab11-FIP4	Rab11 family-interacting protein 4
RACK1	Receptor of activated protein kinase C1
Raf	Rapidly accelerated fibrosarcoma
RAI-R DTC	Radioactive iodine-refractory well-differentiated metastatic thyroid cancer
RCC	Renal cell carcinoma
REML	Restricted Maximum Likelihood
RET	Rearranged during transfection proto-oncogene
RFA	Radiofrequency ablation
RFS	Recurrence-free survival
Rheb	Ras homolog enriched in brain
RNase	Ribonuclease
RNS	Reactive nitrogen species
ROS	Reactive oxygen species
rRNA	Ribosomal RNA
RT-PCR	Reverse transcription PCR
SCCA	Squamous cell carcinoma antigen
SCF	Stem cell factor
SD	Standard deviation
SDS	Sodium dodecyl sulfate
SDS-PAGE	Sodium dodecyl sulfate-Polyacrylamide gel electrophoresis
SHARP	Sorafenib Hepatocellular Carcinoma Assessment Randomized Protocol
SHARP1	Enhancer-of-split and hairy-related protein 1
siRNA	Small interfering RNA
SIRT1	Sirtuin 1
SLC	Solute carriers
Smac	Mitochondria-derived activator of caspase
STAT	Signal transducer and activator of transcription
TACE	Transarterial chemoembolization
TAD	Transactivation domain
TAE	Tris-acetate-EDTA
TARE	Transarterial radioembolization
tBid	Truncated Bid
TCF3	Transcription factor 3
TEMED	Tetramethylenediamine
TERC	Telomerase RNA component
TERT	Telomerase reverse transcriptase
TGF-α	Transforming growth factor α
TGF-β	Transforming growth factor β
TIP30	Oxidoreductase HTATIP2

TK	Tyrosine kinase
TK	Tyrosine kinase
TKI	Tyrosine kinase inhibitor
TM	Transmembrane
TNF-R	TNF receptor
TNFRSF10B	TNF receptor superfamily member 10b
TNF-α	Tumor necrosis factor α
TNM	Tumor-node-metastasis
TRADD	TNF-R-associated death domain
TRAIL	TNF-related apoptosis-inducing ligand
TRAIL-R	TRAIL receptor
TSA	Trichostatin-A
TTR	Time to recurrence
Twist1	Twist-related protein 1
UCHL1	Ubiquitin COOH-terminal hydrolase isozyme L1
UDP	Uridine diphosphate
UGT1A9	UDP-glucuronosyltranferase 1A9
US	Ultrasonography
VEGF	Vascular endothelial growth factor
VEGFR	Vascular endothelial growth factor receptor
WebGestalt	WEB-based GEne SeT AnaLysis Toolkit
WEHI	Walter and Eliza Hall Institute
WHO	World Health Organization
WOS	Web Of Science
XTT	(2-methoxy-4-nitro-5-sulfophenyl)-5-[(phenylamino) carbonyl]-2H-tetrazolium hydroxide
YB-1	Y-box binding protein 1
ΔΨm	Mitochondrial membrane potential

Literature review

1 Hepatocellular carcinoma

Liver cancer remains a global health challenge and its incidence is increasing worldwide [1]. This kind of cancer is constituted by a heterogeneous group of malignant tumors with diverse histological features and an unfavorable prognosis, including hepatocellular carcinoma or hepatocarcinoma (HCC), cholangiocarcinoma (CCA), angiosarcoma and hepatoblastoma [2,3]. The most common primary liver cancers are HCC, accounting for 75% to 85% of cases, and intrahepatic CCA that comprises about 10-15% [4,5].

1.1 Epidemiology

Liver cancer currently represents the sixth most usually diagnosed cancer and the third cause of cancer-related mortality worldwide, following lung and colorectal cancers. In 2020, 905,677 new cases and 830,180 deaths were registered; thus, liver cancer presents a high mortality rate, being responsible of 8.3% of cancer deaths around the world [5]. However, the incidence of this pathology varies according to gender and geographic distribution [4,5].

Thereby, both the incidence and mortality rate of liver cancer is 2-3 times greater in men than in women, being the second cause of cancer death in the male population [4,5]. Likewise, according to the geographical distribution, liver cancer rates are higher in transitioning countries and this disease is the most common cancer in diverse countries located in Eastern and South-Eastern Asia, as well as Northern and Western Africa [5] **(Figure 1)**. In fact, Mongolia is the country with the highest incidence and mortality rates of liver cancer in the world [4,5]. On the other hand, the regions with the lowest incidence are South-Central and Western Asia and South America. In Europe, the Southern region displays the highest incidence of liver cancer of the continent [5] **(Figure 1)**. Specifically, 6,630 new cases and a total of 5,570 deaths of liver cancer were registered during 2018 in Spain, whose incidence is higher than the European average [6].

Because main risk factors of liver cancer appear to be in change (as will be explained later), incidence and mortality rates are declining in many high-risk regions,

while in formerly low-risk areas have raised or stabilized at greater levels in recent years [4,5]. Despite these changes, both incidence and mortality of primary liver cancer shows a stable increase worldwide [3] and, from 2025 it is estimated that more than one million individuals will be affected annually by this cancer [1].

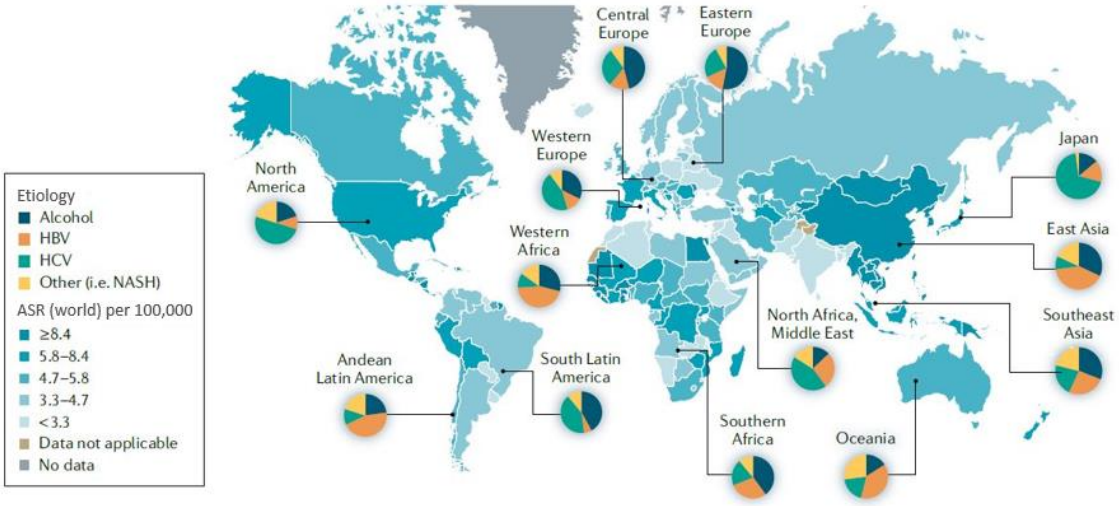

Figure 1. The global incidence of HCC based on geographical distribution and main etiological factors implicated in hepatocarcinogenesis. The greatest incidence of HCC is found in East Asia, with Mongolia being the country with the highest incidence in the world. According to etiology, hepatitis B virus (HBV) is the main etiological factor in most parts of Asia (excluding Japan), South America and Africa; while hepatitis C virus (HCV) is the major risk factor in Western Europe, North America and Japan; and excessive alcohol intake is the predominant etiological cause in Eastern and Central Europe. Moreover, in the "Other" category, the key factor included is non-alcoholic steatohepatitis (NASH), whose incidence is increasing quickly and is expected to become the major factor for HCC in high-income areas in the near future. ASR, age-standardized incidence rate. Estimated age-standardized incidence rates (World) in 2020, liver, both sexes, all ages. Modified from [1].

1.2 Hepatocarcinogenesis

Hepatocytes are the focal functional parenchymal cells in the liver and accomplish most of the metabolic activities of this organ. Moreover, the composition of the liver includes other non-hepatocyte cell types such as (1) stromal cells, including hepatic stellate cells (HSCs) and fibroblasts, which achieve a structural role being responsible for extracellular matrix (ECM) generation; (2) immune cells, which largely involve resident macrophages (Kupffer cells), but comprise inflammation-recruited

leukocytes; (3) endothelial cells, lining the blood vessels; (4) cholangiocytes, which are epithelial cells that line the bile ducts; and (5) liver progenitor cells, in charge of the generation of both hepatocyte and non-hepatocyte intrahepatic cell populations [7].

The pathophysiology of HCC is a complex and multistep process that promotes the malignant transformation predominantly from mature hepatocytes, but also from stem or progenitor cells [1]. Regardless of etiology, development of HCC arises from the inflammation-fibrosis-cirrhosis cascade in most cases; accordingly, cirrhosis precedes HCC in 80-90% of patients [3,8]. To date, the sequential development of liver carcinogenesis starting from preneoplastic nodules to dysplastic hepatocytes and culminating HCC is not fully understood [2,3] **(Figure 2)**.

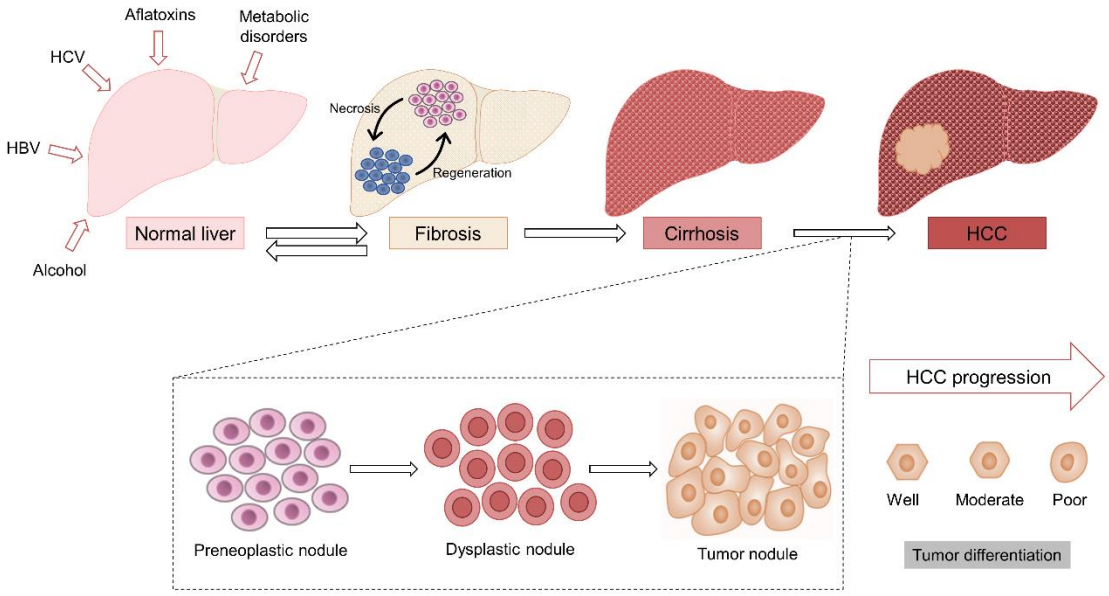

Figure 2. Sequential progression in liver during hepatocarcinogenesis. Hepatic injury incurred by any etiology induces continuous cycles of necrosis-regeneration of hepatocytes. In the first place, chronic liver injury progresses to a fibrotic liver, which can be reversed if the agent responsible for the damage is removed. However, persistent injury can culminate in liver cirrhosis, characterized by the abnormal formation of liver nodules surrounded by collagen deposition and scarring of the liver. Afterwards, hyperplastic or preneoplastic nodules develop, followed by dysplastic nodules and eventually HCC nodules. The progression of HCC is marked by the degree of differentiation, which can be classified into well, moderate and poor. Poorly differentiated tumors represent the most malignant form that can promote invasion and metastasis.

Nevertheless, it is widely accepted that hepatocarcinogenesis occurs from a combination of genetic and environmental factors, comprising the collective action of several cellular mechanisms that in summary are represented by alterations in tumor microenvironment, along with molecular events like genetic and epigenetic alterations, and altered molecular pathways [2,3,8]. All these mentioned mechanisms do not act independently, but all of them are tightly interconnected with extensive crosstalk [2], leading to the development of HCC, progression and eventually metastasis [2,3,7]. As a consequence, there is elevated heterogeneity in HCC, leading to the classification of various subtypes of this tumor [7].

1.2.1 Microenvironmental influence on HCC pathogenesis

The tumor microenvironment constitutes a highly-interconnected network of malignant and stromal cells [7,9]. Different aspects of the liver microenvironment including chronic inflammation, oxidative stress, tissue remodeling and hypoxia have been reported to drive HCC initiation and progression [2,3,7].

Despite the intrinsic variances among etiological and risk factors for HCC, **chronic inflammation** is one of the main and common contributors to HCC initiation and progression [2,10]. Different host cell types release a multitude of cytokines, chemokines, growth factors and other molecules to eliminate damage hepatocytes and, consequently, induce compensatory hepatocyte regeneration [2,3]. In general, the persistent cycle of necro-inflammation and hepatocyte regeneration associated with chronic inflammation is able to increase the risk of genetic mutations in hepatocytes and promote survival and expansion of initiated cells, by making the hepatic milieu a favorable zone for hepatocyte transformation [2,11]. In this sense, alterations in different pro-inflammatory (such as interleukin-6 (IL-6) or tumor necrosis factor α (TNF-α)) and anti-inflammatory cytokines (transforming growth factor α (TGF-α) and β (TGF-β)), or transcription factors (nuclear factor kappa B (NF-κB)), are involved in HCC development [3]. This persistent hepatic injury and concurrent regeneration, progress to sequential development of fibrosis, cirrhosis, and eventually HCC [2].

In addition to inflammation, **oxidative stress** occurs via generation of reactive oxygen species (ROS) and reactive nitrogen species (RNS) by both initiated and inflammatory cells. Oxidative stress could accelerate liver carcinogenesis through several mechanisms, such as the activation of cytokines, induction of oxidative DNA damage, mutations and methylation, as well as increase hepatocyte injury [2,7].

Tumor microenvironment can cause the **remodeling of the ECM**. In this way, chronic inflammation can stimulate ECM synthesis by HSCs and besides, the switch from HSCs synthesis of more proteolysis-resistant collagen types decelerates ECM degradation. This change on the balance between ECM degradation and synthesis leads to ECM accumulation. Excessive ECM is categorized as fibrosis and progresses to cirrhosis when the excess fibrotic bands start to enclose whole liver lobules. As mentioned above, cirrhosis precedes the majority of HCCs; hence, the excess of fibrotic ECM in cirrhotic liver suggest that abnormal ECM accumulation is a significant driver of HCC advancement [7,12].

In consequence, ECM accumulation comprises liver vasculature, altering blood flow and provoking poor oxygen exchange or **hypoxia**. Response to hypoxic conditions includes the upregulation of pro-angiogenic factors such as vascular endothelial growth factor (VEGF) by stromal cells to encourage vascular growth [7,9,12]. However, overexpression of VEGF stimulates a chaotic angiogenesis in tumors, formed by leaky vessels with abnormal vasculature structure and function. This inefficient angiogenesis is not enough to alleviate tumor-associated hypoxia, inducing even greater angiogenesis [7,9]. Definitely, areas of hypoxia have been proposed as driving mechanism of HCC, since promote alterations in molecular signaling in non-tumor cells [7,12].

1.2.2 Genetic and epigenetic changes on HCC carcinogenesis

Development of HCC involves the accumulation of multitude **genetic alterations** during initiation, promotion and progression events, counting somatic mutations, chromosomal aberrations, genomic instability and copy number variants [2,3,8].

Telomere shortening is one of the most frequent chromosomal aberrations. Telomeres are repetitive sequences of nucleotides that protect the end of the chromosomes; and the enzyme telomerase maintains telomere length by adding specific telomeric DNA sequences to compensate telomere shortening after duplication [8,13]. Nonetheless, chronic liver injury increases hepatocytes proliferation, which prompt telomere shortening [7,8]. This is synergized by somatic mutations of the telomerase reverse transcriptase (TERT) and the telomerase RNA component (TERC) genes that compose active telomerase [8,14]. Then, during early steps in HCC development, telomere shortening results in chromosomal instability that drives cancer initiation [3,7,8]. Once the tumor is advanced, telomerase is reactivated allowing to immortalization of malignant cells [13].

According to copy number variants, in most cancers, mutations occur in tumor suppressor genes and proto-oncogenes [3]. In HCC, most common alterations in tumor suppressor genes are the inactivation of p53 and retinoblastoma (pRb) pathway. The loss of tumor suppressor p53 is a major driver of HCC progression, irrespective of etiology and mutations of this gene has been observed in 30-60%, thereby affecting p53-mediated cell cycle regulation or apoptosis [3,8,14]. In contrast, several proto-oncogenes such as Ras family, c-Myc or c-Fos are frequently over-activated in HCC [3]. Overall, these mutations predispose to promote HCC pathogenesis [8,14].

Epigenetic modifications are defined by the presence of heritable stats of gene expression without alteration in DNA sequences. Deregulated epigenetics contributes to carcinogenesis by influencing multiple mechanisms, including gene transcription, chromosomal stability and cell differentiation. Epigenetic mechanisms include alterations in DNA methylation, histone modification, chromatin modification and mechanisms of gene regulation by non-coding RNAs (ncRNAs) [8,15].

The CpG sites are regions of DNA where a cytosine nucleotide is followed by a guanine nucleotide in the linear sequence, which occur with high frequency in genomic regions named CpG islands. DNA methylation patterns occur at promoter CpG islands of genes, regulating gene expression [8,14,15]. In human HCC, promoter hypermethylation and subsequent epigenetic silencing of tumor suppressor genes such

as, p53 or epithelial cadherin (E-cadherin), has been identified [3]. Typically, aberrant methylation occurs in the initiation and progression stages of HCC carcinogenesis [3,7,14]. Furthermore, histone modifications mainly include acetylation, methylation, phosphorylation and ubiquitination, have been implicated in altering expression in HCC pathways [8,15].

Otherwise, chromatin remodeling describes the process of dynamic changes in chromatin structure that regulate gene expression, apoptosis and DNA repair. Disruption in chromatin remodeling can contribute to cancer initiation and progression [8,15]. Some of well-studied chromatin modifiers in HCC include enhancer of zeste homologue 2 (EZH2) and Adenine/Thymine-rich interaction domain 1A (ARID1A) and 2 (ARID2) [15].

Among ncRNAs, a broad range of oncogenic microRNAs (miRNAs) has been described as drivers of development to HCC being upregulated in this neoplasia, such as miR-21, miR-221, miR-222 and miR-224. Moreover, long non-coding RNAs (lncRNAs) are also important modulators of HCC progression [8,15].

1.2.3 Key signaling pathways linked to HCC carcinogenesis

Increasing evidence proves that unusual dysregulation of several molecules involved in signaling pathways controlling cell cycle, proliferation, differentiation, cell survival and apoptosis are related to HCC progression [3].

Likewise, the main signaling pathways altered in HCC are Wnt/β-catenin; Ras/rapidly accelerated fibrosarcoma (Raf)/mitogen-activated protein kinase kinase (MEK)/extracellular signal-regulated kinase (ERK), also known as the mitogen-activated protein kinase (MAPK)/ERK pathway; phosphatidylinositol 3-kinase (PI3K)/protein kinase B (AKT)/mammalian target of rapamycin (mTOR); Janus kinase (JAK)/signal transducer and activator of transcription (STAT); Hedgehog; and angiogenesis (mediated by VEGF and platelet-derived growth factor (PDGF)) [2,3,7].

1.3 Etiology and risk factors

In the most of cases, about 80-90%, HCC occurs in the setting of liver cirrhosis [8]; thus, cirrhosis from any etiology is the strongest risk factor that precedes the development of HCC [1]. Broadly, a multitude of environmental and genetic risk factors have been associated with HCC including chronic viral infections, environmental toxins, excessive alcohol intake, comorbid conditions and metabolic or autoimmune disorders [4,5,16]. The unique geographic, gender, and age distributions of HCC are largely the consequence of the specific patterns of these risk factors, highlighting hepatitis B and C viral infections and alcoholic liver disease [3] **(Figure 1)**.

1.3.1 Viral-induced HCC

The World Health Organization (WHO) estimates that around 257 and 71 million people are chronically affected by hepatitis B virus (HBV) or hepatitis C virus (HCV), respectively [17]. Chronic infection with hepatitis is a major risk cause of HCC, since approximately 54% of HCC cases are attributed to HBV infection and 31% to HCV, leaving around 15% to other factors [18].

Based on geographical distribution, HBV infection accounts for approximately 60% of HCC cases in Asia and Africa [1] **(Figure 1)**. This infection is the main determinant condition of HCC in South-Eastern Asia and Sub-Saharan Africa regions where HBV is endemic [1,4,19]. In these regions, infections are acquired during the perinatal period or during childhood due to HBV transmission happens mainly via perinatal, blood and sexual practices. In fact, most individuals with chronic HBV infection acquire the virus through vertical transmission [19]. Otherwise, chronic HCV infection is the most common underlying liver disease among HCC patients in developed areas like North America, Europe and Japan [1] **(Figure 1)**. Outside of endemic areas, HBV and HCV infections occur during middle age and transmission channels include intravenous drug users, transfusion of contaminated blood, high-risk sexual behaviors and risk of occupational exposure [19].

HBV is a double-stranded non-cytopathic DNA virus of the *Hepadnaviridae* family [19,20]. HBV infection triggers hepatocyte injury and chronic necro-

inflammation in the liver, succeeding hepatocyte proliferation, fibrosis and cirrhosis. The greater rate of hepatocyte turnover in cirrhotic liver together with accumulation of mutations in the host genome may result in genetic alterations, chromosomal aberrations, inactivation of tumor suppressor genes and activation of oncogenes, leading to HCC. However, although most HCC cases arise in cirrhotic livers, HBV-associated HCC can also occur in the absence of previous cirrhosis by directly integration of HBV DNA into the host genome, which results in chromosomal rearrangement and, in that way, improves genomic instability [3,20]. Moreover, the viral oncogenic HBV protein X (HBx) plays a crucial role in HBV-associated HCC development. HBx is considered essential for HBV replication and activates oncogenes like c-Myc and a wide range of pathways involved in cell proliferation such as Ras/MAPK or PI3K/AKT [9,20]. Additionally, HBx can bind and suppress genes that regulate cell cycle, DNA repair and apoptosis, such as the tumor suppressor p53 [3].

Unlike HBV, **HCV** is a single-stranded RNA virus that belongs to *Flaviviridae* family, being incapable to integrate into the host cell genome and prompt direct carcinogenesis. Consequently, HCV causes liver carcinogenesis in an indirect manner preceded by cirrhosis [1,20]. HCV is a non-cytopathic virus and HCV-mediated liver carcinogenesis is regulated by interactions between the viral-induced factors and host-induced immune response. This immunologic response is different for each individual and is mediated by factors like TNF-α, resulting in hepatocyte injury and several cycles of hepatocyte death and regeneration leading to a fibrotic liver [3,9]. Besides, the virus and host immune response prompt oxidative stress by ROS production, which has been suggested to be involved in HCV-mediated carcinogenesis [9]. The core HCV proteins non-structural protein 5A (NS5A) and non-structural protein 3 (NS3) trigger oxidative stress, activating NF-κB and MAPK to raise inflammatory response and disturb proliferation and apoptosis pathways [3]. In both cases, permanent damage and regeneration lead to mutations that increase the risk of cirrhosis and, eventually, the development of HCC [3,9].

HBV and HCV share the methods of transmission, great diffusion worldwide, and the capability to trigger a viral chronic infection that might leads to HCC [20].

Epidemiological data suggest that co-infection with HBV and HCV intensifies the risk of HCC progression [9,20]. Likewise, the human immunodeficiency virus (HIV) is considered as another prime modulator of HCC development, since HIV co-infection can accelerate the progression of chronic HBV or HCV infections and increase the chance of liver cirrhosis and HCC [9,20]. Hepatitis D virus (HDV) is an RNA virus that needs the HBV surface antigens for its replication and infectivity. HBV/HDV co-infection is related to an increased risk of HCC in comparison with single HBV infection [1].

Therefore, disease progression from HBV or HCV chronic hepatitis to cirrhosis and HCC depends on a broad range of factors such as presence of viral co-infections, gender, age of infection, and the exposure of other risk factors of HCC like alcohol or environmental toxins [5,14].

Primary prevention of most cases of liver cancer has been possible by the development and introduction, in 1982, of a vaccine against HBV. The HBV vaccine has radically reduced the prevalence of HBV infection globally, as well as the incidence of HCC at early ages in Eastern Asia, where mass vaccination was first introduced [4,5,17,19]; but it is required to implement the vaccination programs around the world [1]. Globally, it has been estimated that between 1990 and 2020, HBV vaccination reduced approximately 83% of new HBV infections [17]. Nonetheless, at present there is no vaccine available to prevent HCV infection [4,5,17]. In addition to prevention, the progression of chronic viral disease can be abrogated by different antiviral therapies [17,19].

1.3.2 Aflatoxins

Another key agent in the pathologic progression of HCC is the ingestion of food contaminated with aflatoxins. Aflatoxins are secondary metabolites produced by the fungi *Aspergillus flavus* and *Aspergillus parasiticus* species [17,20]. These fungal toxins are well-known food contaminant, which may be present in an extensive variety of foodstuffs as for example peanuts, soya, meat, milk, rice, corn, and dried fruits, which have been stored in a hot and humid environment [17,20,21]. Aflatoxin B1 (AFB1) is a

potent human carcinogen and, once consumed, AFB1 is metabolized in the liver by cytochrome P450 (CYP450) to a functional transitional compound, AFB1-exo-8,9-epoxide. This metabolite is highly reactive and can attach to DNA forming adducts causing nucleotide modification. Specifically, AFB1 generates a mutation at serine 249 in the tumor suppressor gene p53 [20–22].

Aflatoxin intake is frequent in South-East Asia and Sub-Saharan Africa regions, where HBV infection is endemic [1]. Hence, AFB1 is an important cofactor in these regions, acting synergistically with HBV infection to improve from 5 to 10-fold the likelihood of HCC development [1,3,18]. In Africa, this synergistic effect is responsible for an HCC developed at an early age, around 30-40 years [1].

The prevalence of HBV and HCV is declining worldwide as a result of the success of HBV vaccination programs and the development of antiviral therapies, as well as the huge effort to prevent and reduce exposure to aflatoxins [4,5,17]. Therefore, the main risk factors of HCC appear to be in transition, as the incidence of other non-viral risk factors, such as alcohol abuse, obesity or type 2 diabetes, is enhancing the rate of HCC in developed regions [4,5].

1.3.3 Alcohol

Excessive alcohol consumption, defined as the ingestion of 50-70 g per day, origins liver injury leading to alcohol-related cirrhosis [9,22]. Alcohol intake constitutes the main etiological factor of cirrhosis in Central and Eastern Europe [1], representing a great risk of HCC in countries such as France and Spain [18] **(Figure 1)**.

Although alcohol can individually cause HCC by inducing cirrhosis, is commonly associated with virus-mediated HCC (primarily to HCV) to increase the probability of HCC development compared to non-drinkers [9]. The precise mechanism by which heavy alcohol consumption exacerbates virus-related disease are not entirely clear; nevertheless, weakened immune response, improved viral replication, and upper hepatocyte toxicity are considered key effects that drive to liver disease progression [3]. Furthermore, alcohol-promoted hepatocarcinogenesis is largely associated with excessive ROS production by ethanol metabolites [9,22]. This severe oxidative stress

releases pro-inflammatory cytokines, principally TNF-α, occasioning chronic damage and regeneration of hepatocytes that can progress to cirrhosis and, ultimately, HCC [3,22].

1.3.4 Metabolic disorders

In developed regions, increasing evidence suggest an enlarged HCC incidence in patients with non-alcoholic fatty liver disease (**NAFLD**) associated with metabolic syndrome, type 2 diabetes mellitus and obesity [9,18]. Besides, for patients with chronic viral hepatitis, metabolic syndrome represents an additive risk [18]. NAFLD is considered a benign metabolic disorder that from the hepatic deposition of triglycerides and steatosis can progress to non-alcoholic steatohepatitis (**NASH**), fibrosis, cirrhosis and finally HCC [22]. The rate of progression to cirrhosis or HCC is slower in the presence of NAFLD/NASH than in other chronic liver diseases, occurring in 2.4-12.8% of these patients [22,23]. Additionally, insulin resistance, hyperinsulinemia, visceral obesity, dyslipidemia and arterial hypertension play a significant role in altering NASH, which increases the risk of cirrhosis and HCC [22]. In the coming years, the prevalence of these factors will become one of the leading causes of HCC [23] **(Figure 1)**.

1.3.5 Other factors

In addition to environmental factors, α1-antitrypsin deficiency, glycogen storage disease type I, hemochromatosis, porphyria, hereditary tyrosinemia, autoimmune hepatitis, hypothyroidism, among other several autoimmune diseases and metabolic disorders also show an increased risk of HCC [3,18,24].

The gut microbiota contributes to NAFLD and can stimulate progression to NASH, principally in obese patients. Thus, dysbiosis, defined as any change in the composition of the microbiota compared to healthy conditions, is an emergent factor of HCC [22,23].

Moreover, recently also some sociodemographic features have been related to HCC [1,25]. As previously mentioned, gender is a prime risk factor that predominates in male population, probably associated with a collecting of risk factors among men

and the existing variances in sex hormones [1,4]. Also, ageing is an important risk factor, with a greater age-specific prevalence described in individuals older than 70 years [1]. Furthermore, some differences between racial/ethnic groups have been described; in particular, black and Hispanic HCC patients present worse outcomes than white individuals [25]. Finally, epidemiological studies have also highlighted the increased risk of HCC associated with lifestyle and smoking [25].

1.4 Surveillance and diagnosis

In addition to prevention, diagnosis in early stages when liver function is still preserved, could constitute a key strategy to improve the prognosis of HCC, favoring more effective therapies with survival benefit [26]. However, HCC is usually diagnosed in advanced stages due to most of patients are asymptomatic or present symptoms that are often related to those of precedent chronic liver disease [16]. Only in advanced stages, when curative treatment is not applicable, patients show symptoms associated with liver failure [27]. The main symptoms of HCC are epigastric or abdominal pain, abdominal swelling, jaundice, weakness, unintentional weight loss and fever [16].

Guidelines recommend surveillance based on cost-effective and risk of HCC development in the at-risk subgroups of the population, including individuals with cirrhosis and with chronic HBV infection. In consequence, a continuous surveillance of individuals at specific predisposition to develop HCC can improve early diagnosis, reducing HCC-related mortality [18,26].

In addition to clinical examination, multiple techniques can be performed to establish the diagnosis of HCC, being classified into radiological or imaging techniques, molecular markers and liver biopsy [27] **(Figure 3)**.

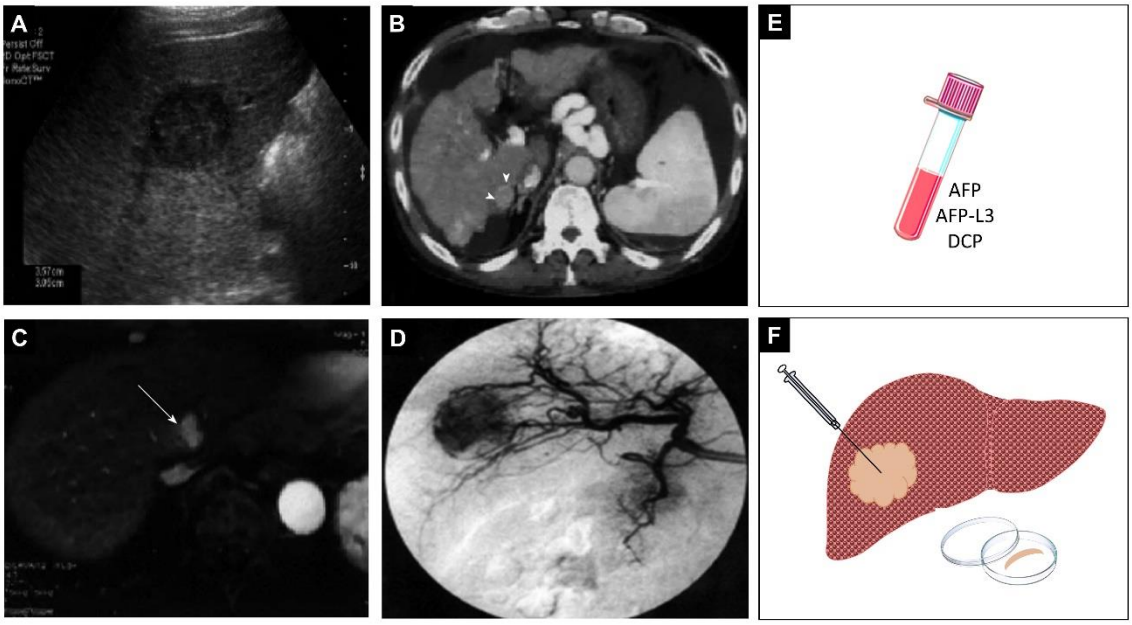

Figure 3. Leading diagnostic techniques employed for the detection of HCC. Figures A-D show the main radiological or imaging methods for HCC diagnosis. (A) Transverse abdominal sonogram obtained by ultrasonography (US) shows a small tumor mass (3 cm) in the right liver lobe; **(B)** HCC is visualized as an enhanced nodule through late arterial phase of multi-detector computed tomography (MDCT) (arrowheads); **(C)** The arterial phase of dynamic magnetic resonance imaging (MRI) reports a tumor mass next to the portal vein (white arrow); **(D)** Detection of HCC by hepatic angiography as a hypervascularizated region into the liver. **(E)** Major serum biomarkers used: α-fetoprotein (AFP), the AFP-L3 isoform, and des-γ-carboxyprothrombin (DCP). **(F)** Illustrative liver biopsy. Figures A-D were retrieved from [27].

1.4.1 Radiological diagnosis

Imaging-based diagnosis can be performed using different non-invasive techniques such as ultrasonography (US), computed tomography (CT) or magnetic resonance imaging (MRI), and also using the invasive method of angiography [27].

Abdominal US is first-choice method for the surveillance of hepatic focal lesions in high-risk patients **(Figure 3A)** (alone or in combination with the α-fetoprotein (AFP) biomarker) [16,27], as well as for early HCC diagnosis, due to ease of procedure, reliability, real-time results, cost-effectiveness and non-invasiveness [28]. US recognizes signs related to malignancy, including portal vein thrombosis, a mass that protrudes from the liver surface or dilated intrahepatic bile duct, even in the lack of a well-defined liver mass [27]. Nonetheless, most HCCs occur in the context of cirrhosis,

which impairs identification of small tumors by US, since the cirrhotic liver is nodular [18,29]. The sensitivity of US for the detection of HCC is highly dependent on operator expertise, as well as tumor and patient features such as tumor size or obesity. In standard backgrounds the sensitivity of US is around 60-65% [26,27]. Most lesions <1 cm in diameter detected on US are not HCC or are very difficult to diagnose [18,29]; actually, only 50% of tumors lower than 1 cm are detected by US [29]. In this situation, short-term follow-up with a repeat US after three months is required. For lesions ≥1 cm, additional diagnostic techniques should be performed [18]. Different US variants have been developed with different clinical utility. For instance, US-Doppler, contrast-enhanced US (CEUS) or the endoscopic US, improved the sensitivity and specificity of HCC identification and can provide further data about the characteristics of liver lesions than conventional US [27,28].

CT and MRI scans are largely used imaging methods to confirm the radiological diagnosis of HCC patients with anomalous results after US and serum AFP screening [28,30].

CT has excellent performance in early detection of focal liver lesions and HCC staging [27] and is also applied to determine the response of HCC to locoregional treatment [27,28]. Besides, CT has other wide uses in clinical practice including tridimensional vascular reconstruction, measurement of liver or tumor volume, and assessment of extrahepatic metastasis [28]. Most innovative the multi-detector computed tomography (MDCT) comprises four analytical phases after injection of the contrast agent **(Figure 3B)**. This technique shows greater sensitivity in the identification of HCC lesions inside the cirrhotic parenchyma due to quick washout of contrast, allowing the identification of focal hepatic lesions smaller than 2 cm [27]. However, persistent exposure to this method carries a significant radiation risk, limiting its use in long-term diagnosis of HCC [26,30].

MRI allows the diagnosis, staging and response assessment of HCC without employ ionizing radiation or nephrotoxic contrast agents **(Figure 3C)**, and provides higher resolution images of the liver tissue than CT [27,28,30]. Thus, MRI may be useful in patients with renal insufficiency or those with hypersensitivity to CT contrast agents.

Even though MRI displays a similar diagnostic precision to MDCT in the early detection of HCC, it is superior to both US and CT in discerning regenerative nodules from HCC nodules in cirrhotic liver. However, MDCT scanning remains the preferred method for most radiologists, as result of the elevated cost and the long time needed to obtain good quality MRI images [27]. Hence, surveillance is not cost-effective by MRI [26].

In conclusion, for surveillance of high-risk individuals, US screening is recommended every six months single or with AFP. CT or MRI are greater techniques of diagnosis but are not recommended for surveillance because of the radiation and contrast agent risks, the higher cost and the detection of false positive signals [16,26].

Finally, **angiography** is an invasive procedure of imaging-based diagnosis that involves the injection of intra-arterial contrast dye [27,28], resulting a useful method owing to HCC is a hypervascular tumor [27] **(Figure 3D)**. Angiography checks liver tumor vessels and the number, size and bloodstream of hepatic tumors. Furthermore, provides data on vascular anatomic changes and the anatomic relationship between liver tumor and important blood vessels, as infiltration of the portal vein that is fundamental for prognosis [28]. Angiography can improve HCC detection if combined with CT or MRI. But less invasive and novel procedures described above have limited the employ of this technique for delivering of hepatic locoregional therapy or for the management of acute bleeding from local rupture [27,28].

1.4.2 Diagnostic biomarkers

During HCC development, liver cells may present altered molecular signatures and release tumor-associated molecules, which could be monitored for HCC diagnosis [31] **(Figure 3E)**.

AFP is the main well-studied and usually biomarker employed for the diagnosis and prognosis of HCC [31]. As mentioned above, AFP can be used as a supplementary tool for surveillance of high-risk individuals together US [16,31]. AFP is a serum glycoprotein synthesized by the fetal liver, which serum levels decline quickly after birth and remain low during adulthood [31,32]. Nonetheless, this protein can be overexpressed again under pathological conditions including chronic liver disease,

germ cell tumors, HCC and gastric cancer [32]. The use of AFP as diagnostic biomarker is controversial; although several researches regarding the diagnostic usefulness of AFP suggest that elevated serum levels are correlated with HCC, the use of this biomarker presents some limitations [31,32]. On the one hand, due to the higher heterogeneity of HCC, elevated AFP levels are not detected in most HCC tumors at early stage, reducing its sensitivity [26,32]. On the other hand, sensitivity and specificity are variable depending on the cut-off value used [32]: a lower specificity cut-off value (>20 ng/ml) may detect elevated AFP levels in the situation of cirrhotic patients with active hepatitis, increased serum alanine aminotransferase (ALT), or non-HCC-related malignancies [16,31,32]. To date, although the use of AFP constitutes an effective support method for the detection and surveillance of HCC, the use of this biomarker alone is not recommended [31]. In this way, fucosylated fraction of AFP (**AFP-L3**), an isoform of AFP, has demonstrated better specificity in discerning HCC patients from those with cirrhosis and regenerating nodules, but shows poorer sensitivity than AFP [27,31]. The AFP-L3 percentage is measured as a ratio between AFP-L3 and total AFP [27].

The limitations of AFP use highlight the need to identify novel biomarkers or a combination of them can constitute an optimal performance in the diagnosis, prognosis, treatment response, and surveillance of HCC [32]. Des-γ-carboxyprothrombin (**DCP**), another well-studied and approved serum biomarker, is a non-functional prothrombin induced by vitamin K absence and is overproduced in HCC patients [27,31,32]. In HCC, DCP acts as an autologous growth factor that stimulates tumor growth and as a paracrine factor implicated in the crosstalk between tumor and vascular endothelial cells [31]. Compared to AFP, DCP does not provide substantial improvements [32], although some results revealed that DCP was superior to AFP in detecting tumors greater than 5 cm in diameter [31]. Moreover, this biomarker is not suitable for early HCC diagnosis, but DCP levels have been correlated to advanced HCC stages and portal vein invasion [32]. In addition, DCP is a likely prognostic marker for HCC patients after treatment [31]. Serum DCP-based diagnosis displays suboptimal sensitivity but adequate specificity for HCC patients [32].

Furthermore, there are many other molecules under investigation that have been considered as potential HCC biomarkers for future clinical practice, such as glypican 3 (GPC-3), osteopontin (OPN), heat shock protein 70 (Hsp70), Golgi protein 73 (GP73), glutamine synthetase (GS), squamous cell carcinoma antigen (SCCA), miRNAs, lncRNAs, among others [31,32].

1.4.3 Liver biopsy

Liver biopsy is an invasive method that involves the extraction of a small portion of the tumor mass for its histological evaluation **(Figure 3F)**. This technique presents more complications than the radiological diagnostic tools [33]. For instance, severe bleeding is usually evident within 2-4 h after biopsy, and tumor spread through the needle track is other possible risk [27,33]. Therefore, advances in imaging tools have decreased the need for biopsy of liver nodules. Tissue-biopsy is then limited to the diagnosis of HCC when imaging-based techniques are inconclusive and for HCC developed in non-cirrhotic patients [33].

1.5 HCC staging and management

Once the diagnosis is established, prognostic assessment is a fundamental step in the management of HCC. Clinical classification of HCC is intended to establish prognosis and allow the selection of the best treatment strategy for each candidate [18]. Management of HCC depends on the tumor stage, liver function reserve, and tumor-related health patient status [18,27].

Numerous staging systems have been developed around the world to provide a clinical classification of HCC that allows for proper management. The main recognizes systems are tumor-node-metastasis (TNM), Okuda, Cancer of the Liver Italian Program (CLIP), *Groupe d'Etude et de Traitement du Carcinome Hépatocellulaire* (GRETCH), Barcelona Clinic Liver Cancer (BCLC), Chinese University Prognostic Index (CUPI), Japan Integrated Staging (JIS), Tokyo score, and Hong Kong Liver Cancer (HKLC) [34–36]. Despite this wide range of classification systems, nowadays there is no universally accepted staging system to compare management alternatives in different populations [35].

In oncology, TNM staging is the standard classification of cancer based on tumor characteristics [18]. This method examines the extent of the primary tumor (T), the presence of lymph node involvement (N) and/or the presence of extrahepatic metastasis (M) [34].

1.5.1 BCLC staging

BCLC system has been widely validated and is the most frequently used staging system for HCC [36]. BCLC staging clarifies the decision-making process of HCC patients according to tumor extension, liver functional reserve and physical status. Tumor extension involves the size and number of the tumors as well as the presence of portal vein invasion or extrahepatic metastasis; the liver functional reserve is determined by the Child-Pugh score; and the physical condition of individuals is determined according to the Eastern Cooperative Oncology Group Performance Status (ECOG-PS). Then, HCC patients are assigned to one of the five categories (0, A, B, C and D) in accordance to these features [34,35] **(Figure 4)**.

As shown in **Figure 4**, BCLC 0 (very early stage) involves a solitary nodule measuring ≤2 cm, while BCLC A (early stage) comprises single or up to three nodules ≤3 cm in diameter. In both stages, HCC patients preserve liver function and there is no presence of vascular invasion or extrahepatic propagation. Thus, curative therapies including surgical resection, liver transplant and ablation, are suggested for BCLC 0 and BCLC A patients. The selection of each curative option attends to different parameters. In other hand, BCLC B (intermediate stage) includes HCC patients without symptoms, but diagnosed with multifocal tumors without vascular invasion or extrahepatic spread. If liver function is preserved, these BCLC B patients are candidates for locoregional treatment by transarterial chemoembolization (TACE). In BCLC C (advanced stage), patients present one or more of the following: vascular invasion, tumor spread beyond the liver, and minor cancer-related symptoms. For this situation, systemic therapy is recommended. Finally, BCLC D (end stage) assigned patients show impaired liver function or marked symptomatology and require best supportive care [30,34–36].

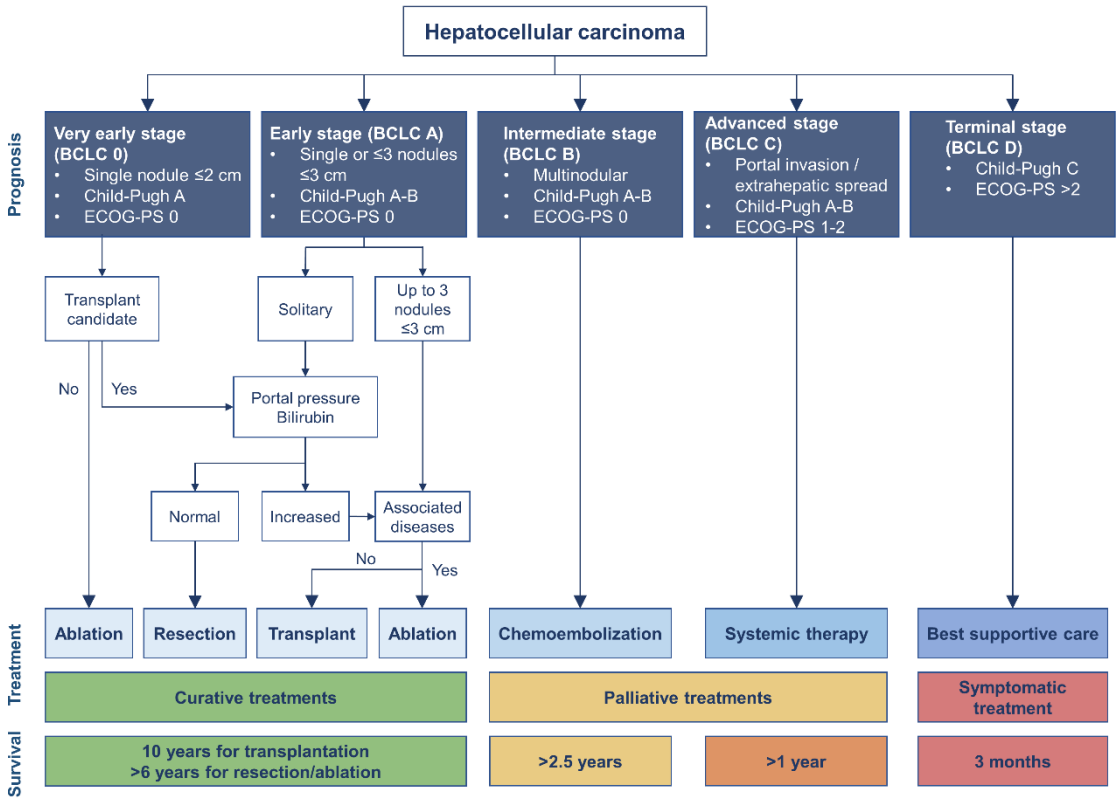

Figure 4. BCLC staging system and treatment strategy. The BCLC staging system establishes five prognostic stages (BCLC 0, A, B, C and D) linked to the recommendation of first-line treatment options in accordance with disease extension, liver function (Child-Pugh score) and performance status (ECOG-PS). The expected outcome is expressed as the median survival of each tumor stage based on the available scientific evidence [1,36]. Liver function can be classified as well compensated (Child-Pugh A), significant functional compromise (Child-Pugh B) or decompensated (Child-Pugh C) [16]. Preserved liver function includes patients with varying degrees of liver function reserve that must be cautiously assessed. For most treatment options, compensated liver disease (Child-Pugh stage A without ascites) is required for optimal results [36]. Liver transplantation is the only option that could be applied regardless of liver function. Patients with end-stage liver disease due to severely impaired liver function (Child-Pugh stage C or earlier stages with poor prognosis predictors) should be considered for liver transplant [1,36]. According to performance status, patients may be fully active (ECOG-PS 0), have restricted functional capacity (ECOG-PS 1-2) or be disabled (ECOG-PS 3-4) [16]. Figure adapted from [1,18,36].

1.6 HCC treatment landscape

HCC treatment aimed at increase patient survival whereas maintaining the highest quality of life and consists in different curative and palliative options. As previously mentioned, HCC patients are usually diagnosed in advanced stages because

the absence of symptoms, where only palliative therapies are available [16,36]. Hence, the development of novel drugs and therapies can improve the outcome of patients with HCC, but the crucial aspect in the management of HCC remains to achieve an early-stage diagnosis and constant surveillance of the high-risk population [16].

1.6.1 Curative treatments

Curative options for HCC patients include surgical resection, liver transplantation and ablation, which are recommended for patients assigned to BCLC stages 0 or A [36].

Hepatic **surgical resection** constitutes the treatment option in patients with resectable tumors in the lack of substantial portal hypertension [36,37]. Moreover, bilirubin levels are another variable considered [36]. Resection is the standard treatment for individuals without cirrhotic liver, in whom major resections can be performed without severe complications [1,36]. Even though surgical resection is a potentially curative treatment, tumor recurrence occurs in approximately 70% of cases at 5 years [1,36,37]. One of the benefits of hepatic resection is the obtainability of the surgical histopathological specimen, which can be useful to predict the chance of recurrence [36,37]. The BCLC group has suggested and corroborated the rescue transplant procedure after resection for those patients with high-risk histological markers, as for example microvascular invasion or satellites [37].

Liver transplantation is the treatment option for early diagnosed HCC in cases where hepatic resection is contraindicated, including those patients with decompensated cirrhosis [36]. Liver transplantation is the best curative option for individuals with early-stage HCC, as it removes both the tumor and the unhealthy liver tissues, avoiding the underlying cirrhosis that could limit the functional capacity of the liver and develop recurrent tumors. Therefore, this procedure seems to be the most effective management to prevent intrahepatic recurrence [36,37]. Unfortunately, the main limitation of liver transplantation is the shortage of liver donors [36]. Based on the Milan criteria, a solitary lesion ≤5 cm or up to three nodules ≤3 cm is the standard for tumor burden to achieve the best long-term outcomes after liver transplantation.

This benchmark allows obtaining an overall survival (OS) at 5 years greater than 70% with a recurrence rate of less than 10-15% [1,36,37].

As mentioned earlier, histopathological analysis after resection can identify a high risk of recurrence, which primes the indication of liver transplantation in these patients. This strategy allows patients to be successfully treated by resection avoiding liver transplant and, thereby, achieves optimal employment of the limited number of organs, since only those patients who are really going to benefit will undergo transplantation [36].

Local tumor **ablation** is a broadly recognized treatment for small, early-stage tumors [1,36]. Image-guided tumor ablation is used in patients who are not candidates for liver transplantation or hepatic resection due to medical comorbidities or liver dysfunction [37,38]. When liver transplantation is not possible, ablation can be selected as the first-line option for patients with a small single nodule (very early stage) and surgery as second-line treatment if ablation is not feasible or after ablation failure. In fact, this technique is almost 100% effective in HCC nodules less than 2 cm in diameter [36]. Moreover, clinical data suggest that local ablation can be used in a satisfactory manner as a bridge therapy to liver transplantation [37]. Ablation induces direct tumor necrosis by thermal, chemical or electrical methods [1]. The two most ordinarily used modalities are radiofrequency ablation (RFA) and microwave ablation (MWA), and both tactics induce tumor necrosis by supplying heat straight into tumors [18,37]. MWA has emerged as a potential technique, owing to it is less susceptible to heat sink effect, is further effective for larger tumors from 3 cm to 5 cm, and requires fewer sessions than RFA [36–38]. RFA is the first-line ablation method, as it provides better control and outcomes than percutaneous ethanol injection (PEI). Nonetheless, PEI still has a role in HCC treatment in resource-limited situations, since RFA cannot be applied near the gallbladder, colon, stomach or other viscera; or when nodule is adjacent to large intrahepatic vessels or bile ducts to evade heat injury by RFA or MWA [18,36–38].

1.6.2 Palliative treatments

Palliative therapy for HCC tries to improve survival while remains an acceptable quality of life without achieving the complete remission of the malignance [18].

The predominant arterial vascularization of HCC, in comparison to the adjacent liver parenchyma, allows the selective intravascular shipment of drugs, embolization particles, or radioactive gadgets by image-guided transcatheter treatments [36]. **TACE** is considered the first-line treatment in patients with intermediate-stage HCC, and involves the injection of cytotoxic chemotherapeutic agents and delivery of embolic agents into the tumor-feeding artery to barrier the arterial bloodstream, triggering tumor necrosis [14,36–38]. Nowadays, the most used drugs throughout conventional TACE in HCC patients are doxorubicin or cisplatin [14,37]. It has been indicated that the proper patient choice and optimal administration of the treatment can improve survival around 30-40 months [36,37].

Otherwise, although radiotherapy is not very used for HCC treatment, transarterial radioembolization (**TARE**) is another locoregional treatment that has recently been included to the offered palliative options. This method delivers a carrier-based cargo of radioactivity directly into the arteries that feed HCC tumors, resulting in tumor necrosis. The most popular TARE technique employs microspheres coated with yttrium-90, a β-emitting isotope [37,38].

Finally, **systemic therapy** is applied for the treatment of patients with advanced HCC. HCC is accepted as one of the most chemotherapy-resistant tumors, and until 2007 no effective systemic therapy was available for patients with advanced stage, a situation unprecedented in clinical oncology [18]. After 30 years of research, the multi-tyrosine kinase inhibitor (TKI) sorafenib appeared in 2007 as the first effective systemic drug against HCC, and constitutes at present the gold standard for patients with advanced tumors [3,18]. After the success of sorafenib, next additional attempts at developing new systemic therapies for advanced HCC were unsuccessful, and for over a decade this chemotherapeutic agent was the only standard for the treatment of these patients [1,38]. Lessons from these failures have contributed greatly in recent years to the improvement in trial design for the development of new treatments

against HCC [18,39]. In this way, recently other first or second-line therapeutic options have displayed efficacy against advanced HCC. Such as sorafenib, other multi-TKIs have been approved including lenvatinib as alternative first-line option, or regorafenib and cabozantinib for treatment after progression on sorafenib [1,39–41].

Moreover, immunotherapy has emerged as a promising strategy against HCC, being approved several monoclonal antibodies and immune-checkpoint inhibitors. Specifically, ramucirumab (anti-VEGF receptor 2 (VEGFR2) monoclonal antibody), nivolumab and pembrolizumab (anti-programmed cell death 1 (PD1) inhibitor) were approved as second-line single agents, while ipilimumab (anti-cytotoxic T-lymphocyte-associated antigen 4 (CTLA4) monoclonal antibody) was approved in combination with nivolumab. The latest incorporation to advanced HCC treatments was the combination of atezolizumab (anti-programmed cell death 1 ligand 1 (PDL1) antibody) and bevacizumab (anti-VEGF antibody), which was the first regimen that improve OS compared with sorafenib [1,39–42]. In **Figure 5**, timeline of approved systemic treatments for advanced HCC is represented.

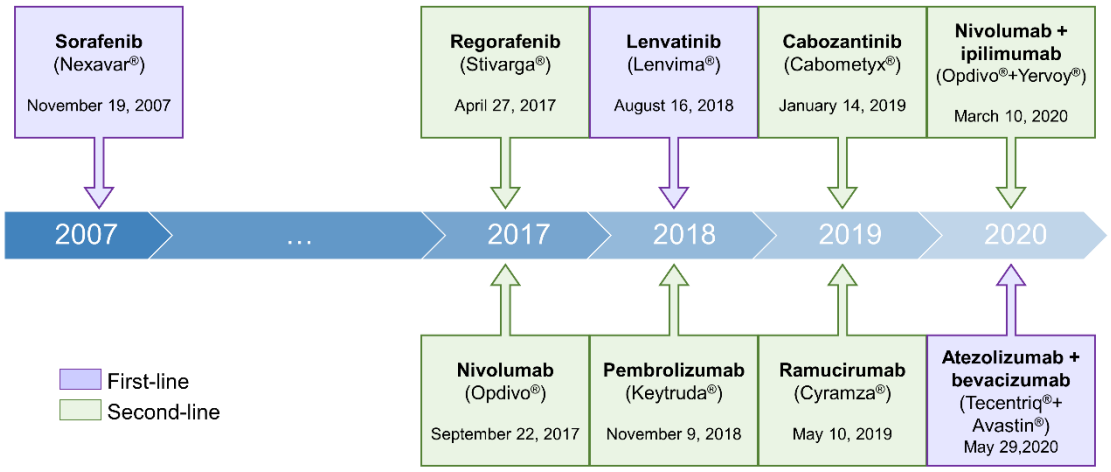

Figure 5. Timeline of approved drugs for systemic therapy of advanced HCC. The generic and commercial names of the different drugs are indicated, as well as the date of approval for HCC by the American Food and Drug Administration (FDA). Purple boxes indicate drugs approved as first-line treatment, while second-line regimens approved for HCC patients previously treated with sorafenib are reported in green boxes.

2 Sorafenib

Sorafenib (BAY 43-9006, Nexavar®) is a bi-aryl urea chemotherapeutic drug developed in 1995 by Bayer and Onyx against the Raf1 or c-Raf oncogene [43]. This drug was the first systemic treatment authorized by the American FDA and by the European Medicines Agency (EMA) entities to be administered as the first-line therapy in advanced HCC [42,44]. As well, sorafenib has also been approved for the treatment of other cancers, including in first place for renal cell carcinoma (RCC) [45–47], and more recently for radioactive iodine-refractory well-differentiated metastatic thyroid cancer (RAI-R DTC) [48,49].

2.1 Clinical trials in HCC

Early phase I studies were undertaken to conclude the maximum tolerated dose, safety profile, dose-limiting toxicities, pharmacokinetics, and tumor response profile of oral administration of sorafenib in patients with advanced refractory solid tumors. These researches established that sorafenib was well tolerated, safe, and provided anti-tumor clinical benefits. Moreover, a dosage of 400 mg bid continuous was suggested for further phase II testing [50,51].

A phase II study tested the efficacy, toxicity, pharmacokinetics, and biomarkers of sorafenib in 137 patients with advanced and unresectable HCC (ClinicalTrials.gov identifier NCT00044512). These patients received 400 mg bid oral sorafenib in 4-week cycles. In this phase II trial, sorafenib was normally well tolerated and revealed anti-tumor activity in patients with advanced HCC, enabling a median OS of 9.2 months [52].

Following, approval of sorafenib for HCC by regulatory agencies was based on two phase III clinical trials [43,44,53]. On the one hand, the Sorafenib HCC Assessment Randomized Protocol (**SHARP**) trial was conducted in a double-blind, placebo-controlled manner (ClinicalTrials.gov identifier NCT00105443). The SHARP trial evaluated 602 patients with advanced HCC who preserved liver function (Child-Pugh A) and none received prior systemic therapy. Patients were given continuous oral administration with either 400 mg of sorafenib (consisting of two 200 mg tablets)

twice daily or placebo in 6-week cycles. Results showed that the median OS of patients in the sorafenib group was 10.7 months compared to 7.9 months in the placebo group (hazard ratio (HR), 0.69; 95% confidence interval (CI), 0.55-0.87; p<0.001), which demonstrates a significant improvement in survival **(Table 1)**. Median time to radiologic progression was also longer in the sorafenib group than in the placebo group (5.5 *vs.* 2.8 months; HR, 0.58; 95% CI, 0.45-0.74; p<0.001). In conclusion, median survival and time to radiological progression were about 3 months extended for patients treated with sorafenib [54].

On the other hand, these outcomes were affirmed by the randomized, double-blind, placebo-controlled **Asia-Pacific** parallel phase III clinical trial (ClinicalTrials.gov identifier NCT00492752). In this trial, 271 patients from different centers in China, South Korea and Taiwan were selected and, like SHARP, had not received preceding systemic treatment and had Child-Pugh liver function class A. Patients enrolled also underwent the same dosage and schedule than those from SHARP. The main difference was the study population, since the Asia-Pacific trial was conducted in Asiatic population where existed a strong prevalence of HBV-related HCC. Nevertheless, significant results were also obtained, as the median OS of individuals who were treated with sorafenib was 6.5 months and with placebo 4.2 months (HR, 0.68; 95% CI, 0.50-0.93; p=0.014). In addition, the time to progression was twice as long in sorafenib-treated patients than for those given placebo (2.8 *vs.* 1.4 months; HR, 0.57; 95% CI, 0.42-0.79); p=0.0005). Hence, the Asia-Pacific trial confirmed the efficacy of sorafenib informed by SHARP trial [55].

Although both SHARP and Asia-Pacific trials described an augmented incidence of adverse events in sorafenib-treated groups, this drug was well tolerated and side effects were acceptable. As a result, sorafenib received approval in 2007 [43,44,53]. Succeeding the approval of sorafenib, other different phase III trials compared sorafenib with investigational drugs, obtaining a median OS ranged between 6.5 and 11.8 months [18]. Besides, some post-marketing surveillance studies reported real-life records in which the OS for BCLC B patients was of 15.6-20.1 months and for those with BCLC C of 8.4-13.6 months [56–59].

Consequently, sorafenib was recommended as the routine systemic therapy for HCC in patients with well-preserved liver function (Child-Pugh A) and with advanced tumors (BCLC C), or tumors progressing on locoregional treatments. However, no clear recommendation has not yet been established in patients assigned to Child-Pugh B [18].

The prospective observational Global Investigation of therapeutic DEcisions in HCC and Of its treatment with sorafeNib (**GIDEON**) is a large phase IV study of 3,213 patients with HCC who were treated with sorafenib, including patients with liver dysfunction (ClinicalTrials.gov identifier NCT00812175). The study revealed that the safety and tolerability profile of sorafenib was consistent in HCC patients with preserved liver function (Child-Pugh A) and with poor liver function (Child-Pugh B). However, the reported outcome for Child-Pugh B individuals was shorter compared with Child-Pugh A patients [60,61]. Other cohort studies have informed a similar safety profile and benefit from sorafenib treatment in Child-Pugh B patients [62,63]. These results suggest that sorafenib may be used for some patients with liver impairment, but this have to be carefully considered after conscientious patient evaluation [61–63].

2.2 Pharmacokinetics and metabolism

Sorafenib is a lipophilic drug with poor hydro-solubility and great membrane permeability [64,65]. Sorafenib film-coated tablets contain 274 mg of sorafenib-tosylate, which means 200 mg of sorafenib as the active ingredient (the recommended full dose regimen is 400 mg bid) [65].

Sorafenib is administered orally in fasted condition and is metabolized in the liver in two steps. The first phase consists of oxidative metabolism mediated by CYP450 3A4 (CYP3A4) and then, in the second step, is glucuronidated through uridine diphosphate (UDP)-glucuronosyltranferase 1A9 (UGT1A9) [65–67]. It has been indicated that eight active metabolites of sorafenib can be found in plasma after this hepatic metabolism [64,65].

Sorafenib tablets present a bioavailability of 38-49%, which can be reduced by 30% with a high-fat meal in contrast to a fasted state. This drug is 99.5% bound to

plasma proteins, reaching a peak plasma level after 1-2 h and a steady-state concentration within 7 days [65–67]. Bacterial glucuronidase cleaves sorafenib glucuroconjugates, enabling reabsorption of the non-conjugated active agent into the enterohepatic circulation [65,67]. Mean half-life of sorafenib is around 24-48 h, being excreted about 77% in feces and 19% in urine, mostly as glucuronidated metabolites. Moreover, the unchanged drug represents 51% of the dose found in feces, but it was not identified in urine [65–67].

2.3 Sorafenib-related side effects

Although sorafenib have been described as safety and well-tolerated drug by several clinical trials previously mentioned, the phase III trials SHARP and Asia-Pacific, and the GIDEON non-interventional study displayed some common side effects in patients receiving this drug [54,55,61,66]. The most common sorafenib-related adverse events include dermatologic toxicities like hand-foot skin reaction (HFSR) and rash, diarrhea, fatigue, and hypertension [66,68]. These adverse events are generally grade 1 or 2 (mild or moderate). HFSR and diarrhea have been reported as the most frequent grade 3/4 adverse events in the sorafenib-treated group [54,55,61,65]. In consequence, temporary interruption and/or dose adjustment of sorafenib, or in severe or persistent situations permanent discontinuation of sorafenib treatment, may be necessary [66,69].

Adverse **dermatological events** occur in 90% of patients who receive sorafenib [70]. HFSR, which is characterized by diffuse painful edema and redness in palms and soles of the feet, and rash or desquamation are the most frequent [66,68,70,71]. These skin reactions are usually grade 1 or 2 and generally appear within first 6 weeks of treatment initiation [66,68]. Moreover, alopecia, erythematous eruptions, dry skin and pruritus are also common dermatological adverse events [54,66,70]. The management of mild to moderate dermatologic toxicities includes preventive actions and topical remedies for symptomatic relief [66,71].

Gastrointestinal toxicities are also common in HCC patients under sorafenib treatment. Diarrhea in grade 1 or 2 is the most frequent gastrointestinal adverse event

occurring after the first cycle of sorafenib [68]. Patients should sustain a stool diary, report any irregularities or weakening symptomatology, maintaining a healthy diet and adequate fluid intake. For the treatment of mild to moderated diarrhea related to sorafenib therapy, loperamide administration is employed [66]. Moreover, other gastrointestinal side effects, such as nausea and vomiting, have been also described after sorafenib treatment [54].

Some **cardiovascular effects** have been reported, for instance, sorafenib-related hypertension which is typically mild to moderate, usually occurs early in treatment and can be managed with standard anti-hypertensive treatments [66,68]. In addition, sorafenib administration increases the risk of cardiac ischemia, infarction and bleeding [66].

Furthermore, **constitutional symptoms**, mainly fatigue, have been found in sorafenib-treated patients. Nevertheless, the incidence is similar in sorafenib and placebo groups, suggesting that fatigue is more probable due to the underlying illness rather than sorafenib [54,66]. Weight loss, anorexia and abdominal pain are other constitutional effects that have been commonly reported in the sorafenib group [54].

Curiously, recent data demonstrated that the manifestation of sorafenib-related side effects such as diarrhea, hypertension and skin toxicities, is related to improved OS in sorafenib-treated HCC patients [69,71].

2.4 Pharmacodynamics

Sorafenib is a dual action multi-TKI that targets both tumor cells and tumor-associated endothelial cells, exerting anti-proliferative, anti-angiogenic and pro-apoptotic activities [44,67]. As indicated above, sorafenib was originally developed to inhibit c-Raf, but it also inhibits wild-type or mutated B-Raf [43,44,64,67]. These Raf serine/threonine kinases are involved in the MAPK/ERK pathway, leading to a phosphorylation cascade that eventually promotes the transcription of genes implicated in cell proliferation and survival [43,44,65,67]. ERK activates c-Myc, a transcription factor for cyclin D1 that encourages cell proliferation; it has been reported that low cyclin D1 levels decline transcription of genes involved in cell

proliferation [43]. Additionally, c-Raf interacts directly with anti-apoptotic and apoptotic regulatory proteins to stimulate cell survival [44]. Hence, by inhibiting Raf kinases sorafenib is able to exert its anti-proliferative activity against HCC [43,44,65,67] **(Figure 6)**.

In contrast, sorafenib can act on several MAPK-independent signaling pathways to induce apoptosis of tumor cells [65]. This drug suppresses phosphorylation of the eukaryotic translation initiation factor 4E (eIF4E) hindering translation of the anti-apoptotic protein myeloid cell leukemia-1 (Mcl-1), a B-cell lymphoma 2 (Bcl-2) family member [43,44,65,67]. Sorafenib also increases the expression of p53-upregulated-modulator of apoptosis (Puma) [65,67]. Both mechanisms provoke the activation of intrinsic apoptosis in the tumor cells [43,44,65,67] **(Figure 6)**. Curiously, some authors have indicated that sorafenib can cause DNA fragmentation [43].

On the other hand, sorafenib treatment also abrogates angiogenesis by inhibition of multiple cell surface tyrosine kinases including VEGFR-1/2/3, PDGF receptor β (PDGFR-β), KIT, FMS-like tyrosine kinase 3 (FLT-3), and the rearranged during transfection proto-oncogene (RET) [64,65,67]. These TK receptors activate Ras and the subsequent Raf/MAPK cascade, which allow to induction proliferation and survival of vascular endothelial cells as well as transcription of genes that lead to angiogenesis [43,44]. By decreasing angiogenesis, sorafenib allow to reduction in tumor vessel formation, which enables to cell death by arresting the blood supply to the tumor and inducing tumor cells starvation [43] **(Figure 6)**.

Finally, it has been suggested that sorafenib may also display some immunomodulatory properties, improving the action of tumor-specific T cells and decreasing immune-suppressive cell populations [65,67].

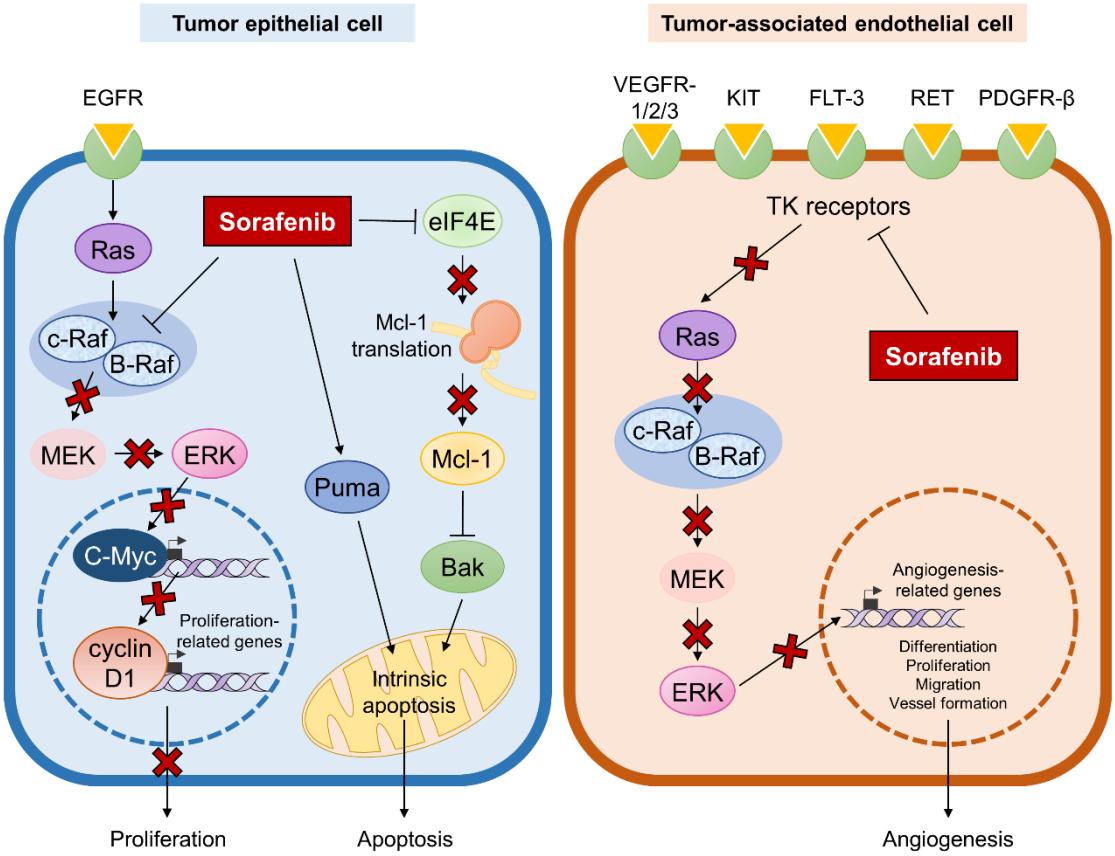

Figure 6. Molecular mechanisms of action of sorafenib. The left panel represents the anti-proliferative and pro-apoptotic effects of sorafenib on HCC cells. Sorafenib inhibits B-Raf and c-Raf kinases involved in the MAPK pathway, so these kinases can no longer activate MEK, ERK and c-Myc cascade and subsequent cyclin D1 transcription. Decreased levels of cyclin D1 are available to induce the transcription of proliferation-related genes, and therefore cell proliferation is slowed. On the other hand, sorafenib also promotes apoptosis by both activating the pro-apoptotic protein Puma and preventing the phosphorylation of eIF4E. eIF4E is the translation initiation factor for Mcl-1 and, in consequence, reduced translated levels of Mcl-1 are not capable of fully inhibiting the pro-apoptotic protein Bcl-2 homologous antagonist/killer (Bak). Hence, apoptosis is promoted. The right panel describes the anti-angiogenic action of sorafenib on tumor-associated endothelial cells. This drug inhibits the TK receptors VEGFR-1/2/3, PDGFR-β, KIT, FLT-3 and RET in endothelial cells. These receptors can no longer activate Ras and MAPK cascade that promote the transcription of genes leading to angiogenesis.

2.5 Sorafenib resistance

Unfortunately, despite systemic chemotherapy with sorafenib has demonstrated a significant increase in mean OS, the amount of HCC patients who

obtain a real and long-term benefit from this treatment is limited. This is explained by the existence of a high rate of primary and acquired sorafenib resistance in HCC cells [72–74]. Sorafenib is beneficial in only about 30% of patients, and acquired resistance often appears within 6 months after the treatment initiation [73,75]. Thus, several mechanisms that may be responsible for sorafenib resistance in HCC have been proposed in recent years [72–80].

2.5.1 Primary resistance

Primary or intrinsic resistance, which is characterized by the presence of sorafenib resistance factors in HCC cells prior to drug treatment, is mainly due to the genetic heterogeneity of this type of tumors [74,77]. Management of this topic is based on the identification of crucial biomarkers potentially useful to identify sorafenib-responsive patients from non-responders before to prescribing sorafenib, according to variances in the genetic features and expression profiles of tumors [74,78]. Some molecules have been identified to be related with sorafenib sensitiveness, such as epidermal growth factor receptor (EGFR), phosphorylated ERK (p-ERK), c-Jun NH_2-terminal kinase (JNK), c-Jun, VEGF or angiopoietin 2 (ANG-2) [81–85], among others [78]. Moreover, multiple tumor-specific miRNAs and lncRNAs have recently identified as novel prognostic biomarkers for sorafenib response in HCC [86]. Despite these findings, currently available biomarkers for sorafenib sensitivity still have an uncertain clinical value. Further investigations and well-designed prospective trials are required to corroborate their exact role in predicting the primary resistance to sorafenib as well as to identify additional and more clinical valuable markers [74,77,78].

2.5.2 Acquired resistance

Long-term exposure to sorafenib can result in reduced sensitivity of tumor cells during sorafenib treatment, leading to acquired resistance [72,74]. Elucidating the mechanisms involved could be useful for develop new approaches to prevent resistances instauration or to overcome when have already appeared [74]. As

described below, several mechanisms account for development of sorafenib resistant HCC cells have been suggested and are summarized in **Figure 7**.

Some studies reported the activation of **escape signaling pathways** from the MAPK cascade. Because sorafenib targets the MAPK pathway, PI3K/AKT and JAK/STAT are the main overactivated pathways in sorafenib-resistant cells as a consequence of compensatory mechanisms [72,77]. Higher levels of AKT have been described in resistant HCC cells than in parental cells, and thus the inhibition of AKT can reverse acquired resistance to sorafenib [72,74,77]. In addition, resistance can often be due to reactivation of the signaling molecules directly repressed by sorafenib, effects that occur through changes in upstream or downstream regulatory pathways or via secondary modifications of the drug target [79]. Consistent with these reactivation mechanisms, elevated levels of VEGFRs and p-ERK have been reported in HCC patients under sorafenib treatment [72,77,79].

Autophagy, which is an adaptive catabolic process crucial to preserving cellular homeostasis, has also been linked to sorafenib resistance. In this process useless or damaged organelles, proteins or other cytoplasmic components are delivered to lysosomal network for degradation [74,75,78,87]. Sorafenib treatment induces autophagy in HCC cells by rise autophagosome formation and expression of autophagy-related genes (ATGs) [74]. However, although some studies established that sorafenib-induced autophagy enhances its cytotoxicity against tumor cells, other works reported that autophagy can act as a pro-survival response. Therefore, the induction of cytoprotective autophagy can play an important role in desensitizing HCC cells to sorafenib [74,87].

Epithelial-mesenchymal transition (**EMT**) is a process characterized by the loss of cell–cell interactions and epithelial apico-basal polarity contributing to cell migration [73]. EMT also appear to be a key mechanism in the acquisition of sorafenib chemoresistance [73,74,76,77,80]. Sorafenib-resistant cells showed a reduced expression of epithelial-related proteins, such as E-cadherin, while mesenchymal markers as neural cadherin (N-cadherin), vimentin, and Snail are enhanced [74,88].

Furthermore, EMT is regulated by several pathways including PI3K/AKT or MAPK, and by hypoxic conditions [72,77].

Increasing evidence suggests that **epigenetic modifications** are critical for the emergence of sorafenib resistance. In some cases, prolonged sorafenib treatment may influence the methylations status of cancer-associated genes in HCC, mainly oncogenes and tumor suppressor genes [75,77]. Moreover, several miRNAs and lncRNAs can confer sorafenib resistance inducing some of these epigenetic modifications [75,77,86].

Other findings suggested the relevance of liver **cancer stem cells (CSCs)** subpopulation in sorafenib resistance [73,75,77,79,89]. Long-term treatment with sorafenib leads to enrichment of hepatic CSCs, while differentiated cells growth was inhibited [74,80,89]. CSCs have the capacity of self-renewal, differentiation, and tumorigenicity, conducting to sorafenib resistance and HCC progression [73,89]. Moreover, stemness is associated with mesenchymal status, and typical liver CSCs and EMT markers have been related to invasive, metastatic and sorafenib-resistant phenotype [74,79].

Despite these previously reported mechanisms, recent studies show other emerging mechanisms related to acquired resistance to sorafenib including changes in **drug transport, pharmacokinetics, metabolism and DNA repairing mechanisms** [78,79,89]**.** Thus, changes causing a decrease in the intracellular accumulation of sorafenib can compromise the efficacy of the drug: weakened expression or function of plasma membrane proteins involved in sorafenib transport may also participate in resistant development. In this way, reduced drug uptake by solute carriers (SLC) and enhanced activity of some drug efflux transporters of adenosine triphosphate (ATP)-binding cassette (ABC) families have been associated with acquired resistance. Besides, prolonged exposure of HCC cells to sorafenib leads to metabolic reprogramming, such as genetic variations affecting CYP450s and UGT1A9 which have been related to alterations in the metabolism of this drug [78,79,89].

Finally, changes in the **tumor microenvironment** has been considered a hallmark in sorafenib failure and the onset of resistance in HCC. This mechanism comprises not only modification on immune microenvironment, chronic inflammation, remodeling of ECM, fibrosis, oxidative stress or viral reactivation but also hypoxia [73,75,79]. Among them, hypoxia is probably one of the most studied key features, since it facilitates the selection of resistant clones to adapt to oxygen deprivation. This ability is carried out by the activation of different pro-survival pathways in tumor cells, including induction of EMT [72–77,79]. The role of hypoxia on acquired resistance to sorafenib will be explained in more detail later in the present PhD Thesis.

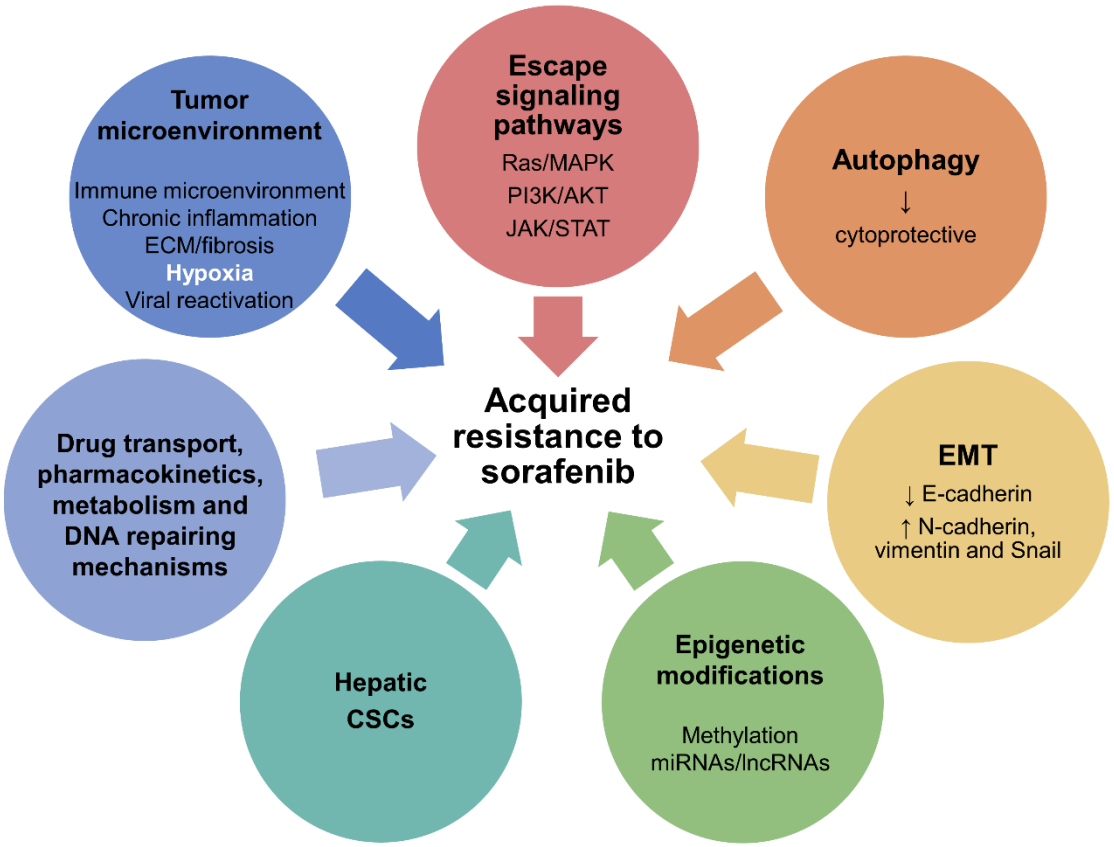

Figure 7. Mechanisms involved in the acquisition of sorafenib resistance. Sustained treatment with sorafenib can lead to activation of escape signaling pathways, cytoprotective autophagy, and EMT in HCC cells. Furthermore, enrichment of hepatic CSCs, epigenetic modifications and alterations in tumor microenvironment, sorafenib transport, pharmacokinetics, metabolism and DNA repairing mechanisms are adaptive changes that HCC cells can develop to resist sorafenib treatment.

2.5.3 Management of systemic therapy and sorafenib resistance

Due to the wide range of factors that appear to be involved in the effectiveness of sorafenib in HCC, the development of new approaches that can prolong the use of or replace sorafenib after its failure has been required. Accordingly, different drugs and combinations have been tested in the last decade [72,74]. Since 2017, the FDA has approved some drugs as alternative first-line treatment or as second-line for sorafenib-refractory HCC patients. In addition to sorafenib, other first-line available agents are lenvatinib (which showed non-inferiority to sorafenib) and atezolizumab plus bevacizumab (which could potentially substitute sorafenib as standard treatment for advanced HCC patients). Moreover, second-line regimen includes nowadays regorafenib, cabozantinib, ramucirumab, nivolumab, pembrolizumab or ipilimumab plus nivolumab [1,39–42]. **Table 1** summarizes the clinical trials that led to approval of these treatments.

Table 1. Summary of clinical trials that lead to approval of first- and second-line regimens for systemic therapy in advanced HCC.

FDA approval (year)	Trial name	Experimental and control arms	OS (months) Median HR (95% CI)	Study identifier*	Reference
First-line therapy					
2007	SHARP	Sorafenib *vs.* placebo	10.7 *vs.* 7.9 0.69 (0.55-0.87)	NCT00105443	[54]
2018	REFLECT	Lenvatinib *vs.* sorafenib	13.6 *vs.* 12.3 0.92 (0.79-1.06)	NCT01761266	[90]
2020	IMbrave 150	Atezolizumab + bevacizumab *vs.* sorafenib	Median OS not reached [a]	NCT03434379	[91]
Second-line therapy					
2017	RESORCE	Regorafenib *vs.* placebo	10.6 *vs.* 7.8 0.63 (0.50-0.79)	NCT01774344	[92]
2017	CheckMate-040	Nivolumab	15.0 [b]	NCT01658878	[93]
2018	KEYNOTE-224	Pembrolizumab	12.9 [c]	NCT02702414	[94]
2019	CELESTIAL	Cabozantinib *vs.* placebo	10.2 *vs.* 8.0 0.76 (0.63-0.92)	NCT01908426	[95]

2019	REACH-2	Ramucirumab *vs.* placebo	8.5 *vs.* 7.3 0.71 (0.53-0.95)	NCT02435433	[96]
2020	CheckMate-040: cohort 4	Nivolumab + ipilimumab	Median OS not reached [d]	NCT01658878	[97]

* https://clinicaltrials.gov/

[a] At the time of the primary analysis (August 29, 2019), the HR for death with atezolizumab plus bevacizumab compared to sorafenib was 0.58 (95% CI, 0.42- 0.79). OS at 12 months was 67.2% (95% CI, 61.3-73.1) with atezolizumab plus bevacizumab and 54.6% (95% CI, 45.2-64.0) with sorafenib.

[b] The phase I/II dose escalation and expansion trial Checkmate-040 was carried out in patients who were either treatment-naïve or pretreated with sorafenib. The median OS was 15 months in patients already treated with sorafenib and the treatment with nivolumab showed a manageable safety profile.

[c] The non-randomized, open-label phase II trial KEYNOTE-224 demonstrated similar anti-tumor activity and safety of pembrolizumab as second-line therapy compared to nivolumab, achieving a median OS of 12.9 months.

[d] Cohort 4 of the phase I/II trial CheckMate-040 evaluates three different dosages (Arm A, B and C) of nivolumab plus ipilimumab. At this time, median OS was 22.8 months (95% CI, 9.4-not reached) in arm A *vs.* 12.5 months (95% CI, 7.6-16.4) in arm B and 12.7 months (95% CI, 7.4-33.0) in arm C. In arm A, the 12-month OS rate was 61% (95% CI, 46%-73%) and the 24-month OS rate was 48% (95% CI, 34%-61%). Thus, arm A was approved by FDA.

Nevertheless, although different systemic options have been approved in the last years, sorafenib resistance remains a major challenge in the treatment of advanced HCC [74]. Increasing evidences suggest that a better understanding of the mechanisms implicated in sorafenib resistance will lead to the identification of key biomarkers for a better prognosis as well as more valuable targets to improve therapeutic strategies against advanced HCC [73,79].

3 Hypoxia

Mammalian cells need to maintain appropriate oxygen homeostasis towards perform aerobic metabolism and energy production required for their vital functions [98]. Hypoxia arises when oxygen demand exceeds oxygen supply, which normally occurs owing to abnormalities of the vasculature, anemia, or malfunction of hemoglobin [99]. Hepatocytes are especially susceptible to hypoxia after toxins exposure, viral infection, or chronic inflammation. Thus, hypoxia is implicated in alterations in hepatocytes that can lead to hepatocarcinogenesis [100].

Cellular oxygen balance is severely affected in cancer, chronic obstructive pulmonary disorders and heart diseases, and cells become hypoxic (oxygen levels less than 2%) [98,101]. While acute hypoxia is resolute by physiologic homeostasis in normal tissues, chronic hypoxia is more likely to appear in cancerous tissues [99]. Albeit both normal liver and HCC are highly vascularized, the rapid and uncontrolled growth of HCC cells requires increased consumption of oxygen and nutrients and, therefore, triggers tumor angiogenesis. However, the resulting tumor neo-vasculature is vastly chaotic and inefficient and cannot meet the drastic increase of oxygen demand, leading to oxygen deprivation or hypoxia in tumor regions that are far from functional blood vessels [99,102,103]. Indeed, with a median oxygen level of 0.8%, HCC is one of the most hypoxic tumors [103].

Although hypoxia itself results toxic to normal and cancer cells, this stress can trigger a wide range of adaptive changes that enable tumor cells to survive, such as an increase in erythropoietin (EPO) to rise hemoglobin, a switch from aerobic to anaerobic metabolism, promotion of EMT, and stimulation of growth factors that lead to angiogenesis [101,104,105]. This hypoxia-mediated response is carried out mainly by the hypoxia-inducible factors (HIFs) [98,100,102–104]. Therefore, hypoxia is a hallmark in solid tumors like HCC and has been associated with higher aggressiveness, selection of more invasive clones and resistance to chemotherapy and radiotherapy, leading to poor clinical outcomes [99,103,104].

3.1 HIF isoforms

HIF transcription factors are heterodimeric complexes consisting of an oxygen-sensitive α-subunit (HIF-α) and a constitutively expressed β-subunit (HIF-β). Three isoforms of HIF-α subunit have been described: HIF-1α, HIF-2α (also termed endothelial PAS domain-containing protein 1 (EPAS-1)) and HIF-3α, and among them HIF-1α and HIF-2α are the best characterized [101,106–108]. On the other hand, three constitutively expressed β-subunits, also called aryl hydrocarbon receptor nuclear translocator (ARNT), have been currently characterized: HIF-1β (ARNT1), HIF-2β (ARNT2) and HIF-3β (ARNT3), being HIF-1β the most studied [103,109].

Both subunits belong to the basic helix-loop-helix-Per-ARNT-Sim (bHLH-PAS) protein family and the three α-subunit show substantial structure homology [101,107,110]. As transcription factors, these proteins contain nuclear localization signals (NLS) that allow their translocation to the nucleus. The NH_2-terminal bHLH domains enable specific binding to the hypoxia-response element (HRE) in the promoter regions of HIFs target genes, by the recognition of a specific nucleotide sequence (5'-RCGTG-3', where R is either A or G). The two tandem PAS domains (PAS A and B) facilitate heterodimerization between the α and β subunits. Additionally, the COOH-terminal end of the HIF subunits constitutes the regulatory region of the protein, composed by transactivation domains (TADs) that are responsible for triggering their transcriptional activity. The first TAD that is situated near the NH_2-terminal region (N-TAD) appears only in HIF-α subunits at the oxygen-dependent regulation site, which is also known as the oxygen-dependent degradation domain (ODDD) [107,108,110]. ODDD serves as the recognition site for the von Hippel-Lindau disease tumor suppressor (pVHL) and is involved in the stabilization of α-subunits depending on the intracellular oxygen concentration [108]. Finally, the TAD located in the COOH-terminal region (C-TAD) is in charge of recruiting the co-activators, such as p300/cAMP response element-binding (CREB)-binding protein (CBP), to initiate transcription. These co-activators facilitate HIF-mediated transcription by enabling the chromatin remodeling [98,110]. However, different splice variants of HIF-3α, no containing C-TAD or lacking the bHLH DNA-binding domain, have been identified, being

the inhibitory PAS domain protein (IPAS) the best characterized [98,110,111] **(Figure 8)**.

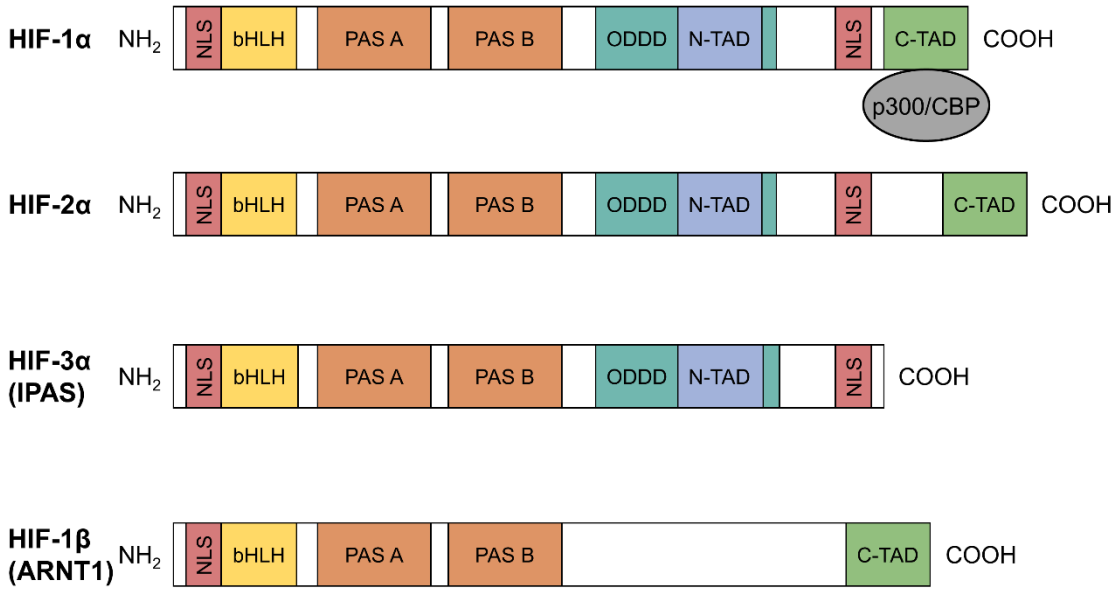

Figure 8. Domain structure of the HIF-α isoforms and binding partner HIF-1β. As transcription factors, canonical HIF proteins contain NLS sequences that allow their nuclear translocation. Moreover, HIF isoforms consist of a bHLH domain that recognizes the HRE in the promoter regions of target genes and two PAS domains responsible for the heterodimerization of the HIF-α/HIF-β subunits in the NH_2-terminal region. The COOH-terminal region presents two TAD sequences, which trigger HIF-related transcription and only HIF-α subunits present a unique ODDD that overlaps N-TAD, in charge of oxygen-dependent regulation of these factors. The C-TAD domain also binds to the p300/CBP co-activator to facilitate transcription. However, HIF-3α lacks the C-TAD domain and HIF-1β lacks the N-TAD one.

The fact that HIF-3α variants only present one TAD could explain their weaker transcriptional activity when compared with HIF-1/2α activity [111]. It has been suggested that the HIF-3α isoforms act as negative pathway regulators by forming transcription-incompetent heterodimers [110,111]. Therefore, these molecules mainly act as antagonists of HIF-1α and HIF-2α activity by occupying the HIF-β subunit. However, depending on the variant and the context, can also act as transcriptional activators of target genes, providing evidence that HIF-3α plays an important role as oxygen-dependent transcriptional activator. Furthermore, other findings suggest

supplementary roles, independent to hypoxic stress regulation, for some specific HIF-3α variants [112].

3.2 HIFs regulation

3.2.1 Oxygen-dependent regulation of HIF-α subunits

Under normal oxygen conditions or normoxia, HIFs activity is not required and, hence, their degradation takes place. This degradation requires hydroxylation of the conserved proline residues located in the ODDD of the α-subunit by the prolyl hydroxylase domain proteins (PHDs) [98,101,105–107,110]. Hydroxylated α-subunit acts as a recognition signal to pVHL binding, which recruits an E3 ubiquitin ligase complex resulting in ubiquitination and the consequent proteasomal degradation of HIF-α [98,101,105,106]. However, under hypoxic conditions, PHDs are inactive and HIF-α does not undergo hydroxylation, leading to its stabilization and translocation to the nucleus, where it heterodimerizes with HIF-β through their PAS domains to form the HIF transcription factor. Once in the nucleus, the HIF-α/β dimer binds to the HRE of the promoter region of its target genes and to transcriptional co-activators such as p300/CBP by C-TAD, promoting target gene expression [101,105–107] **(Figure 9)**.

There are three identified PHD isoforms (PHD1, PHD2 and PHD3). Among them, PHD2 has been characterized as the main regulator of this hypoxia pathway [105]. PHDs need oxygen and α-ketoglutarate as substrates, and Fe^{2+} and ascorbate as co-factors [98,108]. PHD activity can be blocked by numerous metabolites, including ROS, nitric oxide, fumarate and succinate. Otherwise, the amino acid cysteine can enhance PHD2 activity by inhibiting its oxidative self-inactivation [108,113].

Moreover, also another oxygen-dependent mechanism, which does not involve PHDs and pVHL, is responsible for negative regulation of HIFs under normoxia through controlling HIFs transactivation. In normoxia, factor inhibiting HIF (FIH), also known as asparginyl hydroxylase, catalyzes the hydroxylation of an asparagine residue in the C-TAD of HIF-α, in that way preventing interaction with the p300/CBP co-activator and subsequent transcription [98,105,107,108,114]. Although all three HIF-α isoforms are

regulated by prolyl hydroxylation, only HIF-1α and HIF-2α are controlled by asparaginyl hydroxylation because HIF-3α lacks C-TAD domain [114] **(Figure 9)**.

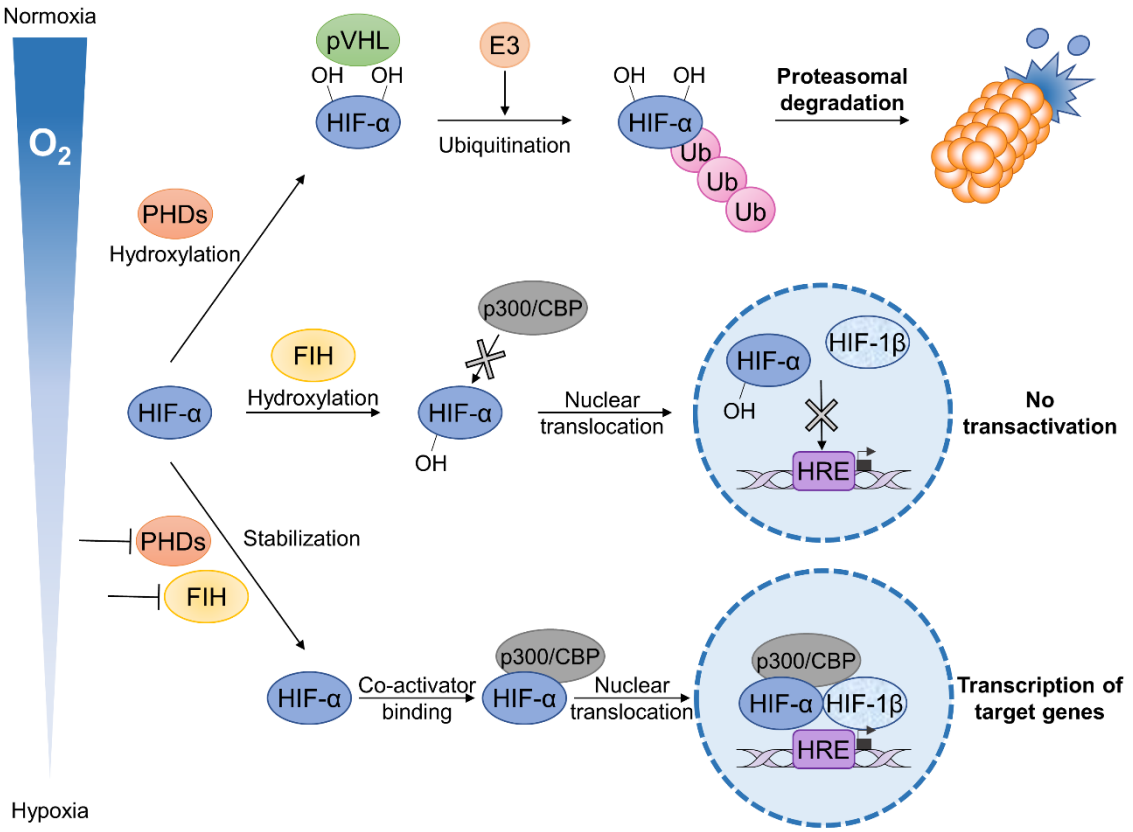

Figure 9. Oxygen-dependent regulation of HIF-α subunits. Under normoxic conditions, HIF-α subunits are continuously degraded through the oxygen-dependent hydroxylases PHD1–3, especially PHD2, which enable pVHL binding to HIF-α, subsequent ubiquitination by the E3 ubiquitin ligase complex and proteasomal degradation. FIH also inhibits HIF-α by hydroxylation that prevents the between HIF-α and its transcriptional co-activator p300/CBP, blocking transactivation. Under hypoxic conditions, hydroxylation of HIF-α by PHDs or FIH is restrained, leading to HIF-α stabilization. Following, HIF-α binds to the co-activators and dimerizes with HIF-1β to form a transcriptional activation complex, which binds to the HREs of target genes and promotes their transcription.

Similar to the PHDs, the catalytic effect of FIH also requests oxygen and α-ketoglutarate as substrates, and the establishment of hypoxia promotes the blockade of FIH hydroxylation, resulting in transcriptional activation of the target genes [98,107,108]. Intriguingly, HIF-1α is more susceptible to FIH-mediated abrogation than HIF-2α owing to a specific amino acid variance between the C-TAD

domain of both HIFs [107,110]. Besides, the oxygen affinity differs for PHDs and FIH: under low oxygen environment, PHDs are more rapidly inhibited as FIH has a greater affinity for oxygen. Consequently, when PHDs are inactive the HIF-α subunit stabilizes but FIH can still prevent the transcription of genes that require HIF-1α C-TAD activity [107].

In summary, the pVHL-dependent pathway regulates HIF-α stabilization, while the FIH-dependent mechanism controls HIF-α transactivation, both being regulated by the oxygen levels [98] **(Figure 9)**.

3.2.2 Oxygen-independent regulation of HIF-α subunits

In addition to the main role of hydroxylases in controlling HIFs activity, there are a number of pathways that regulate HIFs levels in an oxygen-independent manner. Various non-hypoxia-driven stimuli including growth factors, cytokines and other molecules lead to HIF-α accumulation, while different mechanism can allow to HIF-α degradation [98,107].

On the one hand, ubiquitination and proteasomal degradation of HIF-α can be induced by proteins other than pVHL and independently of hydroxylation [113]. For instance, the hypoxia-associated factor (HAF) is an E3 ubiquitin ligase that switches from HIF-1α to HIF-2α signaling via both HIF-1α degradation and HIF-2α transactivation [107]. HAF specifically targets HIF-1α for its ubiquitination and degradation under normoxia and hypoxia conditions. Otherwise, HAF binds to HIF-2α at a different site than HIF-1α, and instead of triggering HIF-2α degradation by ubiquitination, HAF enhances the transactivation capacity of HIF-2α [113] **(Figure 10)**.

The interplay between HIFs and the p53 family also intervenes in HIFs regulation. The E3 ubiquitin ligase murine double minute 2 (Mdm2), is responsible for ubiquitination and proteasomal degradation of HIF-1α in a p53-dependent manner [98,107,110]. In hypoxic tumors, loss or mutations in the tumor suppressor p53 impedes Mdm2-mediated degradation of HIF-1α [98]. Moreover, p53 also competes with HIF-α for the co-activator p300, decreasing the hypoxic response by avoiding transcriptional activation of HIFs [110] **(Figure 10)**.

Similarly, the eukaryotic translation initiation factor 3 subunit E (eIF3e) also produces the oxygen and pVHL-independent degradation of the α-subunit, being specific towards HIF-2α [110,113]. The enhancer-of-split and hairy-related protein 1 (SHARP1) induces the degradation of HIF-1α and HIF-2α by promoting their binding to the proteasome in an oxygen and ubiquitination-independent way. In contrast, deubiquitination by ubiquitin COOH-terminal hydrolase isozyme L1 (UCHL1) allows to HIF-1α stabilization by blocking pVHL-mediated ubiquitination [113] **(Figure 10)**.

Another oxygen-independent pathway for HIF-1α degradation involves receptor of activated protein kinase C1 (RACK1) and heat shock protein 90 (Hsp90) [108,115]. RACK1 enhances the binding of HIF-1α to the E3 ubiquitin ligase complex promoting its ubiquitination and degradation [108,110,115], whereas Hsp90 upregulates the stability of the HIF-1α protein through competition with RACK1 for binding to the PAS domain of HIF-1α [98,108,110,115] **(Figure 10)**. In addition, Hsp90 controls folding and thus function of many different proteins including TK receptors, serine/threonine kinases and other transcription factors involved in stabilizing HIF-α such as MAPK [110].

On the other hand, HIF-α levels can also be controlled by oxygen-independent mechanisms that do not focus on proteasomal degradation [108,113]. For instance, the Y-box binding protein 1 (YB-1) binds to HIF-1α messenger RNA (mRNA), but not to HIF-2α, activating its translation [113] **(Figure 10)**.

Furthermore, growth factors such as PDGF, insulin-like growth factor 1 (IGF-1), insulin and heregulin are able to regulate HIF expression [108]. Certain growth factors, and their cognate receptors that signal through the PI3K/AKT/mTOR or Ras/MAPK pathways, induce HIF expression [98,107,116]. Activation of PI3K regulates protein syntheses by its target AKT and downstream component mTOR [98]. The mTOR kinase functions in two multiprotein complexes termed mTOR complex 1 (mTORC1) and complex 2 (mTORC2) [117]. mTORC1 regulates HIF-1α protein translation via phosphorylation of their downstream effectors, eIF4E binding protein 1 (4E-BP1) and ribosomal protein S6 kinase beta-1 (p70S6K) [98,118]. In addition, HIF-1α and HIF-2α can be modulated by the PI3K-dependent induction of mTORC2 [117,119]. This

pathway is antagonized by phosphatase and tensin homolog (PTEN) which reverses the phosphorylation of PI3K products [98]. Additionally, growth factors activate Ras which in turn stimulates Ras/MAPK cascade [98,107,110,116]. Moreover, activated ERK phosphorylates 4E-BP1, p70S6K, and MAPK-interacting protein kinase (MNK) [98,116]. Finally, MNK can also phosphorylate eIF4E directly. Altogether, these signaling events result in an improved rate of mRNA translation into HIF-α proteins. Interestingly, ERK also regulates HIF-1α transcriptional activation by phosphorylation of the co-activator p300/CBP, enhancing HIF-1α/p300 complex formation [98,113] **(Figure 10)**.

HIFs are also regulated by a wide array of epigenetic modifications including changes in their methylation or acetylation status as well as miRNAs and lncRNAs [109,111,113,120]. For example, the enzyme sirtuin 1 (SIRT1) can bind to both HIF-1α and HIF-2α and deacetylate them, which produces opposite effects on their function. Curiously, HIF-1α activity is suppressed by preventing the recruitment of p300, but HIF-2α activity is increased [113] **(Figure 10)**.

Definitely, HIF-α regulation is complex and involves many pathways yet to be discovered and many of those identified have not yet been fully elucidated. It is clear the key role of oxygen-dependent regulation and that the level of HIF-α expression is the result of the balance between both synthesis and degradation rates, determined by the net result of the above pathways.

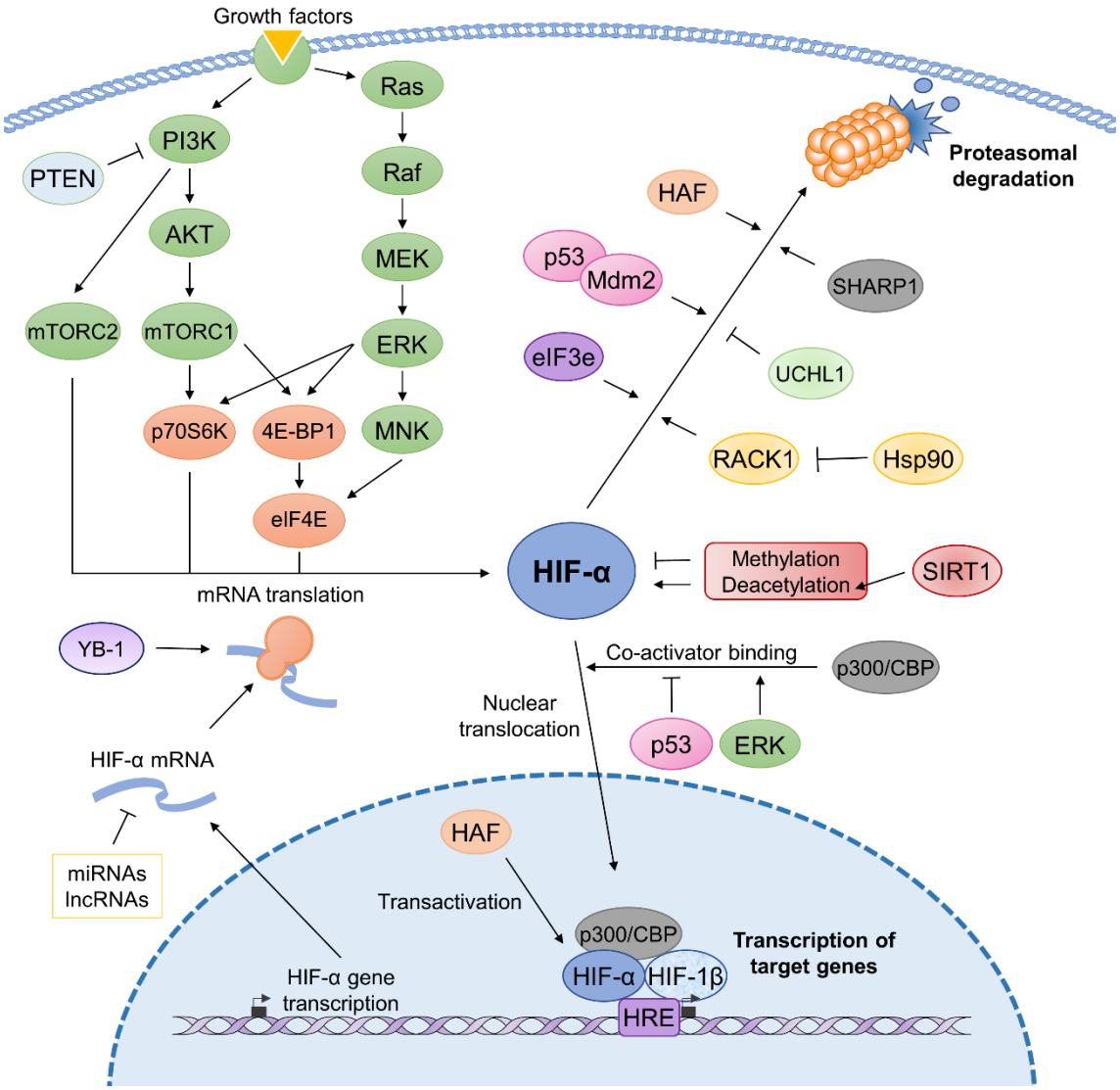

Figure 10. Oxygen-independent regulation of HIF-α subunits. HIF-α mRNA translation can be upregulated by YB-1 or by several growth factors that activate various signaling pathways, such as PI3K/AKT/mTOR and Ras/MAPK. In contrast, HIF-α mRNA can be inhibited by miRNAs and lncRNAs. Furthermore, HIF-α proteasomal degradation can be promoted in an oxygen-independent manner by numerous factors, including HAF, Mdm2 in a p53-dependent way, eIF3e, SHARP1, and RACK1, or inhibited by UCHL1 and Hsp90 (by competition with RACK1). Alterations in the methylation or acetylation status can modify HIF-α activity, for instance, SIRT1 promotes deacetylation. Stabilized HIF-α requires binding to the p300/CBP co-activator, which can be either hindered by p53 or improved by ERK. Finally, HAF may also facilitate the transactivation ability of HIF-α.

3.3 HIFs target genes in HCC and their functional contributions

HIF-1, HIF-2, and HIF-3 trigger the transcription of thousands of target genes that can be shared or specific, based on the target gene, the cell type, and the own expression of each HIF-α subunit in the cell [114].

Although HIF-1α and HIF-2α exhibit high homology (~48%), similar oxygen-dependent degradation and share overlapping target genes, both also regulate a set of exclusive targets that are concerned in unrelated processes, and remarkably, they may display even contrary effects [102,105,121]. This can be explained by the less sequence homology in the HIF-1α and HIF-2α transactivating domains N-TAD and C-TAD than the DNA-binding and heterodimerization domains bHLH-PAS [107]. Thus, HIF-1α is more implicated in endothelial cell proliferation, migration and vessel sprouting, while HIF-2α plays a more significant role in the regulation of vascular morphogenesis, integrity and assembly [121]. Moreover, HIF-1α is ubiquitously expressed across all tissues, while HIF-2α is only expressed by certain cell-types including hepatocytes, endothelial cells, cardiomyocytes, glial cells, kidney fibroblasts, type II pneumocytes and interstitial cells of the pancreas and duodenum [121,122]. Also, differences between time-dependent stabilization patterns have been informed: HIF-1α is activated in response to acute hypoxia, whereas HIF-2α plays a leading role in the chronic hypoxia response [122,123]. Interestingly, the depletion of HIF-1α increases the expression of HIF-2α in HCC cells by a reciprocal feedback mechanism, and this switch between both α-subunits gives the tumor a more aggressive phenotype under hypoxia [80,122–124].

HIF-1α and HIF-2α overexpression has been reported in liver diseases, such as NAFLD and HCC [106]. Both HIF-1α and HIF-2α have been shown higher expressed in HCC tissues than in adjacent tissues [106,108,125]. The high expression levels of HIF-1α or HIF-2α have been correlated with worse clinical outcomes, including invasion, metastasis, and poor prognosis in patients with HCC [106,108]. Even though some researches support the role of HIF-1α overexpression in prompting invasion, tumor recurrence and survival shortening of HCC patients [125,126], the relationship of HIF-1α with clinicopathological features and prognosis in HCC still remains inconclusive. Additionally, HIF-2α has shown to promote invasion and metastasis in HCC. However,

there is a lack of data on the association between HIF-2α overexpression and patient outcome in HCC, since the current results are controversial and inconsistent [127,128].

Notably, HIF-1- and HIF-2-induced genes display key roles in regulating different aspects of tumor biology, such as tumor survival and proliferation, metabolism, angiogenesis, invasion and metastasis as well as tumor cell death and chemo- and radio-resistance [103,105,106].

3.3.1 Cell proliferation and survival

HIF-1α targets and activates growth factors, including TGF-α and insulin-like growth factor 2 (IGF-2), to induce cell survival and proliferation [106,115]. Moreover, HIF-1α directly binds to the promoter of oncogenes implicated in HCC cell replication, such as forkhead box protein M1 (FOXM1) and aurora kinase A (AURKA), stimulating cell proliferation [103,104,106] **(Figure 11)**. Nevertheless, the role of HIF-2α in HCC remains unclear, since some studies report that HIF-2α overexpression is related to HCC progression, while other evidences suggest a tumor suppressor role for HIF-2α in HCC [106].

3.3.2 Metabolism

Unlike non-malignant tissues, tumor cells use more anaerobic glycolysis than oxidative phosphorylation to meet their energy requirements, even when oxygen is available, a phenomenon named the Warburg effect [106,108]. Only HIF-1α, but not HIF-2α, participates in metabolic reprogramming in HCC by its related target genes [108]. Many critical enzymes involved in glycolysis and glucose metabolism have been revealed to be direct HIF-1α targets in HCC cells, including enolase 1 (ENO1), glyceraldehyde-3-phosphate dehydrogenase (GAPDH), hexokinase 1 (HK1) and 2 (HK2), L-lactate dehydrogenase A chain (LDHA), pyruvate dehydrogenase kinase 1 (PDK1), phosphofructokinase (PFK) and phosphoglycerate kinase 1 (PGK1), among others [103,106,108]. For instance, the transcriptional action of HIF-1, induces the expression of mitochondrial-associated enzymes, like PDK1, which represses the tricarboxylic acid cycle and hence decreases oxidative phosphorylation and oxygen consumption of mitochondria [103,108]. HK2 and LDHA, both direct HIF-1α targets, enhance the

glycolytic adjustment from glucose to pyruvate [103]. Furthermore, HIF-1α contributes to glucose uptake through direct upregulation of glucose transporter 1 (GLUT1) and 3 (GLUT3) [103,108] **(Figure 11)**.

3.3.3 Angiogenesis

Elevated HCC vascularization results from the upregulation of angiogenic factors, and hypoxia is the major stimulus responsible for angiogenesis induction. As a well-characterized direct target of both HIF-1α and HIF-2α, VEGF is a potent pro-angiogenic factor that stimulate the proliferation and migration of endothelial cells required for new blood vessel formation. Aside from VEGF, hypoxia also stimulates angiogenesis through other different mechanisms: HIF-1α-mediated expression of ANG-2 and bone morphogenetic protein 4 (BMP4); HIF-2α-dependent expression of plasminogen activator inhibitor-1 (PAI-1) and stem cell factor (SCF); and by other direct targets of both HIFs such as EPO and PDGF [103,106] **(Figure 11)**.

3.3.4 Invasion and metastasis

Under a hypoxic environment, HIF-1α and HIF-2α play a major role in EMT through downregulation of E-cadherin and increase vimentin [106,129]. Both HIFs activate genes that are E-cadherin repressors, such as Snail, Twist-related protein 1 (Twist1) and transcription factor 3 (TCF3), leading to EMT promotion [101–103,106]. In addition, HIFs facilitate ECM degradation by metalloproteinases (MMPs), another key mechanism in tumor metastasis: both HIF-1α and HIF-2α are important transcription factors in upregulating the expression of MMP2 and MMP9 [102,106]. Further, the induction of the HIF-1α targets C-X-C motif chemokine 6 (CXCL6) and Rab11 family-interacting protein 4 (Rab11-FIP4), and the HIF-2α targets SerpinB3 and SCF, can promote the migratory and metastatic potentials of HCC cells [103] **(Figure 11)**.

3.3.5 Apoptosis and autophagy

Studies focused on the role of HIFs on apoptosis have reported controversial results, proposing that they can induce as well as antagonize this cell death mechanism. HIF-1α and HIF-2α are known to regulate both pro-apoptotic and anti-apoptotic proteins of the Bcl-2 family [115,121,124,130]. HIF-1α leads to cell growth

arrest and apoptosis via inducing the expression of target genes such as p53, Bcl-2/adenovirus E1B 19 kDa-interacting protein 3 (BNIP3), and caspase-3 [115,124]. BNIP3 is a pro-apoptotic member of the Bcl-2 family directly targeted by HIF-1α. HIF-1α is also involved in regulating mitochondrial autophagy (mitophagy) by upregulating expression of the Bcl-2 homology 3 (BH3)-only proteins BNIP3 and BNIP3-like protein X (NIX) [115,124,130]. In addition, p53 is considered the main inhibitor of proliferation as well as an inductor of apoptosis, and can be stabilized by HIF-1α. In contrast, other studies propose that HIF-1α can also act as anti-apoptotic factor in HCC by enhancing the expression of survivin and Bcl-2 [115]. The impact of HIF-2α on apoptosis has been less studied, but specifically points to an anti-apoptotic role [121,130] **(Figure 11)**.

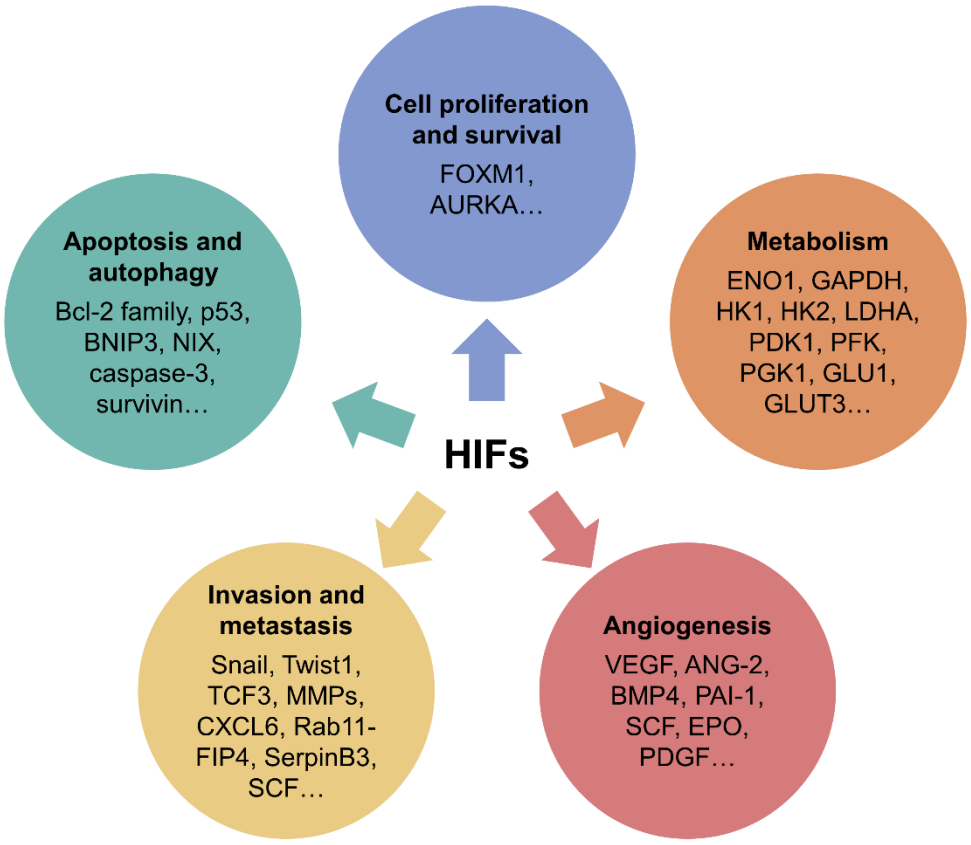

Figure 11. Role of HIFs in cancer progression: major target genes and processes controlled by HIF-1α and HIF-2α. HIF-1α and HIF-2α have a wide range of target genes that regulate different signaling pathways in cancer. In general, HIFs modulate cell proliferation and survival, metabolic reprogramming, angiogenesis, invasion and metastasis, as well as apoptosis and autophagy.

3.4 Hypoxia and HIFs on sorafenib resistance

The tumor microenvironment plays a crucial role in the onset and development of tumors. Anti-angiogenic drugs are responsible for tumor vessels shrinkage and decrease bloodstream, resulting in a shortage of oxygen and nutrients reaching the tumor. It is extensively recognized that hypoxia in solid tumors, such as HCC, is related to selection of more invasive and resistant clones, chemotherapy failure and worse prognosis. Hypoxic cells within solid tumors are extremely resistant to therapies, since their survival capability is improved owing to the adaptive response to hypoxia principally controlled by HIFs [77,123].

In HCC, hypoxia drives angiogenesis through HIF-1α activation and subsequent VEGF production [75,131–133]. Thus, the anti-angiogenic activity of sorafenib are derived from blockade of the HIF-1α/VEGF pathway [131,133,134]. Specifically, sorafenib prevents hypoxia-promoted HIF-1α protein synthesis, which leads to declined VEGF expression and reduced vasculature in HCC [131,134]. Nonetheless, there is a close correlation between the hypoxic microenvironment and acquired sorafenib resistance: the long-term anti-angiogenic effect of sorafenib treatment causes tumor starvation and following intratumoral hypoxia, which favors the selection of resistant cell clones adapted to oxygen deficiency, limiting the efficacy of this drug [75,118,135,136].

It has been described that hypoxia confers sorafenib resistance in RCC and myeloid leukemia cells [137–139]; and is responsible for the development of resistance to many other chemotherapeutic drugs in HCC cells, including cisplatin, doxorubicin, etoposide, SN38, and 5-fluorouracil (5-FU) [140–144]. Liang *et al.* [135], using an HCC subcutaneous tumor model in mice, reported that the sustained administration of sorafenib upregulates the HIF-1α protein levels and its transcriptional activity. Similarly, HCC tissues from sorafenib-resistant patients exhibits greater intratumor hypoxia and HIF-1α expression in comparison to untreated or sorafenib-sensitive HCCs [135]. HIF-1α protein stabilization is associated with sorafenib resistance by the enhanced expression of the multidrug resistance protein 1 (MDR1), VEGF and GLUT1 [135,145]. Moreover, galectin-1, a protein that modulates cell-cell and cell-matrix

interactions, has been suggested as a predictive marker of sorafenib resistance, being regulated by the AKT/mTOR/HIF-1α axis [146]. β-2 adrenergic receptor (ADRB2) signaling can modulate autophagy negatively in an AKT-dependent manner, which promotes the stabilization of HIF-1α and induces the reprogramming of glucose metabolism in HCC cells, favoring the acquisition of sorafenib resistance [147]. This implication of glycolysis in sorafenib resistance was supported by another research in which HIF-1α activation induces the expression of GLUT1 and HK2 to accelerate the glycolytic rate, allowing cell survival [148]. Moreover, mitophagy, a specific mitochondrial autophagy, is activated under hypoxia in HCC cells by the promotion of the mitophagy targets of HIF-1α, BNIP3 and NIX; mitophagy could exert a cytoprotective function on HCC cells and sorafenib cannot block this process [118] **(Figure 12)**.

Considering the feedback loop between HIF-1α and HIF-2α subunits, it can be assumed that sorafenib treatment may overexpress HIF-2α as consequence of the HIF-1α inhibition, enhancing sorafenib resistance and promoting a more aggressive HCC growth [75,122,123,136,149]. It has been confirmed that sorafenib upregulates HIF-2α by the hypoxic response switch from HIF-1α inhibition, contributing to sorafenib resistance by inducing the HIF-2α/TGF-α/EGFR pathway [149] and activating the expression of VEGF and cyclin D1 [122]. Moreover, Xu *et al.* [150] reported that sorafenib treatment improves HIF-2α accumulation and succeeding decrease of the androgen receptor (AR), which is associated with HCC progression and metastasis [150]. Another study found this feedback mechanism and showed that high HIF-2α levels positively modulates β-catenin/c-Myc expression in HCC cells, thus enhancing the proliferation involved in sorafenib resistance [136]. Zhu *et al.* [151] also supported that HIF-2α is involved in the hypoxia-mediated adaptation process of HCC cells against sorafenib. Hepatopoietin Cn (HPPCn) is a growth factor that leads to sorafenib resistance in HCC through the increase of HIF-2α levels and the promotion of cell growth and metastasis [151]. Moreover, another study reaffirmed that the overexpression of HIF-2α caused by sorafenib induces HCC invasion and metastasis via the downregulation of oxidoreductase HTATIP2 (TIP30) [152] **(Figure 12)**.

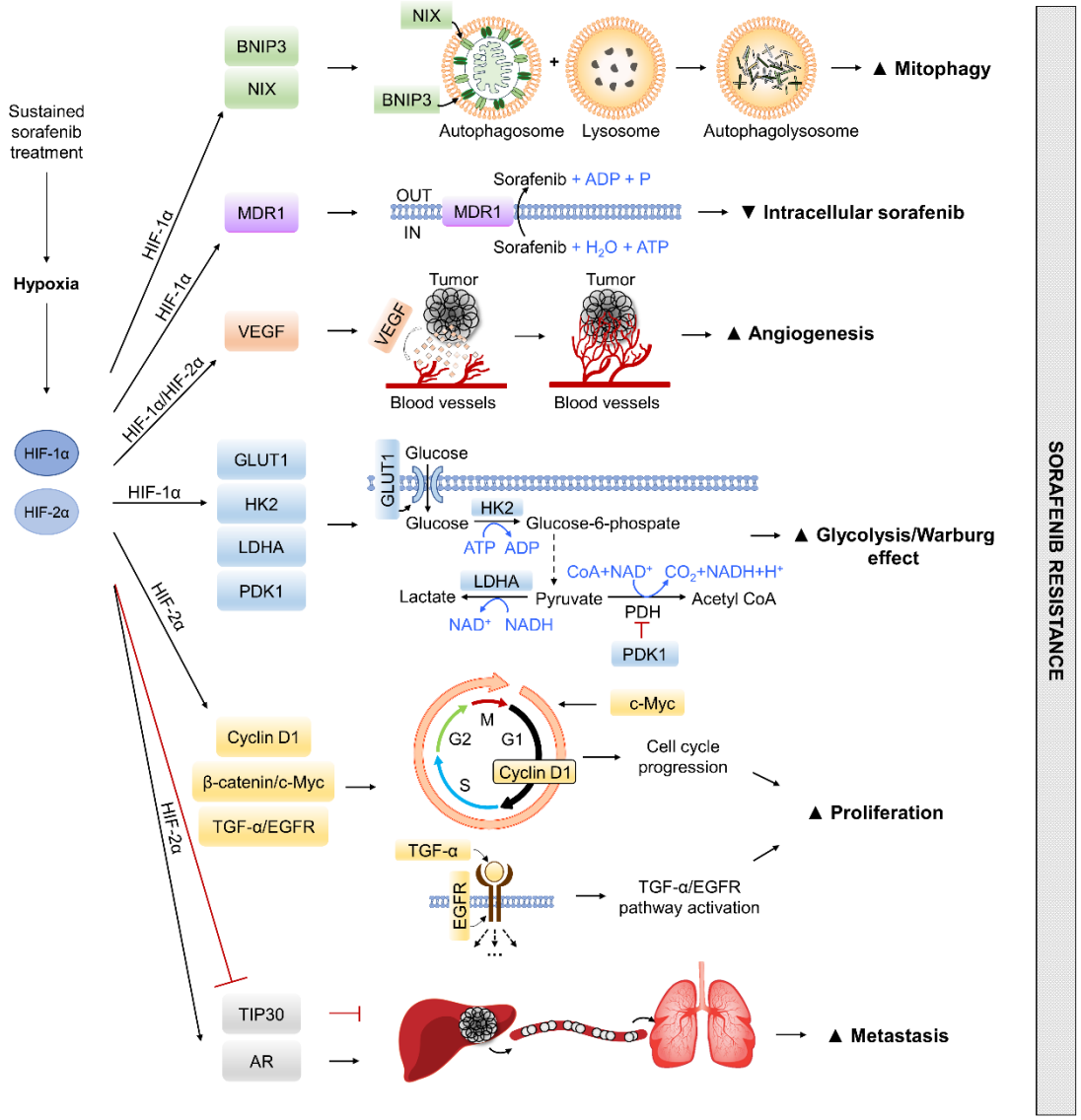

Figure 12. Mechanisms of sorafenib resistance related to hypoxia in HCC. Prolonged exposure to sorafenib promotes hypoxia and thereby stabilization of HIF-1α and HIF-2α. Both factors are involved in different signaling pathways and transcription of target genes that reduce intracellular accumulation of sorafenib and enhance mitophagy, angiogenesis, glycolysis, proliferation and metastasis as adaptive mechanisms in HCC cells, leading to sorafenib resistance.

Additionally to HIFs, hypoxia also upregulates the C-X-C motif chemokine 12 (CXCL12)/C-X-C chemokine receptor type 4 (CXCR4)/C-X-C chemokine receptor type 7 (CXCR7) chemokine axis, which can activate the ERK/MAPK and JAK/STAT signaling pathways, enabling tumor progression and promoting chemoresistance to sorafenib [77].

These evidences endorse the present relationship between the HIFs overexpression and the phenomenon of sorafenib resistance, suggesting that hypoxia and HIFs significantly affects sorafenib therapy [123].

4 Cell death by apoptosis

Cell death is an essential mechanism in development, homeostasis and integrity of multicellular organisms. The balance between cell proliferation and elimination is required to preserve the stability of physiological processes [153,154]. Cell death involves two well-defined mechanisms, programmed cell death (PCD) and necrosis. Necrosis is characterized as uncontrolled cell death by a nonspecific swelling of cells and their membrane organelles that promotes disruption of their integrity, leading to externalization of cell content and inflammatory processes in multicellular organisms. In contrast, PCD is formed by genetically programmed 'cellular suicide' programs in response to particular signals [154,155]. About 15 types of PCD are described and, the most common of which are apoptosis, autophagy, pyroptosis and programmed necrosis (necroptosis) [153,155–157].

Apoptosis, the most important and best-known form of PCD, is caused by the activation of a 'suicide' machinery within the cell in response to internal or external stress. Mechanism of action of apoptotic cell death is defined by chromatin condensation, DNA fragmentation, cell shrinkage, dynamic membrane blebbing, and loss of adhesion to ECM or to neighbor cells, which finally leads to cell death without provoking damage to adjacent cells [153,154,156,158]. Therefore, apoptosis is a protective mechanism against damaged or stressed cells by any agent to avoid the accumulation of non-functional cells in tissues, maintaining homeostasis [153,157,158]. Failure to regulate apoptosis allows the continued accumulation of mutations in cells that could lead to the development of many pathologies, including cancer, autoimmune diseases, or neurodegenerative disorders [153,157].

The different pathways that regulate apoptosis are complex and appear to be tissue-specific and agent-dependent [156]. On the one hand, the cell itself can promote apoptosis after damage is detected through various intracellular sensors, a process termed as the intrinsic pathway. Alternatively, apoptosis can occur from the interplay between immune cells and damaged cells, which is known as the extrinsic pathway [153]. After the activation of different intermediate molecules, both intrinsic and extrinsic pathways converge in the final execution pathway mediated by caspase

activation and cleavage of essential cellular components [157,158] **(Figure 13)**. In addition to these main apoptotic pathways, a third way has been described: the perforin/granzyme pathway, which is caspase-independent, specific to cytotoxic T lymphocytes and natural killer cells, and mediated by single-stranded DNA damage [156,159].

4.1 Intrinsic pathway of apoptosis

The intrinsic pathway, also known as the mitochondrial pathway of apoptosis, involves a diversity of intracellular stimuli that act on several targets within the cell [153,154,156]. This pathway depends on factors released by the mitochondria and is originated either from a positive or negative pattern. Negative signal arises from the absence of pro-survival signals such as cytokines, growth factors, and hormones in the cell environment. This leads to the activation of pro-apoptotic proteins that are ordinarily inhibited, initiating apoptosis. Nevertheless, the positive pattern is facilitated by direct exposure to environmental factors such as toxins, radiation, hypoxia, and viral infections, even though in some cases, hypoxia can promote cell survival [153,156].

The first step of mitochondrial apoptosis is regulated by proteins of the Bcl-2 family [158], which can be grouped in three major groups based on their pro- or anti-apoptotic function, as well as according to the Bcl-2 homology (BH) regions in their structure [160,161]. Anti-apoptotic members Bcl-2, such as Bcl-2-like protein 1 (Bcl-x_L), Bcl-2-like protein 2 (Bcl-w) and Mcl-1, contain four BH domains (BH1-4). Nonetheless, pro-apoptotic proteins are classified in two types: multi-domains members (such as Bcl-2-associated X protein (Bax) and Bak, that contain and share homology in the four BH domains), and the BH3-only proteins, also named apoptosis initiator group (which include Bcl-2-associated agonist of cell death (Bad), BH3-interacting domain death agonist (Bid), Bcl-2-like protein 11 (Bim), Bcl-2-interacting killer (Bik), Bcl-2-modifying factor (Bmf), Puma and phorbol-12-myristate-13-acetate-induced protein 1 (Noxa)) [160]. In absence of apoptotic stress, the anti-apoptotic proteins like Bcl-2 and Bcl-x_L form heterodimers with Bax and Bak (pro-apoptotic) to preserve the outer mitochondrial membrane (OMM) integrity and impede mitochondrial apoptosis [161].

Under presence of apoptotic stimuli, the expression of pro-apoptotic proteins and/or BH3-only proteins (apoptosis initiator) is improved, binding to pro-survival Bcl-2 proteins to release Bax and Bak from inhibition. Free Bax and Bak form oligomers that insert into OMM and produce OMM permeabilization (MOMP), leading to the release of cytochrome c from the intermembrane space of mitochondria into the cytoplasm [158,161] **(Figure 13)**.

The next step in mitochondrial apoptosis is the apoptosome formation [161]. In this way, the released cytochrome c binds to apoptotic protease-activating factor 1 (APAF-1) monomers, resulting in a conformational change in APAF-1 to expose a nucleotide binding that binds to deoxy ATP (dATP). This binding induces a further conformational modification in APAF-1, exposing both its recruitment and oligomerization domains, thus allowing APAF-1 monomers to assemble into a wheel-shaped homo-heptameric APAF-1 complex called apoptosome [153,161]. The apoptosome recruits and cleaves the initiator pro-caspase-9, and converts it to its active form caspase-9 [161] **(Figure 13)**.

Bax and Bak also cause the release of other mitochondrial proteins that act as secondary apoptosis mediators. Second mitochondria-derived activator of caspase (Smac)/ direct inhibitor of apoptosis-binding protein with low pI (DIABLO) and the serine protease high-temperature requirement protein A2 (Omi/HtrA2) provides a supplementary process for caspase activation by antagonizing inhibitors of apoptosis (IAPs) [153,158]. Smac/Diablo and Omi/HtrA2 assist the apoptosis initiation but, without cytochrome c release, inhibition of IAPs alone is not enough to initiate apoptosis [153]. On the other hand, apoptosis-inducing factor (AIF) and endonuclease G are also released. These pro-apoptotic proteins can induce caspase-independent cell death via chromatin condensation and nuclear DNA cleavage [153,157,158].

4.2 Extrinsic pathway of apoptosis

The extrinsic pathway, also termed as the death receptor pathway of apoptosis, triggers apoptosis by signaling through the interaction between ligands that belong to cytokines of the TNF superfamily and membrane-bound death receptors belonging to

the TNF receptor (TNF-R) superfamily [155,157]. Almost 40 ligand-receptor pairs have been defined. The most common ligand-receptor couples responsible for promoting extrinsic apoptosis are first apoptosis signal (Fas) ligand (FasL) that specifically binds to Fas receptor, TNF-related apoptosis-inducing ligand (TRAIL) that can bind to TRAIL receptors 1, 2, 3 and 4 (TRAIL-R1, TRAIL-R2, TRAIL-R3, and TRAIL-R4), and TNF-α interaction with TNF-R1 and TNF-R2 [155].

Upon ligand binding, active death receptors recruit and bind through their intracellular death domain to adapter proteins such as Fas-associated death domain (FADD) and TNF-R-associated death domain (TRADD). These adapter proteins also contain another protein interaction domain to bind with initiator pro-caspase-8 and pro-caspase-10. Then, a death-inducing signaling complex (DISC) is developed, promoting autocatalytic activation of pro-caspases and leading to activation of caspase-8 and caspase-10 initiating caspases to cause cell death [153,157,158,162]. Moreover, the activation of initiator caspases-8 and -10 also leads to the cleavage and myristoylation of cytoplasmic Bid protein, generating the active form truncated Bid (tBid) that is translocated to the mitochondria. tBid is able to activate Bax, contributing to the release of cytochrome c and apoptosis via the mitochondrial pathway. Therefore, Bid constitutes a common molecule between intrinsic and extrinsic pathways of apoptosis [155,157,162] **(Figure 13)**.

4.3 Execution phase

As shown in **Figure 13**, both extrinsic and intrinsic pathways converge in the final pathway of apoptosis. This execution phase begins with the activation of the executioner caspases (3, 6 and 7) by the initiator caspases (8, 9 and 10) [153,156,158]. Executioner caspases promote a cascade of events by stimulating endonucleases and proteases, which leads to the destruction of nuclear materials and cytoskeleton [156]. This results in cleavage of many substrates such as poly (adenosine diphosphate (ADP)-ribose) polymerase (PARP), as well as chromatin condensation, DNA fragmentation, degradation of nuclear and cytoskeletal proteins, etc., to orchestrate proteolytic dismantling of the cell. Finally, the dead cell components are encompassed in apoptotic bodies and the expression of ligands for phagocytic cells facilitates non-

inflammatory phagocytosis by surrounding cells, thus allowing their elimination [153,156].

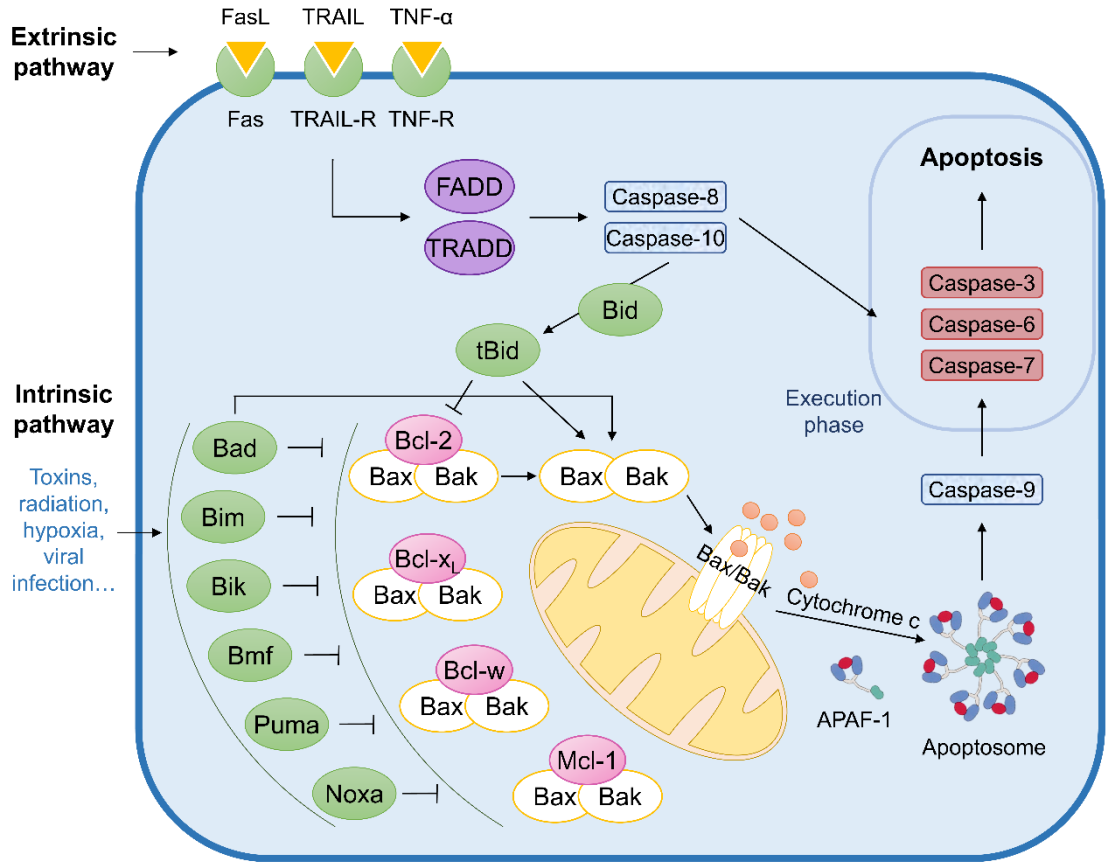

Figure 13. Extrinsic and intrinsic pathways of apoptosis. The onset of apoptosis is controlled by numerous interrelated processes. The extrinsic pathway is activated by external signals through ligands such as FasL, TRAIL or TNF-α, which act via death receptors Fas, TRAIL-R or TNF-R. Subsequently, caspase-8 and caspase-10 are activated through the adapter domains FADD and TRADD. Otherwise, the intrinsic pathway is initiated by different signals, primarily extracellular stimuli. Mitochondria are a key element of the intrinsic pathway and host an array of apoptotic factors. In first place, mitochondrial apoptosis is regulated by proteins of the Bcl-2 family. In the absence of apoptotic stress, anti-apoptotic proteins (Bcl-2, Bcl-x_L, Bcl-w and Mcl-1) form heterodimers with the pro-apoptotic proteins Bax and Bak to maintain the integrity of the OMM and prevent apoptosis. In the presence of apoptotic stimuli, the expression of pro-apoptotic proteins and/or the BH3-only initiator proteins (Bad, Bid, Bim, Bik, Bmf, Puma and Noxa) is enhanced, achieving their binding to pro-survival Bcl-2 proteins to release Bax and Bak from the blockade. Free Bax and Bak form oligomers that insert into OMM and produce MOMP, leading to the release of cytochrome c. Then, cytochrome c binds to APAF-1 monomers, resulting in the apoptosome formation, which recruits and cleaves the initiator pro-caspase-9 inducing its active

caspase-9 form. Both extrinsic and intrinsic pathways converge in the execution phase, which begins with the activation of the executioner caspases (3, 6 and 7) by the initiator caspases (8, 9 and 10). Executioner caspases promote a cascade of events that leads to the demolition of nuclear materials and cytoskeleton, dismantling the cell. Besides, the initiator caspases-8 and -10 also cause the cleavage and myristoylation of Bid, producing active tBid, which is translocated to the mitochondria where it activates Bax, contributing to the release of cytochrome c and apoptosis by the mitochondrial pathway. Hence, Bid is a mutual molecule of intrinsic and extrinsic pathways of apoptosis.

4.4 Apoptosis and sorafenib resistance

Dysregulation of cell death constitutes a key hallmark in tumorigenesis and tumor progression [161]. In cancer, aberrant apoptotic signaling allows cancer cells to escape apoptosis, which leads to uncontrolled proliferation and thereby tumor survival, therapy resistance and cancer recurrence. This resistance is a complex phenomenon that originates from the interactions of several molecules and signaling pathways [163].

In HCC, despite the fact that sorafenib exerts a pro-apoptotic effect, sustained treatment allows the development of mechanisms that induce apoptotic resistance and survival advantage of cancer cells [74,123]. Evasion of apoptosis by activation of anti-apoptotic proteins or/and downregulation of pro-apoptotic proteins has been associated with resistance to sorafenib [74]. Particularly, some studies have reported overexpression of Bcl-2 and Bcl-x_L [164–166], as well as a lower apoptotic rate in sorafenib-resistant samples from patients with HCC [135]. Interestingly, hypoxia and HIFs can promote alterations in this cell death process to regulate survival of tumor cells [115,121,124,130].

5 BNIP3

BNIP3 is an atypical member of the Bcl-2 family, which belongs to the pro-apoptotic protein subfamily with BH3-only domain, and is located in the OMM [167–169]. BNIP3 is highly expressed specifically in muscle, heart and liver [170]; and is closely related to hypoxic conditions, being directly activated by the HIF-1α factor by presenting the HRE in its gene promoter [169,170]. This mitochondrial protein mainly functions as a cell death regulator under hypoxia, being involved in various cell death processes, including apoptosis, necrosis, autophagy, and its specific form, mitophagy [171,172].

5.1 BNIP3 structure

The BNIP3 protein consists of 194 amino acids and is composed by different domains [168,172]. The NH_2-terminal region contains the microtubule-associated protein 1A/1B-light chain 3 (LC3)-interacting region (LIR) motif. LIR domain allows the interaction between the homodimer BNIP3 and LC3, anchored in the phagophore membrane, which leads mitochondria directly to the autophagosome for degradation [169,170,172,173]. Thus, the LIR motif mediates the activity of BNIP3 as mitochondrial autophagy initiator [172] **(Figure 14)**.

The NH_2-terminal region also has a proline, glutamic acid, serine, threonine (PEST) domain. These PEST sequences are flanked by histidine and arginine/lysine amino acid residues and are responsible for proteasome-mediated degradation [168,172]. Besides, there is a conserved cysteine residue, Cys64, towards the NH_2-terminus that establish a disulfide linkage in the homodimer encouraging its stability [168] **(Figure 14)**.

BNIP3 also presents the motif $L^{1}KKNSD^{6}W^{7}IWDW^{11}$ related to the BH3-only domain of the Bcl-2 family members. This motif contains highly conserved leucine residue at position 1 and aspartic acid at position 6 as other BH3 domains [167]. Nonetheless, this motif exhibits evolutionarily non-conserved tryptophan residues at positions 7 and 11 rather than aspartic or glutamic acid residues found in other BH3-only proteins [167,172]. These tryptophan residues have been related to a decreased

selectivity of interactions with pro-survival Bcl-2 proteins, weakening the pro-apoptotic ability of BNIP3 [172]. Consequently, BNIP3 appears to be an atypical member of the BH3-only subfamily [167]. Different studies support the apoptosis inducting effect of the BH3 domain of BNIP3. On the contrary, other reports show that the lack of the BH3-domain does not suppress the BNIP3 pro-apoptotic activity, so this domain is dispensable for cell death promotion, indicating that the main interaction with anti-apoptotic proteins is carried out via the transmembrane (TM) domain. Therefore, the role of the BH3 domain in cell death-promoting activity of BNIP3 is controversial [167,169,172]. In addition, BNIP3 has a highly 16 amino acid conserved domain (CD) just after the BH3 domain [168] **(Figure 14)**.

Finally, the COOH-terminal region of BNIP3 contains a TM domain (amino acids 164–184) in charge its mitochondrial localization, dimerization, and pro-death activity [168,172]. BNIP3 is anchored to the OMM by this TM domain, which is crucial for its functioning [168,172,173]. In addition to the mitochondrial localization of BNIP3, the COOH-terminal TM domain presents a glycine zipper AXXXG responsible for formation of stable dimers [168,173]. On the one hand, BNIP3 homodimerization is essential for its interaction with LC3 to promote mitochondrial autophagy [173]. On the other hand, the heterodimerization of BNIP3 with anti-apoptotic Bcl-2 proteins is necessary to induce apoptosis by cytochrome c release [172] **(Figure 14)**.

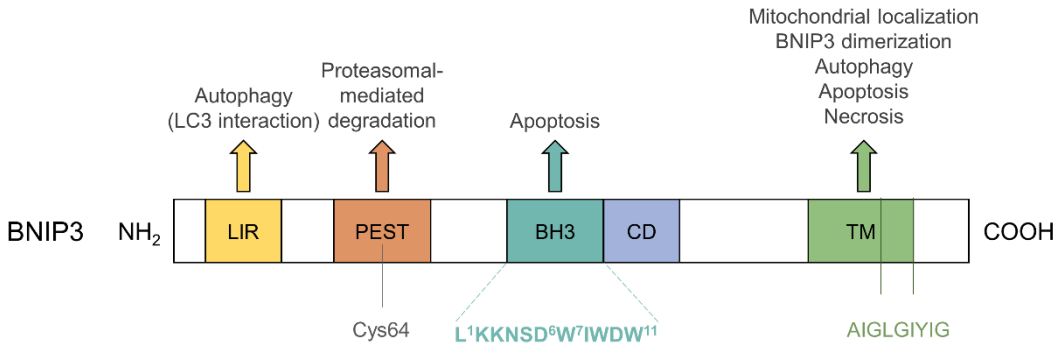

Figure 14. Domain structure of BNIP3 protein and its domain-dependent functions. The NH_2-terminal region is composed by the LIR domain that mediates the activity of BNIP3 as mitochondrial autophagy initiator, and the PEST sequence in charge of its proteasomal degradation. As BH3-only protein of the Bcl-2 family, BNIP3 also exhibits a

unique BH3 domain, responsible for part of BNIP3-mediated apoptosis. However, BNIP3 is an atypical member since motif $L^{1}KKNSD^{6}W^{7}IWDW^{11}$ related to the BH3-only domain contains evolutionarily non-conserved tryptophan residues at positions 7 and 11. Besides, BNIP3 has a conserved residue (Cys64) and a CD. At the COOH-terminal is located the TM domain, which allows for mitochondrial localization, dimerization, and pro-death activity of BNIP3. AIGLGIYIG represents the AXXXG glycine zipper motif that promotes dimer stability.

5.2 BNIP3 function

There is no a unique mechanism through which BNIP3 can induce necrosis, apoptosis, autophagy or mitophagy. In fact, the different mechanisms appear to depend on cell type and context [172,174].

BNIP3-induced cell death is controlled by both the BH3 domain and TM domain, in contrast with other BH3-only proteins, promoting **apoptosis and necrosis** [168]. In one way, upon activation, BNIP3 inserts into the OMM and causes the opening of a mitochondrial permeability transition pore (MPTP), loss of mitochondrial membrane potential (ΔΨm), ROS generation, and finally necrosis [174]. BNIP3 also can function as typical BH3-only proteins, binding to anti-apoptotic Bcl-2 family members located in the OMM to trigger Bax/Bak-dependent MOMP or directly activates Bax/Bak, to release cytochrome c and promote caspase-mediated apoptosis by the intrinsic pathway. This mechanism may also be performed by the TM domain [167–169]. In addition, BNIP3 may modulate endoplasmic reticulum-sarcoplasmic reticulum (ER-SR) Ca^{2+} stores. Enlarged ER-SR Ca^{2+} stores cause improved mitochondrial Ca^{2+} uptake, which in turn activates the MPTP, mitochondrial depolarization, and the release of caspase-dependent and -independent intermediaries of cell death [167,168]. However, BNIP3 may also function through interaction between the TM domain of BNIP3 and optic atrophy protein 1 (Opa1), a mitochondrial fusion protein, which causes disruption of Opa1 complexes and facilitates mitochondrial fission. This process, which is dependent on Bax or Bak, provokes mitochondrial fragmentation and apoptosis [167–169,175] **(Figure 15)**.

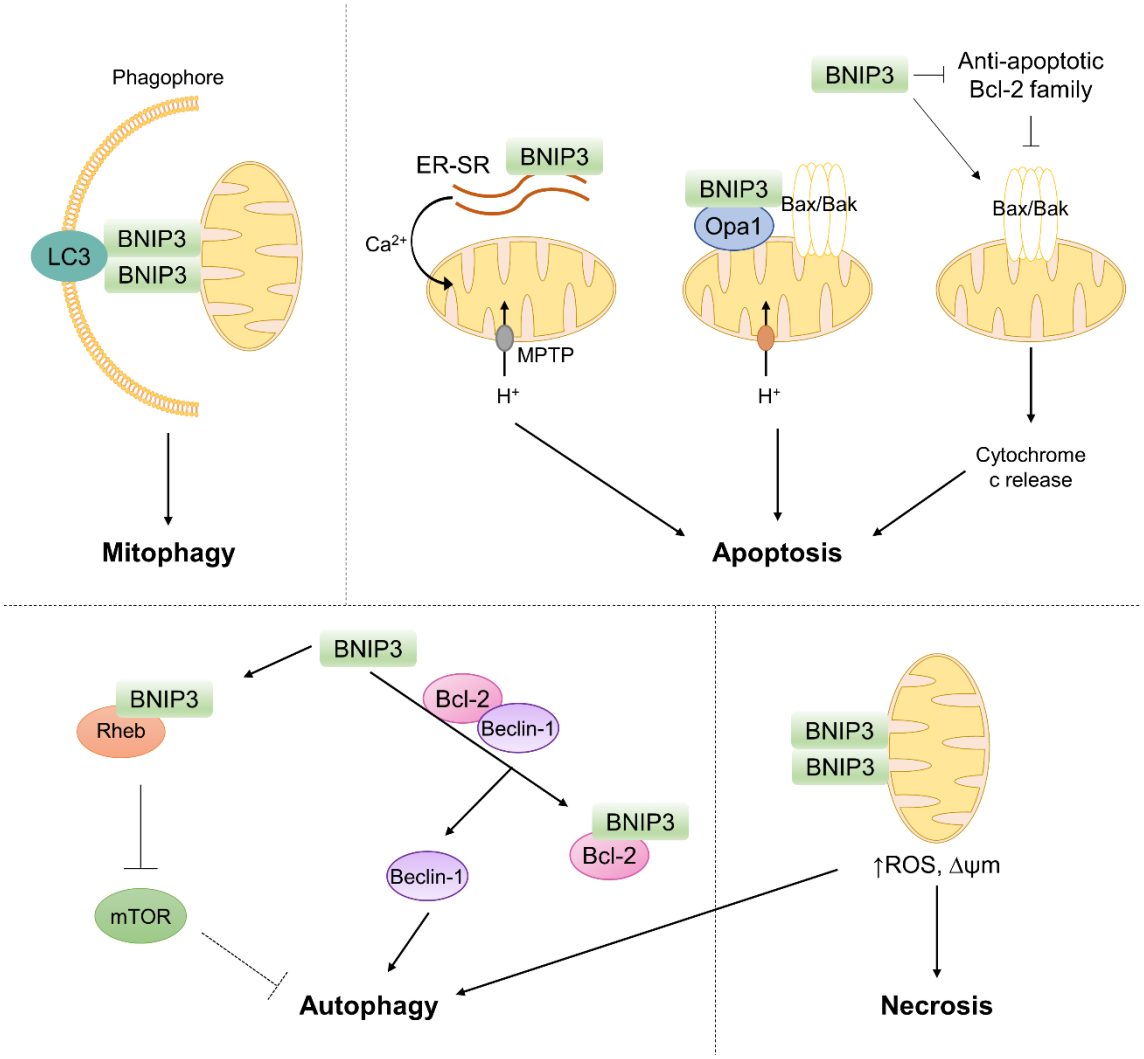

Figure 15. BNIP3-dependent mechanisms for induction of cell death and autophagy. BNIP3 can induce apoptosis by three different mechanisms: via binding to anti-apoptotic or pro-apoptotic (Bax and Bak) Bcl-2 proteins to trigger Bax/Bak-dependent MOMP, cytochrome c release and promote caspase-mediated apoptosis; alternatively, enhancing ER-SR Ca^{2+} stores to improve mitochondrial Ca^{2+} uptake, MPTP activation, and mitochondrial depolarization; or by interaction with Opa1, a process dependent on Bax or Bak, which facilitates mitochondrial fission. Alternatively, BNIP3 may promote necrosis through causing loss of ΔΨm and ROS generation. This process also can trigger autophagy. Other autophagy mechanisms include BNIP3 competition with Beclin-1 for binding to Bcl-2 that disrupts the Beclin-1-Bcl-2 complexes to release Beclin-1, and the binding and inhibition Rheb to block the inhibitory effect of mTOR. Finally, BNIP3 homodimers bind to LC3 and induce mitophagy-mediated by hypoxia.

Furthermore, although BNIP3 is not part of the core machinery of autophagy, is linked to the induction of **autophagy and mitophagy**, also by various mechanisms and in a context-dependent manner. These mechanisms are regulated by TM and LIR

domains [167,169,170,172,173]. As noted above, BNIP3 can promote mitochondrial depolarization and dysfunction leading to elevated ROS, which also may induce autophagy. Second, by challenging with Beclin-1 for binding to Bcl-2, BNIP3 can disrupt Beclin-1-Bcl-2 complexes to release Beclin-1, a central initiator of autophagy [167,169]. Another mechanism is the binding and inhibition of Ras homolog enriched in brain (Rheb) protein, an upstream activator of mTOR; thereby, by preventing mTOR activation, BNIP3 can trigger autophagy [167,169,173,175]. Finally, by homodimerization of BNIP3 in the OMM, BNIP3 dimer binds to LC3 and induce mitophagy-mediated by hypoxia through LIR domain [170,173,175] **(Figure 15)**. BNIP3-mediated auto- and mitophagy exhibit a dual role in cancer, acting as pro-death or pro-survival mechanisms in certain conditions [87,173,175].

These mentioned processes are also implicated in **EMT** and **metastasis**. Besides contributing to cell death and metastasis-associated processes, BNIP3 is capable to controlling diverse metabolic pathways, such as **mitochondrial bioenergetics**, **lipid metabolism** and **glycolysis**. Consequently, BNIP3 is a crucial mediator between cell death and survival [172].

5.3 Role and regulation of BNIP3 in cancer

BNIP3 plays an important role in carcinogenesis in different types of tumors. Some studies informed that BNIP3 overexpression was correlated with more aggressive tumor phenotype and poor prognosis, as well as a higher risk of recurrence in several types of cancer, including prostate, lung, cervical, and breast carcinomas [176–179]. On the contrary, decreased mRNA and protein levels of BNIP3 were associated with poor outcomes in other reports on leukemia, RCC, pancreatic, colorectal and HCC tumors [171,180–190]. Actually, the loss of BNIP3 expression contributed to therapy resistance and a worse prognosis for patients with pancreatic cancer [183].

BNIP3 is a strongly hypoxia-induced stress sensing protein. Despite BNIP3 is a direct target of HIF-1 as contains HRE and is implicated in hypoxia-induced cell death, other transcription factors act as regulators of BNIP3 expression, such as pleiomorphic

adenoma-like protein 2 (PLAGL2), Forkhead box protein O3 (FOXO3), E2F transcription factor 1 (E2F1), and NF-κB [168,175,191]. Moreover, the activity of the BNIP3 promoter is also modulated by epigenetic modifications, being commonly silenced by methylation and histone deacetylation [168,172,175,191]. These modifications have been described in different types of cancer, and play a key role in tumor development. For instance, the BNIP3 promoter is aberrant methylated in colorectal and pancreatic cancer, abrogating hypoxia-inducible cell death by silencing BNIP3 [171,182,184,185,190]. Alternatively, BNIP3 expression is suppressed by histone deacetylation in RCC [181]. In both situations, low BNIP3 levels lead to cell death resistance that favors the survival of tumor cells [172].

Introduction and aims

HCC constitutes the major primary liver cancer, which currently represents the sixth most prevalent malignancy and the third cause of cancer-related mortality worldwide. The high mortality rate of HCC is due to the difficulty of early diagnosis and the lack of curative treatments for the advanced stage of this type of tumor, where most cases are diagnosed, which leads to a worse prognosis of this pathology. Moreover, HCC exhibits a high recurrence rate after treatments.

HCC is a highly vascularized tumor; nonetheless, the tumor vasculature is chaotic and inefficient, leading to intratumoral hypoxia. Hypoxia is a common feature of solid tumors and, although initially supposes a stress, it can trigger adaptive changes that allow tumor cells to survive. Accordingly, hypoxia has been associated with tumor aggressiveness, recurrence, selection of more invasive clones, resistance to therapies, and poor clinical outcomes. Hypoxia-mediated response is carried out mainly by HIF-1α and HIF-2α, key transcription factors on modulation of expression of several genes involved in cell proliferation, evasion of cell death, metabolic reprogramming, angiogenesis, invasion and metastasis.

Furthermore, the treatment landscape in advanced stages of HCC is based on sorafenib, the first drug approved for this purpose. Sorafenib is a multi-TKI drug that exerts anti-proliferative, anti-angiogenic and pro-apoptotic activities against HCC cells. Despite its effectiveness in prolonging the survival of HCC patients, sensitivity to sorafenib is reduced after long-term exposure owing to the emergence of resistant HCC cells by different adaptive mechanisms. In fact, sustained anti-angiogenic activity of sorafenib promotes intratumoral hypoxia.

Considering the above data, the main objective of the present dissertation was to study the significance of HIF-1α or HIF-2α overexpression on the prognosis and clinicopathological features of patients with HCC, as well as the relationship between hypoxia-mediated response and chemoresistance using an *in vitro* model of HCC with acquired resistance to sorafenib.

For this, the following specific aims were proposed:

First

To evaluate the association of high expression of HIF-1α and HIF-2α with survival-related parameters in HCC patients subjected to surgical resection by means of a systematic review with meta-analysis.

Second

To meta-analyze the correlation between the overexpression of the HIF-1α and HIF-2α proteins and several clinicopathological features in patients with HCC.

Third

To characterize the growth dynamics and proliferation of HepG2S1 and HepG2S3 sorafenib-resistant cells in comparison with the parental HepG2 cell line sensitive to this drug.

Fourth

To assess the protein expression and regulation of the main intermediaries of the hypoxia-mediated response, HIF-1α and HIF-2α, between resistant and parental sensitive cell lines.

Fifth

To determine the status of apoptotic cell death among parental sensitive and resistant cells to sorafenib, and the possible involvement of HIF-1α and HIF-2α expression on the survival capacity of resistant HepG2S1 and HepG2S3 cells.

Sixth

To analyze the expression and regulation of the key apoptotic mediator under hypoxic conditions, BNIP3, in the resistant phenotype.

Material and methods

The methodology employed in the present work is divided into two parts: systematic review with meta-analysis and *in vitro* study.

1 Workspace

The present Doctoral Thesis has been carried out at the Institute of Biomedicine (IBIOMED) of the University of León. In addition, confocal microscopy analyses were performed at the Microscopy Service of the University of León.

2 Systematic review with meta-analysis

A meta-analysis is a statistical technique for combining the results obtained from multiple studies that attempt to answer the same research question. The purpose of the meta-analysis is to provide one unified conclusion by integrating all the findings [192,193].

In the meta-analysis performed in this PhD Thesis, we primarily aimed at evaluating the prognostic significance of HIF-1α or HIF-2α expression in HCC patients who underwent surgical resection, regarding OS and disease-free survival (DFS)/recurrence-free survival (RFS). Our second goal was to examine the relationship of HIF-1α or HIF-2α expression with several tumor and patient characteristics.

This meta-analysis was accomplished according to the Preferred Reporting Items for Systematic Reviews and Meta-Analyses (PRISMA) guidelines (Supplemental Table 1) [194,195]. Furthermore, the protocol design was previously recorded in the International Prospective Register of Systematic Reviews (PROSPERO) (National Institute for Health Research (NIHR), York, UK) (https://www.crd.york.ac.uk/prospero/) with the registration code CRD42020191977.

2.1 Search strategy

To assess the role of HIFs expression in HCC patients, a comprehensive systematic literature search was carried out in Embase, Cochrane, PubMed, Scopus and Web Of Science (WOS) databases, with a completion date of May 31st, 2020. All eligible studies were identified using the following search terms ("HCC" OR

"hepatocarcinoma" OR "hepatocellular carcinoma") AND ("HIF" OR "hypoxia-inducible factor") in each database, as reported in **Table 2**.

Table 2. Search strategy for each database (until May 31st, 2020 included).

DATABASE	SEARCH STRATEGY
Cochrane Library	(("HCC" OR "hepatocarcinoma" OR "hepatocellular carcinoma") AND ("HIF" OR "hypoxia-inducible factor")):ti,ab,kw
Embase	('hcc' OR 'hepatocarcinoma' OR 'hepatocellular carcinoma') AND ('hif' OR 'hypoxia-inducible factor')
PubMed	("HCC"[All Fields] OR "hepatocarcinoma"[All Fields] OR "hepatocellular carcinoma"[All Fields]) AND ("HIF"[All Fields] OR "hypoxia-inducible factor"[All Fields])
Scopus	TITLE-ABS-KEY (("HCC" OR "hepatocarcinoma" OR "hepatocellular carcinoma") AND ("HIF" OR "hypoxia-inducible factor"))
WOS Core Collection	TS=(("HCC" OR "hepatocarcinoma" OR "hepatocellular carcinoma") AND ("HIF" OR "hypoxia-inducible factor")) *Indexes=SCI-EXPANDED, SSCI, A&HCI, CPCI-S, CPCI-SSH, BKCI-S, BKCI-SSH, ESCI, CCR-EXPANDED, IC Timespan=All years*

2.2 Eligibility criteria

In order to be included, studies had to meet the following inclusion criteria: (1) patients with a distinctive diagnosis of HCC by pathology; (2) expression of HIF-1α or HIF-2α protein determined using immunohistochemistry (IHC); (3) samples obtained through surgical resection; (4) relationship between HIF-1α or HIF-2α expression levels in HCC and survival-related or clinicopathological parameters was examined; (5) an adequate statistical methodology was used.

In the same way, any study that met the following exclusion criteria was omitted: (1) studies conducted only in preclinical models; (2) reviews, case reports, letters, book chapters or meeting communications; (3) samples without intratumoral tissues, or involving only paracarcinoma tissues; (4) the detection method was different from IHC; (5) studies in which the required data were not provided and could not be estimated; (6) articles without full-text in English.

2.3 Data collection and quality assessment

The full-text of selected studies was exhaustively analyzed to confirm eligibility, evaluate quality, and extract applicable data.

The Newcastle-Ottawa scale (NOS) was employed to determine the quality of the selected studies, with total NOS total scores ranging from 0 to 9 [196]. Those studies scoring ≥5 were considered as high-quality studies; otherwise, studies were regarded to have a low-quality and were not included in the quantitative synthesis.

The baseline characteristics of each included study comprehending study (first author and reference), year of publication, sample size, sample size based on gender, clinical intervention, age range, mean/median age, study quality (NOS score), method to measure HIF expression, type of survival analysis, source of HR data, definition of high HIF expression, and number of patients with high HIF-1α or HIF-2α expression, were recorded in **Table 3**.

Moreover, in Supplemental Table 2 the antibodies and the staining procedure used for the IHC of HIFs in each of the included articles were collected.

To perform the statistical analysis, HR and 95% CI for OS, DFS/RFS and time to recurrence (TTR) were extracted. OS was calculated from the medical intervention date until the last follow-up visit or the patient's death. DFS, RFS and TTR were defined as the period from the intervention date until the last follow-up or when tumor recurrence was diagnosed. The Parmar method was employed to calculate HR and 95% CI when direct data were not detailed in the primary study [197]. For the clinicopathological features, we collected the number of patients with high and low expression of HIF-1α or HIF-2α for the two comparative conditions of each feature. Specific thresholds or cut-off values were required to be established for some parameters. The comparative conditions and the cut-off values used are detailed in **Table 4**. These data allow the calculation of the odds ratio (OR) and 95% CI necessary for the statistical analysis.

Table 3. Baseline characteristics of included articles.

Study (first author and reference)	Year	Sample size	Sample size (M/F)	Intervention	Age range	Mean/ median age	Study quality (NOS score)	HIF-1α measurement method	Survival analysis	HR source	High HIF-1α definition	Number of patients with high HIF-1α
Huang *et al.* [198]	2005	36	32/4	Resection	19-77	45.90	6/9	IHC	OS	Estimated	Positive staining[a]	24
Wada *et al.*[199]	2006	60	45/15	Resection	44-79	63	6/9	IHC	DFS	Reported	>1% nuclear staining and/or strong cytoplas-mic staining	7
Xie *et al.* [200]	2008	72	59/13	Surgical resection	23-71	50.57	7/9	IHC	OS/DFS	Reported	III and IV[b]	37
Dai *et al.* [201]	2009	110	95/15	Hepatectomy	28-75	52.40	7/9	IHC/qRT-PCR	OS/DFS	Reported	III and IV[b]	39
Liu *et al.* [202]	2010	200	169/31	Radical resection	NR	NR	7/9	IHC	OS/TTR	Reported	>50% with nuclear staining	126
Xiang *et al.* [203]	2011	309	262/47	Curative resection	NR	NR	7/9	IHC	NR	NR	≥10% nuclear staining	85
Li *et al.* [204]	2012	35	30/5	Curative hepatectomy	34-68	50±9.19	5/9	IHC	NR	NR	Positive staining[c]	28
Xia *et al.* [205]	2012	406	331/75	Curative resection	NR	51.10	7/9	IHC	OS/TTR	Estimated	4-5 (+) or 6-7 (++)[d]	212
Xiang *et al.* [206]	2012	69	61/8	Curative resection	NR	NR	7/9	IHC	OS/RFS	Reported	≥10% nuclear staining	30
Cui *et al.* [207]	2013	55	34/21	Surgery	20-73	41	7/9	IHC	OS	NEP	3 (moderate staining) and 4-6 (strong staining)[e]	30

Ma *et al.* [208]	2013	207	156/51	Resection	23-80	57	6/9	IHC	NR	NR	≥4[f]	147
Wang *et al.* [209]	2014	45	34/11	Hepatectomy	36-78	NR	6/9	IHC/qRT-PCR	OS	NEP	≥3[g]	32
Yang *et al.* [210]	2014	126	110/16	Surgical resection	19-66	48.80	7/9	IHC/WB/qRT-PCR	CS/DFS	Estimated	III and IV[b]	72
Huang *et al.* [211]	2015	47	35/12	Surgery	33-74	53	6/9	IHC	NR	NR	≥10% cytoplasmic staining	19
Li *et al.* [212]	2015	102	87/15	Hepatectomy	NR	NR	6/9	IHC	OS/DFS	Estimated	2-4[h]	64
Srivastava *et al.* [213]	2015	179	142/37	Curative hepatectomy	NR	57.50	5/9	IHC	OS/RFS	Reported	III and IV[b]	108
Zhao *et al.* [214]	2015	97	NR	Surgical resection	NR	NR	5/9	IHC	CS	Estimated	3-6[i]	63
Tang *et al.* [215]	2016	143	130/13	Curative resection	21-70	49.47	6/9	IHC	CS/TTR	Estimated	Scores evaluated by software based on the percentage of positively stained cells and the staining intensity	72
Wang *et al.* [216]	2017	201	169/32	Hepatectomy	NR	NR	6/9	IHC	CS	Estimated	≥4[j]	94
Dai *et al.* [217]	2018	90	84/6	Curative hepatectomy	13-81	54	6/9	IHC	OS/DFS	Reported	2 and 3[b]	39
Tian *et al.* [218]	2018	65	38/27	Surgery	25-77	46.50± 2.80	6/9	IHC/WB	NR	NR	>3[k]	30
Wang *et al.* [219]	2018	419	313/106	Surgery	NR	NR	7/9	IHC	OS	Reported	≥30%	223 (6 missing)

Zou *et al.* [220]	2018	138	116/22	Surgery	NR	NR	6/9	IHC/qRT-PCR/WB	CS/TTR	Estimated	Optimal cut-off point of the relative integrated optical densities based on patients' outcome	73
Gong *et al.* [221]	2019	137	115/22	Primary surgical resection	NR	NR	7/9	IHC	OS/TTR	Estimated	≥6[l]	68
Wu *et al.* [222]	2019	119	NR	Curative resection	NR	NR	5/9	IHC	OS	Estimated	≥6[l]	67
Zhou *et al.* [223]	2020	90	74/16	Surgery	NR	NR	2/9	IHC	OS	NEP	NR	NR
Qian *et al.* [224]	2020	111	NR	Surgery	NR	NR	5/9	IHC	OS	Estimated	>2[f]	57 (2 missing)
Study (first author and reference)	**Year**	**Sample size**	**Sample size (M/F)**	**Intervention**	**Age range**	**Mean/ median age**	**Study quality (NOS score)**	**HIF-2α measurement method**	**Survival analysis**	**HR source**	**High HIF-2α definition**	**Number of patients with high HIF-2α**
Bangoura *et al.* [225]	2004	97	76/21	Resection	34-78	61.40± 8.90	6/9	IHC	NR	NR	++ (dark brown)	31
Bangoura *et al.* [226]	2007	315	260/55	Curative surgical resection	46-79	60.80	7/9	IHC	CS	Estimated	positive staining[m]	219
Sun *et al.* [227]	2013	246	198/48	Curative resection	NR	NR	6/9	IHC/WB/qRT-PCR	OS	Reported	>50%	118
Yang *et al.* [210]	2014	126	110/16	Surgical resection	19-66	48.80	7/9	IHC/WB/qRT-PCR	CS/DFS	Estimated	III and IV[b]	17

Yang *et al.* [228]	2016	206	177/29	Radical resection	31-84	57.20	7/9	IHC/WB	OS/RFS	Reported	>50%	67
Jiang *et al.* [229]	2018	84	70/14	Curative surgery	NR	NR	7/9	IHC/WB/qRT-PCR	NR	NR	≥4[n]	34
Chen *et al.* [230]	2019	139	116/23	Hepatectomy	NR	NR	7/9	IHC/WB/qRT-PCR	OS/DFS	Estimated	Median value of final scores (product of the percentage of stained cells by the staining strength) as a cut-off	67
Cao *et al.* [231]	2020	328	NR	Surgery	NR	NR	5/9	IHC	OS	NEP	3-9[j]	NR

CS, cumulative survival; F, female; M, male; NEP, no estimation possible; NR, not reported; qRT-PCR, quantitative reverse transcription-polymerase chain reaction; WB, Western blot.

[a]The sum of sections with weak and strong staining

[b]Nuclear staining in 10–50% of cells and/or distinct/moderate cytoplasmic staining (III or 2), and nuclear staining in >50% of cells and/or strong cytoplasmic staining (IV or 3)

[c]The sum of cases with weak (10%-25%), moderate (26%-50%) and strong staining (>51%)

[d]Final scores were assessed by the sum of the intensity (0, negative; 1, weak; and 2, strong), and the staining extent based on the percentage of positive tumor cells (0, negative; 1, 1–25%; 2, 26–50%; 3, 51–75%; and 4, 76–100%)

[e]Final scores were assessed by the sum of the intensity (0, negative; 1, weak; 2, intermediate; 3, strong), and the extent of immunoreaction (0,0%; 1, <5%; 2, 5–50%; and 3, >50%)

[f]Final scores were assessed by multiplying the result of the percentage of positive cells (≤5%, 0; -25%, 1; -50%, 2; -75%, 3; >75%, 4) by the staining intensity (colorless, 0; pale yellow, 1; deep yellow and brownish red, 2; sepia, 3)

[g]Final scores were assessed by the sum of the cytoplasmic staining degree (0, no or negligible staining; 1, pale yellow staining; 2, brown-yellow staining; 3, brown staining) and the punctuation obtained based on the percentage of positively stained cells (0, <5%; 1, 5-25%; 2, >25-50%; and 3, >50%)

[h]Final scores were assessed by determining the percentage of immunoreactive tumor cells (0, 0%; 1, 1-25%; 2, 26-50%; 3, 51-75%; 4, 76-100%)

[i]Final scores were assessed by the sum of the positivity extent (0, <10%; 1, <25%; 2, <50%; 3, >50%) and the staining intensity (0, no appreciable; 1, barely detectable; 2, readily visible; 3, dark brown staining)

[j]Final scores were assessed by multiplying the positivity extent (0, <10%; 1, <25%; 2, <50%; 3, >50%) by the staining intensity (0, no appreciable; 1, barely detectable; 2, readily visible; 3, dark brown staining)

[k]Final scores were assessed by multiplying the degree of staining (negative control, 0; light yellow, 1; tan, 2; sepia, 3) by the scoring of the positive cells proportion (≤10%, 1; 11%-50%, 2; 51%-75%, 3; >75%, 4)

[l]Final scores were assessed by multiplying the stained area (1, 1-25%; 2, 26-50%; 3, 51-75%; 4, 76-100%) by the staining intensity (0, 1, 2, or 3)

[m]More than 65% of cells were stained intensely (+++) or moderately (++) or weakly (+)

[n]Final scores were assessed by multiplying the results of the percentage (0, <10%; 1, 10-30%; 2, 31-60%; 3, >61%) and the intensity (0, lack of any immunoreactivity; 1, light-yellow; 2, yellow-brown; and 3, brown) of immune-staining cells

Table 4. Comparative conditions and cut-off values used to evaluate the possible correlation between HIF-1α or HIF-2α and clinicopathological features of patients with HCC.

Clinicopathological feature	Comparative conditions	Cut-off values
HIF-1α		
AFP	High *vs.* low levels	20 ng/ml 400 ng/ml
Age	Older *vs.* younger	50 years 60 years
Albumin	High *vs.* low levels	35 U/L
ALT	High *vs.* low levels	40 U/L 80 U/L
BCLC staging	BCLC B+C *vs.* BCLC A	
Bilirubin	High *vs.* low levels	1 µmol/L
Capsule formation	Positive *vs.* negative	
Capsule infiltration	Positive *vs.* negative	
Child-Pugh score	B *vs.* A	
Cirrhosis	Positive *vs.* negative	
Distant metastasis	Positive *vs.* negative	
Edmondson grading	III-IV *vs.* I-II	
Gender	Male *vs.* female	
Hepatitis B	Positive *vs.* negative	
Hepatitis C	Positive *vs.* negative	
Histological grade	Moderate/poor *vs.* well differentiated	
Intrahepatic metastasis	Positive *vs.* negative	
Lymph node metastasis	Positive *vs.* negative	
TNM staging	II-III *vs.* I III *vs.* I-II III-IV *vs.* I-II	
Tumor differentiation	Moderate/poor (III-IV) *vs.* well differentiated (I-II)	
Tumor number	Multiple *vs.* single	
Tumor size	High *vs.* low size	3 cm 5 cm
Vascular invasion	Positive *vs.* negative	
Vasculogenic mimicry	Positive *vs.* negative	
HIF-2α		
AFP	High *vs.* low levels	400 ng/ml
Age	Older *vs.* younger	50 years
Capsule formation	Positive *vs.* negative	
Capsule infiltration	Positive *vs.* negative	

Cirrhosis	Positive *vs.* negative	
Edmondson grading	III-IV *vs.* I-II	
Gender	Male *vs.* female	
Hepatitis B	Positive *vs.* negative	
Histological grade	Moderate/poor *vs.* well differentiated	
Necrosis	Positive *vs.* negative	
TNM staging	III-IV *vs.* I-II	
Tumor number	Multiple *vs.* single	
Tumor size	High *vs.* low size	5 cm
Vascular invasion	Positive *vs.* negative	

2.4 Statistical Analysis

The STATA software version 16 (Stata Corporation, College Station, TX, USA) was used to analyze the possible correlation of HIF-1α or HIF-2α expression with prognosis and several clinicopathological features of HCC patients.

The outcome of HIFs expression on HCC was measured in two steps. On the one hand, we pooled the OS and DFS/RFS by HR and 95% CI to determine the overall value that examine the association between HIF-1α or HIF-2α and HCC prognosis. On the other hand, the strength of correlation between HIF-1α or HIF-2α overexpression and each clinicopathological feature was tested by estimating OR with 95% CI. In both situations, HR or OR with the corresponding 95% CI were combined across studies and overall effect size was calculated and represented by forest plot. Global HR>1 and OR>1 suggested a raised risk of worse prognosis and a higher incidence on the feature considered, respectively, related to the overexpression of the corresponding HIF. These correlations were statistically significant when $p<0.05$.

Moreover, heterogeneity across studies was checked through the chi-square-based Q-test and I^2 statistic. I^2 statistic, a quantitative measure of inconsistency across studies range from 0% (no detected heterogeneity) to 100% (maximal heterogeneity). When Q-test p-value<0.1 or $I^2 \geq 50\%$ was considered significant and substantial heterogeneity. Accordingly, the Restricted Maximum Likelihood (REML) method as the random-effect model was applied when heterogeneity was found by at least one test. Otherwise, the fixed-effects model with Inverse Variance (IV) method was employed.

To explore possible heterogeneity sources, we performed subgroup analyses based on sample size, NOS score, follow-up time and median age. Other parameters such as HIF antibody used or gender were considered to examine subgroups, but data was not reported in all studies.

Finally, we examined the presence of publication bias by funnel plot and Egger's test. When funnel plot was asymmetric and Egger's p-value<0.05, significant publication bias was confirmed. Then, trim-and-fill method was used to adjust the number of studies and estimate a corrected overall effect size, allowing to determine whether publication bias influenced the robustness of the pooled results.

3 Experimental *in vitro* study

3.1 Cell culture and treatments

To carry out the *in vitro* study of the relationship between resistance to sorafenib and hypoxia-mediated response in HCC, we employed the human HCC cell line HepG2 obtained from the American Type Culture Collection (ATCC) (Manassas, VA, USA); and two HepG2-derived cell lines which undergo acquired resistance to sorafenib, named HepG2S1 and HepG2S3, which were generated by the group from KU Leuven University (Belgium) [88] **(Figure 16)**.

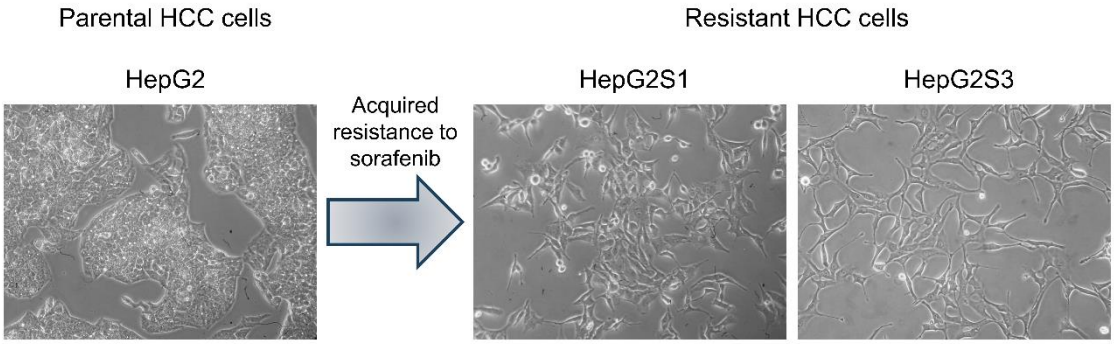

Figure 16. Optical microscopy images of the different cell lines employed: parental cell line HepG2, and sorafenib resistant cell lines HepG2S1 and HepG2S3. Magnification: 10X.

3.1.1 Development of cell lines with acquired resistance to sorafenib

The first step in the development of resistant cell lines was to determine the half maximal inhibitory concentration (IC_{50}) for HepG2 cells exposed to sorafenib (Bayer HealthCare, Leverkusen, Germany). For this, cells were seeded in a 96-well plate and treated with a wide range of doses of sorafenib. After 72 h, cell viability was evaluated by 2,3-bis (2-methoxy-4-nitro-5-sulfophenyl)-5-[(phenylamino) carbonyl]-2H-tetrazolium hydroxide (XTT) assay as reported by van Malenstein *et al*. [88].

HepG2 cells were then cultured in 6-well plates at a density of 7.5×10^4 cells/well and incubated with sorafenib concentrations just below their IC_{50}. During the following weeks, the sorafenib dose was slowly increased with 0.25 µM every time. After 5-7 months, the first HepG2 cell line resistant to sorafenib, HepG2S1, was

developed. The process was repeated obtaining a new HepG2-derived resistant line, HepG2S3 [88].

3.1.2 Cell culture conditions

Cells were grown in monolayer using Dulbecco's Modified Eagle's Medium (DMEM) with high glucose content (4500 mg/l) (Sigma-Aldrich, San Luis, MO, USA) supplemented with 10% fetal bovine serum (FBS) (Gibco™, Gaithersburg, MD, USA) and 100 U/ml penicillin/streptomycin (Gibco™). The cell lines were cultured in 75 cm^2 flasks maintaining controlled incubation conditions of CO_2 (5%), temperature (37°C) and humidity (95%), and a medium change was carried out every two days. After establishment, the resistant cell lines were continuously cultured in the presence of 6 µM sorafenib (Santa Cruz Biotechnology, Dallas, TX, USA) to preserve drug resistance. Sorafenib was dissolved in dimethyl sulfoxide (DMSO) (Sigma-Aldrich).

Cells were subcultured when they reached a confluence around 80%. For this, cells were washed with phosphate buffered saline (PBS) (Sigma-Aldrich) and then incubated with trypsin-ethylenediaminetetraacetic acid (EDTA) at 0.05% (Gibco™). After remaining at 37°C for approximately 5 min for HepG2 and 2 min for HepG2S1 and HepG2S3 for hydrolysis, this enzyme was neutralized by adding complete medium. Cells were centrifuged at 1,100 rpm for 3 min and pellet obtained was resuspended in fresh complete medium. Finally, each HCC line was plated in 75 cm^2 flask at a density about 2×10^6 cells for its maintenance, or in the corresponding plates to perform the different experiments.

3.1.3 Reagents and treatments

In addition to sorafenib, other compounds were used to carry out the experiments. To establish hypoxic conditions, 100 µM cobalt chloride ($CoCl_2$) (PanreacAppliChem, Barcelona, Spain) dissolved in medium was added to culture cells. $CoCl_2$ acts as a hypoxia mimetic preventing hydroxylation and subsequent degradation of HIFs owing to cobalt antagonizes Fe^{2+}-mediated PHD activity [232].

We employed 300 µM cycloheximide (CHX) and 30 µM MG132 (Tocris Bioscience, Bristol, UK) as protein synthesis and proteasome inhibitors, respectively.

Besides, we repressed histone deacetylation using 10, 50 and 100 nM of the histone deacetylases (HDACs) inhibitor trichostatin-A (TSA) (AdooQ® Bioscience, Irvine, CA, USA) and methylation with 10 and 100 µM of the DNA methyltransferase (DNMT) inhibitor 5-aza-2'-deoxycytidine (5-Aza or decitabine) (MedChemExpress, Sollentuna, Sweden). CHX was dissolved in milli-Q H_2O; while MG132, TSA and 5-Aza were dissolved in DMSO.

3.2 Cell growth, viability and death assays

3.2.1 Growth curve based on crystal violet staining

Crystal violet or methyl violet is a frequently used dye in microbiology for the classification of bacteria, allowing purple Gram-positive staining [233]. It is also used in cell growth and viability assays due to its ability to bind to cellular DNA [234].

To carry out crystal violet staining, the cells were seeded in 48-well plates at a density of 7.5×10^3 cells/well, considering that one plate was used for each day (days 0, 1, 2, 3, 4 and 5). Once treated with or without sorafenib and/or $CoCl_2$, cells were washed with ice-cold PBS and fixed for 10 min with 4% formaldehyde solution (Thermo Fisher Scientific, Waltham, MA, USA) dissolved in PBS. Then, cells were washed with milli-Q H_2O and stained for 20 min with 0.1% crystal violet (Labkem, Barcelona, Spain) dissolved in 10% ethanol. After 3 washes, 10% acetic acid (Sigma-Aldrich) was added to each well followed by 20 min incubation under shaking. We diluted 1:4 with milli-Q H_2O and measured absorbance at a wavelength of 590 nm using the microtiter plate reader Synergy™ HT Multi-Mode Microplate Reader (BioTek Instruments, Inc., Winooski, VT, USA) and Gen 5 software (BioTek Instruments, Inc.).

3.2.2 Cell viability assay

Thiazolyl blue tetrazolium bromide (MTT) (Sigma-Aldrich) can be used as a colorimetric metabolic activity indicator for cell viability assay termed MTT assay [235].

Cells were seeded in 96-well plate at a density of 1×10^4 cells/well. After gene silencing and treatments with $CoCl_2$ and with or without 5-Aza for different experiments, the medium was removed and PBS washing was made followed by incubation for 3 h at

37°C with a 1:10 free-FBS medium solution of MTT dissolved in PBS at 5 mg/ml. MTT generates a yellowish solution that is turned into dark blue H_2O-insoluble formazan crystals through mitochondrial dehydrogenases of living cells. Then, MTT-containing medium was substituted by DMSO and shaken for 5 min to solubilize the formazan crystals. The optical intensity was measured colorimetrically at a spectral wavelength of 570 nm by the Synergy™ HT Multi-Mode Microplate Reader and Gen 5 software.

3.2.3 Flow cytometry of subG1 cell population

Propidium iodide (PI) is a fluorescent intercalator that binds to double-stranded DNA by intercalating between base pairs. Thus, it is commonly used in flow cytometry to assess cell viability or DNA content in cell cycle evaluation. DNA fragmentation is a characteristic feature of apoptotic cells. Therefore, apoptotic cells contain fractional DNA and, following PI staining, can be recognized as those cells with deficit in DNA content named “subG1” or “hypodiploid” peak subpopulation [236].

For subG1 population analysis, cells were seeded in 75 cm^2 flasks at a density of 2×10^6 cells/flask and, 48 h after treatment with $CoCl_2$ and with/ without sorafenib, cells were harvested. Trypsinized cells were centrifuged at 350 g and 4°C for 5 min, washed with ice-cold PBS and centrifuged again under the same conditions. The cells were fixed for 2 h at 4°C with 70% ethanol in PBS. To prepare samples, approximately 1×10^6 fixed and permeabilized cells per sample were centrifuged at 850 g for 5 min and washed with PBS. After another round of centrifugation, these 1×10^6 cells were incubated with 0.5 mL PI/ribonuclease (RNase) Staining Buffer (BD Pharmingen™, Franklin Lakes, NJ, USA) for 15 min at room temperature under dark conditions. RNAse was used to remove RNA present in cells, since PI also has affinity for RNA.

Finally, using a FACSCalibur flow cytometer (Becton Dickinson, San José, CA, USA) and CellQuest Pro™ software (Becton Dickinson), 5,000 events were acquired for each sample and the percentage of cells in subG1 phase was evaluated by WEASEL analytical software (Walter and Eliza Hall Institute (WEHI), Melbourne, VIC, Australia).

3.3 Evaluation of protein expression

3.3.1 Immunocytochemistry and immunofluorescence (ICC/IF)

ICC is a technique that allows the use of antibodies to detect and locate a certain protein in cell samples, either from isolated cells or from cell cultures. Antigen-antibody interaction can be visualized by chromogenic labeling, where an enzyme conjugated to an antibody reacts with its specific substrate producing a colored precipitate; or by IF detection, where the antibody is conjugated to a fluorophore visible by a fluorescence microscope [237].

HepG2, HepG2S1 and HepG2S3 cells were seeded in 24-well plates containing a coverslip, at a density of 2.5×10^4. The coverslips were pretreated with 0.2% gelatin (Sigma-Aldrich) dissolved in deionized H_2O (diH_2O) by incubation for 10 min at room temperature, since the addition of a thin layer of gelatin improves the adhesion of cells to the glass. Then, the gelatin solution was removed and allowed to dry for at least 15 min.

After treatment with CoCl2 and with or without sorafenib, cells were fixed with 4% formaldehyde solution (Thermo Fisher Scientific) for 15 min, permeabilized for 20 min with 0.2% saponin (Sigma-Aldrich) and blocked for 30 min with 1% fatty acid-free bovine serum albumin (FAF-BSA) (Sigma-Aldrich) in PBS. These steps were performed at room temperature and with 3 washes with PBS between each of them. The cells were then incubated overnight at 4°C with the primary antibodies against Ki67 (1:200; reference sc-23900, Santa Cruz Biotechnology), HIF-1α (1:300; reference ab2185, Abcam, Cambridge, UK), HIF-2α (1:300; reference ab199, Abcam) or BNIP3 (1:200; reference sc-56167, Santa Cruz Biotechnology). Cells were washed with PBS and incubated for 1 h at room temperature with the secondary antibodies anti-mouse immunoglobulin G (IgG) conjugated with Alexa Fluor® 488 (1:1,000; reference ab150113, Abcam) or anti-rabbit IgG conjugated with Alexa Fluor® 647 (1:1,000; reference ab150079, Abcam). The coverslips were washed with PBS and mounted on glass slides with Fluoroshield™ (Sigma-Aldrich), a fluorescent mounting medium containing 4'6-diamidino-2-phenylindole (DAPI) for nuclei staining. Results were visualized in a Zeiss LSM 800 confocal laser scanning microscope (Zeiss AG, Jena, Germany) and the images obtained

with the ZEN software (Zeiss AG). Fluorescence quantification was performed using ImageJ software (National Institutes of Health (NIH), Bethesda, MD, USA) and the corrected total cell fluorescence (CTCF) formula [238,239]:

CTCF = integrated density − (area of selected cell × mean fluorescence of background readings)

3.3.2 Western blot assay

The Western blot or immunoblot technique allows the separation, immunodetection and quantification of the expression levels of specific proteins in a complex mixture of proteins. This process was carried out through multiple steps [240]:

Cell collection and lysis

Cells were seeded onto p60 plates at a density of 7.5×10^5 cells/plate. After the corresponding treatments with $CoCl_2$, sorafenib, CHX, MG132, TSA, 5-Aza and/or gene silencing for several experiments, cells were washed with ice-cold PBS and collected in a homogenization buffer (0.25 mM sucrose, 10 mM Tris and 1 mM EDTA; pH 7.4) supplemented with protease and phosphatase inhibitor cocktails (Roche Diagnostics, Basel, Switzerland), in order to avoid protein degradation by action of these enzymes. Cells were lysed by sonication during 2 pulses of 20 s at 60% amplitude using the UP50H Compact Ultrasonic Processor (Hielscher-Ultrasound Technology, Teltow, Germany), and centrifuged at 14,000 g for 10 min.

Quantification of the amount of protein

Subsequently, the protein concentration of collected samples was measured by the Bradford dye-binding method, a colorimetric assay based on the binding of the Bradford reagent or Coomassie® Brilliant Blue G-205 dye (Bio-Rad, Hercules, CA, USA) to the basic and aromatic amino acid residues, mainly arginine. The procedure was performed according to the manufacturer's instructions. Using the Synergy™ HT Multi-Mode Microplate Reader and the software Gen 5, the absorbance was read at a wavelength of 595 nm. Changes in coloration/absorbance are directly proportional to the amount of dye bound to the proteins and, therefore, to the concentration of

proteins in the solution. A relationship was established from the absorbance obtained, which allows the concentration of protein present in each sample to be calculated using a BSA standard (Sigma-Aldrich).

Handcasting polyacrylamide gels

Polyacrylamide gels employed for electrophoresis were prepared by mixing acrylamide and bis-acrylamide, forming a cross-linked gel matrix. Furthermore, it was added the polymerizing agent ammonium persulfate (APS) and tetramethylenediamine (TEMED) that catalyzes the polymerization. Polyacrylamide gels are composed by two differentiated parts: stacking and resolving gels. The purpose of stacking gel is to align all protein samples loaded on the gel, so that they can enter the resolving gel at the same time. The resolving gel enables the separation of proteins based on their molecular weight [241].

Resolving gels were prepared by mixing 30% acrylamide/bis-acrylamide solution (Bio-Rad), diH_2O, 1.5 M Tris-HCl (pH = 8.8), 10% sodium dodecyl sulfate (SDS), 10% APS, and TEMED (Bio-Rad). Depending on the molecular weight (kDa) of the proteins to be analyzed, the pore size of the resolving gel should be different. The size of the pores created in the gel is inversely related to the polyacrylamide percentage or concentration. Thus, gels between 9 and 14% were required to analyze the different proteins. On the other hand, stacking gels were made at 4% through mixing 30% acrylamide/bis-acrylamide solution, diH_2O, 0.5 M Tris-HCl (pH = 6.8), 10% SDS, 10% APS, and TEMED. All handcasting gel supplies were purchased from Bio-Rad and gels were elaborated as indicated by the manufacturer's instructions.

SDS-Polyacrylamide gel electrophoresis (PAGE) and electrotransfer

The samples were prepared with the same amount of protein and subjected to a denaturation process by adding 1:4 of the 4x Laemmli sample buffer (Bio-Rad) and heating at 100°C for 3 min. Equal amount of denaturalized samples and the PageRuler^{TM} Prestained Protein Ladder (Thermo Fisher Scientific) or the Precision Plus Protein Dual Color Standards (Bio-Rad) were then loaded into a polyacrylamide gel and subjected to SDS-PAGE, which separates the different proteins based on their

molecular weight by applying an electric field of 100 V. Electrophoresis chamber and power supplies were purchased from Bio-Rad.

Subsequently, the resulting gel was transferred to a polyvinylidene difluoride (PVDF) membrane (Bio-Rad) by employing the Trans-Blot® Turbo™ Transfer System (Bio-Rad) according to the manufacturer's instructions. Hydrophobic PVDF membranes were previously prepared for blotting by prewetting in methanol (VWR International, Radnor, PA, USA) for 20 s and, then, submerged in milli-Q H_2O during 2 min until fully equilibrated for easy immersion into the aqueous solution.

Membrane blocking and antibodies incubation

Transferred PVDF membranes were blocked with 5% milk dissolved in 0.05% PBS-Tween 20 (Bio-Rad) (PBS-T) for 1 h at room temperature to avoid nonspecific binding. Then, each membrane was incubated overnight at 4°C with the corresponding primary antibody **(Table 5)**. Proliferating cell nuclear antigen (PCNA) was used as housekeeping. The next day, the membranes were incubated for 1 h at room temperature with the secondary antibodies anti-rabbit IgG (1:20,000; reference 31460, Thermo Fisher Scientific) or anti-mouse Ig (1:5,000; reference P0206, Dako, Glostrup, Germany), which are conjugated to horseradish peroxidase (HRP). Between each step, membranes were washed 3 times with PBS-T.

Table 5. List of the primary antibodies used for protein detection by Western blot. The target protein, antibody host and type, source, reference, molecular weight of protein and dilution are detailed.

Target protein	Antibody host and type	Source	Reference code	Molecular weight (kDa)	Dilution
Bax	Rabbit policlonal	Santa Cruz Biotechnology	sc-493	23	1:100
BNIP3	Mouse monoclonal	Santa Cruz Biotechnology	sc-56167	22/30	1:200
Cleaved caspase-3	Rabbit policlonal	Cell Signaling Technology, Danvers, MA, USA	#9661	17/19	1:1,000
HIF-1α	Rabbit policlonal	Abcam	ab2185	100	1:500

HIF-2α	Rabbit policlonal	Abcam	ab199	100	1:500
PCNA	Mouse	Santa Cruz Biotechnology	sc-56	36	1:200
β-actin	Mouse monoclonal	Sigma-Aldrich	A3854	42	1:50,000*

* Anti-β-actin antibody is already HRP-conjugated

Development and quantification

Finally, the membranes were incubated with the Pierce™ enhanced chemiluminescence (ECL) Western Blotting Substrate (Thermo Fisher Scientific), an enhanced luminol-based chemiluminescent substrate for the detection of HRP on immunoblots, as reported by the manufacturer's instructions. This enables the detection of proteins using a photographic method, by exposing the membranes to X-Ray films Amersham Hyperfilm™ ECL (VWR International), and submerging these films in developer (Rosex Medical, SL., Barcelona, Spain), H_2O and fixer (Rosex Medical) solutions in order, to obtain the different protein bands. The density of the protein bands was quantified with ImageJ software.

3.4 Analysis of nucleic acids levels

3.4.1 Gene expression analysis by microarray

Oligonucleotide microarray is a technique that provides the most accurate, sensitive, and comprehensive simultaneous measurement of the expression level of thousands of genes [242].

To perform the gene expression analysis, the group from KU Leuven University (Belgium) seeded HepG2 and HepG2S1 cells at 1×10^6 in 25 cm² flasks. After 72 h in maintenance conditions, cells were harvested with TRIzol™ reagent (Invitrogen, Carlsbad, CA, USA) and RNA was isolated using the RNeasy Kit (Qiagen, Chatsworth, CA, USA) as stated in the manufacturer's protocol. Then, RNA quality was tested through the 2100 BioAnalyzer Instrument (Agilent, Palo Alto, CA, USA). The GeneChip® Human Gene 1.0 ST Array (Affymetrix, Santa Clara, CA, USA) was employed as platform for microarray.

3.4.2 Reverse transcription polymerase chain reaction (RT-PCR) and real-time quantitative (q)RT-PCR (qRT-PCR)

RT-PCR is a powerful method for studying gene expression, allowing mRNA levels to be compared across samples to identify gene expresion patterns. For this, reverse transcription is required to generate complementary DNA (cDNA) from mRNA, so that the cDNA serves as template for PCR [243].

Cells were seeded in 6-well plates at a density of 2.5×10^5 cells/plate. Following treatment with $CoCl_2$ and with or without sorafenib and 5-Aza for diverse experiments, total RNA was isolated with TRIzol™ Reagent (Invitrogen) and quantified using the Nanodrop™ ND-1000 Spectrophotometer (Thermo Fisher Scientific). RQ1 RNase-free deoxyribonuclease (DNase) (Promega, Madison, WI, USA) was employed to remove residual single- and double-stranded DNA and, afterwards, equal amounts of RNA (500 ng) were reverse transcribed to cDNA with the High-Capacity cDNA Reverse Transcription Kit (Applied Biosystems, Carlsbad, CA, USA). All procedures were performed as indicated by the manufacturer's instructions.

For qRT-PCR analysis, cDNA was amplified using Power SYBR™ Green PCR Master Mix (Applied Biosystems) according to the manufacturer's protocol and with the following conditions: initial denaturation for 10 min at 95°C, and 40 cycles of denaturation for 15 s at 95°C and annealing for 60 s at 60°C, by using the StepOnePlus™ Real-Time PCR System and StepOne™ software (Applied Biosystems). Relative changes in gene expression levels were evaluated by the $2^{-\Delta\Delta CT}$ method [244].

While for RT-PCR, cDNA amplification was performed using the KAPA HiFi HotStart ReadyMix PCR Kit (Kapa Biosystems, Wilmington, MA, USA) and the MJ Research PTC-200 Thermal Cycler (Marshall Scientific, Hampton, NH, USA) under the next conditions: initial denaturation for 5 min at 95°C; 30 cycles of denaturation for 30 s at 94°C, annealing for 45 s at 60°C, extension for 30 s at 72°C; and an ending extension step for 10 min at 72°C. The obtained RT-PCR products were subjected to agarose gel electrophoresis together with a 100 base pair (bp) DNA ladder (Invitrogen). Handcast agarose gels were prepared by dissolving 2% agarose (Biotools, Madrid, Spain) in 1:50 of 50X Tris-acetato-EDTA (TAE) buffer (2 M Tris, 1M glacial acetic acid, 50

mM EDTA) and adding GelRed® Nuclei Acid Gel Stain (Biotium, Fremont, CA, USA), which allow the bands to be visualized using the ChemiDoc™ XRS Universal Hood II and the Quantity One® software (Bio-Rad).

Human primers employed in qRT-PCR and RT-PCR were as detailed: BNIP3 forward 5'-CGCAGACACCACAAGATACC-3' and reverse 5'-TCTTCATGACGCTCGTGTTC-3'; 18S forward 5'-GGCGCCCCCTCGATGCTCTTAG-3' and reverse 5'-GCTCGGGCCTGCTTTGAACACTCT-3'. 18S ribosomal RNA (rRNA) was used as endogenous control.

3.4.3 Methylation-Specific PCR (MSP)

Among PCR techniques, MSP is a specific method to determine the methylation status of a region of interest by the selective amplification of methylated and unmethylated alleles [245].

Cells were seeded in 6-well plates at a density of 2.5×10^5 cells/plate. After the treatments with $CoCl_2$ and with or without sorafenib and 5-Aza, the DNA was extracted using Phenol:Chloroform:Isoamyl Alcohol 25:24:1 (Sigma-Aldrich) and DNA was modified using the bisulfite conversion EZ DNA Methylation™ Kit (Zymo Research, Irvine, CA, USA). Both procedures were employed following the manufacturer's instructions.

MSP was carried out using specific primers to detect BNIP3 methylated (M) and unmethylated (U) DNA: M-BNIP3 forward 5'-TAGGATTCGTTTCGCGTACG-3' and reverse 5'-ACCGCGTCGCCCATTAACCGCG-3'; U-BNIP3 forward 5'-TAGGATTTGTTTTGTGTATG-3' and reverse 5'-ACCACATCACCCATTAACCACA-3'. Amplification was made employing the KAPA HiFi HotStart ReadyMix PCR Kit in the MJ Research PTC-200 Thermal Cycler, and the optimal MSP settings were as follows: preliminary denaturation for 15 min at 95°C; 35 cycles of denaturation for 30 s at 94°C, annealing for 50 s at 58°C, elongation for 1 min at 72°C; and a final elongation for 10 min at 72°C. The MSP products were loaded onto 2% agarose gels for electrophoresis along with a 100 bp DNA ladder, and visualized with the ChemiDoc™ XRS Universal Hood II and the Quantity One® software.

3.5 Gene silencing

Small interfering RNAs (siRNAs) are processed from long double-stranded RNA and a selected guide strand, allowing the recognition and cleavage of a target mRNA, thus blocking gene expression [246].

Commercial siRNAs against HIF-1α (sc-35561), EPAS-1 (i.e., HIF-2α) (sc-35316) and BNIP3 (sc-37451), as well as a control siRNA encoding a nontargeting sequence (sc-36869) were purchased from Santa Cruz Biotechnology. These siRNAs are a pool of different target-specific 19-25 nucleotides siRNAs designed to knockdown the expression of the gene of interest. The siRNAs were introduced into cells by reverse transfection using Lipofectamine® RNAiMAX Reagent (Invitrogen) according to the manufacturer's protocol. Lipofectamine acts as delivery agent, facilitating the crossing of siRNA to the cell by the plasma membrane. After preparing the siRNA-lipofectamine complexes within the 6-well plates, cells were added at a density of 5×10^5 cells/well. 5 h after transfection, medium was replaced with complete fresh medium and, 24 h after transfection, cells were treated with $CoCl_2$ and with or without sorafenib and 5-Aza to finally be subjected to MTT and Western blot assays.

3.6 Statistical analysis

Microarray data arise from three independent experiments and were analyzed with the Limma package from Bioconductor (http://www.bioconductor.org) [247]. Differentially expressed genes were measured by performing a moderated t-test. The resulting p-values were corrected for multiple testing with Benjamini-Hochberg to control false discovery rate [248]. To select genes with differentiated expression, a cut-off of Δlog (^{2}log fold change (FC))>+0.7 or <−0.7 and a corrected p<0.05 was applied.

Pathway analysis, with gene-annotation enrichment analysis, functional clustering and Kyoto Encyclopedia of Genes and Genomes (KEGG) pathway mapping, was carried out using the bioinformatic tools WEB-based GEne SeT AnaLysis Toolkit (WebGestalt) (http://webgestalt.org/) [249] and Database for Annotation, Visualization and Integrated Discovery (DAVID) (https://david.ncifcrf.gov/) [250], in parallel. These data

are available at National Center for Biotechnology Information (NCBI), GEO DataSets, series GSE62813 (https://www.ncbi.nlm.nih.gov/geo/query/acc.cgi?acc=GSE62813).

The rest of results were reported as mean values ± standard deviation (SD) of three independent experiments. Data were analyzed with the statistical package GraphPad Prism 6 (GraphPad Software, San Diego, CA, USA), checking the normality of the data with the Kolmogorov-Smirnov test. According to the different experiments, we performed unpaired t-test, or one-way or two-way analysis of variance (ANOVA) followed by Tukey post-hoc test to examine differences between the different groups evaluated. The results were considered statistically significant when $p<0.05$.

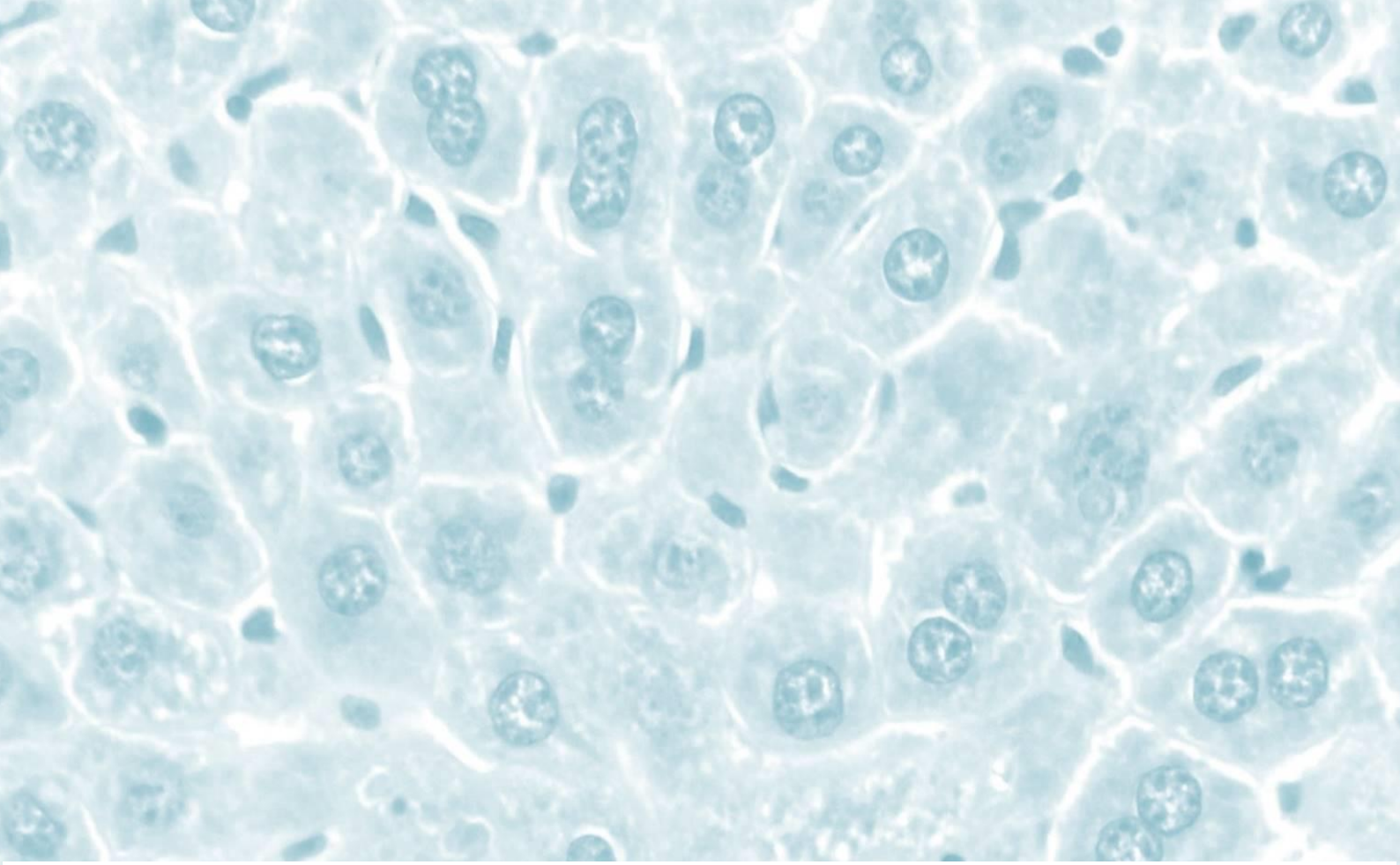

Results

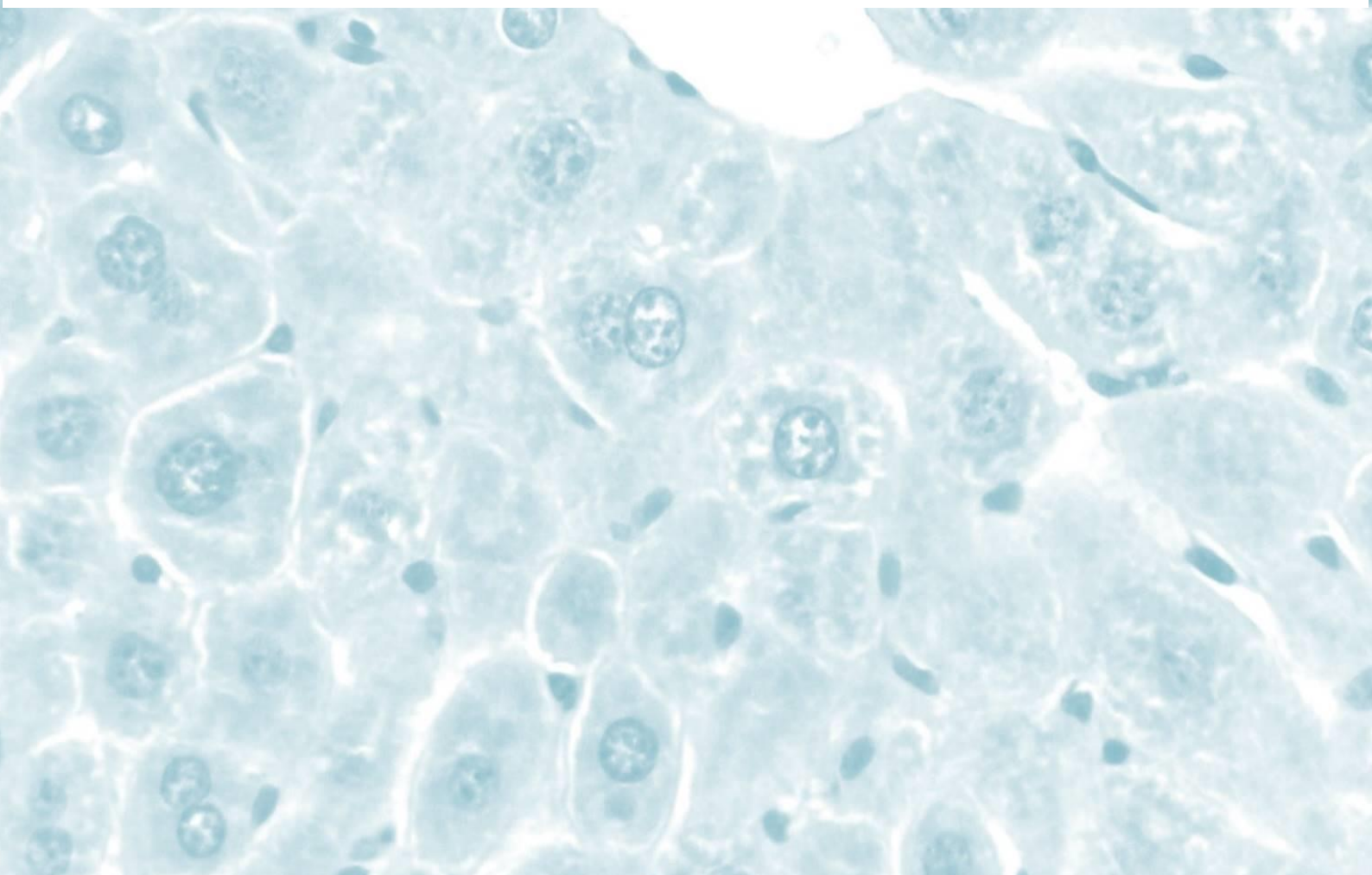

1 Prognostic and clinicopathological significance of HIF-1α and HIF-2α in HCC: A systematic review with meta-analysis

Hypoxia is a common phenomenon among solid tumors, including HCC, which plays a key role in tumor development and progression. The cellular response to low oxygen tension is principally mediated by HIF-1α and HIF-2α [103]. Thus, in the present study we performed a systematic review with meta-analysis of the available scientific evidence of the role of these transcription factors in the outcomes of patients with HCC, finding the next results:

1.1 Study selection and characteristics

Based on the search terms listed above, a total of 3,888 potentially relevant studies were identified from the databases searching. Among them, 2,172 duplicated records were removed. After screening for titles and abstracts, other 1,386 studies were excluded according to the following reasons: non-original research articles (reviews, book chapters, or similar), studies in animal or cellular models, and non-HCC or HIF related articles. The full-text of 330 articles was examined to determine their eligibility, identifying 24 studies with full-text in Chinese, 264 without HIF IHC and/or without analysis of survival or clinicopathological features, one about HIF-3α and seven where surgical resection was not employed. Hence, these 296 papers were also omitted of our study and 34 articles [198–231] were subjected to data extraction and quality assessment in the qualitative synthesis. Cao *et al*. [231] and Zhou *et al*. [223] did not provide sufficient data to estimate HR and its 95% CI by the Parmar method. Besides, Zhou *et al*. [223] did not reach the quality threshold of the NOS scale **(Table 3)**. Finally, 32 publications were eligible for quantitative meta-analysis: 25 about HIF-1α, six on HIF-2α and one about both factors **(Figure 17)**.

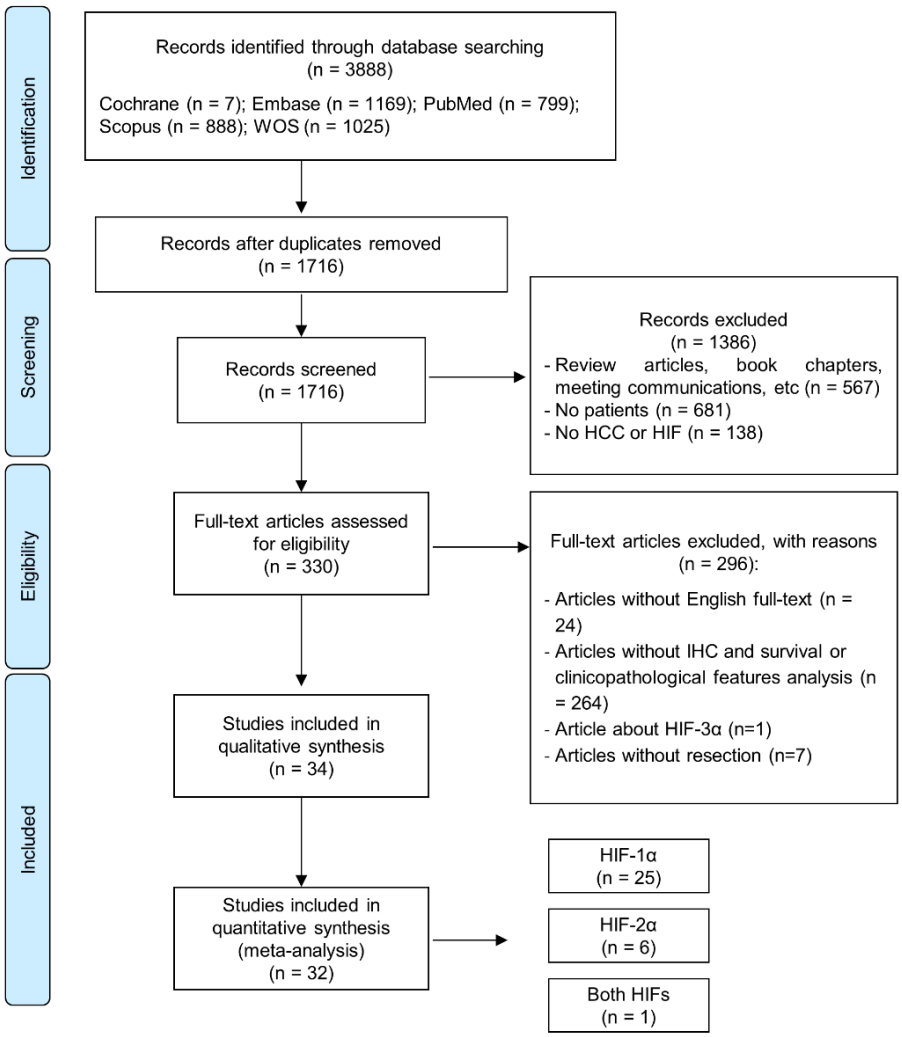

Figure 17. PRISMA flowchart of the study selection process. The PRISMA flow diagram for the systematic review detailing the databases searching, the number of abstracts screened, and the full-text articles assessed for eligibility.

Table 3 summarizes the baseline characteristics of the involved articles, including scores of quality assessment. The 32 studies eventually included in the quantitative analysis were published from 2004 to 2020 and comprised a total of 3,578 (eigth were "missing" in the analysis of HIF-1α expression) and 1,213 HCC patients to HIF-1α and HIF-2α evaluation, respectively. The studies selected for HIF-1α study included a number of patients ranging from 35 to 419, and 1,846 patients (51.7%) exhibited HIF-1α overexpression. For HIF-2α articles, between 84 and 315 patients were registered from each study, showing a total of 553 patients (45.6%) with HIF-2α overexpression.

Regarding the data required for the quantitative assessment of the present meta-analysis, within the 25 articles comprised for HIF-1α, 18 supplied data about OS, eigth on DFS/RFS and 23 concerning several clinicopathological features; whereas for the seven studies for HIF-2α, five provided OS, three DFS/RFS and all of them clinicopathological features. Moreover, although five of the HIF-1α researches determined TTR, only one reported the HR and HR estimation and its 95% CI was not possible consistent with Parmar method for the remaining studies. Therefore, association between HIF-1α and TTR was not feasible to include.

All enrolled patients were subjected to surgical resection. However, some of the included patients in Wada *et al*. [199] and Dai *et al*. [201] studies received preoperative antitumor therapy. Likewise, in Xiang *et al*. [206] the patients underwent external beam radiotherapy as postoperative adjuvant treatment. The rest of the patients evaluated did not receive any additional intervention to surgery.

All the patients involved came from Asia: one study from Japan (1.3%) [199], another from Singapore (3.8%) [213] and the rest from China (94.9%). Concerning etiology, 21 of the 32 articles assessed the number of patients with hepatitis B [198–200,202–208,210,212,213,215,219–221,226–228,230], nine checked the patients with hepatitis C [199,203,205,210,212,213,226–228], and only one the alcoholic patients [213]. This correlates with the fact that all the studies were conducted in the Asian population, where hepatitis B is the main etiological factor [1]. Moreover, 20 articles explored the number of HCC patients derived from cirrhosis [198–203,205,208,210,212,213,215,217,219–221,225–228]. We determined that 78.2% of the patients included in the present meta-analysis had hepatitis B, 6.6% hepatitis C and 66.1% cirrhosis.

1.2 Correlation of HIF-1α and HIF-2α protein expression with prognosis

To start the quantitative synthesis of the meta-analysis, we assessed the association between each HIF and survival-related parameters. As shown in **Figure 18A**, the prognostic significance of HIF-1α overexpression showed a strength correlation with both OS (HR, 1.73; 95% CI, 1.54-1.94; p=0.00) and DFS/RFS (HR, 1.64; 95% CI, 1.36-1.99; p=0.00) in HCC patients, not displaying significant heterogeneity.

Moreover, the results indicated that there was not significant association between HIF-2α overexpression and OS in HCC patients (HR, 1.25; 95% CI, 0.68-2.32; p=0.48), denoting elevated heterogeneity across studies (I^2=91.46%, Q-test p=0.00). Conversely, high HIF-2α expression correlated with DFS/RFS (HR, 1.37; 95% CI, 1.05-1.79; p=0.02), and no heterogeneity was revealed **(Figure 18B)**.

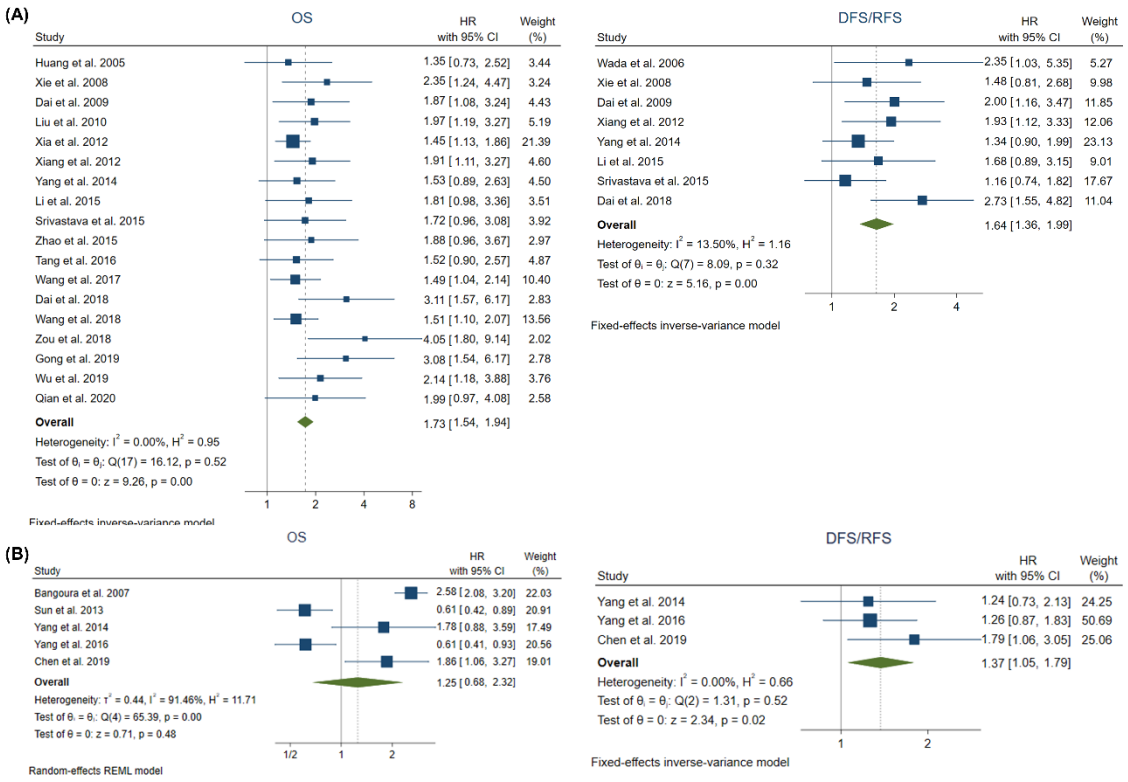

Figure 18. Meta-analysis of the prognostic significance of HIF-1α and HIF-2α in the survival of HCC patients. Forest plots of OS and DFS/RFS for **(A)** HIF-1α and **(B)** HIF-2α.

1.3 Correlation of HIF-1α and HIF-2α protein expression with clinicopathological features

To further investigate the role of HIFs on HCC, we analyzed their possible correlation with several clinical and pathological characteristics.

On the one hand, various clinicopathological features were positively associated with high HIF-1α expression, including BCLC staging (OR, 2.49; 95% CI, 1.56-3.98; p=0.00), capsule infiltration (OR, 2.48; 95% CI, 1.29-4.77; p=0.01), intrahepatic metastasis (OR, 2.90; 95% CI, 1.62-5.20; p=0.00), lymph node metastasis (OR, 3.74; 95% CI, 1.73-8.07; p=0.00), TNM staging (I, II-III) (OR, 1.59; 95% CI, 1.21-2.09; p=0.00), TNM staging (I-II, III) (OR, 2.62; 95% CI, 1.69-4.08; p=0.00), TNM staging (I-II, III-IV) (OR, 2.23; 95% CI, 1.37-3.64; p=0.00), tumor differentiation (OR, 1.78; 95% CI, 1.07-2.96; p=0.03), tumor number (OR, 1.50; 95% CI, 1.15-1.96; p=0.00), tumor size (cut-off 3 cm) (OR, 3.70; 95% CI, 1.29-10.63; p=0.02), vascular invasion (OR, 2.61; 95% CI, 1.82-3.75; p=0.00), and vasculogenic mimicry (OR, 2.61; 95% CI, 1.67-4.09; p=0.00) **(Figures 19 and 20)**. Among them, marked heterogeneity was found for tumor differentiation (I^2=66.79%, Q-test p=0.00), and vascular invasion (I^2=69.59%, Q-test p=0.00) **(Figure 20)**.

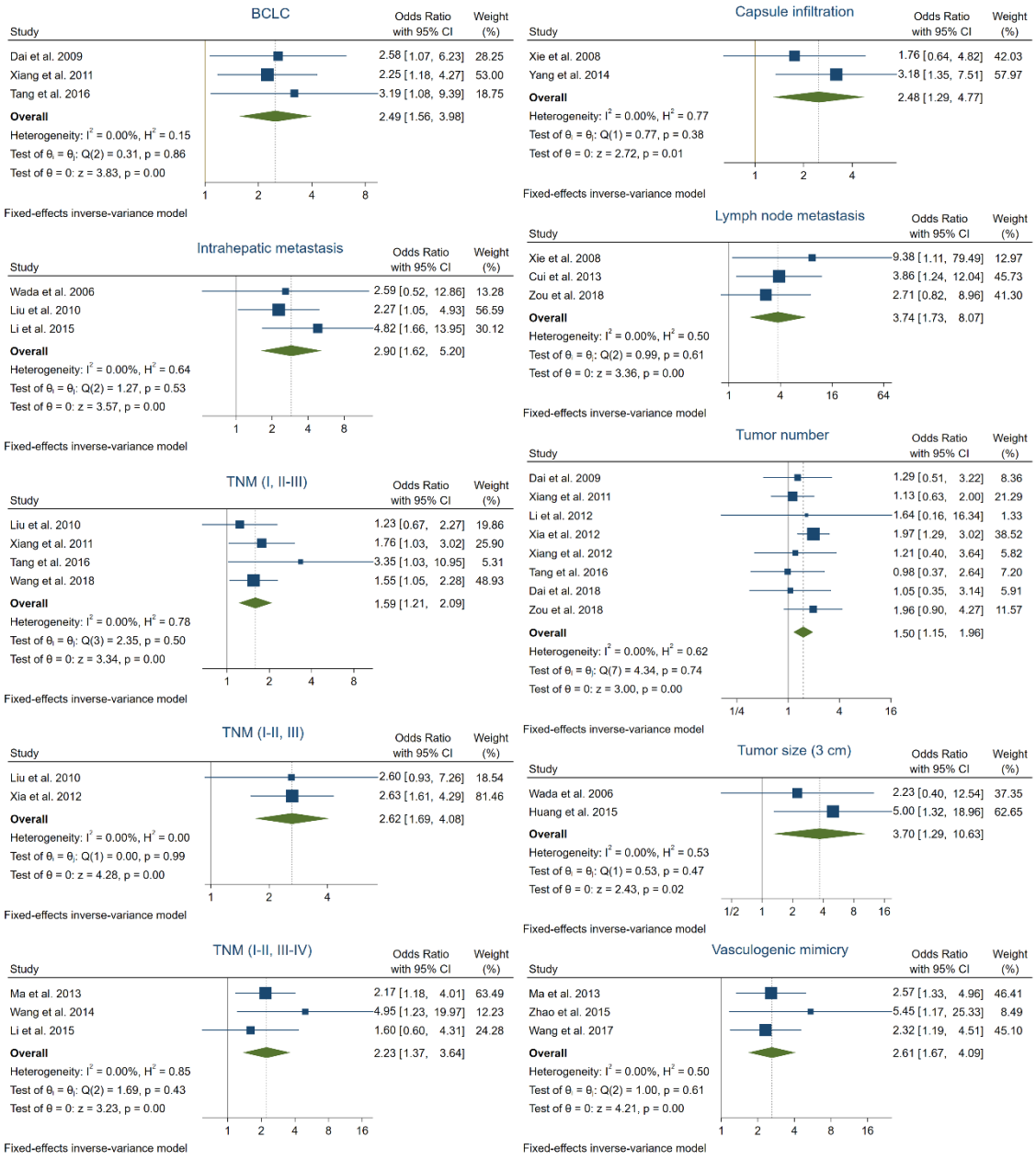

Figure 19. Meta-analysis of the correlation between HIF-1α overexpression and clinicopathological features in patients with HCC: characteristics significantly associated with HIF-1α and showing acceptable heterogeneity between studies. Forest plots of HIF-1α association with BCLC staging, capsule infiltration, intrahepatic metastasis, lymph node metastasis, TNM staging, tumor number, tumor size (3 cm), and vasculogenic mimicry.

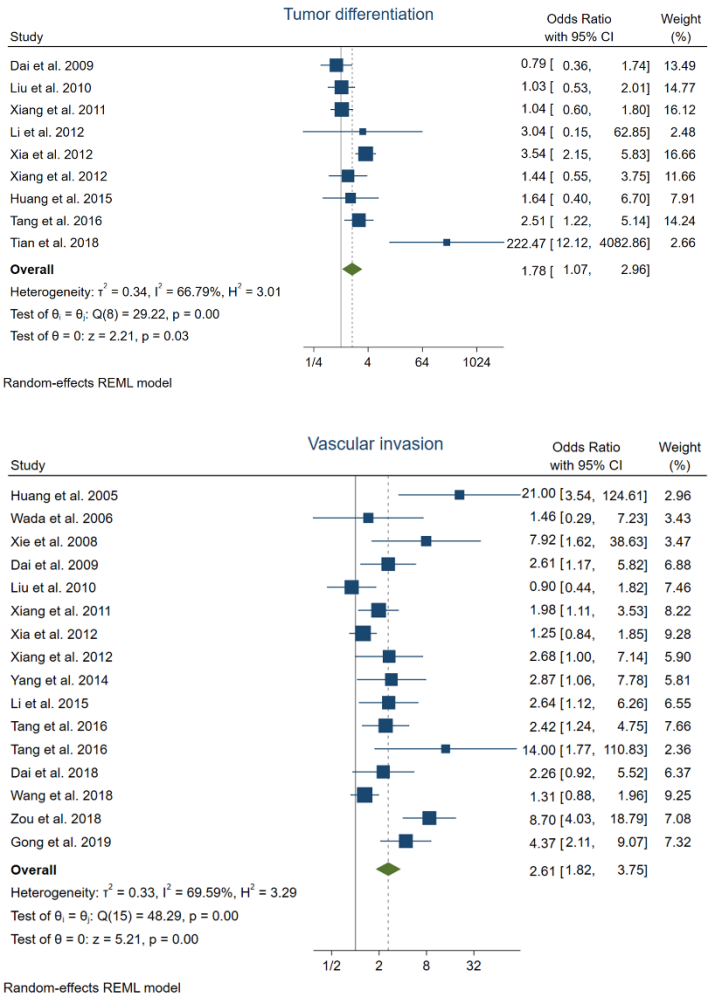

Figure 20. Meta-analysis of the association between HIF-1α overexpression and clinicopathological features in patients with HCC: characteristics significantly related to HIF-1α but denoting high heterogeneity across studies. Forest plots of the relationship between HIF-1α expression with tumor differentiation and vascular invasion.

On the other hand, no significant relationship was found between the positive HIF-1α expression and other features such as AFP levels (cut-off 20 ng/ml) (OR, 1.39; 95% CI, 0.92-2.09; p=0.11), AFP levels (cut-off 400 ng/ml) (OR, 1.49; 95% CI, 0.67-3.33; p=0.33), age (cut-off 50 years) (OR, 0.86; 95% CI, 0.57-1.31; p=0.49), age (cut-off 60 years) (OR, 1.03; 95% CI, 0.68-1.55; p=0.90), albumin levels (cut-off 35 U/L) (OR, 0.60; 95% CI, 0.26-1.38; p=0.23), ALT levels (cut-off 40 U/L) (OR, 0.86; 95% CI, 0.60-1.24; p=0.42), ALT levels (cut-off 80 U/L) (OR, 1.04; 95% CI, 0.67-1.62; p=0.86), bilirubin levels (cut-off 1 µmol/L) (OR, 1.65; 95% CI, 1.00-2.73; p=0.0501), capsule formation (OR, 0.89; 95% CI, 0.69-1.13; p=0.33), Child-Pugh score (OR, 1.52; 95% CI, 0.91-2.53; p=0.11), cirrhosis (OR, 1.32; 95% CI, 0.97-1.80; p=0.08), distant metastasis (OR, 6.14; 95% CI, 0.83-45.48; p=0.08), Edmondson grading (OR, 1.35; 95% CI, 0.83-2.20; p=0.22), gender (OR, 0.93; 95% CI, 0.77-1.14; p=0.51), hepatitis B (OR, 0.99; 95% CI, 0.82-1.21; p=0.96), hepatitis C (OR, 1.25; 95% CI, 0.72-2.16; p=0.42), histological grade (OR, 1.54; 95% CI, 0.70-3.40; p=0.28), and tumor size (cut-off 5 cm) (OR, 1.40; 95% CI, 0.88-2.22; p=0.16) **(Figures 21 and 22)**. Besides, substantial heterogeneity was showed in AFP (20 ng/ml) (I^2=54.11%, Q-test p=0.05), AFP (400 ng/ml) (I^2=73.88%, Q-test p=0.01), age (50 years) (I^2=47.38%, Q-test p=0.07), albumin (35 U/L) (I^2=51.97%, Q-test p=0.13), cirrhosis (I^2=44.47%, Q-test p=0.03), distant metastasis (I^2=82.75%, Q-test p=0.02), histological grade (I^2=49.79%, Q-test p=0.09), and tumor size (5 cm) (I^2=85.08%, Q-test p=0.00) **(Figure 22)**.

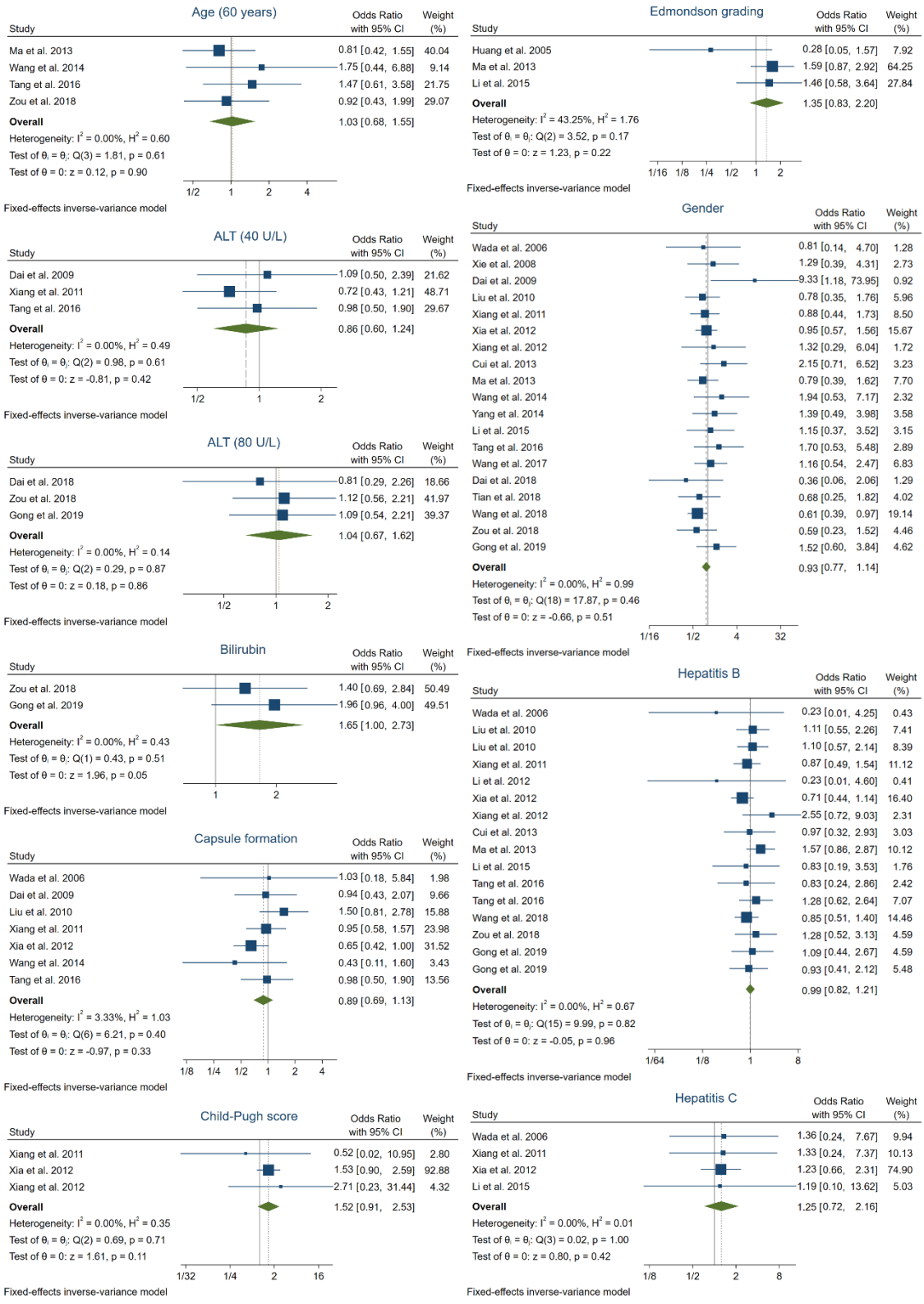

Figure 21. Meta-analysis of the relationship between HIF-1α overexpression and clinicopathological features in patients with HCC: characteristics not significantly associated with HIF-1α and displaying acceptable heterogeneity between studies. Forest plots of correlation of HIF-1α levels with age (60 years), ALT levels, bilirubin

levels, capsule formation, Child-Pugh score, Edmondson grading, gender, hepatitis B and hepatitis C.

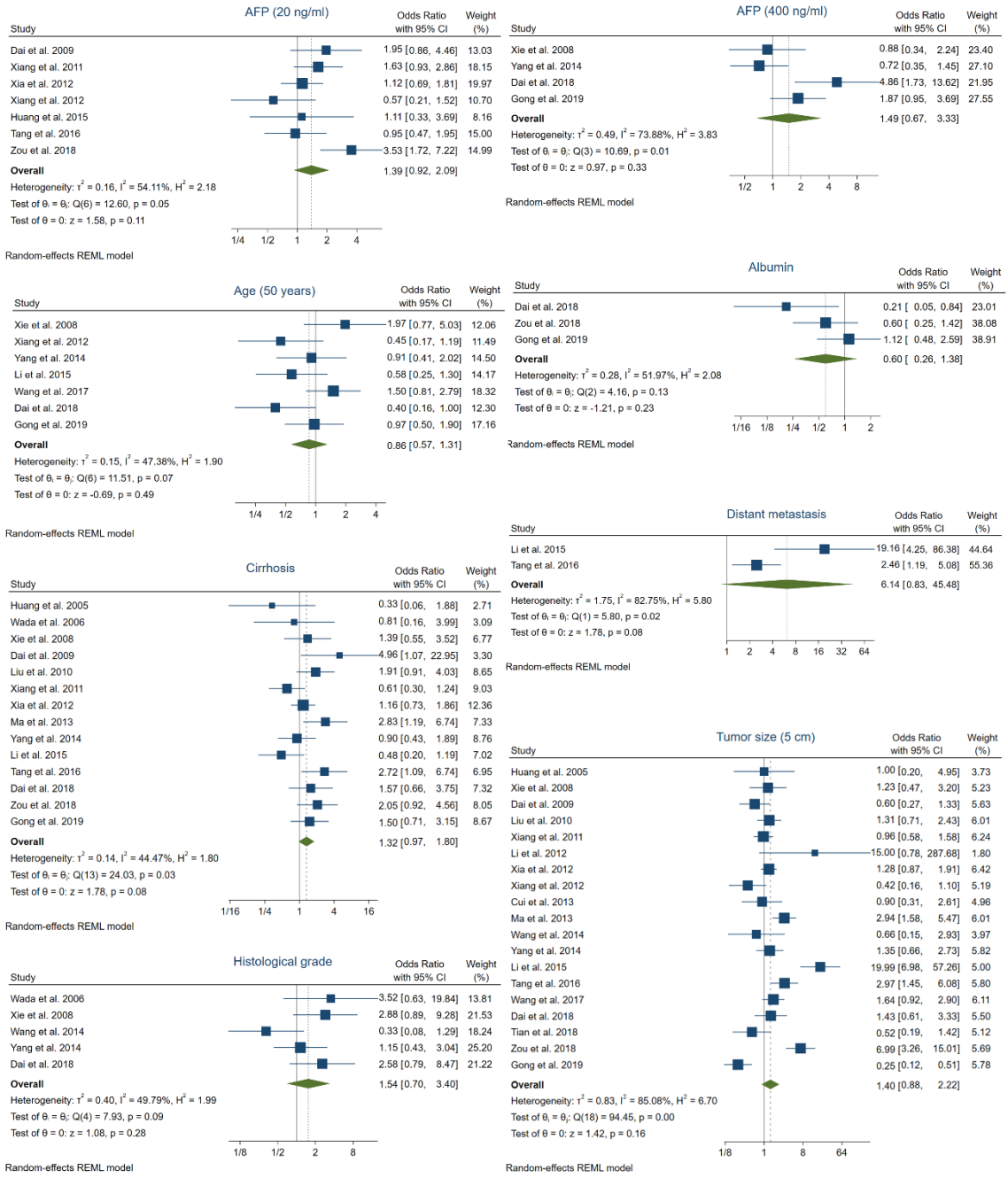

Figure 22. Meta-analysis of the association between HIF-1α overexpression and clinicopathological features in patients with HCC: characteristics not significantly correlated to HIF-1α and with elevated heterogeneity across studies. Forest plots of HIF-1α expression associated with AFP levels, age (50 years), albumin levels, cirrhosis, distant metastasis, histological grade and tumor size (5 cm).

All HIF-2α studies were incorporated for the meta-analysis of clinicopathological features. However, the results did not report a significant relationship between HIF-2α overexpression and any parameter tested: AFP levels (cut-off 400 ng/ml) (OR, 0.88; 95% CI, 0.60-1.30; p=0.52), age (cut-off 50 years) (OR, 1.17; 95% CI, 0.79-1.73; p=0.44), capsule formation (OR, 1.31; 95% CI, 0.93-1.83; p=0.12), capsule infiltration (OR, 1.82; 95% CI, 0.54-6.13; p=0.33), cirrhosis (OR, 1.22; 95% CI, 0.91-1.64; p=0.19), Edmondson grading (OR, 11.05; 95% CI, 0.02-6,167.72; p=0.46), gender (OR, 0.95; 95% CI, 0.68-1.35; p=0.79), hepatitis B (OR, 1.03; 95% CI, 0.76-1.39; p=0.86), histological grade (OR, 0.93; 95% CI, 0.43-1.99; p=0.85), necrosis (OR, 1.32; 95% CI, 0.25-6.98; p=0.74), TNM staging (I-II, III-IV) (OR, 1.12; 95% CI, 0.40-3.10; p=0.83) tumor number (OR, 1.44; 95% CI, 0.92-2.27; p=0.11), tumor size (cut-off 5 cm) (OR, 1.20; 95% CI, 0.36-3.99; p=0.77) and vascular invasion (OR, 1.16; 95% CI, 0.67-2.00; p=0.60) **(Figures 23 and 24)**. Furthermore, heterogeneity was substantial for some features including capsule infiltration (I^2=77.06%, Q-test p=0.03), Edmondson grading (I^2=94.64%, Q-test p=0.00), necrosis (I^2=89.88%, Q-test p=0.00), TNM staging (I-II, III-IV) (I^2=56.26%, Q-test p=0.13), tumor size (5 cm) (I^2=94.27%, Q-test p=0.00) and vascular invasion (I^2=62.18%, Q-test p=0.02) **(Figure 24)**.

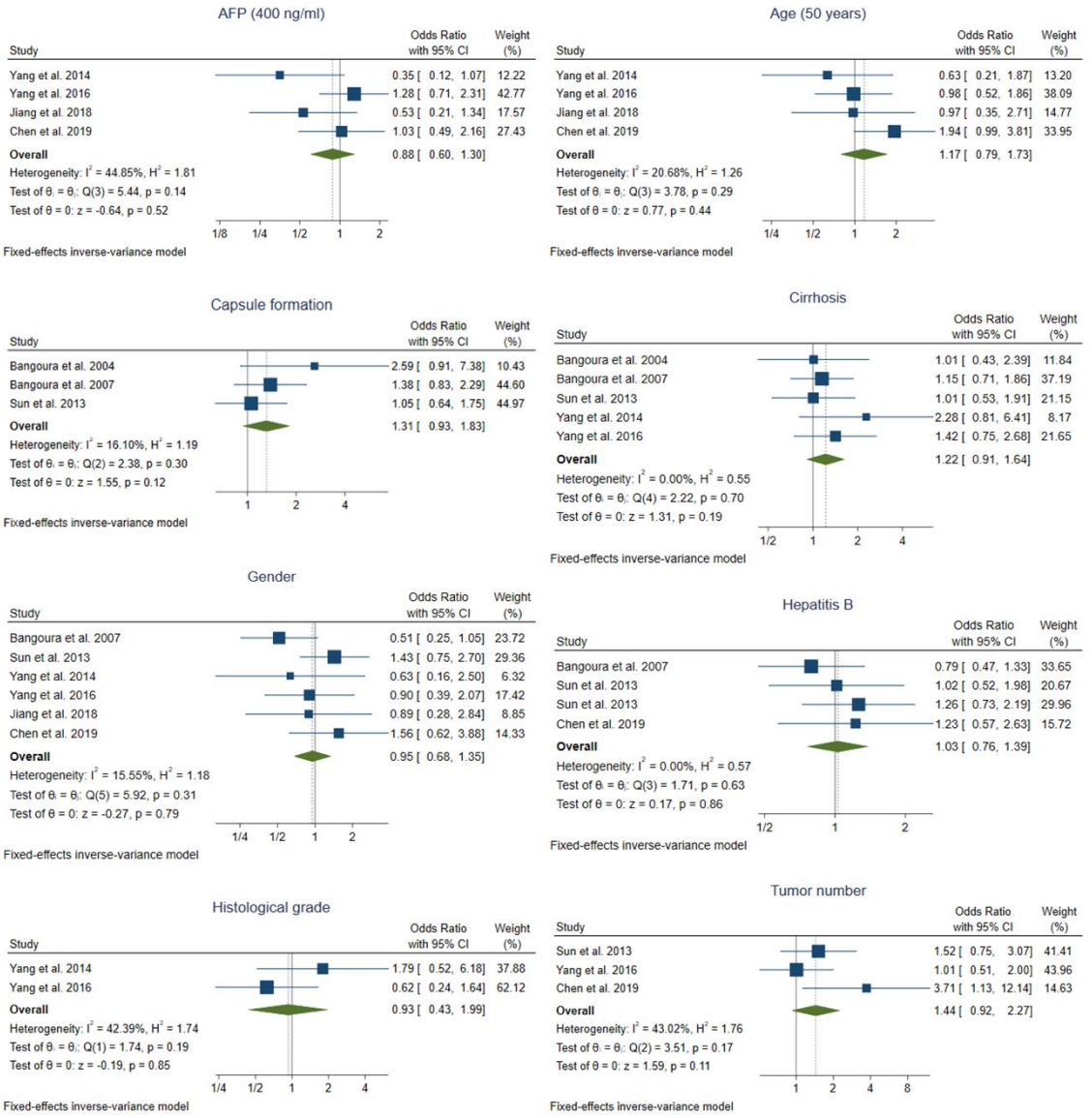

Figure 23. Meta-analysis of the association between HIF-2α overexpression and clinicopathological features in patients with HCC: characteristics not significantly related to HIF-2α and without heterogeneity across studies. Forest plots of HIF-2α expression associated with AFP levels (400 ng/ml), age (50 years), capsule formation, cirrhosis, gender, hepatitis B, histological grade and tumor number.

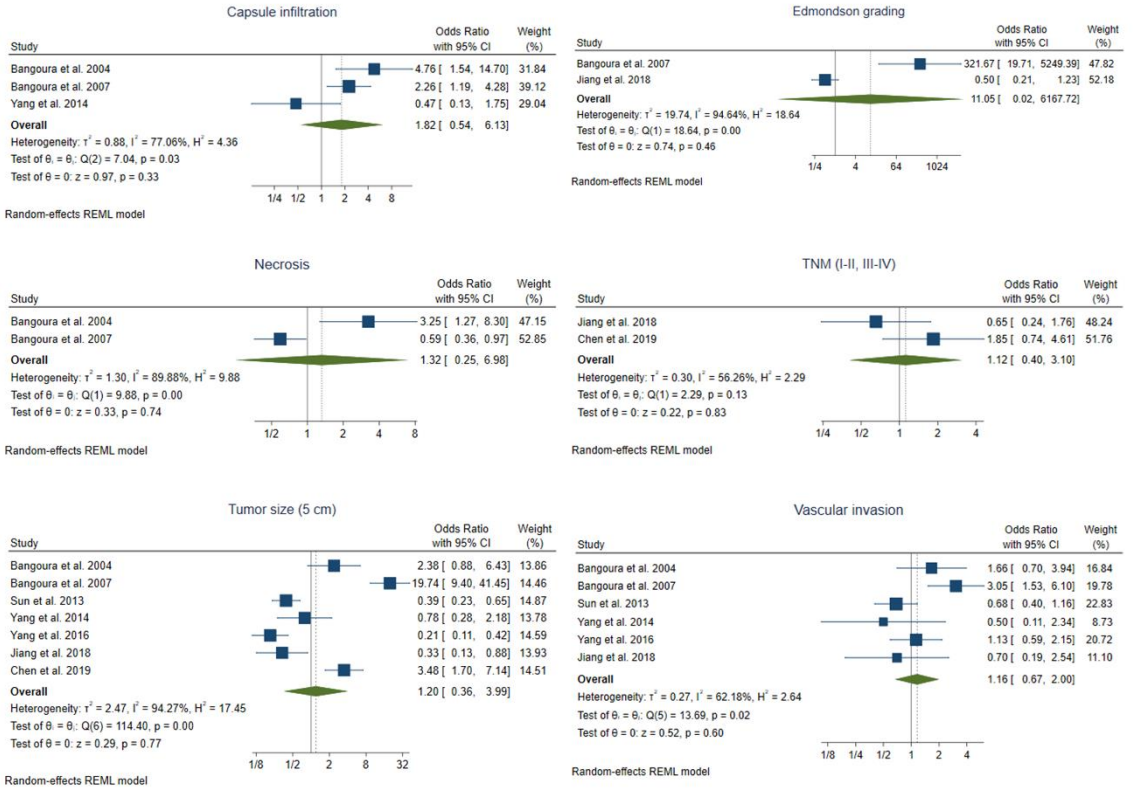

Figure 24. Meta-analysis of the relationship between HIF-2α overexpression and clinicopathological features in patients with HCC: characteristics not significantly related to HIF-2α and showing high heterogeneity between studies. Forest plots of HIF-2α expression associated with capsule infiltration, Edmondson grading, necrosis, TNM staging, tumor size (5 cm) and vascular invasion.

1.4 Subgroup analysis

To explore the potential sources of high heterogeneity, we performed subgroup analysis using sample size, NOS score, follow-up time and median age as moderators, which is summarized in **Table 6**. It should be mentioned that subgroups composed by a single study were not considered.

According to results of subgroups evaluation for HIF-1α based on sample size, HIF-1α overexpression was linked to AFP levels (20 ng/ml) (n≥100: OR, 1.59; 95% CI, 1.03-2.46; p=0.04), cirrhosis (n<300: OR, 1.48; 95% CI, 1.06-2.07; p=0.02), tumor size (5 cm) (n≥200: OR, 1.46; 95% CI, 1.04-2.06; p=0.03) and various subgroups of vascular invasion (n≥100: OR, 2.39; 95% CI, 1.58-3.61; p=0.00) (n<100: OR, 3.22; 95% CI, 1.87-5.55; p=0.00) (n≥200: OR, 1.32; 95% CI, 1.04-1.68; p=0.02) (n<200: OR, 3.54; 95% CI, 2.69-4.66; p=0.00) (n≥300: OR, 1.39; 95% CI, 1.08-1.79; p=0.01) (n<300: OR, 3.22; 95%

CI, 2.13-4.88; p=0.00) (n<400: OR, 3.04; 95% CI, 2.08-4.45; p=0.00); however, heterogeneity remained substantial in many cases. Subgroups by sample size in which heterogeneity was resolved were AFP levels (20 ng/ml) (n<100: I^2=0.00, Q-test p=0.40; n≥200/300: I^2=0.00, Q-test p=0.32), age (50 years) (n≥100: I^2=13.66, Q-test p=0.32; n<200: I^2=38.69, Q-test p=0.15), albumin (n≥100: I^2=2.23, Q-test p=0.31), cirrhosis (n<100: I^2=0.00, Q-test p=0.42), tumor size (5 cm) (n<100: I^2=20.05, Q-test p=0.27; n≥300: I^2=0.00, Q-test p=0.37) and vascular invasion (n<100: I^2=44.29, Q-test p=0.13; n≥200: I^2=2.54, Q-test p=0.38; n<200: I^2=35.11, Q-test p=0.11; n≥300: I^2=0.00, Q-test p=0.41; n≥400: I^2=0.00, Q-test p=0.87) **(Table 6)**.

Subgroups employing NOS score as moderator showed correlation between high HIF-1α levels and albumin (NOS<7: OR, 0.45; 95% CI, 0.21-0.93; p=0.03), tumor differentiation (NOS≥6: OR, 1.76; 95% CI, 1.04-2.97; p=0.04), tumor size (5 cm) (NOS=6: OR 2.27; 95% CI, 1.10-4.70; p=0.03) (NOS<7: OR, 2.45; 95% CI, 1.20-4.99; p=0.01) and vascular invasion (NOS≥7: OR, 1.99; 95% CI, 1.36-2.90; p=0.00) (NOS<7: OR, 4.00; 95% CI, 2.14-7.46; p=0.00), and among them only the albumin subgroup for NOS<7 exhibited an acceptable heterogeneity (NOS<7: I^2=36.71%, Q-test p=0.21). Additionally, subgroup based on NOS score solved heterogeneity for AFP levels (20 ng/ml) (NOS≥7: I^2=35.04%, Q-test p=0.20), AFP (400 ng/ml) (NOS≥7: I^2=49.57%, Q-test p=0.14), age (50 years) (NOS≥7: I^2=35.07%, Q-test p=0.20), cirrhosis (NOS≥7: I^2=35.56%, Q-test p=0.16) and histological grade (NOS≥7: I^2=28.40%, Q-test p=0.24) subgroups, although none of them reported a relationship with HIF-1α protein expression **(Table 6)**.

Interestingly, the removal of Zou *et al.* [220] in the AFP (20 ng/ml) analysis led to a greater decrease in heterogeneity (I^2=3.17, Q-test p=0.40), although there was no correlation with HIF-1α overexpression (OR, 1.21; 95% CI, 0.91-1.60; p=0.19). In the same way, the deletion of Xia *et al.* [205] and Tian *et al.* [218] for tumor differentiation resolved heterogeneity (I^2=3.09, Q-test p=0.40) and showed no association (OR, 1.25; 95% CI, 0.92-1.69; p=0.16). Nevertheless, for cirrhosis, reject the data from Xiang *et al.* [203] and Ma *et al.* [208] achieved low heterogeneity (I^2=33.52, Q-test p=0.12) and a significant association with HIF-1α protein levels (OR, 1.33; 95% CI, 1.05-1.69; p=0.02).

Likewise, heterogeneity for histological grade was eliminated through excluding Wang *et al.* [209] (I^2=0.00, Q-test p=0.53), also showing correlation to HIF-1α (OR, 2.04; 95% CI, 1.12-3.69; p=0.02) **(Table 6)**.

For HIF-2α, subgroups according to sample size as moderator showed that high expression of the HIF-2α protein was related to OS (n<200: HR, 1.83; 95% CI, 1.18-2.84; p=0.01), removing heterogeneity (n<200: I^2=0.00; Q-test p=0.93). Besides, sample size subgroups resolved heterogeneity in vascular invasion (n<100: I^2=16.26, Q-test p=0.27; n<200: I^2=15.06, Q-test p=0.31; n<300: I^2=3.84, Q-test p=0.38), but no relationship with HIF-2α levels was found. Similarly, follow-up subgroups denoted a correlation between OS and HIF-2α overexpression (follow-up>72: HR, 2.47; 95% CI, 2.02-3.03; p=0.00) with reduced heterogeneity (follow-up>72: I^2=11.74, Q-test p=0.29). Capsule infiltration was also examined based on median age, exhibiting correlation to HIF-2α (years≥50: OR, 2.71; 95% CI, 1.55-4.73; p=0.00) and reduced heterogeneity (years≥50: I^2=21.15, Q-test p=0.26). Classification of subgroups by NOS score did not reveal any adjustment. Accordingly, the heterogeneity for tumor size (5 cm) characteristic of the HIF-2α study could not be resolved. **(Table 6)**.

Overall, these results of the subgroup analysis revealed that sample size, NOS score, median age and follow-up time appear to be triggers for the heterogeneity found.

Table 6. Subgroup analysis of heterogeneous prognostic and clinicopathological features.

HIF-1α										
Subgroups	**Number of studies (n)**	**Number of cases (n)**	**HIF-1α⁺ (n)**	**HIF-1α⁺ (%)**	**Pooled data**			**Test for heterogeneity**		**Model used**
					OR	**95% CI**	**p-value**	**Q-test p-value**	**I^2 (%)**	
AFP (20 ng/ml)										
Sample size (n)										
≥100	5	1106	481	43.49	1.59	1.03-2.46	0.04*	0.06	55.89	REM
<100	2	116	49	42.24	0.74	0.35-1.59	0.45	0.40	0.00	FEM
≥200/300	2	715	297	41.54	1.31	0.91-1.89	0.15	0.32	0.00	FEM
<200/300	5	507	233	45.96	1.39	0.73-2.64	0.31	0.02	64.06	REM
≥400	1	406	212	52.22	1.12	0.69-1.81	–	–	–	–
<400	6	816	318	38.97	1.45	0.88-2.40	0.14	0.04	57.84	REM
NOS score										
≥7	4	894	366	40.94	1.27	0.93-1.75	0.13	0.20	35.04	FEM
<7	3	328	164	50.00	1.61	0.67-3.88	0.29	0.03	68.87	REM
Without Zou *et al*. [220]	6	1084	457	42.16	1.21	0.91-1.60	0.19	0.40	3.17	FEM
AFP (400 ng/ml)										
Sample size (n)										

≥100	2	263	140	53.23	1.16	0.45-2.98	0.75	0.06	72.69	REM
<100	2	162	76	46.91	2.03	0.38-10.90	0.41	0.02	82.78	REM
NOS score										
≥7	3	335	177	52.84	1.11	0.72-1.71	0.65	0.14	49.57	FEM
<7	1	90	39	43.33	4.86	1.73-13.62	–	–	–	–
Age (50 years)										
Sample size (n)										
≥100	4	566	298	52.65	1.00	0.70-1.43	0.99	0.32	13.66	FEM
<100	3	231	106	45.89	0.70	0.26-1.94	0.50	0.03	71.05	REM
≥200	1	201	94	46.77	1.50	0.81-2.79	–	–	–	–
<200	6	596	310	52.01	0.77	0.55-1.09	0.14	0.15	38.69	FEM
NOS score										
≥7	4	404	207	51.24	0.95	0.63-1.43	0.82	0.20	35.07	FEM
<7	3	393	197	50.13	0.74	0.33-1.66	0.46	0.03	68.99	REM
Albumin										
Sample size (n)										
≥100	2	275	141	51.27	0.82	0.45-1.51	0.53	0.31	2.23	FEM
<100	1	90	39	43.33	0.21	0.05-0.84	–	–	–	–
NOS score										
≥7	1	137	68	49.64	1.12	0.48-2.59	–	–	–	–

<7	2	228	112	49.12	0.45	0.21-0.93	0.03*	0.21	36.71	FEM
Cirrhosis										
Sample size (n)										
≥100	10	1878	958	51.01	1.40	0.95-2.07	0.09	0.01	59.07	REM
<100	4	258	107	41.47	1.18	0.67-2.06	0.56	0.42	0.00	FEM
≥200	4	1122	570	71.36	1.35	0.73-2.48	0.34	0.03	68.62	REM
<200	10	1014	495	48.82	1.32	0.90-1.95	0.16	0.08	36.74	REM
≥300	2	715	297	41.54	0.89	0.48-1.66	0.72	0.14	54.49	REM
<300	12	1421	768	54.05	1.48	1.06-2.07	0.02*	0.07	35.53	REM
≥400	1	406	212	52.22	1.16	0.73-1.86	–	–	–	–
<400	13	1730	853	49.31	1.35	0.95-1.92	0.10	0.02	48.04	REM
NOS score										
≥7	7	1360	639	46.99	1.20	0.91-1.58	0.19	0.16	35.56	FEM
<7	7	776	426	54.90	1.37	0.76-2.45	0.30	0.03	57.23	REM
Without Xiang *et al.* [203] and Ma *et al.* [208]	12	1620	833	51.42	1.33	1.05-1.69	0.02*	0.12	33.52	FEM
Histological grade										
Sample size (n)										
≥100	1	126	72	57.14	1.15	0.43-3.04	–	–	–	–

<100	4	267	115	43.07	1.70	0.58-4.95	0.33	0.06	60.50	REM
NOS score										
≥7	2	198	109	55.05	1.67	0.79-3.54	0.18	0.24	28.40	FEM
<7	3	195	78	40.00	1.40	0.32-6.02	0.65	0.04	68.67	REM
Without Wang *et al.* [209]	4	348	155	44.54	2.04	1.12-3.69	0.02*	0.53	0.00	FEM
Tumor differentiation										
Sample size (n)										
≥100	5	1168	534	45.72	1.53	0.86-2.74	0.15	0.00	76.26	REM
<100	4	216	107	49.54	4.82	0.59-39.55	0.14	0.01	81.86	REM
≥200	3	915	423	46.23	1.59	0.70-3.60	0.27	0.00	83.89	REM
<200	6	469	218	46.48	2.36	0.85-6.51	0.10	0.01	75.68	REM
≥300	2	715	297	41.54	1.93	0.58-6.40	0.28	0.00	90.39	REM
<300	7	669	344	51.42	1.68	0.92-3.07	0.09	0.01	53.66	REM
≥400	1	406	212	52.22	3.54	2.15-5.83	–	–	–	–
<400	8	978	429	43.87	1.42	0.93-2.17	0.10	0.01	37.68	REM
NOS score										
5	1	35	28	80.00	3.04	0.15-62.85	–	–	–	–
6	3	255	121	47.45	7.25	0.47-111.92	0.16	0.01	90.53	REM
7	5	1094	492	44.97	1.38	0.79-2.43	0.26	0.00	72.22	REM

NOS (threshold 6)										
≥6	8	1349	613	45.44	1.76	1.04-2.97	0.04*	0.00	70.54	REM
<6	1	35	28	80.00	3.04	0.15-62.85	–	–	–	–
NOS (threshold 7)										
≥7	5	1094	492	44.97	1.38	0.79-2.43	0.26	0.00	72.22	REM
<7	4	290	149	51.38	5.47	0.79-37.76	0.08	0.03	80.72	REM
Without Xia *et al.* [205] and Tian *et al.* [218]	7	913	399	43.70	1.25	0.92-1.69	0.16	0.40	3.09	FEM
Tumor size (5 cm)										
Sample size (n)										
≥100	11	2079	1052	50.60	1.75	0.90-3.39	0.10	0.00	91.66	REM
<100	8	467	250	53.53	0.88	0.59-1.31	0.53	0.27	20.05	FEM
≥200	5	1323	664	50.19	1.46	1.04-2.06	0.03*	0.08	51.84	REM
<200	14	1223	638	52.17	1.37	0.71-2.65	0.35	0.00	84.81	REM
≥300	2	715	297	41.54	1.15	0.84-1.57	0.38	0.37	0.00	FEM
<300	17	1831	1005	54.89	1.45	0.85-2.46	0.17	0.00	84.36	REM
≥400	1	406	212	52.22	1.28	0.87-1.91	–	–	–	–
<400	18	2140	1090	50.93	1.41	0.86-2.31	0.18	0.00	84.50	REM
NOS score										

5	1	35	28	80	15.00	0.78-287.68	–	–	–	–
6	9	1027	575	55.99	2.27	1.10-4.70	0.03*	0.00	84.53	REM
7	9	1484	699	47.10	0.84	0.57-1.24	0.38	0.01	65.64	REM
NOS (threshold 6)										
≥6	18	2511	1274	50.74	1.34	0.84-2.13	0.22	0.00	85.49	REM
<6	1	35	28	80	15.00	0.78-287.68	–	–	–	–
NOS (threshold 7)										
≥7	9	1484	699	47.10	0.84	0.57-1.24	0.38	0.01	65.64	REM
<7	10	1062	603	56.78	2.45	1.20-4.99	0.01*	0.00	83.02	REM
Vascular invasion										
Sample size (n)										
≥100	11	2233	1106	49.53	2.39	1.58-3.61	0.00*	0.00	75.38	REM
<100	5	327	137	41.90	3.22	1.87-5.55	0.00*	0.13	44.29	FEM
≥200	4	1334	646	48.43	1.32	1.04-1.68	0.02*	0.38	2.54	FEM
<200	12	1226	597	48.69	3.54	2.69-4.66	0.00*	0.11	35.11	FEM
≥300	3	1134	520	45.86	1.39	1.08-1.79	0.01*	0.41	0.00	FEM
<300	13	1426	723	50.70	3.22	2.13-4.88	0.00*	0.00	57.60	REM
≥400	2	825	435	52.73	1.28	0.97-1.70	0.08	0.87	0.00	FEM
<400	14	1735	808	46.57	3.04	2.08-4.45	0.00*	0.00	57.00	REM
NOS score										

≥7	9	1848	892	48.27	1.99	1.36-2.90	0.00*	0.01	63.60	REM
<7	7	712	351	49.30	4.00	2.14-7.46	0.00*	0.02	58.51	REM
HIF-2α										
Subgroups	**Number of studies (n)**	**Number of cases (n)**	**HIF-2α⁺ (n)**	**HIF-2α⁺ (%)**	**Pooled data**			**Test for heterogeneity**		**Model used**
					HR	**95% CI**	**p-value**	**Q-test p-value**	**I^2 (%)**	
Overall Survival										
Sample size (n)										
≥200	3	767	404	53.67	1.00	0.39-2.60	1.00	0.00	96.06	REM
<200	2	265	84	31.70	1.83	1.18-2.84	0.01*	0.93	0.00	FEM
≥300	1	315	219	69.52	2.58	2.08-3.20	–	–	–	–
<300	4	717	269	37.52	1.01	0.55-1.87	0.97	0.00	84.09	REM
NOS score										
≥7	3	660	353	53.48	1.44	0.61-3.42	0.41	0.00	93.51	REM
<7	2	372	135	36.29	1.00	0.35-2.84	1.00	0.01	85.67	REM
Follow-up (months)										
>72	2	454	286	63.00	2.47	2.02-3.03	0.00*	0.29	11.74	FEM
≤72	3	578	202	34.95	0.82	0.44-1.54	0.54	0.02	81.14	REM
Subgroups	**Number of studies (n)**	**Number of cases (n)**	**HIF-2α⁺ (n)**	**HIF-2α⁺ (%)**	**Pooled data**			**Test for heterogeneity**		**Model used**
					OR	**95% CI**	**p-value**	**Q-test p-value**	**I^2 (%)**	

Capsule infiltration										
Sample size (n)										
≥100	2	441	236	53.51	1.15	0.25-5.27	0.85	0.04	77.39	REM
<100	1	97	31	31.96	4.76	1.54-14.70	–	–	–	–
≥200	1	315	219	69.52	2.26	1.19-4.28	–	–	–	–
<200	2	223	48	21.52	1.54	0.16-14.79	0.71	0.01	85.41	REM
NOS score										
≥7	1	315	219	69.52	2.26	1.19-4.28	–	–	–	–
<7	2	223	48	21.52	1.54	0.16-14.79	0.71	0.01	85.41	REM
Median age (years)										
≥50	2	412	250	60.68	2.71	1.55-4.73	0.00*	0.26	21.15	FEM
<50	1	126	17	13.49	0.47	0.13-1.75	–	–	–	–
Tumor size (5 cm)										
Sample size (n)										
≥100	5	1032	488	47.29	1.34	0.27-6.71	0.72	0.00	96.16	REM
<100	2	181	65	35.91	0.89	0.13-6.10	0.90	0.01	87.06	REM
≥200	3	767	404	52.67	1.17	0.07-18.75	0.91	0.00	98.22	REM
<200	4	446	149	33.41	1.25	0.43-3.60	0.69	0.00	81.42	REM
≥300	1	315	219	69.52	19.74	9.40-41.45	–	–	–	–
<300	6	898	334	37.19	0.74	0.30-1.85	0.52	0.00	88.12	REM

NOS score										
≥7	5	870	404	46.44	1.32	0.26-6.80	0.74	0.00	95.19	REM
<7	2	343	149	43.44	0.91	0.15-5.39	0.92	0.00	90.05	REM
Vascular invasion										
Sample size (n)										
≥100	4	893	421	47.14	1.13	0.53-2.42	0.75	0.01	75.80	REM
<100	2	181	65	35.91	1.27	0.62-2.60	0.51	0.27	16.26	FEM
≥200	3	767	404	52.67	1.30	0.55-3.07	0.54	0.00	82.57	REM
<200	3	307	82	26.71	1.08	0.56-2.06	0.82	0.31	15.06	FEM
≥300	1	315	219	69.52	3.05	1.53-6.10	–	–	–	–
<300	5	759	267	35.18	0.90	0.64-1.27	0.55	0.38	3.84	FEM
NOS score										
≥7	4	731	337	46.10	1.24	0.57-2.70	0.59	0.04	63.40	REM
<7	2	343	149	43.44	1.00	0.42-2.35	0.99	0.09	66.09	REM

* Significant association with HIF, $p<0.05$

1.5 Publication bias

The results obtained from the publication bias assessment are summarized in **Table 7**.

Table 7. Assessment of publication bias on survival-related parameters and clinicopathological features.

HIF-1α					
Survival	**Number of studies**	**Egger's test (p-value)**	**Model used**	**Trim-and-fill HR (95% CI)**	**Imputed studies**
OS	18	0.00*	FEM	1.56 (1.41-1.73)	7
DFS/RFS	8	0.06	FEM	–	–
Clinicopathological feature	**Number of studies**	**Egger's test (p-value)**	**Model used**	**Trim-and-fill OR (95% CI)**	**Imputed studies**
AFP (20 ng/ml)	7	0.59	REM	–	–
AFP (400 ng/ml)	4	0.41	REM	–	–
Age (50 years)	7	0.18	REM	–	–
Age (60 years)	4	0.24	FEM	–	–
Albumin	3	0.07	REM	–	–
ALT (40 U/L)	3	0.33	FEM	–	–
ALT (80 U/L)	3	0.59	FEM	–	–
BCLC	3	0.58	FEM	–	–
Bilirubin	2	0.51	FEM	–	–
Capsule formation	7	0.93	FEM	–	–
Capsule infiltration	2	0.38	FEM	–	–
Child-Pugh score	3	0.85	FEM	–	–
Cirrhosis	14	0.97	REM	–	–
Distant metastasis	2	†	REM	–	–
Edmondson	3	0.08	FEM	–	–
Gender	19	0.03*	FEM	0.83 (0.69-1.00)	5

Hepatitis B	16	0.91	FEM	–	–
Hepatitis C	4	0.94	FEM	–	–
Histological grade	5	0.82	REM	–	–
Intrahepatic metastasis	3	0.70	FEM	–	–
Lymph node metastasis	3	0.39	FEM	–	–
TNM (I, II-III)	4	0.35	FEM	–	–
TNM (I-II, III)	2	0.99	FEM	–	–
TNM (I-II, III-IV)	3	0.50	FEM	–	–
Tumor differentiation	9	0.04*	REM	1.78 (1.07-2.96)	0
Tumor number	8	0.32	FEM	–	–
Tumor size (3 cm)	2	0.47	FEM	–	–
Tumor size (5 cm)	19	0.47	REM	–	–
Vascular invasion	16	0.00*	REM	1.75 (1.12-2.73)	6
Vasculogenic mimicry	3	0.33	FEM	–	–
HIF-2α					
Survival	**Number of studies**	**Egger's test (p-value)**	**Model used**	**Trim-and-fill HR (95% CI)**	**Imputed studies**
OS	5	0.93	REM	–	–
DFS/RFS	3	0.55	FEM	–	–
Clinicopathological feature	**Number of studies**	**Egger's test (p-value)**	**Model used**	**Trim-and-fill OR (95% CI)**	**Imputed studies**
AFP (400 ng/ml)	4	0.02*	FEM	1.00 (0.69-1.44)	1
Age (50 years)	4	0.27	FEM	–	–
Capsule formation	3	0.17	FEM	–	–

Capsule infiltration	3	0.63	REM	–	–
Cirrhosis	5	0.46	FEM	–	–
Edmondson	2	†	REM	–	–
Gender	6	0.67	FEM	–	–
Hepatitis B	4	0.54	FEM	–	–
Histological grade	2	0.19	FEM	–	–
Necrosis	2	†	REM	–	–
TNM (I-II, III-IV)	2	†	REM	–	–
Tumor number	3	0.08	FEM	–	–
Tumor size (5 cm)	7	0.89	REM	–	–
Vascular invasion	6	0.46	REM	–	–

*Significant publication bias, p<0.05; †Convergence not achieved during tau2 estimation

A strong funnel plot asymmetry was identified in the analysis of the OS parameter for HIF-1α evidencing publication bias, which was confirmed by the Egger's test (p=0.00). Therefore, the trim-and-fill method was implemented, where seven studies were imputed and the global effect size was readjusted (HR, 1.56; 95% CI, 1.41-1.73). Conversely, Egger's test did not report asymmetry in DFS/RFS (p=0.06) for HIF-1α, nor in OS (p=0.93) and DFS/RFS (p=0.55) for HIF-2α **(Table 7; Figure 25)**.

Among the clinicopathological features of HIF-1α, asymmetry was detected for gender (p=0.03), tumor differentiation (p=0.04) and vascular invasion (p=0.00). In gender, trim-and-fill analysis imputed five studies and estimated a corrected global effect (OR, 0.83; 95% CI, 0.69-1.00). Similarly, six "missing" reports were added to the improved funnel plot for vascular invasion, correcting for the pooled effect size (OR, 1.75; 95% CI, 1.12-2.73). Conversely, for tumor differentiation the trim-and-fill method did not include any "missing" studies; thus, global effect size remained intact. For HIF-1α parameters, all imputed studies were aggregated on the left side of the funnel plots **(Table 7; Figures 26 and 27)**.

Regarding the clinicopathological characteristics of HIF-2α, the Egger's test only displayed asymmetry for AFP levels (p=0.02). After the trim-and-fill analysis, one study was imputed on the right side of the funnel plot and the global effect was adjusted (OR, 1.00; 95% CI, 0.69-1.44) **(Table 7; Figure 28)**.

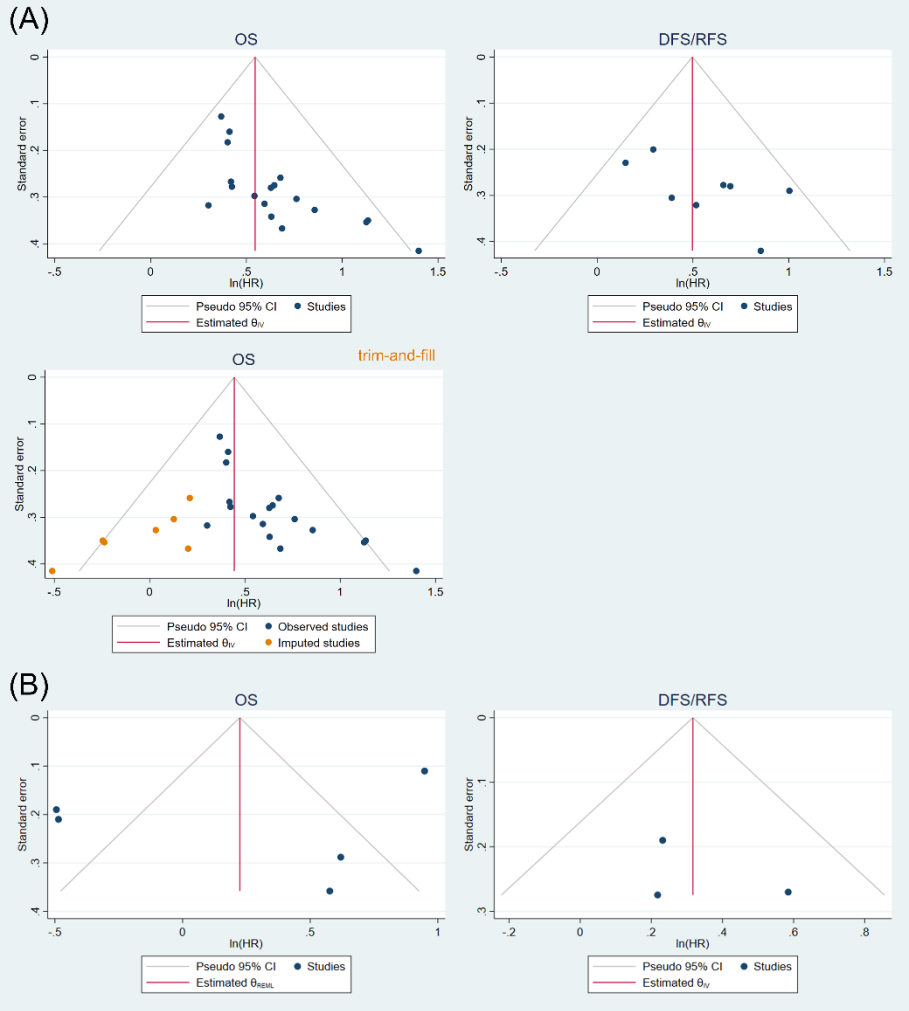

Figure 25. Publication bias evaluation of the relationship between survival-related parameters and the expression of HIF-1α and HIF-2α in patients with HCC. Funnel plots of OS and DFS/RFS for **(A)** HIF-1α, including trim-and-fill funnel plot for OS (orange circles represent imputed articles), and for **(B)** HIF-2α.

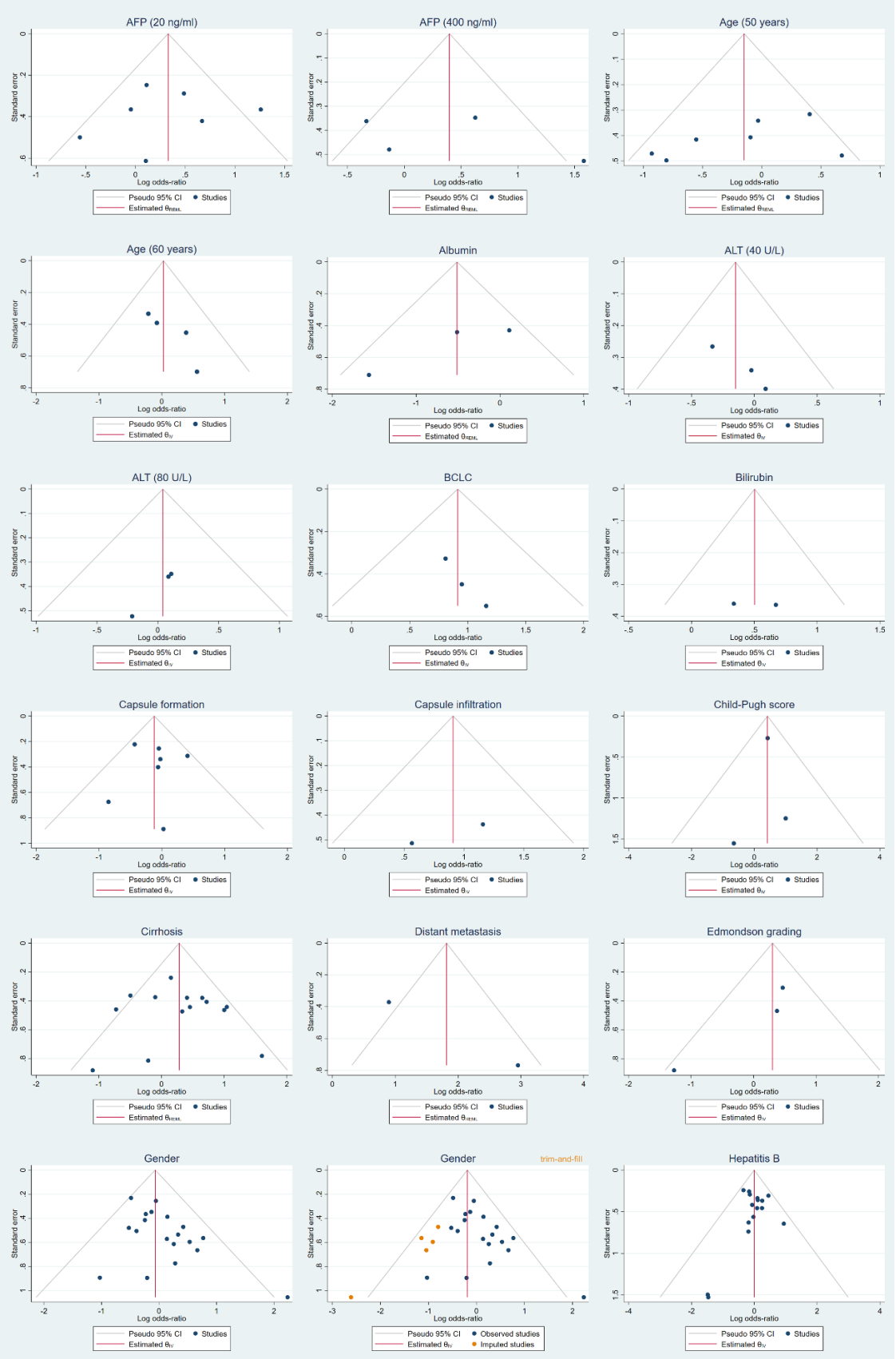

Figure 26. Publication bias assessment of the association of HIF-1α expression with clinicopathological features in patients with HCC (part 1). Funnel plots of the

relationship between HIF-1α expression and AFP, age, albumin, ALT, BCLC staging, bilirubin, capsule formation, capsule infiltration, Child-Pugh score, cirrhosis, distant metastasis, Edmondson grading, gender and hepatitis B. For trim-and-fill funnel plot of gender, orange circles represent the imputed articles.

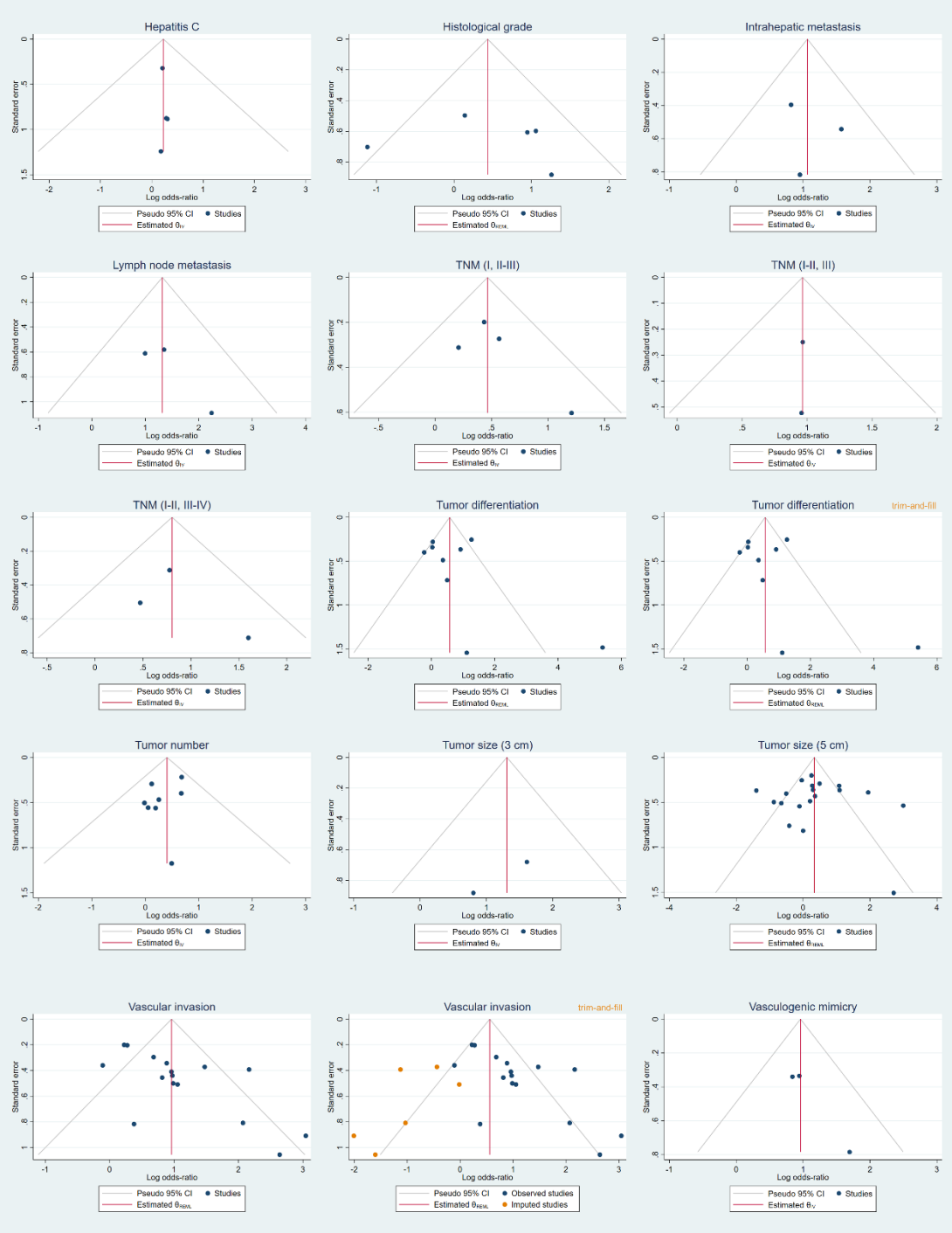

Figure 27. Publication bias analysis of the association of HIF-1α expression with clinicopathological features in patients with HCC (part 2). Funnel plots of the relationship between HIF-1α expression and hepatitis C, histological grade, intrahepatic metastasis, lymph node metastasis, TNM staging, tumor differentiation,

tumor number, tumor size, vascular invasion, and vasculogenic mimicry. Trim-and-fill funnel plot of tumor differentiation and vascular invasion are also included, and orange circles represent the imputed articles.

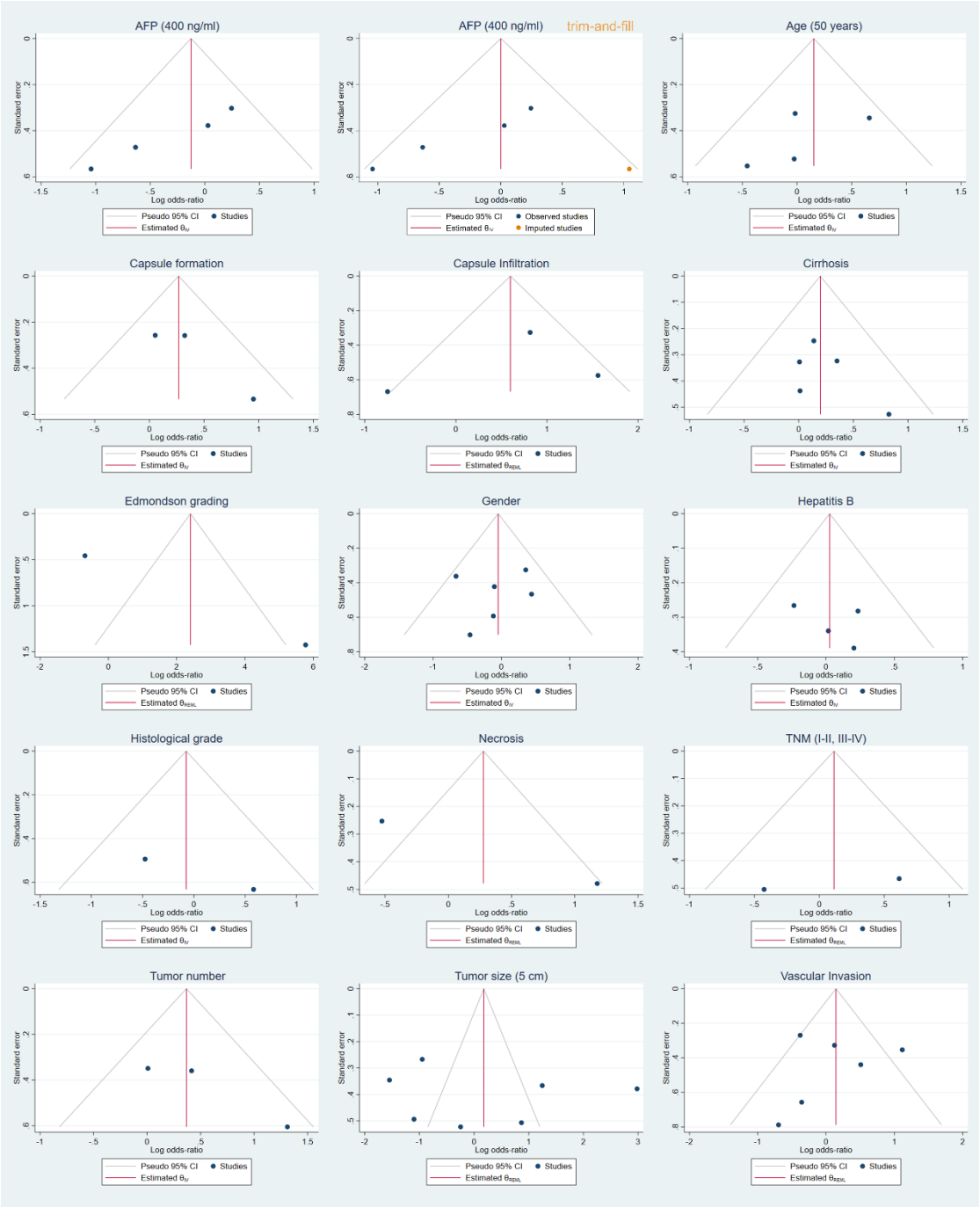

Figure 28. Publication bias assessment of the association of HIF-2α expression with clinicopathological features in patients with HCC. Funnel plots of the relationship between HIF-1α expression and AFP, age, capsule formation, capsule infiltration, cirrhosis, Edmondson grading, gender, hepatitis B, histological grade, necrosis, TNM staging, tumor number, tumor size and vascular invasion. For trim-and-fill funnel plot of AFP, orange circles represent imputed articles.

2 Role of hypoxia-mediated response on acquired resistance to sorafenib: An *in vitro* study

Sorafenib was the first drug approved against advanced HCC. Despite its efficacy, after sustained treatment with this drug, tumor cells are capable of developing resistance mechanisms to evade the anti-tumor effects of sorafenib. Among them, the anti-angiogenic effect of sorafenib can induce intratumoral hypoxia, a characteristic closely related to the selection of more invasive clones, resistance and worse prognosis [123]. In order to study the implication of hypoxia in the phenomenon of sorafenib resistance, we employed the human HCC cell line HepG2 and two cell lines derived from HepG2 with acquired resistance to sorafenib, defined as HepG2S1 and HepG2S3, obtaining the following results that appear below

2.1 Characterization of growth dynamics and cell proliferation of sorafenib-resistant cells

First, we compared the growth dynamics of the two resistant cell lines and the parental line HepG2 in the absence and presence of 6 µM sorafenib over 5 days, both under normoxic and hypoxic conditions. Sorafenib treatment repressed cell growth of the parental HepG2 line under both oxygen conditions. Nevertheless, HepG2S1 and HepG2S3 cells displayed a higher growth rate than HepG2 in normoxia and hypoxia, being even greater than that shown by parental cells in the absence of sorafenib. Concerning resistant cell lines, HepG2S1 exhibited the uppermost growth capacity, being significantly superior to that observed in HepG2S3 cells. Moreover, the hypoxic microenvironment increased the difference in cell growth observed between both resistant lines and the untreated HepG2 **(Figure 29A)**.

These data coincide with those obtained from the study of proliferative capacity by analyzing the expression of the proliferation marker Ki67 under hypoxia. Sorafenib administration reduced proliferation of HepG2 cells, while resistant cells showed greater proliferation capacity than HepG2 cells even compared to HepG2 without treatment **(Figure 30)**. Taken together, these data suggest that resistant cell lines display a more aggressive phenotype than sorafenib-sensitive cells.

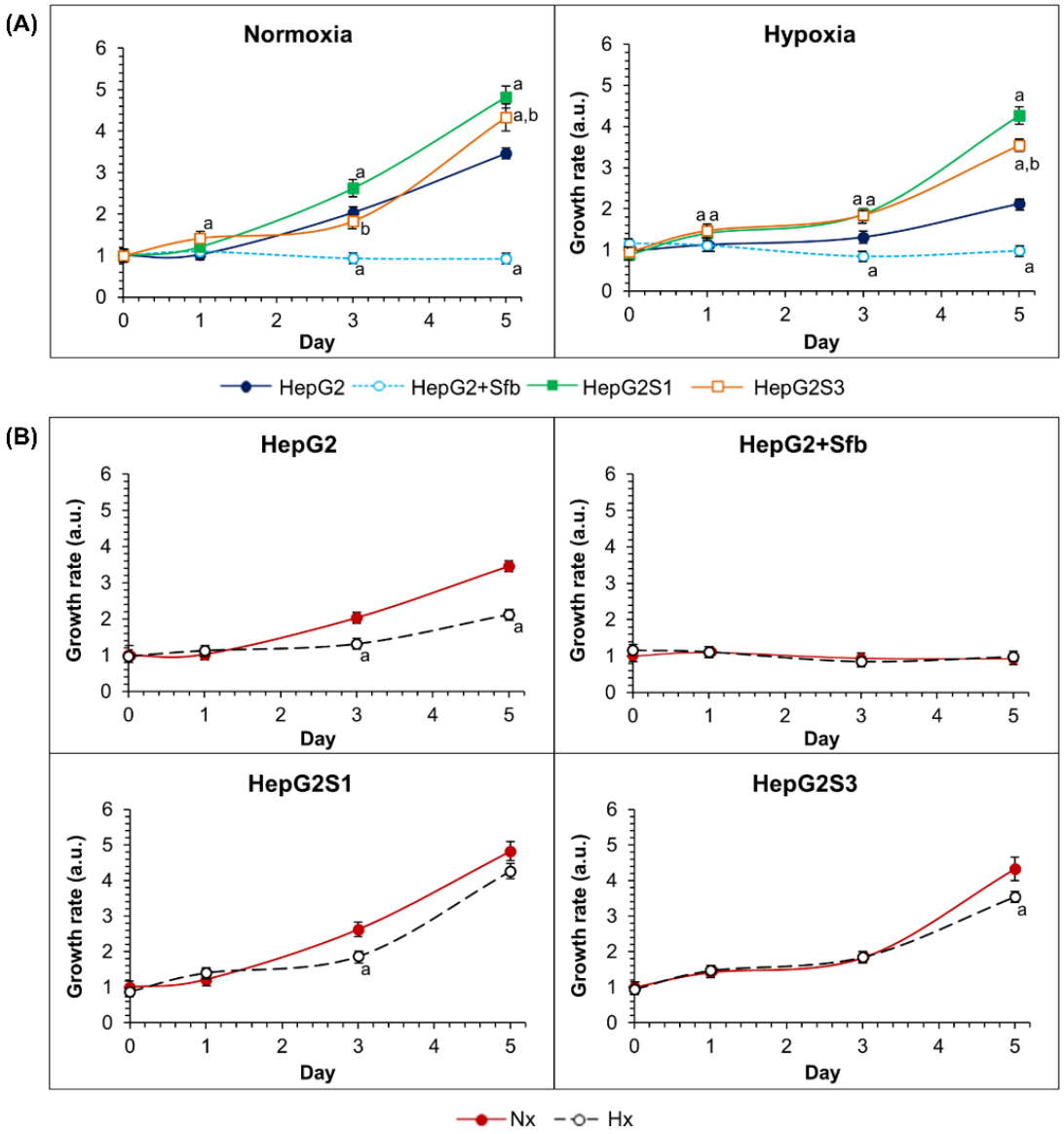

Figure 29. Characterization of growth dynamics by comparing sorafenib-sensitive and sorafenib-resistant cells under normoxia and hypoxia. (A) Contrast of cell growth between sorafenib-resistant cell lines, HepG2S1 and HepG2S3, and HepG2 parental line under both normoxia and hypoxia. [a] $p<0.05$ significant changes *vs.* non-treated HepG2 cells, [b] $p<0.05$ significant differences between sorafenib-resistant cells; **(B)** Comparison of cell growth between normoxia and hypoxia within the same cell line. [a] $p<0.05$ respect to normoxic cells. Data are expressed as mean values of arbitrary units (a.u.) ± SD of three independent experiments.

Furthermore, we contrasted the growth capacity independently for each cell line between normoxia and hypoxia. The results showed that the growth of the untreated HepG2 cells was markedly reduced by hypoxia induction, whereas HepG2S1 and HepG2S3 cells preserved a similar growth rate under both oxygen conditions **(Figure**

29B). These suggest that the resistant cells could have adaptive mechanisms against hypoxia.

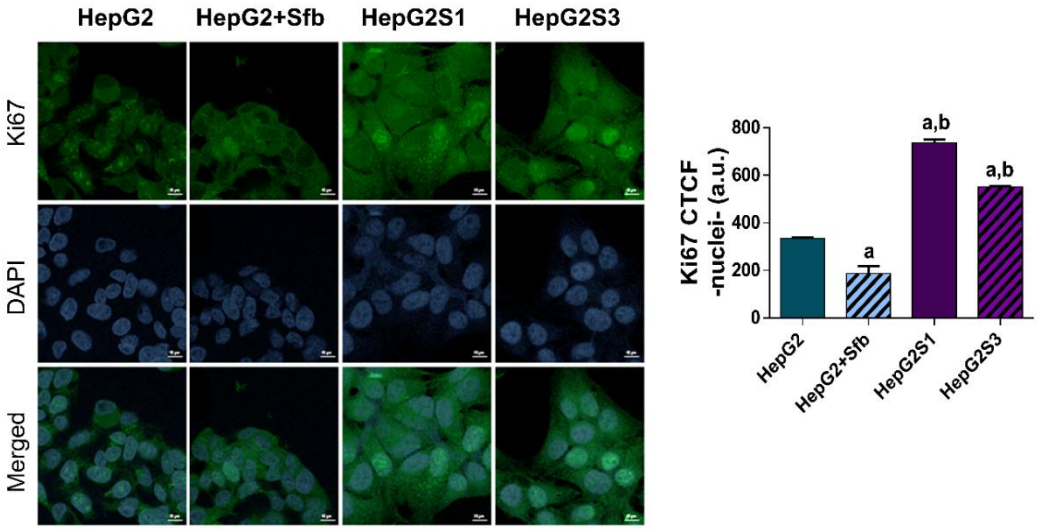

Figure 30. Assessment of cell proliferation by comparing Ki67 expression between sorafenib-sensitive and sorafenib-resistant cells under hypoxic conditions. Comparison of cell proliferation between resistant cell lines and HepG2 cells with or without sorafenib subjected to hypoxia induction for 24 h. Confocal microscopy images show Ki67 expression (green), and DAPI staining (blue) denotes cell nuclei. Bar graph represent nuclear expression of Ki67. Magnification: 63X, scale bar: 10 µm. [a] $p<0.05$ and [b] $p<0.05$ indicate significant differences respect to non-treated and sorafenib-treated HepG2 cells, respectively. Data are expressed as mean values of a.u. ± SD of three independent experiments.

2.2 Evaluation of protein expression and regulation of the major regulators of hypoxia-mediated response, HIF-1α and HIF-2α, in sorafenib-resistant cell lines

Hypoxia is a cellular stress that promotes an adaptive response by stabilizing HIFs [123]. Considering the data previously reported, we evaluated how HepG2S1 and HepG2S3 sorafenib-resistant cells respond against the induction of hypoxia by studying HIF-1α and HIF-2α expression over 48 h.

Based on Western blot analysis, HepG2 cells exhibited a progressive enhance of HIF-1α protein expression owing to the induction of hypoxia, while the administration of sorafenib prevented its increase. Resistant HepG2S3 cells showed a greater expression of HIF-1α compared to HepG2 cells treated with sorafenib, and denoted

similar levels to untreated parental line. However, it was the HepG2S1 cell line in which we found the highest HIF-1α overexpression in a time-dependent manner. Regarding HIF-2α, both sorafenib-resistant cell lines displayed a notable increment of its protein expression in relation to the parental line HepG2 subjected or not to sorafenib, where no detectable HIF-2α expression were found. It should be mentioned that even under normoxia resistant cells revealed a significant expression of HIF-1α and HIF-2α, which is not denoted by parental cells **(Figure 31)**.

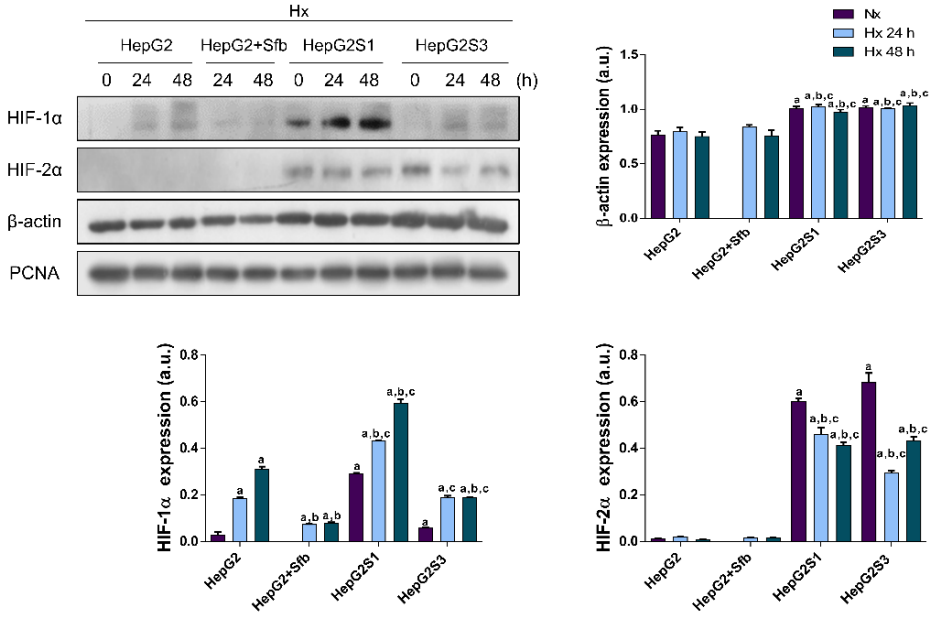

Figure 31. Analysis of HIF-1α and HIF-2α protein expression under normoxic and hypoxic conditions. Lanes 0 h represent basal protein levels under normoxia, and hypoxia was tested after 24 and 48 h. PCNA was used as internal loading control. [a] $p<0.05$ denotes significant changes in comparison with non-treated HepG2 cells in normoxia, [b] $p<0.05$ and [c] $p<0.05$ respect to non-treated and sorafenib-treated HepG2 cells in hypoxia, correspondingly, for each time point. Data are expressed as mean values of a.u. ± SD of three independent experiments.

As a loading control we started using β-actin. Nonetheless, marked changes in the expression levels of β-actin between parental and resistant cell lines were found, being overexpressed in HepG2S1 and HepG2S3 cells **(Figure 31)**. Therefore, since cytoskeletal proteins seemed to be altered, which can be explained by the different morphology of resistant cells **(Figure 16)**, we decided to employ the nuclear protein

PCNA as housekeeping **(Figure 31)**. The validation of PCNA as an internal reference of expression has been tested in several studies, defining its stability [251–253].

The HIFs expression trends in hypoxia were confirmed by determining the expression of both hypoxic factors by ICC/IF. Additionally, since HIFs are transcription factors, the nuclear translocation of HIF-1α and HIF-2α was also evaluated, which shows a greater translocation rate of HIFs in HepG2S1 and HepG2S3 cell lines compared to HepG2 cells **(Figure 32)**.

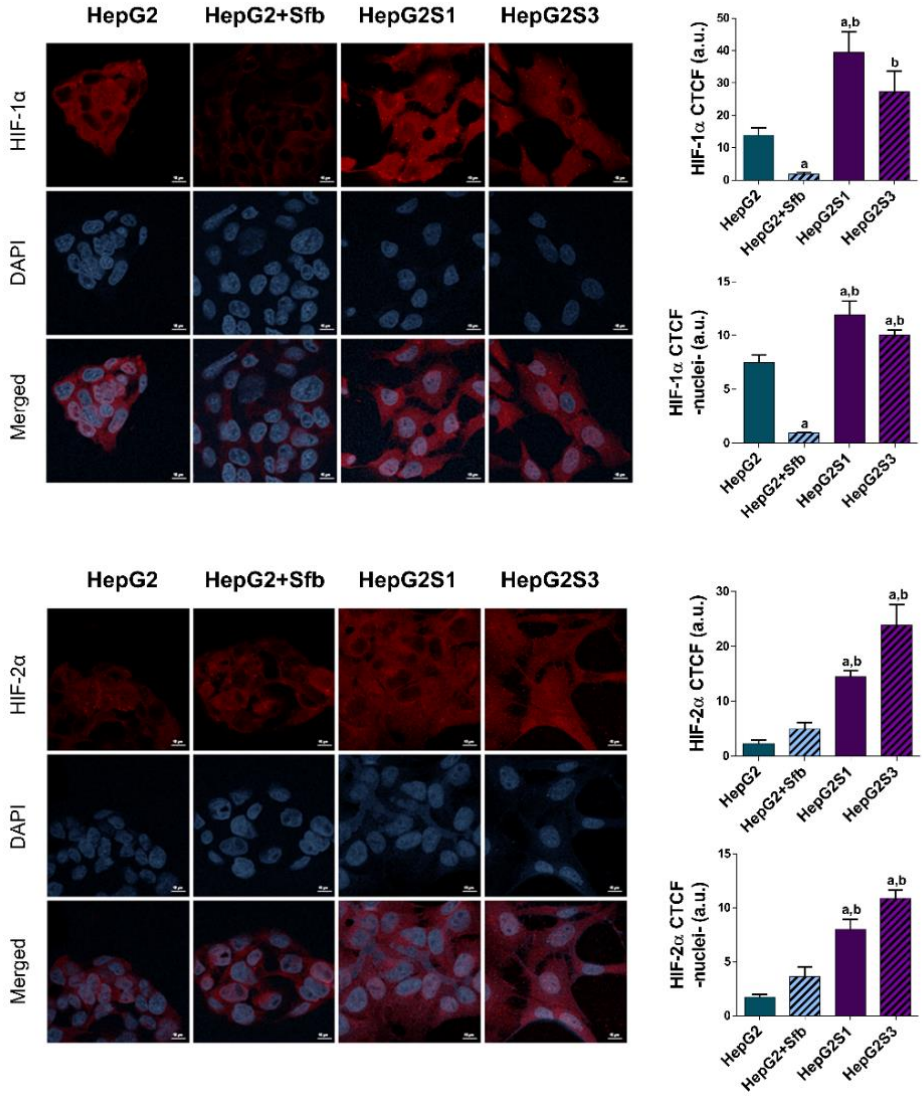

Figure 32. Evaluation of HIF-1α and HIF-2α protein expression and nuclear translocation under hypoxia. Microscopy images of HIF-1α (upper panel) and HIF-2α (lower panel) show HIFs expression (red) after 24 h under hypoxia. DAPI staining (blue) represents cell nuclei. Bar graphs at top position denote total HIFs expression, while

bar graphs at bottom position indicate nuclear translocation for each factor analyzed. Magnification: 63X, scale bar: 10 µm. [a] $p<0.05$ and [b] $p<0.05$ indicate significant differences respect to non-treated and sorafenib-treated HepG2 cells, respectively. Data are expressed as mean values of a.u. ± SD of three independent experiments.

Given the variation observed in HIF-1α and HIF-2α expression patterns in sorafenib-resistant cells, even under normoxia, we explored the regulation of HIFs by studying the synthesis and degradation processes on HIF-1α. In this way, parental and resistant cells were subjected for 24 h to both oxygen conditions, and were individually treated with chemical inhibitors of protein synthesis and degradation during the last 6 h. As shown in **Figure 33**, inhibition of protein synthesis with CHX resulted in a significant decrease in HIF-1α levels in HepG2, while the amount of HIF-1α was not altered in HepG2S1 and HepG2S3. Otherwise, blocking the protein degradation with MG132 promoted a robust accumulation of HIF-1α in all cell lines examined **(Figure 33)**. These results indicate that the HIF-1α degradation process appears to be suppressed in sorafenib-resistant cells.

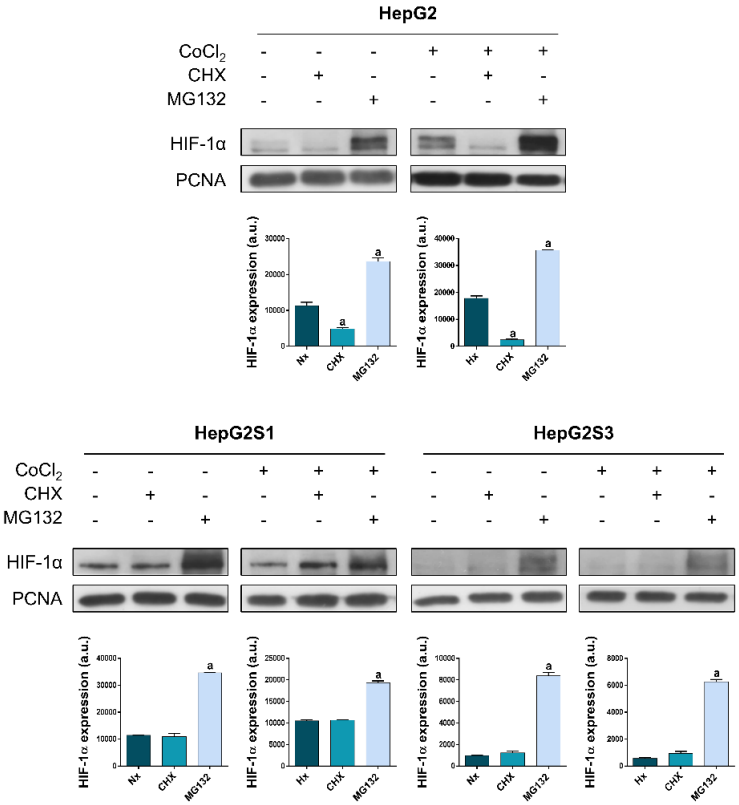

Figure 33. Study of HIF-1α protein synthesis and degradation processes under normoxic and hypoxic conditions. Cells were treated with or without $CoCl_2$ for 24 h,

and CHX and MG132 were used as protein synthesis and protein degradation inhibitors, respectively, for the last 6 h of treatment. PCNA was used as internal loading control. [a] $p<0.05$ in comparison with normoxia or hypoxia control within the same cell type. Data are expressed as mean values of a.u. ± SD of three independent experiments.

2.3 Determination of the apoptotic cell death status in cells resistant to sorafenib and the implication of HIFs on their survival ability

Cell death mechanisms, such as apoptosis, are frequently altered in chemoresistant tumor cells [74]. For this reason, we verified whether our *in vitro* HCC model of resistance to sorafenib shows any disturbance in the apoptosis process compared to the parental cells HepG2.

First, changes in gene expression between HepG2 and HepG2S1 cell lines, as a consequence of the development of resistance to sorafenib, were examined by microarray analysis **(Table 8)**.

Table 8. Relative expression of RNA for apoptosis markers in sorafenib-resistant HepG2S1 cells *vs*. parental HepG2 cells under normoxia determined by microarray *

Gene Symbol	Full Name	Regulation	^{2}log FC HepG2S1/HepG2	Corrected p
Pro-apoptotic genes				
BAX	BCL2 associated X apoptosis regulator	Down	−0.93	5.74×10^{-9}
HRK/BID3	Harakiri BCL2 interacting protein	Up	+1.34	1.17×10^{-7}
PMAIP1/ NOXA	Phorbol-12-myristate-13-acetate-induced protein 1	Up	+2.45	9.17×10^{-13}
TNFRSF10B	TNF receptor superfamily member 10b	Down	−1.23	5.04×10^{-11}
Pro-survival genes				
BCL2	BCL2 apoptosis regulator	Up	+1.25	1.43×10^{-8}
BCL2L1 /BCL-X	BCL2 like 1	Down	−1.21	1.59×10^{-10}
BIRC3	Baculoviral IAP repeat containing 3	Up	+5.06	1.32×10^{-15}

PTPN13	Protein tyrosine phosphatase non-receptor type 13	Up	+1.97	5.59×10^{-10}
Caspases				
CASP2	Caspase-2	Up	+0.95	1.18×10^{-8}
CASP3	Caspase-3	Down	−2.06	4.59×10^{-11}
CASP8	Caspase-8	Down	−0.81	7.98×10^{-9}
CASP9	Caspase-9	Up	+1.21	1.76×10^{-9}
CASP10	Caspase-10	Down	−1.23	6.76×10^{-8}

* Microarray data derive from three independent experiments.

Results showed that KEGG-pathway for apoptosis (hsa04210) was significantly enriched. As shown in **Table 8**, HepG2S1 cells displayed a significant repression of the pro-apoptotic genes BAX and TNFRSF10B compared to HepG2 whereas, according to the anti-apoptotic genes assessed, resistant cells showed a doubling of BCL2, 33-fold upregulation of BIRC3 and 4-fold increment of PTPN13. In addition, we found a differential expression of several caspases in HepG2S1 cell line. It should be noted the approximately 25% reduction of CASP3 relative to HepG2 and furthermore, CASP8 and CASP10 were also significantly suppressed. Inquiringly, since HepG2S1 has taken several months to adapt to sorafenib, it may be inducing other compensatory mechanisms and some genes are shifted in the opposite direction. However, the gene expression data propose a suppression of apoptosis **(Table 8)**.

To confirm these data, the protein expression of Bax and cleaved caspase-3 were evaluated by Western blot. Sorafenib treatment of HepG2 cells under hypoxic conditions for 24 and 48 h enhanced the expression of both apoptosis markers compared to untreated HepG2 cells. On the contrary, Bax and cleaved caspase-3 expression levels were remarkably repressed in the two sorafenib-resistant cell lines, HepG2S1 and HepG2S3, under both normoxic and hypoxic conditions **(Figure 34)**.

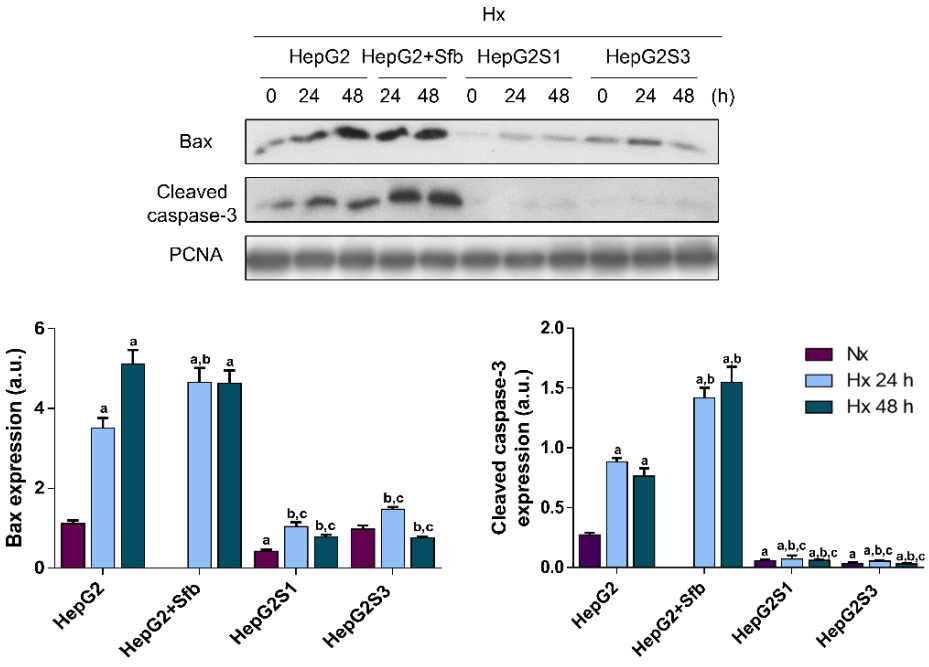

Figure 34. Analysis of protein expression of the pro-apoptotic markers Bax and cleaved caspase-3 under normoxic and hypoxic conditions. Lanes 0 h represent basal protein levels under normoxia, and hypoxia was tested after 24 and 48 h. PCNA was used as internal loading control. [a] $p<0.05$ denotes significant changes in comparison with non-treated HepG2 cells in normoxia, [b] $p<0.05$ and [c] $p<0.05$ respect to non-treated and sorafenib-treated HepG2 cells in hypoxia, correspondingly, for each time point. Data are expressed as mean values of a.u. ± SD of three independent experiments.

Furthermore, the apoptotic cell population was determined by cell cycle assessment. Cell cycle evaluation exhibited a high increase of HepG2 cells in subG1 phase after the addition of sorafenib under hypoxia, reaching around 10% of dead cells, which contrasts with the 3% found in untreated HepG2 cells. On the other hand, the percentage of subG1 cells was analogous between both resistant lines HepG2S1 and HepG2S3 (around 5.5%), but significantly lower than the levels obtained in HepG2 cells treated with sorafenib **(Figure 35)**.

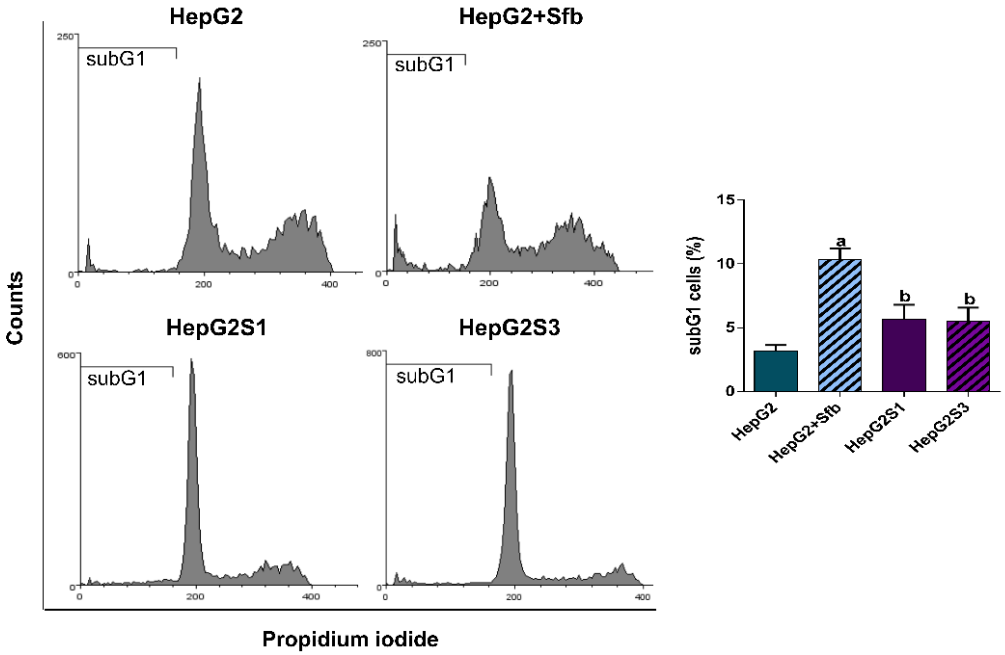

Figure 35. Evaluation of the subG1 population related to apoptotic cell death under hypoxia. SubG1 population was analyzed after 48 h of hypoxia induction. [a] $p<0.05$ indicates significant differences in contrast to non-treated HepG2 cells, [b] $p<0.05$ denotes significant changes respect to sorafenib-treated HepG2 cells Data are expressed as a percentage of mean values ± SD of three independent experiments.

Taken together, these results suggest that sorafenib-resistant HepG2S1 and HepG2S3 cells have established altered mechanisms to evade apoptotic cell death signals.

Finally, the interesting results obtained in sorafenib-resistant cells about HIFs overexpression and apoptosis evasion, likely correlated, we decided to analyze the role of both HIFs on their survival capacity. In this way, we performed gene silencing for both HIF-1α and HIF-2α through siRNA transfection into resistant cells and verified their impact on cell viability. Efficacy of gene silencing was tested by Western blot. HIF-1α knockdown promoted a significant reduction of cell viability in both resistant cell lines, especially in HepG2S1 where it was declined by about 50%. After HIF-2α downregulation, cell death was also triggered in both cell lines, but was more pronounced in HepG2S3 cells in comparison with HepG2S1 **(Figure 36)**. Hence, these data indicate the key involvement of both HIFs in the survival of resistant cells to sorafenib.

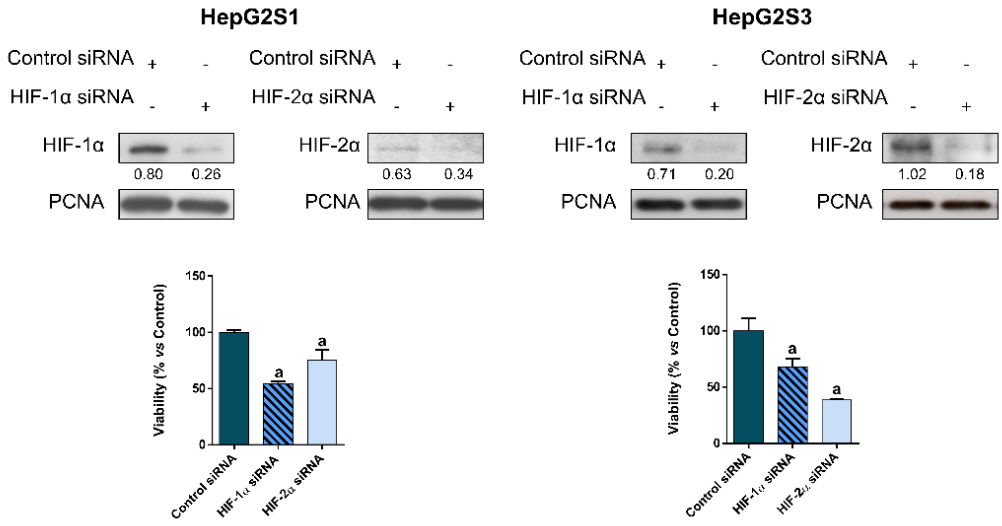

Figure 36. Gene silencing of HIF-1α and HIF-2α in sorafenib-resistant cell lines under hypoxic conditions. Representative immunoblots and cell viability analysis 48 h post-transfection and last 24 h under hypoxia. PCNA was used as internal loading control. Densitometry reading of each band is shown under the immunoblots. [a] $p<0.05$ respect to control siRNA. Data are expressed as a percentage of mean values ± SD of three independent experiments.

2.4 Analysis of expression and regulation of the apoptotic mediator under hypoxia, BNIP3, in sorafenib-resistant cell lines

BNIP3 is a pro-apoptotic protein member of the Bcl-2 family and is regulated by hypoxic conditions, being a well-recognized direct target of HIF-1α [168,172]. Since the demonstrated implication of the hypoxia-mediated response in our model of resistance to sorafenib, we decided to check the expression of BNIP3 between the different cell lines in hypoxia. In HepG2 cells, BNIP3 protein levels decreased in response to sorafenib administration and, surprisingly, a more significant reduction of BNIP3 was found in both HepG2S1 and HepG2S3 cells **(Figure 37A-B)**. Similarly, BNIP3 mRNA levels showed the same tendency, indicating that BNIP3 downregulation in resistant cells to sorafenib is a consequence of an upstream process **(Figure 37C)**.

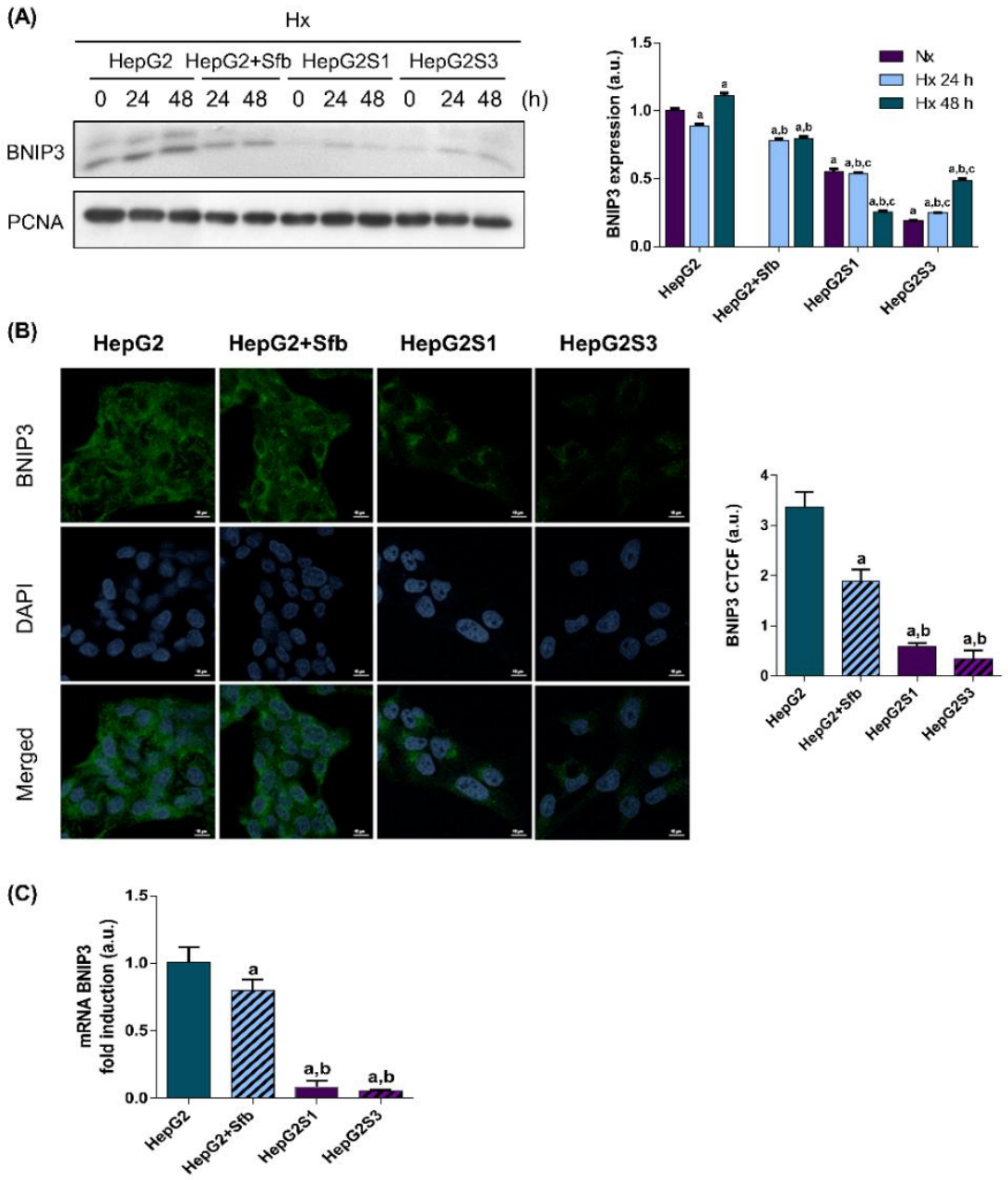

Figure 37. Determination of BNIP3 expression between sensitive and resistant cells to sorafenib. (A) BNIP3 protein expression. Lanes 0 h represent basal protein levels under normoxia, and hypoxia was tested after 24 and 48 h. PCNA was used as internal loading control. [a] $p<0.05$ denotes significant changes in comparison with non-treated HepG2 cells in normoxia, [b] $p<0.05$ and [c] $p<0.05$ respect to non-treated and sorafenib-treated HepG2 cells in hypoxia, correspondingly, for each time point. **(B)** Confocal microscopy images show BNIP3 protein expression (green) after incubation under hypoxia for 24 h. DAPI staining (blue) denotes cell nuclei. Magnification: 63X, scale bar: 10 µm. [a] $p<0.05$ and [b] $p<0.05$ indicate significant differences respect to non-treated and sorafenib-treated HepG2 cells, respectively. **(C)** BNIP3 mRNA levels 24 h under hypoxia were measured by qRT-PCR. [a] $p<0.05$ and [b] $p<0.05$ denote significant changes

compared to non-treated and sorafenib-treated HepG2 cells, respectively. Data from A-C are expressed as mean values of a.u. ± SD of three independent experiments.

Epigenetic modifications have been closely related to gene silencing. In fact, it has been reported that many tumor suppressor genes can be inactivated by epigenetic modifications such as DNA methylation and histone deacetylation [168]. Initially, we examined the possible histone deacetylation by using 10, 50 and 100 nM of the HDACs inhibitor TSA in the resistant cell lines. In HepG2S1 and HepG2S3 resistant cells, BNIP3 expression did not show changes after 24, 48 and 72 h of exposure to any of the TSA doses, discarding histone deacetylation as responsible for BNIP3 downregulation **(Figure 38A)**. Hence, we evaluated the methylation status of the BNIP3 promoter and elevated levels of methylated DNA were detected in both resistant cell lines, which were not found in the parental HepG2 cells **(Figure 38B)**. The DNMT inhibitor 5-Aza proved to be effective in avoiding the methylation of the BNIP3 promoter from the lowest dose employed of 10 µM **(Figure 38C)**. Besides, 5-Aza was able to restore the hypoxia-induced expression of BNIP3 both at mRNA **(Figure 38D)** and protein **(Figure 38E)** levels.

To clarify whether the repression of BNIP3 due to methylation is responsible for the evasion of cell death in cells resistant to sorafenib, we evaluated the effect of 5-Aza treatment on cell viability, as well as its combination with the gene silencing of BNIP3. In HepG2S1 and HepG2S3 cells, recovery of BNIP3 expression by demethylation using 5-Aza significantly induced cell death. On the contrary, the simultaneous silencing of BNIP3 improved the cell viability of resistant cells with respect to those treated only with 5-Aza. Efficacy of gene silencing was tested by Western blot **(Figure 39)**.

Altogether, results suggest that downregulation of BNIP3 by methylation could constitute an adaptive mechanism of sorafenib resistance cells to avoid cell death.

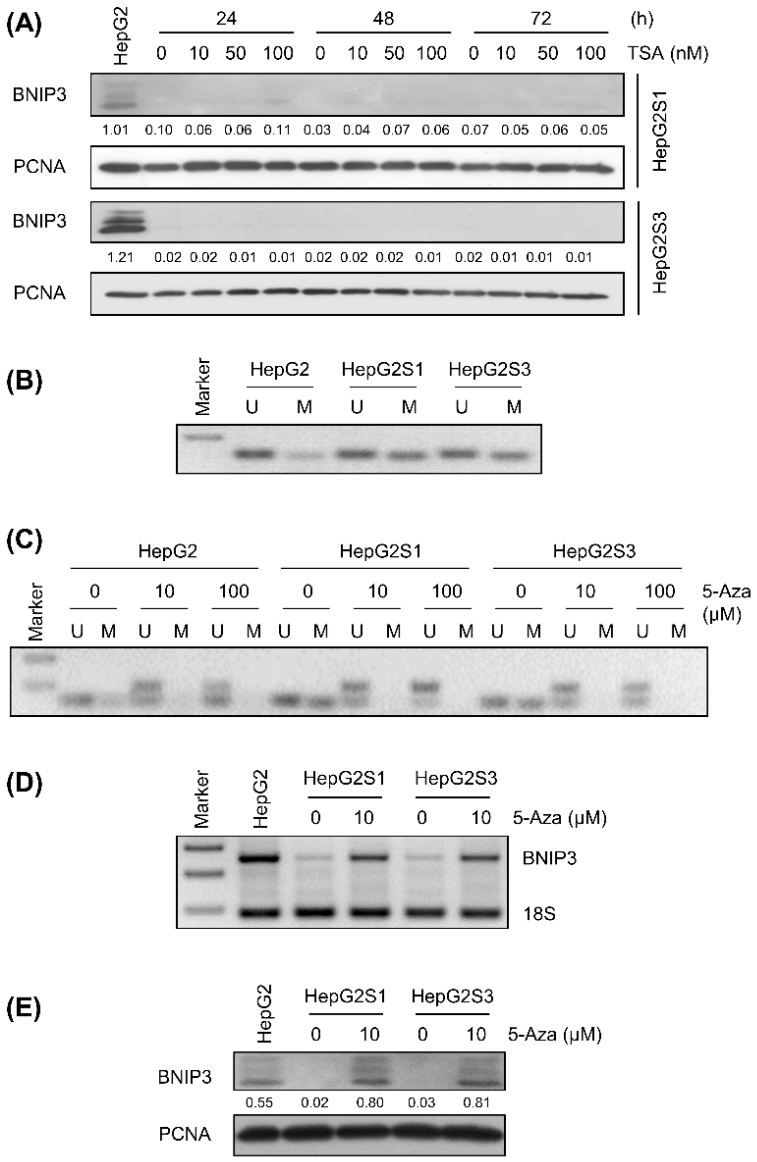

Figure 38. Analysis of epigenetic regulation of BNIP3 in cells resistant to sorafenib under hypoxia. (A) Effect of preventing histone deacetylation on BNIP3 expression using TSA. Resistant cells were subjected to hypoxia for the last 24 h of every TSA treatment. PCNA was used as internal loading control. Densitometry of each band is detailed below the immunoblots. **(B)** Methylation status of the BNIP3 promoter was tested after 24 h of hypoxia by MSP, by using specific BNIP3 primers to amplify U-BNIP3 or M-BNIP3 DNA. **(C)** Effect of 5-Aza treatment on the methylation status of the BNIP3 promoter. Cells were exposed to demethylation agent 5-Aza for 48 h and subsequent treatment to hypoxia plus 5-Aza for further 24 h. **(D-E)** Effect of 5-Aza administration on BNIP3 mRNA and protein levels, using 18S and PCNA as internal control, respectively. HepG2 lanes from A, D-E show basal mRNA or protein levels of BNIP3 after 24 h under hypoxia.

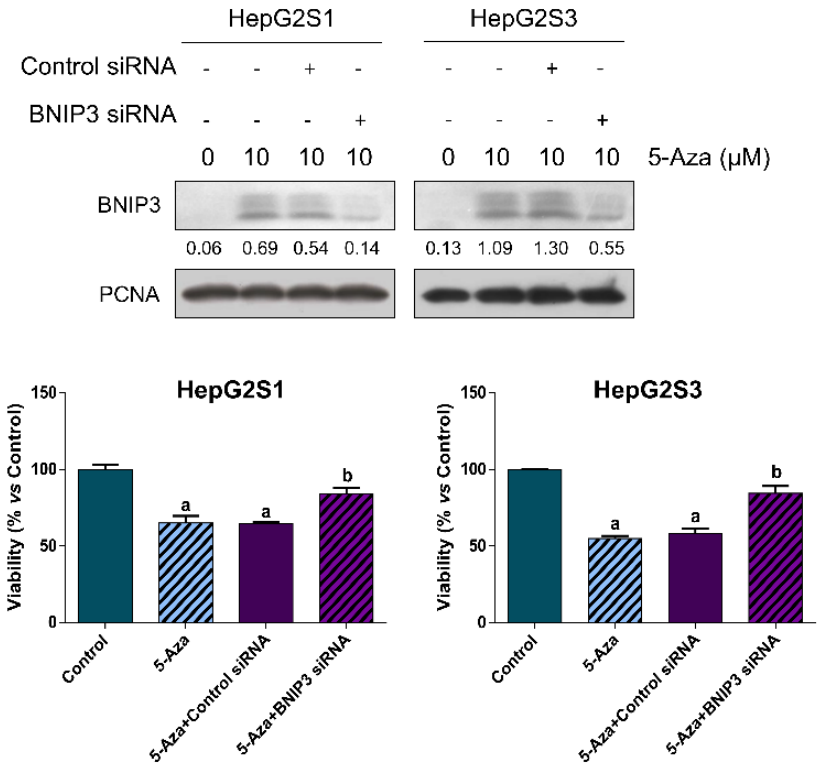

Figure 39. Effect of demethylation by 5-Aza alone or in combination with BNIP3 silencing on the BNIP3 expression and the resistant cell viability under hypoxia. Densitometry of each band is detailed below the immunoblots. PCNA was used as internal loading control. [a] $p<0.05$ indicates significant differences respect to non-treated cells (control), [b] $p<0.05$ reports significant changes in comparison with control siRNA cells also treated with 5-Aza. Data are expressed as a percentage of mean values ± SD of three independent experiments.

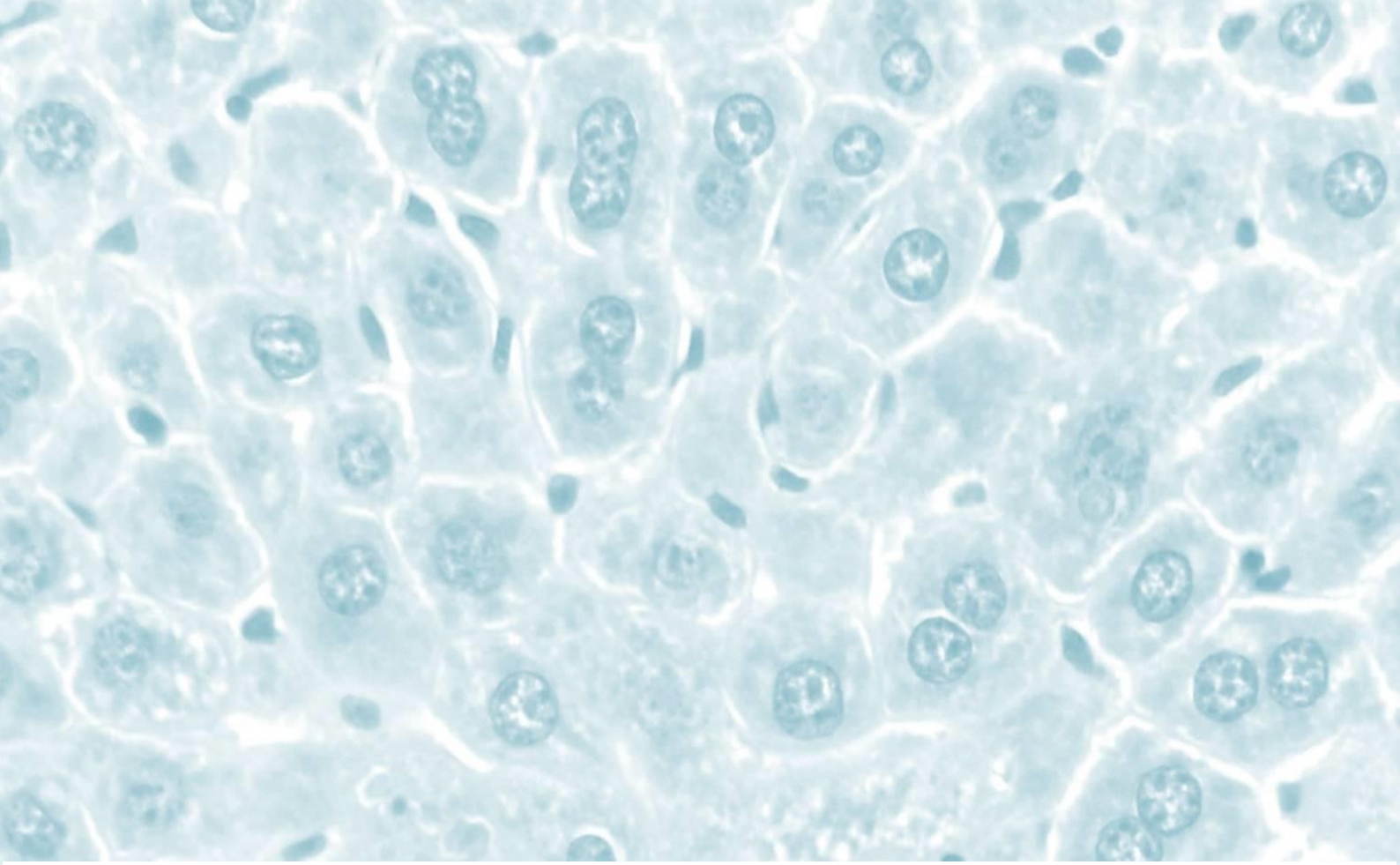

Discussion

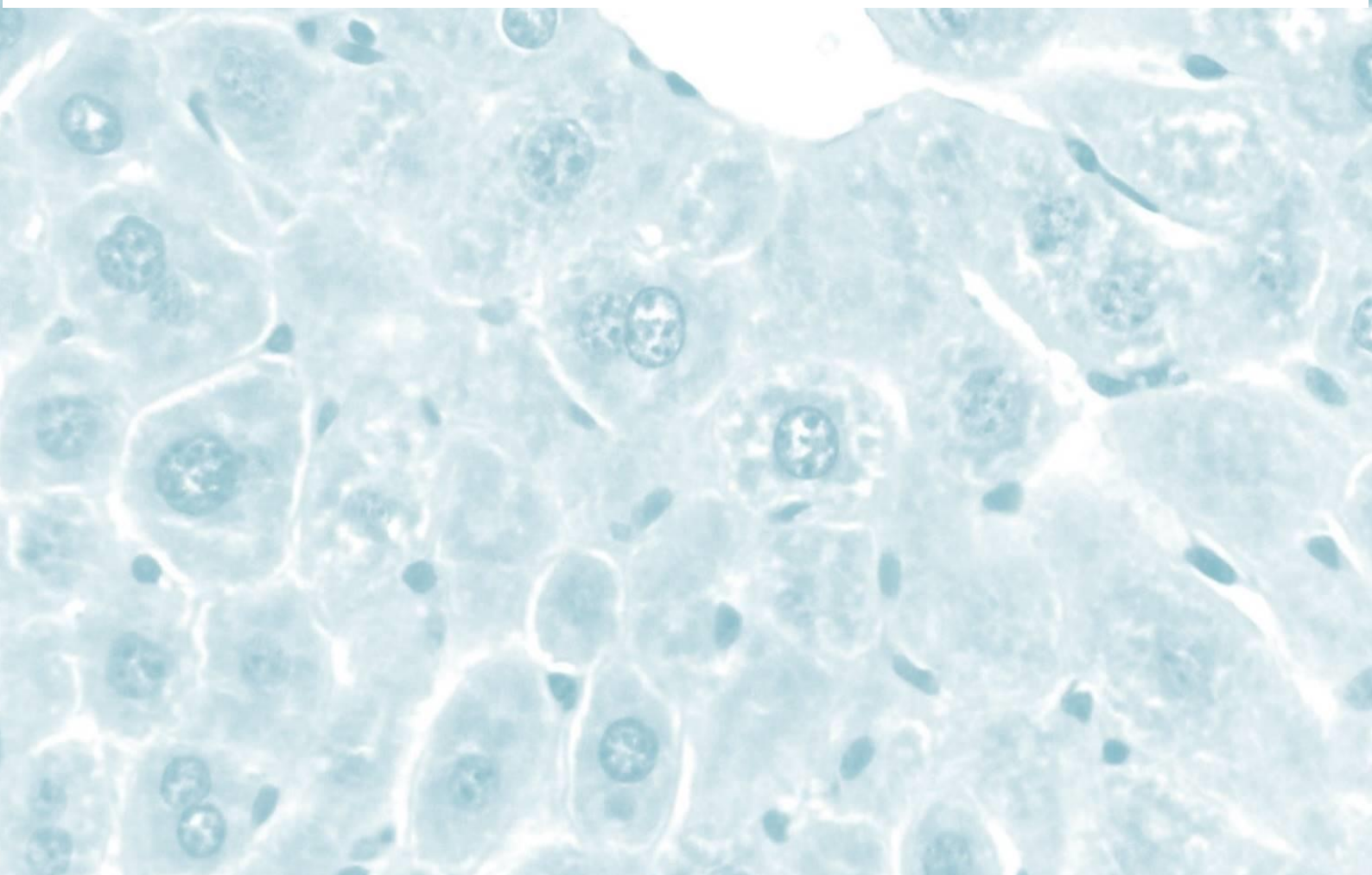

1 Overexpression of HIF-1α and HIF-2α correlates with poor outcomes of patients with HCC

Hypoxia is a frequent feature in solid tumors that arises in response to flawed vascularization and enhanced metabolic activity [123]. Despite the fact that HCC is characterized as one of the most hypervascularized tumors, hypoxic regions are commonly present into this tumor due to the fast proliferation of tumor cells and the development of anomalous blood vessels [126,127]. Even though initially a decrease in oxygen supply is detrimental to cell survival, some tumor cells can develop adaptive changes to survive under the hypoxic microenvironment [128]. This adaptive response is principally facilitated by HIFs, transcription factors that modulate a set of pro-survival genes associated with tumor aggressiveness, recurrence, selection of more invasive clones, resistance to treatments and poor clinical outcomes [103,123].

HCC is the third leading cause of cancer-related death and has been recognized as a poor prognosis tumor [254]. This is a consequence of its difficult early detection and high recurrence rate. Moreover, typical biomarkers like AFP have been revealed to be of insufficient value to predict the prognosis of HCC as well as metastatic recurrence [255]. Hence, novel effective biomarkers need to be defined to accurately determine the clinical prognosis and response to treatment of HCC patients. In the present study, we assessed the main mediators of the response to hypoxia, HIF-1α and HIF-2α, as possible biomarkers to predict HCC prognosis. To examine the correlation between the expression of HIFs and HCC, the present meta-analysis aimed at evaluating the association of the HIF-1α or HIF-2α overexpression with the prognosis and clinicopathological features of HCC patients.

1.1 High HIF-1α and HIF-2α expression are associated with survival-related parameters of HCC patients

A total of 26 high-quality studies comprising 3,570 HCC patients were included for the quantitative analysis of HIF-1α. Pooled results exhibited that high HIF-1α expression is responsible for poor OS and DFS/RFS in HCC, could be employed as a biomarker to predict outcomes and recurrence in HCC patients.

Two previous meta-analysis conducted by Zheng *et al.* [126] and Cao *et al.* [125], which included 7 and 8 articles respectively, also examined the role of HIF-1α expression in individuals with HCC. In accordance to our results, both studies reported a relationship between HIF-1α overexpression and DFS, and Zheng *et al.* [126] also described an association with OS. Also, several researches accomplished in breast cancer [256], non-small cell lung cancer [257], gastric cancer [258], RCC [259], pancreatic cancer [260], bone tumor [261], esophageal carcinoma [262], colorectal cancer [263], head and neck cancer [264,265], endometrial cancer [266], epithelial ovarian cancer [267], and oral squamous cell carcinoma [268], also displayed a significant relation between poor prognosis and HIF-1α overexpression. Additionally, high HIF-1α levels have been correlated to worse prognosis in advanced cancer patients undergoing chemotherapy and/or radiotherapy [269]. Therefore, along with a useful biomarker, targeting HIF-1α could be a promising approach to improve treatments for advanced cancer patients.

On the other hand, for the HIF-2α meta-analysis, 7 high-quality studies enrolling 1213 patients were used. First, only DFS/RFS denoted association with high HIF-2α levels; however, after subgroup analysis HIF-2α overexpression also correlated with lower OS when studies where pooled by sample size and follow-up time. Thus, like HIF-1α, this factor could also be employed as a prognostic and recurrence biomarker.

A previous meta-analysis by Yao *et al.* [127] and another by Luo *et al.* [128] assessed the significance of HIF-2α in HCC and in several types of cancer, respectively. Luo *et al.* [128] observed an association between OS and HIF-2α overexpression in HCC after stratifying by tumor type. Likewise, this meta-analysis determined that high HIF-2α levels also results in poor OS in further tumors such as lung, breast, colorectal and head and neck cancers, and sarcomas [128]. In contrast, Yao *et al.* [127] did not find a significant relationship among OS and HIF-2α expression, which is explained because our work involved most recent articles and excluded those with full-text in Chinese [127]. It should be noted that no prior research has analyzed the effect of this transcription factor on DFS or RFS. Additional studies have detected the correlation between HIF-2α overexpression and a worse prognosis in other tumors including RCC

[259], colorectal cancer [263,270], head and neck cancer [264], non-small cell lung cancer [271], oral squamous cell carcinoma [272] and gastric cancer [273].

Similarly, a recent parallel study by Ding *et al.* [274] evaluated the role of the expression of both factors, HIF-1α and HIF-2α, in HCC patients. Despite this study just involved 25 articles about HIFs, and in concordance to our results, their combined data also suggested that HIF-1α overexpression in HCC was associated with poorer OS and DFS. Contrariwise, this research did not show any significant relationship with HIF-2α expression [274]. This difference could be due to a lower number of articles employed by Ding *et al.* [274] and that they did not perform subgroup analysis.

1.2 High HIF-1α and HIF-2α expression are associated with clinicopathological features of HCC patients

Our results also denoted that various clinicopathological features, including BCLC staging, capsule infiltration, intrahepatic and lymph node metastasis, TNM staging, tumor differentiation, tumor number, tumor size (cut-off 3 cm), vascular invasion and vasculogenic mimicry, were significantly associated with the overexpression of HIF-1α. After subgroup analysis, we also detected a correlation of this factor with AFP levels (cut-off 20 ng/ml), cirrhosis, tumor size (cut-off 5 cm) and histological grade. All of these relationships make that HIF-1α could be useful to establish a more precise prognosis for HCC patients.

The two preceding meta-analysis on HIF-1α, also showed that overexpression of this transcription factor was linked to vascular invasion [125,126]; but Cao *et al*. [125] did not find a significant relationship with capsule formation, cirrhosis, tumor differentiation, or tumor size. Nonetheless, this disagreement can be explained by the smaller number of studies, and therefore of HCC patients, included in such meta-analysis as well as the lack of subgroup analysis [125].

Concerning the clinicopathological characteristics, we found that only capsule infiltration was linked to raised HIF-2α levels after the analysis of subgroups by median age. This result agrees with Yao *et al.* [127] and, furthermore, they also reported that there was no correlation of HIF-2α with cirrhosis, necrosis and tumor size. However,

they showed a relationship of this protein levels with vein invasion and histological grade [127].

In concordance to our results, the parallel study by Ding *et al.* [274] displayed an association between HIF-1α and tumor number, tumor size, and vascular invasion. Conversely, this study did not report a relationship with capsule formation, cirrhosis and tumor differentiation for HIF-1α, nor any significant correlation with HIF-2α expression [274]. As explained above, these differences are due Ding *et al.* [274] employed less articles and they did not perform subgroup analysis.

Hypoxia, via the upregulation of angiogenic factors, constitutes the main physiological stimulus that promotes angiogenesis in HCC. VEGF, a pro-angiogenic factor transcriptionally regulated by both HIFs, is key for blood vessel development through inducing endothelial cell growth and migration [103,275]. Some studies enrolled in our meta-analysis displayed that high VEGF expression was associated with angiogenesis, vasculogenic mimicry, microvessel density, and worse prognosis; showing a positive relationship between VEGF and HIF-1α [198,199,203,214,218]. Other HIFs-mediated angiogenic factors are also involved in angiogenesis in HCC, such as HIF-1α-mediated expression of ANG-2 and BMP4 [103,199], HIF-2α-induced expression of SCF and PAI-1, and both HIFs targets EPO and PDGF expression [103,275]. Definitely, hypoxia and more precisely HIFs contribute to angiogenesis in HCC, which is confirmed by our results associating HIF-1α overexpression with improved vascular invasion and vasculogenic mimicry.

Besides, EMT and metastasis can be promoted under hypoxic conditions in HCC cells [106]. Accordingly, various studies included in our quantitative analysis showed that the increased invasiveness and poor prognosis in HCC patients are associated with the expression of invasion-related proteins like MMPs, E-cadherin, or interleukin-8 (IL-8), also controlled by HIFs [201,203,209,212,213]. In preclinical studies, comparable results were described connecting high invasiveness and metastasis with the HIF-1α-mediated expression of Snail, CXCL6, and Rab11-FIP4 [276–278]; and with the HIF-2α targets SerpinB3, SCF, and CUB domain-containing protein 1 (CDCP1) [279–281]. These confirm the association that we found between both HIFs and the clinicopathological

parameters linked to metastasis, such as capsule infiltration and intrahepatic or lymph node metastasis.

1.3 Advantages and limitations of the study

The present work is a highly comprehensive systematic review with meta-analysis performing an exhaustive quantitative analysis of scientific evidences about HIF-1α and HIF-2α relationship with prognostic parameters, including OS and DFS/RFS, and with clinicopathological features in HCC patients subjected to surgical resection. Furthermore, our work includes evaluation of heterogeneity, subgroup analysis and publication bias. The previous meta-analysis that assessed the correlation between HIF-1α or HIF-2α levels and tumor outcomes, which were described throughout the discussion, included fewer articles and HCC patients, and examined fewer parameters. Moreover, most of these studies did not assess publication bias or subgroup analysis.

However, there are some limitations in the current study that should be considered. First, during the assessment of eligibility, those articles with full-text in Chinese were omitted and, consequently, relevant data were excluded. Second, data extraction was not possible in some cases due to the lack of information required to estimate HR and its 95% CI according to Parmar method, such as follow-up time or the number of patients in each group. Third, comprised studies used varied or unspecified antibodies for HIFs detection, employing inconsistent staining procedures and cut-off values for the definition of high HIF-α expression, which could lead to heterogeneity. Fourth, all the studies were accomplished with Asiatic population, mostly from China, where hepatitis B is the main risk factor [1]. Consistent with this, most articles tested the effect of hepatitis. Hence, additional studies are required to evaluate the role of HIFs expression among other ethnic or geographical regions, such as Occidental countries where other etiologic factors for HCC like NASH prevail [1]. Fifth, the volume of research found on HIF-2α was lower and, therefore, the effect of this factor is underrepresented in this analysis. Finally, publication bias was denoted in some parameters.

In conclusion, HIFs are associated with a more aggressive behavior of HCC. In this meta-analysis, high HIF-1α and HIF-2α expression was found in 51.7% and 45.6% of patient samples, respectively. Results reported that HIF-1α and HIF-2α overexpression is related to poor OS, DFS, RFS and some clinicopathological variables of HCC patients. These findings suggest that both HIFs could be useful biomarkers to predict prognosis and recurrence in patients with HCC, which can improve clinical decisions. The main results obtained have been represented in the **Figure 40**.

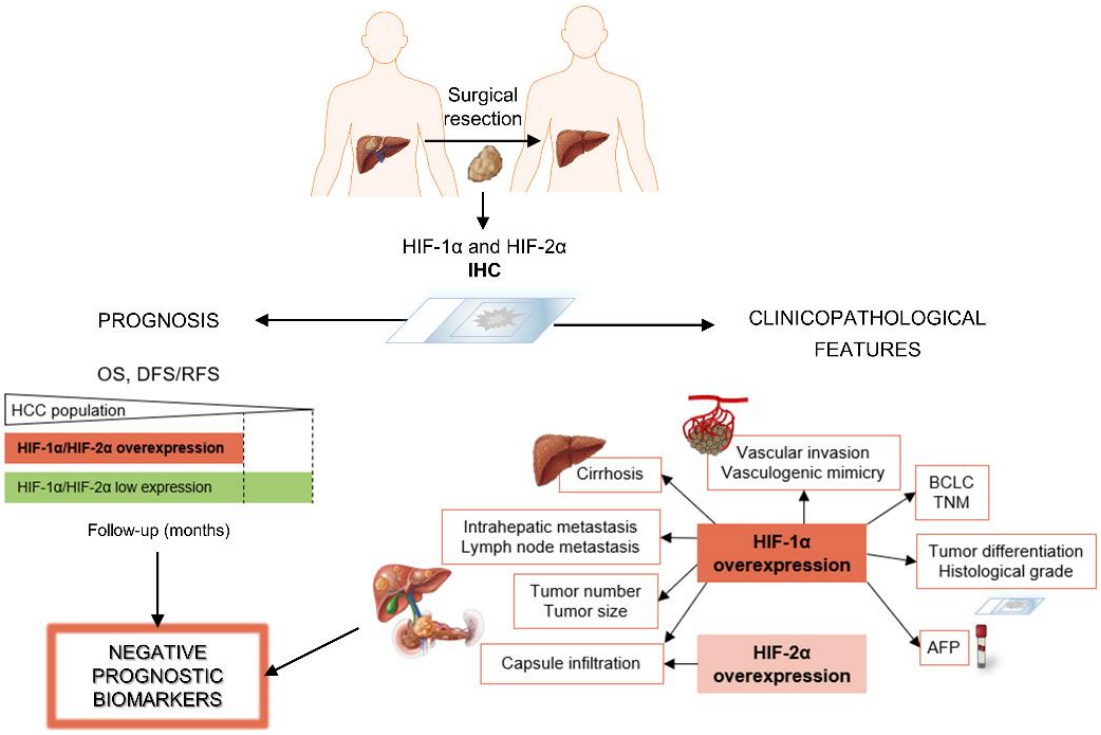

Figure 40. Graphical abstract about the relationship between HIF-1α and HIF-2α overexpression and several parameters related to poor outcomes in patients with HCC. Overexpression of both factors, HIF-1α and HIF-2α, correlates with poor OS and DFS/RFS in HCC patients who underwent surgical resection. Moreover, high HIF-1α expression is linked to a wide range of clinicopathological features of HCC patients, including advanced BCLC and TNM stages, cirrhosis, high AFP levels, poor tumor differentiation and histological grade, larger tumor size and number, intrahepatic and lymph node metastasis, capsule infiltration, vascular invasion and vasculogenic mimicry. Otherwise, elevated HIF-2α protein levels appear to be associated with capsule infiltration. Hence, these transcription factors could be useful biomarkers to predict prognosis and recurrence of HCC patients.

2 Stabilization of HIFs and BNIP3 promoter methylation contribute to acquired resistance to sorafenib in human HCC cells

For advanced HCC, only systemic palliative treatments are available [18]. Moreover, HCC is accepted as one of the most resistant tumors to chemotherapeutic agents, making it difficult the management of patients with HCC [282]. In 2007, systemic treatment with sorafenib was approved for advanced HCC; although is effective to prolong survival, sustained exposure this drug allows to the development of resistant tumor cells. The hypoxia caused as a consequence of its antiangiogenic activity has been suggested as one of the main mechanisms of acquired resistance [123]. In the present PhD Thesis, we performed an *in vitro* study using a model of acquired resistance to sorafenib.

2.1 Resistant HCC cell lines show a more aggressive phenotype and hypoxia-adaptive mechanisms

At first, we characterized the growth dynamics and proliferation of the sorafenib-resistant phenotype. In this way, we evaluated these processes by comparing between two cell lines with acquired resistance to sorafenib, HepG2S1 and HepG2S3, and the parental cell line HepG2 treated or no with sorafenib, under normoxia and hypoxia. Sorafenib treatment reduced the proliferative ability of the HepG2 cells under both oxygen situations. This result was also observed under normoxia with the human HCC cell lines HepG2, Huh7, and Hep3B [283,284], and in Hep3B cells also under hypoxia [118]. Our results also showed that hypoxia repressed the cell growth of HepG2 with respect to normoxic conditions, since hypoxia represents a cellular stress. Contrariwise, Prieto-Domínguez *et al.* [118] did not found that hypoxia decreases cell viability in Hep3B. This study subjected Hep3B cells to hypoxia for 48 h [118], while we observed significant differences in the growth of HepG2 cells from the third day under hypoxia.

Besides, the analysis of growth and expression of Ki67 in both cell lines resistant to sorafenib showed a greater proliferation capacity compared to HepG2 cells treated with sorafenib and even in the absence of sorafenib administration. This faster growth in resistant cells correspond to their higher invasive potential described by van

Malenstein *et al.* [88]. This difference in growth rate between sorafenib-resistant and sorafenib-sensitive cells was enhanced under hypoxia. HepG2S1 and HepG2S3 cells displayed similar growth between normoxia and hypoxia, unlike HepG2 cells, which suggest that resistant cells may contain adaptive mechanisms to deal with hypoxic conditions. It has been reported the influence of hypoxia in the development of HCC resistant cells after treatment with 5-FU [144], doxorubicin, and cisplatin [140]. The acquired resistant to sorafenib related with hypoxia has also been described in other cancer types including RCC [137,138], gastric cancer [285], and acute myeloid leukemia [139]. Moreover, sorafenib-resistant samples from HCC patients presented an increase of intratumoral hypoxia than those untreated or sensitive to sorafenib [135].

2.2 Sorafenib-resistant cell lines display HIFs overexpression and a deregulation in the proteasomal-dependent HIF degradation

Regarding HIF-α expression, under hypoxia, sorafenib decreased protein levels and nuclear translocation of HIF-1α in HepG2, while HIF-2α expression was very low either in the absence or in the presence of sorafenib in these cells. Previous studies have already demonstrated that sorafenib declines HIF-1α levels in HCC cells [122,131], by preventing its protein synthesis [131]. In contrast, both resistant cell lines showed an increase in HIF-1α protein expression and its nuclear translocation, highlighting the marked overexpression of this transcription factor in HepG2S1 with respect to untreated HepG2. Accordingly, in HCC samples from sorafenib-resistant patients, a higher expression of HIF-1α has also been found compared to sorafenib-sensitive or untreated patients [135]. Similarly, prolonged sorafenib treatment in both *in vitro* and *in vivo* HCC models led to enhanced HIF-1α expression [135,146,286]. Remarkably, our results also indicated that protein levels and nuclear translocation of HIF-2α were increased in sorafenib-resistant cells. Preceding investigations in *in vitro* models of HCC reported that high HIF-2α expression stimulates resistance to sorafenib [149], while downregulation of this factor improves the anti-tumor effects of sorafenib [136]. Similar findings were observed in human ovarian cancer lines, where upregulation of HIF-2α mediated resistance to adriamycin [287]. Thus, enhanced expression and

nuclear translocation of both HIF-α factors in resistant cells appear to be related to the acquisition of sorafenib resistance.

In our current study, HepG2S1 and HepG2S3 cells exhibit upregulated protein levels of both HIFs even under normoxia. This curious result could be due to alterations in the synthesis and/or degradation processes of HIFs originated during the acquisition of sorafenib resistance. Since HIF-2α expression is almost undetectable in HepG2 cells, we checked the possible alteration of these mechanisms on HIF-1α expression. While the protein synthesis mechanism did not show differences among cell lines examined, blocking this process using CHX significantly declined HIF-1α expression in HepG2 but did not modify HIF-1α levels in HepG2S1 and HepG2S3 cells. This suggests that the proteasomal degradation process of HIF-α is suppressed in the sorafenib-resistant lines, which may explain the high HIF-α levels found under normoxia and hypoxia. In this way, the stabilization of HIF-1α by avoiding its proteasomal degradation was correlated with chemoresistance to doxorubicin in HCC [288]. Also, the promotion of pVHL-dependent degradation of HIF-1α contributes to improving the sensitivity of sorafenib in HCC [135].

2.3 Resistant cells can evade sorafenib-mediated apoptosis, being HIFs implicated in this lack of sensitivity to sorafenib

Along with hypoxia, mechanisms such as dysregulation of cell cycle and evasion of cell death are common in tumor progression and development of drug resistance [74]. In fact, hypoxia itself can promote alterations in these processes to improve the survival of tumor cells [123]. The percentage of subG1 cell population, associated with apoptotic cells, in HepG2 suffered a pronounced increment when sorafenib was added. These findings are consistent with the sorafenib effect showed on the cell cycle distribution of various HCC cell lines, including HepG2 [289,290]. Nevertheless, we observed a significantly lower percentage of subG1 population in HepG2S1 and HepG2S3 cells than in the HepG2 parental line also treated with the drug, suggesting a reduced apoptotic rate in sorafenib-resistant cells. This result seems to be present not only in HCC sorafenib resistant cells, but has also been reported in tamoxifen-resistant MCF-7 breast cancer cells [291].

Sorafenib addition promoted Bax protein expression and caspase-3 cleavage in HepG2. Likewise, in other studies sorafenib treatment also led to an enhance in pro-apoptotic signals [284,289,292,293]. Oppositely, the protein levels of Bax and cleaved caspase-3 were substantially repressed in resistant lines HepG2S1 and HepG2S3, and gene expression data from microarray analysis also indicated alterations related to apoptosis avoidance. A research carried out by other authors, using also two lines of HCC resistant to sorafenib, showed a higher expression of the anti-apoptotic protein Bcl-2, being responsible for a lower induction of apoptosis [166]. In fact, the overexpression of miRNA-34a, a Bcl-2 inhibitor, induces sensitivity to the anti-tumor effect of sorafenib in human HCC cells [294]. Moreover, inhibition of the anti-apoptotic protein Bcl-x_L potentiated sorafenib-induced apoptosis in both *in vitro* and *in vivo* investigations [164,165]. Finally, Liang *et al.* [135] described a lower apoptotic index in sorafenib-resistant samples from patients with HCC than in susceptible ones. Collectively, these results indicate that HepG2S1 and HepG2S3 cell lines have evolved mechanisms to evade apoptosis as a survival approach against sorafenib treatment.

Diminished expression of pro-apoptotic proteins in our sorafenib-resistant cells were in parallel with the enhanced expression of HIFs. To evaluate whether high HIFs expression is related to the pro-survival ability of the resistant tumor cells, we achieved gene silencing of HIF-1α and HIF-2α in the HepG2S1 and HepG2S3 cell lines. Downregulation of HIF-1α or HIF-2α promoted a significant decrease in the viability of both sorafenib-resistant cell lines. These data highlight the role of HIFs in the survival capacity of sorafenib-resistant cells, which suggest that targeting these transcription factors could be an interesting therapeutic approach to overcome sorafenib resistance.

In agreement, HIF-1α silencing induced sorafenib-mediated apoptosis in HCC cells [295], and improved chemosensitivity to temozolomide of human glioblastoma and astrocytoma cells, reducing their invasive capacity [296]. Moreover, studies in both *in vitro* and *in vivo* HCC models showed that miRNAs targeting HIF-1α sensitizes HCC cells to sorafenib-mediated cell death [145,286]. Also, miRNA-18a inhibits HIF-1α avoiding metastasis in breast cancers [297]. The combination of sorafenib with other molecules, such as EF24, melatonin or genistein, has reported to enhance sorafenib effects under

hypoxia via downregulation of HIF-1α [118,135,148]. Concerning HIF-2α, it was observed that silencing this factor negatively regulates the TGF-α/EGFR pathway to induce apoptosis in HCC [149]; and also targets breast cancer resistance protein (BCRP) to improve adriamycin sensitivity in adriamycin resistant ovarian cancer cells [287]. In addition, resistance to 5-FU and temsirolimus was overcome by their combination with a specific HIF-2α inhibitor in patient-derived primary colon cancer cells [298]. Metformin repressed HIF-2α expression *in vitro* and in an orthotopic mouse model, allowing the recovery of the sensitivity of HCC cells to sorafenib-related apoptosis [152]. Therefore, targeting HIF-1α and HIF-2α simultaneously could constitute an interesting strategy; in this way, Ma *et al.* [122] obtained that 2-methoxyestradiol suppressed protein expression and nuclear translocation of HIF-1α and HIF-2α in HCC cells, synergizing with sorafenib to arrest proliferation and promote apoptosis. Likewise, sodium orthovanadate also declined the expression and transcriptional activity of both factors, overcoming resistance to sorafenib in HCC cells [299]. Together, these findings and previous reports emphasize the key role played by both HIFs in promoting cell survival and drug resistance.

2.4 Methylation-dependent downregulation of BNIP3 contributes to hypoxia-mediated sorafenib resistance

Since the significant role that the hypoxia-mediated response has shown in the acquisition of sorafenib resistance in our model, we tested the possible involvement of BNIP3. BNIP3 is a mitochondrial protein responsible for preserving cellular homeostasis during hypoxia by regulating apoptosis, necrosis, autophagy, and mitophagy [167,168,171,172]. Besides, BNIP3 expression is controlled by HIF-1α, among other transcription factors, containing its promoter HRE. Therefore, this protein is an important regulator of cell death under hypoxia [175,181,191].

In our present work, lower levels of BNIP3 protein and mRNA were observed in sorafenib-resistant cell lines relative to parental HepG2 cells, even when HepG2 cell were treated with sorafenib. In several studies, downregulation of BNIP3 has been associated with worse survival and cell proliferation in leukemia, pancreatic, RCC, colorectal, and HCC tumors [171,180–190]. Additionally, some of these investigations

confirmed a close association between the loss of BNIP3 expression and acquisition of chemoresistance to 5-FU and gemcitabine in pancreatic ductal adenocarcinoma [183], and to oxaliplatin [188] or 5-FU [171,186] in colorectal cancer.

Our prior data suggest that BNIP3 repression is regulated by an upstream mechanism. Numerous genes have been reported to be epigenetically silenced, which is related to pathological effects in cells [168]. Histone deacetylation and hypermethylation at the promoter CpG islands are the most frequent epigenetic modifications [15,168]. To determine the possible histone deacetylation of BNIP3, we used the HDAC inhibitor TSA. After TSA treatment, we found no changes in BNIP3 expression, refusing histone deacetylation as responsible for BNIP3 downregulation in our sorafenib-resistant cells. Subsequently, we examined methylation as possible mechanism for BNIP3 repression by MSP, and reported a hypermethylation of the BNIP3 promoter in both resistant cell lines. Moreover, BNIP3 expression was restored in sorafenib-resistant cells after treatment with the DNMTs inhibitor 5-Aza. This reestablishment of BNIP3 reduced the viability of HepG2S1 and HepG2S3 cells; while BNIP3 silencing increased survival rate of resistant cells also subjected to 5-Aza administration. Hence, acquired resistance to sorafenib seems to be correlated with aberrant methylation and following epigenetic silencing of BNIP3. This indicates that BNIP3 upregulation could improve chemosensitivity of HCC cells to sorafenib.

In agreement, previous studies have associated BNIP3 silencing with BNIP3 promoter methylation as mechanism against cell death in leukemia, pancreatic, and colorectal tumors [171,180,182,184,185,190,300,301]. Hypermethylation was promoted by the activity of DNMT1 in pancreatic cancer [182], and in colorectal cancer by DNMT1/DNMT3B [171]. In most researches, 5-Aza was also employed to return normal BNIP3 expression, sensitizing pancreatic cancer cells [182,184,185] and busulfan-resistant myeloid leukemia cells [180] by inducing hypoxia-mediated apoptosis. This mechanism has been widely reported in colorectal cancer, where 5-Aza restored BNIP3 levels to increase chemosensitivity to 5-FU [171], and as a pretreatment to improved sensitivity to irinotecan [300]. Furthermore, chemotherapy and radiotherapy reduced DNMT1 expression to upregulate BNIP3 and promote

BNIP3-dependent apoptosis [301]. Treatment with verticillin A also restored BNIP3 levels in a DNA demethylation-dependent manner to overcome apoptosis resistance [190].

In contrast, other authors showed that BNIP3 silencing in colorectal cancer cells was jointly caused by promoter methylation and histone deacetylation, demonstrating that 5-Aza and TSA recovered BNIP3 expression [187,189], even more effectively after coadministration [187]. Moreover, Shao *et al.* [181] evidenced that histone deacetylation, but not promoter methylation, is the main responsible for BNIP3 repression in RCC. This study used TSA to restore the acetylation status of BNIP3, blocking cell growth and inducing BNIP3-dependent apoptosis [181].

2.5 Overall *in vitro* findings

Overall, these results highlight the role of HIFs stabilization and methylation-dependent silencing of BNIP3 in the acquisition of sorafenib resistance in HCC, and are represented in **Figure 41**. Hence, targeting these pro-survival mechanisms could overcome drug resistance and improve future therapeutic approaches.

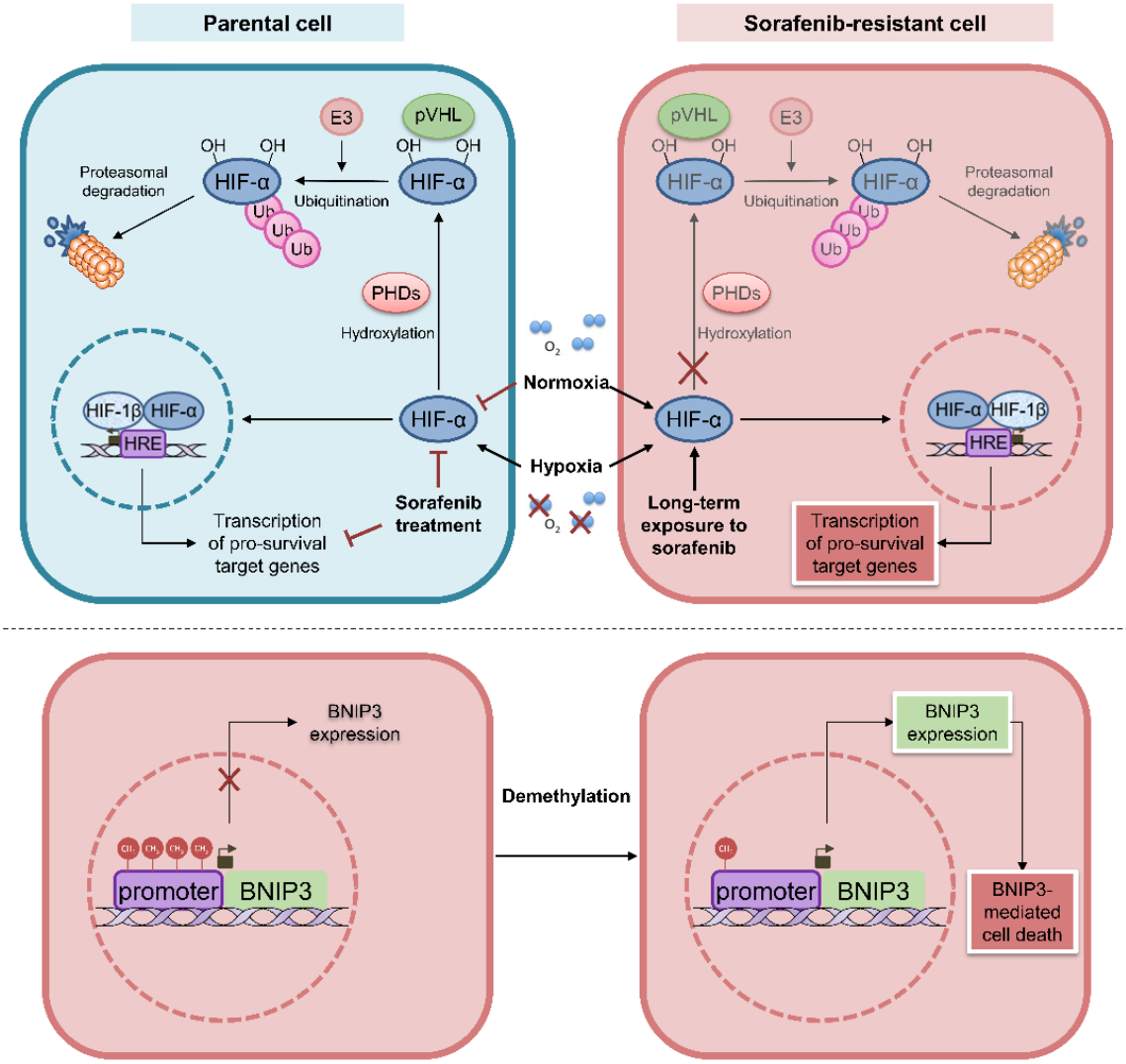

Figure 41. Proposed model about altered hypoxia-mediated response in sorafenib-resistant HCC cells that appear to be associated with the development of acquired resistance to sorafenib. Sorafenib-resistant HCC cells display HIFs overexpression and a repression in the proteasomal-dependent HIFs degradation, which is related to their pro-survival capacity and resistant phenotype. Moreover, methylation-dependent downregulation of BNIP3 contributes to hypoxia-mediated sorafenib resistance by avoiding BNIP3-mediated cell death.

Conclusions

In this chapter, in concordance with the findings obtained in the present PhD Thesis, we detail the conclusions of our work:

First conclusion

Overexpression of both factors, HIF-1α and HIF-2α, correlates with poor OS and DFS/RFS in HCC patients who underwent surgical resection.

Second conclusion

High HIF-1α expression is linked to a wide range of clinicopathological features of HCC patients, including advanced BCLC and TNM stages, cirrhosis, high AFP levels, poor tumor differentiation and histological grade, larger tumor size and number, intrahepatic and lymph node metastasis, capsule infiltration, vascular invasion and vasculogenic mimicry. Otherwise, elevated HIF-2α protein levels only appear to be associated with capsule infiltration.

Third conclusion

HCC cell lines with acquired resistance to sorafenib show more aggressive growth and proliferation rates than the parental HepG2 line sensitive to sorafenib under both oxygen conditions. Moreover, HepG2S1 and HepG2S3 are less affected by hypoxia than parental cells, suggesting that these resistant cells contain adaptive mechanisms to deal with hypoxia.

Fourth conclusion

Sorafenib-resistant HCC cell lines display the stabilization of high protein levels of HIF-1α and HIF-2α, and the subsequent increase in their nuclear translocation, as a consequence of a deregulation in their proteasomal degradation which constitutes a key mechanism on the development of resistance to this drug.

Fifth conclusion

Resistant HCC cells are able to evade sorafenib-mediated apoptosis as a chemoresistance mechanism, being HIF-1α and HIF-2α overexpression involved in this lack of sensitivity to sorafenib.

Sixth conclusion

The apoptotic regulator under hypoxic conditions, BNIP3, is silenced in the sorafenib-resistant phenotype in response to its promoter hypermethylation. This downregulation of BNIP3 participates in hypoxia-mediated sorafenib resistance, by avoiding BNIP3-regulated cell death.

General conclusion

Altogether, the hypoxia-mediated response presents a key role in development, progression, recurrence and drug resistance in HCC. Specifically, HIF-1α and HIF-2α show a relationship with poor outcomes in patients with HCC and with acquired resistance to sorafenib. Therefore, these transcription factors could be useful biomarkers to predict prognosis and recurrence of HCC patients. In addition to the stabilization of HIFs, methylation dependent-silencing of BNIP3 also plays an important role in the acquisition of sorafenib resistance, which suggest that both pro-survival mechanisms are potential therapeutic targets to overcome sorafenib resistance and to improve treatment strategies against HCC.

Resumen en español

universidad de león

Tesis Doctoral

Pronóstico y resistencia adquirida a sorafenib en el carcinoma hepatocelular: papel de la respuesta mediada por hipoxia

Carolina Méndez Blanco
Departamento de Ciencias Biomédicas
Instituto de Biomedicina (IBIOMED)
León, 2021

TABLA DE CONTENIDOS

1 Revisión de la literatura

1.1 Carcinoma hepatocelular

El hepatocarcinoma o carcinoma hepatocelular (HCC, por sus siglas en inglés) es el principal tipo de cáncer hepático primario, que actualmente representa el sexto tipo de cáncer más diagnosticado y la tercera causa de muerte relacionada con el cáncer a nivel mundial [4,5]. En el año 2020, se registraron 830.180 muertes por cáncer de hígado, siendo responsable del 8,3% de las muertes por cáncer en el mundo. De acuerdo con la distribución geográfica, su incidencia es elevada en el este y sudeste de Asia, así como en el norte y oeste de África; mientras que las regiones con menor incidencia son Asia sur-central y occidental y Sudamérica. En Europa, la región sur presenta la mayor incidencia de cáncer hepático del continente [5]. En concreto, durante 2018 se registraron en España 6.630 casos nuevos y un total de 5.570 muertes por cáncer de hígado, cuya incidencia es superior a la media europea [6] **(Figura 1)**. Además de las diferencias entre países y regiones, se ha observado que la incidencia del HCC varía en función del género, siendo 2-3 veces más frecuente en hombres que en mujeres [4,5].

La hepatocarcinogénesis es un proceso complejo que consiste en varias etapas, promoviendo la transformación maligna de los hepatocitos [1]. Con independencia de su etiología, el desarrollo del HCC se asocia principalmente con una cascada de inflamación-fibrosis-cirrosis; de hecho, la cirrosis precede al HCC en torno al 80-90% de los casos [3,8]. Este entorno cirrótico se caracteriza por la formación de nódulos preneoplásicos, que se vuelven displásicos y, finalmente, dan lugar a la instauración del HCC [2,3] **(Figura 2)**. En dicha patogénesis juega un papel importante la combinación de diversos factores, incluyendo variaciones en el microambiente tumoral (inflamación, estrés oxidativo, remodelación tisular e hipoxia), cambios genéticos y epigenéticos, y alteración de múltiples vías moleculares [2,3,7–9]. Todos estos mecanismos están estrechamente relacionados, favoreciendo la aparición del HCC, su progresión y, finalmente, metástasis [2,3,7].

Diversos factores de riesgo se han asociado con el desarrollo del HCC, incluyendo infecciones virales crónicas, toxinas, alcoholismo, trastornos metabólicos o autoinmunitarios, y otras condiciones comórbidas [4,5,16]. Las distribuciones geográficas, de género y de edad únicas del HCC son en gran parte consecuencia de los patrones específicos de estos factores de riesgo, destacando las infecciones por hepatitis B y C, y la enfermedad hepática alcohólica [3] **(Figura 1)**. La infección por el virus de la hepatitis B (HBV, por sus siglas en inglés) constituye el principal factor etiológico en Asia sudoriental y África subsahariana, donde el HBV es endémico, y representa alrededor del 60% de los casos de HCC en Asia y África. Sin embargo, la infección crónica por el virus de la hepatitis C (HCV, por sus siglas en inglés) es la enfermedad hepática subyacente más común entre los pacientes con HCC en áreas desarrolladas como América del Norte, Europa y Japón [1,4,19]. El consumo excesivo de alcohol es el factor etiológico principal en Europa Central y del Este [1], representando un gran riesgo en países como Francia y España [18] **(Figura 1)**. Otro agente clave en el desarrollo del HCC es la ingesta de alimentos contaminados con aflatoxinas, metabolitos secundarios producidos por hongos del género *Aspergillus* [17,20,21]. Así, la ingesta de aflatoxina B1 (AFB1) es frecuente en las regiones de Asia Sudoriental y África Subsahariana, donde la infección por el HBV es endémica, siendo un cofactor importante en estas regiones al actuar de forma sinérgica con el HBV [1,3,18].

La prevalencia de las infecciones por los HBV y HCV está disminuyendo en todo el mundo como resultado exitoso de los programas de vacunación frente al HBV y el desarrollo de terapias antivirales; además, también se ha realizado enorme esfuerzo para prevenir y reducir la exposición a las aflatoxinas [4,5,17,19]. Por ello, los principales factores de riesgo del HCC parecen estar en transición, ya que la incidencia de otros factores de riesgo no virales está aumentando su incidencia en las regiones desarrolladas [4,5]. Entre ellos, se ha visto un aumento de incidencia de HCC en pacientes con enfermedad de hígado graso no alcohólico (NAFLD, por sus siglas en inglés) asociado con síndrome metabólico, diabetes mellitus tipo 2 y obesidad [9,18]. La NAFLD se considera un trastorno metabólico benigno que, a partir del depósito hepático de triglicéridos y esteatosis, puede progresar a esteatohepatitis no alcohólica

(NASH, por sus siglas en inglés), fibrosis, cirrosis y finalmente HCC [22]. Durante los próximos años, se prevé que la prevalencia de estos factores se convierta en una de las principales causas del HCC [23] **(Figura 1)**. Además, enfermedades autoinmunes y trastornos metabólicos [3,18,24]; la disbiosis de la microbiota intestinal [22,23]; el género masculino, previamente mencionado; y otros factores como la edad avanzada, los grupos raciales/étnicos, el estilo de vida y el tabaquismo [1,4,25], también se han asociado con un mayor riesgo de HCC.

El diagnóstico en estadios tempranos es clave dado que permite el uso de terapias curativas [26]. Sin embargo, en la mayoría de los casos el HCC se detecta en fases avanzadas debido a que es asintomático o presenta síntomas que a menudo se relacionan con los de una hepatopatía crónica previa como la cirrosis [16]. Las técnicas de imagen como la ecografía abdominal, la tomografía computarizada, la resonancia magnética, y el método invasivo de angiografía **(Figura 3A-D)**, son ampliamente utilizadas para el seguimiento de pacientes con riesgo elevado y el diagnóstico del HCC [18,26–28]. Además, se emplean biomarcadores séricos con potencial diagnóstico como la α-fetoproteína (AFP), la fracción fucosilada de la AFP (AFP-L3) y la des-γ-carboxiprotrombina (DCP) [16,27,31,32] **(Figura 3E)**. Sin embargo, dichos biomarcadores presentan limitaciones, lo que ha llevado al estudio de nuevos marcadores o combinaciones de ellos que puedan utilizarse en el diagnóstico, pronóstico, respuesta al tratamiento y vigilancia del HCC [31,32]. Finalmente, la biopsia hepática, un método invasivo que implica la extracción de una pequeña porción de la masa tumoral para su evaluación histológica, se limita al diagnóstico del HCC cuando las técnicas de imagen no son concluyentes o para pacientes no cirróticos [33] **(Figura 3F)**.

El tratamiento del HCC depende del estadio en el que se encuentre el tumor, por lo que la correcta categorización pronóstica de los pacientes es fundamental en la selección del tratamiento [18,27]. Entre los numerosos sistemas de estadificación que se han desarrollado, el *Barcelona Clinic Liver Cancer* (BCLC) ha sido ampliamente validado y es el sistema de estadificación más utilizado para el HCC [34–36]. La estadificación BCLC establece el pronóstico de acuerdo con la extensión del tumor, la

reserva funcional del hígado (puntuación de Child-Pugh) y el estado físico del paciente (estado funcional del *Eastern Cooperative Oncology Group* (ECOG-PS, por sus siglas en inglés)), clasificando a los pacientes con HCC en cinco categorías (BCLC 0, A, B, C y D) [34,35] **(Figura 4)**. Como se muestra en la **Figura 4**, los pacientes en fases tempranas (BCLC 0 y A) son susceptibles a los tratamientos curativos como la resección quirúrgica, el trasplante hepático o la ablación. En estadio intermedio (BCLC B), los pacientes son candidatos a tratamientos locales paliativos como la quimioembolización transarterial (TACE, por sus siglas en inglés); mientras que para un pronóstico avanzado (BCLC C), se recomienda el tratamiento quimioterápico sistémico. Por último, en estadio terminal o BCLC D, los pacientes muestran una función hepática deteriorada y/o una sintomatología muy grave, por lo que reciben tratamiento sintomático de apoyo [30,34–36].

En cuanto al tratamiento para estadios avanzados, donde se pronostican la mayoría de los casos tras el diagnóstico, el tratamiento sistémico con el inhibidor tirosina quinasa (TKI, por sus siglas en inglés) sorafenib fue aprobado en 2007, siendo la única opción terapéutica durante una década [1,38]. En los últimos años, otros tratamientos de primera o segunda línea han mostrado eficacia contra el HCC avanzado. Al igual que el sorafenib, se han aprobado otros TKIs, incluido el lenvatinib como opción alternativa de primera línea, o regorafenib y cabozantinib para tumores que continúan su progresión tras el tratamiento con sorafenib [1,39–41]. Además, la inmunoterapia ha surgido como una estrategia prometedora, siendo aprobados varios anticuerpos monoclonales e inhibidores de puntos de control inmunitario. Concretamente, el ramucirumab, nivolumab y pembrolizumab, así como la combinación de ipilimumab y nivolumab, se aprobaron como tratamientos de segunda línea. La última incorporación fue la combinación de atezolizumab y bevacizumab como tratamiento alternativo de primera línea [39–42]. En la **Figura 5**, se representa el cronograma de los tratamientos sistémicos aprobados para el HCC avanzado.

1.2 Sorafenib

El sorafenib fue el primer fármaco sistémico aprobado en 2007 por la *Food and Drug Administration* (FDA) y por la *European Medicines Agency* (EMA) como tratamiento para el HCC avanzado [42,44,53]. Dicha aprobación se basó en dos ensayos clínicos de fase III: el ensayo *Sorafenib HCC Assessment Randomized Protocol* (SHARP) y el ensayo Asia-Pacífico [43]. Así, el ensayo SHARP (identificador de ClinicalTrials.gov NCT00105443) demostró una mejora significativa en la supervivencia de los pacientes con HCC [54] **(Tabla 1)**. Estos resultados fueron confirmados por el ensayo paralelo Asia-Pacífico (identificador de ClinicalTrials.gov NCT00492752) [55]. Además, el sorafenib también ha sido aprobado para el tratamiento del carcinoma de células renales (RCC, por sus siglas en inglés) [45–47] y, por último, para el cáncer de tiroides metastásico bien diferenciado refractario al yodo radiactivo (RAI-R DTC, por sus siglas en inglés) [48,49].

El sorafenib es un TKI de acción dual que se dirige tanto a las células tumorales como a las células endoteliales asociadas, ejerciendo actividades anti-proliferativa, anti-angiogénica y pro-apoptótica [44,67]. Este fármaco se desarrolló originalmente para inhibir el oncogén fibrosarcoma 1 rápidamente acelerado (c-Raf), pero también inhibe B-Raf de tipo tanto *wild-type* como mutado [43,44,64,67]. Esta inhibición conduce al bloqueo de la vía de la proteína quinasa activada por mitógenos (MAPK), concretamente de la quinasa regulada por señales extracelulares (ERK), bloqueando el ciclo celular y, por tanto, la proliferación [43,44,65,67] **(Figura 6)**. Además, el sorafenib reprime la traducción de la proteína 1 de leucemia de células mieloides-1 (Mcl-1) y aumenta la expresión del modulador de apoptosis regulado por p53 (Puma), dos miembros de la familia de la proteína 2 detectada en linfoma de células B (Bcl-2). Ambos mecanismos provocan la activación de la apoptosis por vía intrínseca en las células tumorales [43,65,67] **(Figura 6)**. Por otra parte, el tratamiento con sorafenib también bloquea la angiogénesis mediante la inhibición de múltiples receptores TK de las células endoteliales, incluyendo los receptores del factor de crecimiento del endotelio vascular 1, 2 y 3 (VEGFR-1/2/3), receptor del factor de crecimiento derivado de plaquetas β (PDGFR-β), KIT, tirosina quinasa 3 similar a FMS (FLT-3) y el proto-

oncogén reorganizado durante la transfección (RET) [64,65,67]. La reducción de la angiogénesis por acción del sorafenib provoca la muerte de las células tumorales al reducir el suministro de nutrientes y oxígeno [43] **(Figura 6)**.

Aunque el sorafenib ha sido descrito como un fármaco efectivo, seguro y bien tolerado, los ensayos de fase III SHARP y Asia-Pacífico mostraron algunos efectos adversos comunes en los pacientes que recibieron el fármaco [54,55]. Las reacciones dermatológicas se detectaron en el 90% de los casos, principalmente la reacción cutánea mano-pie (HFSR) y erupciones cutáneas; pero también se han descrito otros efectos frecuentes como diarrea, fatiga e hipertensión [66,68,70]. Sin embargo, en la mayoría de los casos dichos efectos fueron leves o moderados [54,55,61,65].

La principal limitación en el tratamiento con sorafenib es la existencia de una alta tasa de resistencia al mismo por parte de las células de HCC [72–74]. Dicha resistencia puede ser primaria, la cual se caracteriza por la presencia de factores de resistencia a sorafenib antes del tratamiento farmacológico, siendo consecuencia de la elevada heterogeneidad genética del HCC [74,77]. Por ello, es necesario identificar biomarcadores que pueden emplearse para estratificar a los pacientes en respondedores y no respondedores antes de prescribir el sorafenib, según las variaciones en las características genéticas y los perfiles de expresión de los tumores [74,78]. Por otro lado, el tratamiento prolongado con el fármaco conduce al desarrollo de resistencia adquirida, que normalmente aparece durante los 6 primeros meses de tratamiento [73,75].

Como se muestra en la **Figura 7**, se han sugerido diversos mecanismos involucrados en la aparición de células de HCC resistentes al sorafenib. La exposición continua al fármaco provoca la activación de vías de escape de la cascada MAPK o la reactivación de las moléculas inicialmente reprimidas por el sorafenib [72,77,79]; inducción de una autofagia citoprotectora [74,87]; promoción de la transición epitelio-mesénquima (EMT, por sus siglas en inglés) [73,74,76,77,80]; modificaciones epigenéticas [75,77,86]; enriquecimiento de células madre tumorales (CSCs, por sus siglas en inglés) hepáticas [73,75,79,89]; y cambios en el microambiente tumoral, donde destaca la hipoxia [75,79,123]. Recientemente se ha sugerido que cambios en el

transporte del fármaco, farmacocinética, metabolismo y en los mecanismos de reparación del DNA también parecen estar relacionados con la resistencia a sorafenib [78,79,89] **(Figura 7)**.

Debido a la gran cantidad de factores implicados en la eficacia del sorafenib, desde el año 2017 se han aprobado otros regímenes de tratamiento alternativos o de segunda línea para el HCC avanzado [1,39–42]. La **Tabla 1** resume los ensayos clínicos que llevaron a la aprobación de estos tratamientos. No obstante, a pesar de estas nuevas opciones terapéuticas, el uso generalizado de sorafenib como tratamiento estándar hace que la resistencia a dicho fármaco siga constituyendo un desafío importante en el tratamiento del HCC [74]. Por ello, una mayor comprensión de los mecanismos involucrados en la adquisición de resistencia a sorafenib permitirá la identificación de biomarcadores clave para el pronóstico, así como nuevas dianas para mejorar las estrategias terapéuticas [73,79].

1.3 Hipoxia

La hipoxia surge cuando la demanda de oxígeno excede su suministro a los tejidos [99]. Aunque tanto el hígado sano como el afectado por HCC están muy vascularizados, el crecimiento rápido y descontrolado de las células tumorales requiere un mayor consumo de oxígeno y nutrientes y, por lo tanto, desencadena la neoangiogénesis. Sin embargo, la vasculatura tumoral resultante es enormemente caótica e ineficiente y no puede satisfacer el aumento drástico de la demanda de oxígeno, lo que promueve la hipoxia intratumoral [99,102,103]. A pesar de que la hipoxia es dañina para las células, este estrés puede desencadenar cambios adaptativos en las células tumorales que permiten su supervivencia [101,104,105]. Por ello, la hipoxia es un sello distintivo en tumores sólidos como el HCC que se asocia con una mayor agresividad, selección de clones más invasivos, y resistencia a quimioterapia y radioterapia, perjudicando los resultados clínicos [103,104].

La respuesta mediada por hipoxia se lleva a cabo principalmente a través de los factores inducibles por hipoxia (HIFs), factores de transcripción heterodiméricos formados por una subunidad α sensible al oxígeno (HIF-α) y una subunidad β

expresada de forma constitutiva (HIF-β) [98,100,103]. Se han descrito tres isoformas de la subunidad HIF-α, concretamente: HIF-1α, HIF-2α (también denominada proteína del dominio endotelial PAS 1 (EPAS-1)) y HIF-3α (que está menos caracterizada) [101,106–108]. Por otro lado, existen tres subunidades β también conocidas como translocador nuclear del receptor de aril hidrocarburos (ARNT): HIF-1β (ARNT1), HIF-2β (ARNT2) y HIF-3β (ARNT3), siendo HIF-1β la más estudiada [103,109] **(Figura 8)**.

En condiciones normales de oxígeno o normoxia, las subunidades HIF-α son hidroxiladas por las proteínas de dominio prolil hidroxilasa (PHDs), lo que permite su reconocimiento por parte de la proteína von-Hippel Lindau (pVHL), que recluta el complejo ubiquitina ligasa E3 para promover su ubiquitinación y posterior degradación proteasomal [98,101,105,106,110]. Sin embargo, en condiciones de hipoxia, las PHDs se encuentran inactivas impidiendo la hidroxilación de las subunidades α, lo que lleva a su estabilización y translocación al núcleo, donde heterodimerizan con HIF-β para formar el factor de transcripción HIF. El dímero HIF-α/β se une al elemento de respuesta a hipoxia (HRE) de la región promotora de sus genes diana y a coactivadores transcripcionales, promoviendo la expresión de dichos genes diana [101,105–107] **(Figura 9)**. Por otra parte, el factor inhibidor de HIF (FIH) actúa como un segundo regulador de HIF-α dependiente de oxígeno. En condiciones de normoxia, cataliza la hidroxilación de un residuo de asparagina de las subunidades HIF-α impidiendo su interacción con los coactivadores y, por tanto, la transactivación [98,105,107,108,114] **(Figura 9)**.

Además del papel principal de las hidroxilasas en el control de la actividad de los HIF-α, existen numerosas vías que regulan los niveles de HIF de manera independiente del oxígeno. Varios estímulos, incluidos diversos factores de crecimiento, conducen a la acumulación de HIF-α al promover su traducción; mientras que diferentes moléculas pueden modular su transactivación o inducir su degradación por el proteasoma [98,107,110,113] **(Figura 10)**. En definitiva, la regulación de los HIFs es compleja e involucra muchas vías que aún no se han dilucidado por completo. Está claro el papel clave de la regulación dependiente de oxígeno, y que el nivel de expresión de HIF-α es el resultado del equilibrio entre su síntesis y degradación.

Aunque HIF-1α y HIF-2α presentan una alta homología (∼48%), una similar degradación dependiente de oxígeno y comparten genes diana, ambos factores de transcripción respectivamente también regulan un conjunto de dianas exclusivas que están involucradas en procesos no relacionados y, sorprendentemente, pueden mostrar incluso efectos contrarios [102,105,121]. De hecho, HIF-1α tiene una mayor repercusión en la proliferación, migración e invasión vascular, mientras que HIF-2α desempeña un papel más significativo en la regulación de la morfogénesis, la integridad y el ensamblaje de los vasos [121]. Además, HIF-1α se expresa de forma ubicua en todos los tejidos y se activa en respuesta a la hipoxia aguda; mientras que HIF-2α solo se expresa en ciertos tipos celulares, incluidos los hepatocitos, y juega un papel principal en la respuesta hipóxica crónica [121–123]. Curiosamente, la reducción de HIF-1α aumenta la expresión de HIF-2α en las células de HCC mediante un mecanismo de retroalimentación compensatorio, favoreciendo un fenotipo más agresivo [80,122–124].

Se ha descrito que tanto HIF-1α como HIF-2α se encuentran sobreexpresados en tejidos de HCC en comparación con tejidos adyacentes, lo cual se asocia con peores resultados clínicos [106,108,125]. Los múltiples genes diana inducidos por los elevados niveles de HIF-1- and HIF-2 desempeñan importantes funciones en la regulación de diferentes procesos tumorales, tales como la supervivencia y proliferación de las células tumorales, reprogramación metabólica, angiogénesis, invasión y metástasis, así como sobre los mecanismos de muerte celular como la apoptosis y la autofagia [103,105,106] **(Figura 11).**

En el HCC, la hipoxia impulsa la angiogénesis a través de la activación de HIF-1α y la posterior producción de VEGF [75,131–133]. La actividad anti-angiogénica del sorafenib deriva del bloqueo de la vía HIF-1α/VEGF, concretamente previene la síntesis proteica de HIF-1α promovida por la hipoxia, disminuyendo la expresión de VEGF y por ello la vasculatura tumoral [131,133,134]. Aun así, existe una estrecha correlación entre el microambiente hipóxico y la resistencia adquirida a sorafenib. Esto se debe a que el efecto anti-angiogénico a largo plazo provoca la inanición tumoral y posterior hipoxia intratumoral, lo que favorece la selección de clones de células resistentes

adaptadas a la deficiencia de oxígeno, el fracaso de la quimioterapia y un peor pronóstico [75,118,135,136]. Esta respuesta adaptativa, controlada por los HIFs, limita la eficacia del sorafenib [77,123]. De hecho, se han sugerido diversos mecanismos a través de los cuales el tratamiento sostenido con sorafenib es capaz de incrementar los niveles proteicos y la actividad transcripcional de HIF-1α y HIF-2α [123] **(Figura 12)**. Estas evidencias remarcan la relación entre los HIFs y la eficacia del sorafenib en el tratamiento del HCC.

1.4 Muerte celular por apoptosis

La apoptosis, principal mecanismo de muerte celular programada, es causada por la activación de una maquinaria "suicida" dentro de la célula en respuesta a varias situaciones de estrés. Su mecanismo de acción se caracteriza por la condensación de la cromatina, la fragmentación del DNA, la contracción celular, la formación de ampollas dinámicas en la membrana, y la pérdida de adhesión a la matriz extracelular o a las células vecinas, que finalmente conduce a la muerte celular sin provocar daño a las células adyacentes [153,154,156,158]. Por tanto, la apoptosis es un mecanismo protector para evitar la acumulación de células no funcionales o dañadas en los tejidos, manteniendo la homeostasis celular [153,157].

Las diferentes vías que regulan la apoptosis son complejas y parecen ser específicas de tejido y dependientes del agente inductor [156]. Por un lado, la apoptosis puede ocurrir por la interacción entre las células inmunes y las células dañadas, lo que se conoce como la vía extrínseca [153]. Esta ruta se activa mediante señales externas a través de la unión de ligandos como el factor de necrosis tumoral α (TNF-α), el ligando inductor de apoptosis relacionado con TNF (TRAIL) o el ligando primera señal de apoptosis (FasL), a sus respectivos receptores de muerte TNF-R, TRAIL-R o Fas. Posteriormente, se activan la caspasa-8 y la caspasa-10 a través de su asociación con el dominio de muerte asociado a Fas (FADD) o el dominio de muerte asociado a TNF-R (TRADD), y el complejo de señalización inductor de muerte (DISC) [153,155,157,158,162] **(Figura 13)**.

Alternativamente, la propia célula puede inducir su muerte tras detectar el daño a través de sensores intracelulares, ya sea por la ausencia de señales pro-supervivencia como citoquinas, factores de crecimiento y hormonas, o por la exposición directa a factores ambientales como toxinas, radiación, hipoxia e infecciones virales [153,154,156]. Este proceso, conocido como vía intrínseca o mitocondrial, está regulado por proteínas de la familia Bcl-2, que se dividen en tres grupos según su función pro- o anti-apoptótica, así como según las regiones de homología de Bcl-2 (BH) presentes en su estructura [158,160,161]. Así, los miembros anti-apoptóticos, como Bcl-2, contienen cuatro dominios BH (BH1-4) en su estructura. Por otro lado, las proteínas pro-apoptóticas de esta familia se clasifican en dos tipos: en primer lugar, los miembros de múltiples dominios como la proteína X asociada a Bcl-2 (Bax) y el antagonista/asesino homólogo a Bcl-2 (Bak), que contienen y comparten homología en los cuatro dominios BH; y en segundo lugar, las proteínas que solamente poseen el dominio BH3, también denominadas grupo iniciador de apoptosis [160]. En ausencia de estímulo apoptótico, las proteínas anti-apoptóticas forman heterodímeros con Bax y Bak (pro-apoptóticas) para preservar la integridad de la membrana mitocondrial externa (OMM, por sus siglas en inglés) e impedir la apoptosis mitocondrial [161]. En situación de estrés, se incrementa la expresión de las proteínas pro-apoptóticas y de las proteínas iniciadoras de la apoptosis con dominio BH3, que se unen a las proteínas anti-apoptóticas para liberar a Bax y Bak. Bax y Bak forman oligómeros que se insertan en la OMM, permeabilizándola, lo que lleva a la liberación del citocromo c. Luego, el citocromo c se une a monómeros del factor 1 activador de la proteasa apoptótica (APAF-1), formando un complejo homo-heptamérico conocido como apoptosoma, que recluta y escinde la pro-caspasa-9 generando su forma activa, caspasa-9 [153,158,161] **(Figura 13)**.

Además, la activación de las caspasas iniciadoras-8 y -10 también conduce a la escisión y miristoilación de la proteína Bid citoplasmática, generando la forma activa Bid truncada (tBid) que se transloca a las mitocondrias. tBid activa Bax, contribuyendo a la liberación de citocromo c y, por tanto, a la apoptosis mitocondrial. Es decir, Bid es una molécula común entre las vías intrínseca y extrínseca de la apoptosis [155,157,162] **(Figura 13)**.

Por último, ambas vías convergen en la fase de ejecución de la apoptosis, donde las caspasas iniciadoras (8, 9 y 10) activan a las caspasas ejecutoras (3, 6 y 7) responsables de la cascada de eventos que llevan a la destrucción del material nuclear y del citoesqueleto, desmantelando la célula [153,156,158] **(Figura 13)**.

La desregulación de la muerte celular es un sello distintivo clave en la tumorigénesis y la progresión del tumor [161]. En el cáncer, la señalización apoptótica aberrante permite que las células cancerosas escapen de la apoptosis, lo que conduce a una proliferación descontrolada y, por lo tanto, a la supervivencia del tumor, la resistencia al tratamiento y la recurrencia del cáncer [163]. En el HCC, a pesar de que sorafenib ejerce un efecto pro-apoptótico, el tratamiento sostenido permite el desarrollo de mecanismos que inducen la resistencia apoptótica, lo que supone una ventaja para la supervivencia de las células cancerosas [74,123]. La evasión de la apoptosis mediante la activación de proteínas anti-apoptóticas o la inhibición de proteínas pro-apoptóticas se ha asociado con la resistencia al sorafenib [74]. Además, la hipoxia y los HIFs pueden promover alteraciones en este proceso de muerte celular para regular la supervivencia de las células tumorales [115,121,124,130].

1.5 BNIP3

La proteína 3 de interacción con Bcl-2/adenovirus E1B de 19 kDa (BNIP3) es un miembro atípico de la familia Bcl-2, que pertenece a la subfamilia de proteínas pro-apoptóticas con dominio BH3 y se encuentra en la OMM [167–169]. BNIP3 se expresa de forma específica en músculo, corazón e hígado [170]; y está estrechamente relacionada con el microambiente hipóxico, siendo activada directamente por el factor HIF-1α al presentar el HRE en su promotor génico [169,170]. Esta proteína mitocondrial funciona principalmente como un regulador de muerte celular bajo condiciones de hipoxia, estando involucrada en varios procesos de muerte celular, incluyendo apoptosis, necrosis, autofagia, y en la autofagia mitocondrial o mitofagia [171,172].

En su región NH_2-terminal, BNIP3 contiene la región que interactúa con la proteína de cadena ligera 3 asociada a microtúbulos (LC3) (LIR, por sus siglas en inglés)

[168,172]. El dominio LIR permite la interacción entre el homodímero BNIP3 y LC3, anclado en la membrana del fagóforo, dirigiendo a las mitocondrias directamente al autofagosoma para su degradación [169,170,172,173]. BNIP3 también presenta el motivo $L^{1}KKNSD^{6}W^{7}IWDW^{11}$ relacionado con el dominio BH3 de los iniciadores de la apoptosis de la familia Bcl-2. No obstante, este motivo presenta residuos no conservados evolutivamente en las posiciones 7 y 11 en comparación con otras proteínas con dominio BH3, lo que significa que BNIP3 parece ser un miembro atípico de esta subfamilia [167,169,172]. Finalmente, la región COOH-terminal de BNIP3 contiene un dominio transmembrana (TM) multifuncional responsable de su localización mitocondrial, dimerización estable y actividad pro-muerte [168,172] **(Figura 14)**.

No existe un mecanismo único a través del cual BNIP3 induce necrosis, apoptosis, autofagia o mitofagia. De hecho, los diferentes mecanismos parecen depender del tipo celular y de su contexto [172,174]. La muerte celular inducida por BNIP3, apoptosis y necrosis, está controlada tanto por el dominio BH3 como por el dominio TM, en contraste con otras proteínas con dominio BH3 [168]. Además, aunque BNIP3 no es parte de la maquinaria central de la autofagia, es capaz de promover la inducción de autofagia y mitofagia, a través de sus dominios TM y LIR [167,169,170,172,173] **(Figura 15)**. Por lo tanto, BNIP3 se ha descrito como el principal mediador de la muerte celular en condiciones de hipoxia [168,172].

Por todo ello, BNIP3 juega un importante papel en la carcinogénesis. Así, algunos estudios indican que la sobreexpresión de BNIP3 se correlaciona con un fenotipo tumoral más agresivo y un mal pronóstico, así como con un mayor riesgo de recurrencia en cáncer de próstata, pulmón, cuello uterino y mama [176–179]. Por el contrario, la disminución de los niveles de BNIP3 presenta una repercusión negativa en leucemia, RCC, cáncer pancreático, cáncer colorrectal y HCC [171,180–190]. Además, en algunos casos se observó que la expresión de BNIP3 estaba regulada por modificaciones epigenéticas en su promotor, siendo silenciada por metilación y desacetilación de histonas [168,172,175,191]. Estas modificaciones se han descrito en diferentes tipos de cáncer y juegan un papel clave en el desarrollo de tumores. Por

ejemplo, el promotor BNIP3 presenta una metilación aberrante en cáncer colorrectal y pancreático, impidiendo la muerte celular inducida por hipoxia al silenciar BNIP3 [171,182,184,185,190]. Alternativamente, se ha visto que la expresión de BNIP3 se encuentra reprimida mediante la desacetilación de histonas en el RCC [181]. En ambas situaciones, los bajos niveles de BNIP3 conducen a una resistencia a la muerte celular, lo que favorece la supervivencia de las células tumorales [172].

2 Introducción y objetivos

El HCC es el principal cáncer primario de hígado, que actualmente representa la sexta neoplasia más diagnosticada y la tercera causa de mortalidad relacionada con el cáncer a nivel mundial. La alta tasa de mortalidad del HCC se debe a la dificultad de su diagnóstico precoz y a la falta de tratamientos curativos para el estadio avanzado del HCC, donde se diagnostican la mayoría de los casos, lo que conduce a un peor pronóstico de esta patología. Además, el HCC presenta una alta tasa de recurrencia tras los tratamientos.

El HCC es un tumor muy vascularizado; sin embargo, la vasculatura tumoral es caótica e ineficaz, lo que promueve la hipoxia intratumoral. La hipoxia es una característica común de los tumores sólidos y, aunque inicialmente supone un estrés, puede desencadenar cambios adaptativos que permitan la supervivencia de las células tumorales. En consecuencia, la hipoxia se ha asociado con una mayor agresividad del tumor, la recurrencia, la selección de clones más invasivos, la resistencia a las terapias y los malos resultados clínicos. La respuesta mediada por hipoxia se lleva a cabo principalmente por HIF-1α y HIF-2α, factores de transcripción de miles de genes implicados en proliferación celular, evasión de la muerte celular, reprogramación metabólica, angiogénesis, invasión y metástasis.

El tratamiento estándar del HCC en fases avanzadas se basa en el sorafenib, el primer fármaco aprobado para este propósito. El sorafenib es un fármaco TKI que ejerce actividades anti-proliferativa, anti-angiogénica y pro-apoptótica contra las células de HCC. A pesar de su eficacia para prolongar la supervivencia de los pacientes, la sensibilidad a este fármaco se reduce después de una exposición prolongada debido a la aparición de células de HCC resistentes a través de varios mecanismos adaptativos. De hecho, la actividad anti-angiogénica sostenida del sorafenib favorece la hipoxia intratumoral.

Teniendo todo ello en cuenta, el objetivo principal de la presente Tesis fue estudiar la implicación de la sobreexpresión de HIF-1α o HIF-2α en el pronóstico y las características clínico-patológicas de pacientes con HCC, así como la relación entre la respuesta mediada por hipoxia y la quimiorresistencia utilizando un modelo *in vitro* de HCC con resistencia adquirida a sorafenib.

Para ello, se propusieron los siguientes objetivos específicos:

Primero

Evaluar la asociación de la expresión elevada de HIF-1α y HIF-2α con parámetros relacionados con la supervivencia en pacientes con HCC sometidos a resección quirúrgica mediante una revisión sistemática con meta-análisis.

Segundo

Meta-analizar la correlación entre la sobreexpresión de las proteínas HIF-1α y HIF-2α y varias características clínico-patológicas en pacientes con HCC.

Tercero

Caracterizar la dinámica de crecimiento y la proliferación de las células HepG2S1 y HepG2S3 resistentes a sorafenib en comparación con la línea celular parental HepG2 sensible al fármaco.

Cuarto

Evaluar la expresión proteica y la regulación de los principales intermediarios de la respuesta mediada por hipoxia, HIF-1α y HIF-2α, entre las líneas celulares resistentes y la línea parental sensible.

Quinto

Determinar el estado de la muerte celular apoptótica entre células parentales y resistentes a sorafenib, y la posible implicación de la expresión de HIF-1α y HIF-2α sobre la capacidad de supervivencia de las células resistentes HepG2S1 y HepG2S3.

Sexto

Analizar la expresión y regulación del principal mediador apoptótico en condiciones de hipoxia, BNIP3, en el fenotipo resistente.

3 Material y métodos

La metodología empleada en el presente trabajo se divide en dos partes: revisión sistemática con meta-análisis y trabajo *in vitro*.

3.1 Espacio de trabajo

La presente Tesis Doctoral ha sido realizada en el Instituto de Biomedicina (IBIOMED) de la Universidad de León. Además, los análisis de microscopía confocal se llevaron a cabo en el Servicio de Microscopía de la Universidad de León.

3.2 Revisión sistemática con meta-análisis

Nuestro primer objetivo fue evaluar la importancia pronóstica de la expresión de HIF-1α o HIF-2α en pacientes con HCC sometidos a resección quirúrgica, analizando su relación con la supervivencia global (OS, por sus siglas en inglés) y la supervivencia libre de enfermedad/supervivencia libre de recurrencia (DFS/RFS, por sus siglas en inglés respectivamente). Nuestro segundo objetivo fue examinar la relación de la expresión de HIF-1α o HIF-2α con las características del tumor y del paciente.

Este meta-análisis se realizó de acuerdo con las pautas *Preferred Reporting Items for Systematic Reviews and Meta-Analyses* (PRISMA) (Tabla Suplementaria 1) [194,195]. Además, el diseño del protocolo se registró previamente en el *International Prospective Register of Systematic Reviews* (PROSPERO) (National Institute for Health Research (NIHR), York, Reino Unido) (https://www.crd.york.ac.uk/prospero/) con el código de registro CRD42020191977.

3.2.1 Estrategia de búsqueda

Para evaluar el papel de la expresión de los HIFs en pacientes con HCC, se llevó a cabo una búsqueda bibliográfica sistemática exhaustiva en las bases de datos *Embase, Cochrane, PubMed, Scopus* y *Web Of Science* (WOS), con una fecha de finalización del 31 de mayo de 2020. Todos los estudios elegibles fueron identificados utilizando los siguientes términos de búsqueda (“HCC” OR “hepatocarcinoma” OR “hepatocellular

carcinoma") AND ("HIF" OR "hypoxia-inducible factor") en cada base de datos, como se detalla en la **Tabla 2**.

3.2.2 Criterios de inclusión y exclusión

Para ser incluidos, los estudios debían cumplir los siguientes criterios de inclusión: (1) pacientes con un diagnóstico distintivo de HCC por patología; (2) expresión de la proteína HIF-1α o HIF-2α determinada usando inmunohistoquímica (IHC, por sus siglas en inglés); (3) muestras obtenidas mediante resección quirúrgica; (4) examinar la relación entre los niveles de expresión de HIF-1α o HIF-2α en el HCC y los parámetros relacionados con la supervivencia o clínico-patológicos; (5) utilizar una metodología estadística adecuada.

De la misma manera, se omitió cualquier estudio que cumpliera con los siguientes criterios de exclusión: (1) estudios realizados solo en modelos preclínicos; (2) revisiones, informes de casos, cartas, capítulos de libros o comunicaciones a congresos; (3) muestras sin tejido intratumoral o que involucren solo tejidos adyacentes; (4) método de detección diferente a la IHC; (5) estudios en los que no se proporcionaron los datos requeridos y no se pudieron estimar; (6) artículos sin texto completo en inglés.

3.2.3 Extracción de datos y evaluación de la calidad

El texto completo de los estudios seleccionados se analizó de manera exhaustiva para confirmar su elegibilidad, evaluar su calidad y extraer los datos necesarios.

Se empleó la escala Newcastle-Ottawa (NOS, por sus siglas en inglés) para determinar la calidad de los estudios seleccionados para la síntesis cualitativa, que establece una puntuación con valores de 0 a 9 [196]. Los estudios con una puntuación ≥5 se consideraron estudios de alta calidad; de lo contrario, se consideraron de calidad insuficiente y no se incluyeron en la síntesis cuantitativa.

Las características básicas de cada artículo, que comprenden estudio (primer autor y referencia), año de publicación, tamaño de la muestra, tamaño de la muestra

según el sexo, intervención clínica, rango de edad, edad media de los pacientes, calidad del estudio (puntuación NOS), método usado para medir la expresión de HIF, el tipo de análisis de supervivencia, fuente de obtención del cociente de riesgo instantáneo o *hazard ratio* (HR), definición de la elevada expresión de HIF, y número de pacientes con alta expresión de HIF-1α o HIF-2α, se registraron en la **Tabla 3**. Además, en la Tabla Suplementaria 2 se detallaron los anticuerpos y el procedimiento de tinción utilizado para la IHC de HIF en cada uno de los artículos.

Para realizar el análisis estadístico, se extrajeron los HR con su intervalo de confianza (CI, por sus siglas en inglés) del 95% de OS, DFS/RFS y tiempo hasta la recurrencia (TTR, por sus siglas en inglés). La OS se calculó desde la fecha de la primera intervención médica hasta la última visita de seguimiento o la muerte del paciente. DFS, RFS y TTR se definieron como el período desde la fecha de la primera intervención hasta el último día de seguimiento o cuando se diagnosticó la recidiva tumoral. Se empleó el método de Parmar para calcular el HR y el CI 95% cuando el estudio no indicó los datos de forma directa [197]. Para las características clínico-patológicas, recopilamos el número de pacientes con alta y baja expresión de HIF-1α o HIF-2α para las dos condiciones comparativas de cada característica. Se requirió establecer umbrales específicos o valores de corte (*cut-off*) para algunos parámetros. Las condiciones comparativas y los *cut-off* utilizados se detallan en la **Tabla 4**. Estos datos se utilizaron para el cálculo de la razón de momios u *odds ratio* (OR) y su CI 95% necesarios para el análisis estadístico.

3.2.4 Análisis estadístico

Se utilizó la versión 16 del *software STATA* (Stata Corporation, College Station, TX, EE. UU.) Para analizar la posible correlación de la expresión de HIF-1α o HIF-2α con el pronóstico y varias características clínico-patológicas de los pacientes con HCC.

El resultado de la expresión de los HIFs en HCC se midió en dos pasos. Por un lado, agrupamos los datos de los HR y los CI 95% de OS y DFS/RFS para determinar el valor general que examina la asociación entre HIF-1α o HIF-2α y el pronóstico del HCC. Por otro lado, la fuerza de correlación entre la sobreexpresión de HIF-1α o HIF-2α y

cada característica clínico-patológica se evaluó mediante la estimación global de los OR con CI del 95%. En ambas situaciones, los HR y OR se combinaron entre los estudios y el tamaño del efecto general se calculó y representó mediante un diagrama de bosque o *forest plot*. Los valores globales de HR>1 y OR>1 sugirieron un riesgo elevado de peor pronóstico y una mayor incidencia en la característica considerada, respectivamente, en relación con la sobreexpresión del HIF correspondiente. Estas correlaciones fueron estadísticamente significativas cuando p<0,05.

Además, la heterogeneidad entre los estudios se examinó mediante la prueba Q-test basada en chi cuadrado y el estadístico I^2. El estadístico I^2 es una medida cuantitativa de la inconsistencia entre los estudios que varía del 0% (sin heterogeneidad) al 100% (heterogeneidad máxima). Cuando el valor de Q-test p<0,1 o $I^2 \geq 50\%$, se consideró que existía una heterogeneidad significativa. En consecuencia, se aplicó el método *Restricted Maximum Likelihood* (REML) como modelo de efectos aleatorios cuando se encontró heterogeneidad en al menos una prueba. En caso contrario, se utilizó el modelo de efectos fijos con el método de *Inverse Variance* (IV).

Para explorar las posibles fuentes de heterogeneidad, se realizaron análisis de subgrupos según el tamaño de la muestra, la puntuación NOS, el tiempo de seguimiento y la edad media. Se consideraron otros parámetros como el anticuerpo utilizado para cada HIF o el género para examinar los subgrupos, pero no todos los estudios aportaban dicha información.

Finalmente, analizamos la presencia de sesgo de publicación mediante gráfico de embudo o *funnel plot* y mediante el test de Egger. Cuando se obtuvo asimetría en el *funnel plot* y el valor p de Egger<0,05, se consideró la existencia de un sesgo de publicación significativo. En caso de sesgo, se utilizó el método de recorte y relleno o *trim-and-fill* para ajustar el número de estudios y estimar el efecto global corregido, lo que permite determinar si el sesgo de publicación pudo influir en la solidez de los resultados.

3.3 Estudio experimental *in vitro*

3.3.1 Cultivo celular y tratamientos

Para llevar a cabo el estudio *in vitro* de la relación entre la resistencia a sorafenib en el HCC y la respuesta mediada por hipoxia, se utilizó la línea celular de HCC humano HepG2 obtenida de la *American Type Culture Collection* (ATCC) (Manassas, VA, EE. UU.); y dos líneas celulares derivadas de HepG2 con resistencia adquirida a sorafenib, denominadas HepG2S1 y HepG2S3, que fueron generadas por el grupo de la Universidad KU Leuven (Bélgica) tal y como describen van Malenstein *y cols.* [88] **(Figura 16)**.

Las células se cultivaron en monocapa usando *Dulbecco's Modified Eagle's Medium* (DMEM) con alto contenido en glucosa (4500 mg/l) (Sigma-Aldrich, San Luis, MO, EE. UU.) suplementado con suero bovino fetal (FBS, por sus siglas en inglés) al 10% (Gibco™, Gaithersburg, MD, EE. UU.) y 100 U/ml de penicilina/estreptomicina (Gibco™). Las líneas celulares se mantuvieron en condiciones de incubación controladas de CO_2 (5%), temperatura (37°C) y humedad (95%), y se realizó un cambio de medio cada dos días. Las líneas celulares resistentes se cultivaron continuamente en presencia de sorafenib 6 µM (Santa Cruz Biotechnology, Dallas, TX, EE. UU.) para preservar el fenotipo resistente. El sorafenib se disolvió en dimetilsulfóxido (DMSO) (Sigma-Aldrich). Las células fueron subcultivadas cuando alcanzaban una confluencia de alrededor del 80% utilizando tripsina-ácido etilendiaminotetraacético (EDTA) al 0,05% (Gibco™). Cada línea celular se sembraba a razón de 2×10^6 células en *flasks* de 75 cm^2 para su mantenimiento, o bien en distintas placas para realizar los experimentos correspondientes.

Además de sorafenib, se utilizaron otros compuestos para realizar los experimentos. Así, para establecer las condiciones de hipoxia, se añadió cloruro de cobalto ($CoCl_2$) 100 µM (PanreacAppliChem, Barcelona, España) disuelto en medio. El $CoCl_2$ actúa como hipoximimético al prevenir la hidroxilación y la posterior degradación proteasomal de las subunidades HIF-α debido a que el cobalto inhibe la actividad de las PHDs [232]. Empleamos cicloheximida (CHX) 300 µM y MG132 30 µM (Tocris Bioscience, Bristol, Reino Unido) como inhibidores de la síntesis de proteínas y

del proteasoma, respectivamente. Además, reprimimos la desacetilación de histonas utilizando 10, 50 y 100 nM del inhibidor de histona deacetilasas (HDACs) tricostatina-A (TSA) (AdooQ® Bioscience, Irvine, CA, EE. UU.) y la metilación con 10 y 100 µM del inhibidor de la DNA metiltransferasa (DNMT) 5-aza-2'-desoxicitidina (5-Aza) (MedChemExpress, Sollentuna, Suecia). La CHX se disolvió en H_2O milli-Q; mientras que MG132, TSA y 5-Aza en DMSO.

3.3.2 Ensayos de crecimiento, viabilidad y muerte celular

Curva de crecimiento basada en tinción con cristal violeta

Para realizar la tinción con cristal violeta, las células se sembraron en placas de 48 pocillos a una densidad de $7{,}5\times10^3$ células/pocillo, utilizándose una placa para cada día (días 0, 1, 2, 3, 4 y 5). Una vez tratadas con o sin sorafenib y/o $CoCl_2$, las células se lavaron con tampón fosfato salino (PBS, por sus siglas en inglés) (Sigma-Aldrich) frío y se fijaron durante 10 min con una solución de formaldehído al 4% (Thermo Fisher Scientific, Waltham, MA, EE. UU.) disuelta en PBS. Tras la fijación, las células se lavaron con H_2O milli-Q y se tiñeron durante 20 min con cristal violeta al 0,1% (Labkem, Barcelona, España) disuelto en etanol al 10%. Después de 3 lavados, se añadió ácido acético al 10% (Sigma-Aldrich) a cada pocillo seguido de 20 min de incubación en agitación. Diluimos 1:4 con H_2O milli-Q y medimos la absorbancia a una longitud de onda de 590 nm utilizando el lector de placas de microtitulación *Synergy™ HT Multi-Mode Microplate Reader* (BioTek Instruments, Inc., Winooski, VT, EE. UU.) y el *software Gen 5* (BioTek Instruments, Inc.).

Ensayo de viabilidad celular

Se utilizó el bromuro de tetrazolio azul de tiazolilo (MTT) (Sigma-Aldrich) disuelto en PBS a una concentración de 5 mg/ml como indicador colorimétrico de la actividad metabólica para el ensayo de viabilidad celular denominado ensayo MTT.

Las células se sembraron en placas de 96 pocillos a una densidad de 1×10^4 células/pocillo. Después de los silenciamientos génicos y de los tratamientos con $CoCl_2$ y con o sin 5-Aza realizados en diferentes experimentos, se efectuó un lavado con PBS seguido de la incubación durante 3 h a 37°C con una solución 1:10 de MTT en medio

libre de FBS. El MTT genera una solución amarillenta que se convierte en cristales de formazán de color azul oscuro insolubles en H_2O por acción de las deshidrogenasas mitocondriales de las células vivas. A continuación, se sustituyó el medio que contenía MTT por DMSO y se agitó durante 5 min para solubilizar los cristales de formazán. La intensidad óptica se midió a una longitud de onda de 570 nm mediante el lector de placas *Synergy™ HT Multi-Mode Microplate Reader* y el *software Gen 5*.

Estudio de la población subG1 por citometría de flujo

Para el análisis de la población apoptótica subG1, las células se sembraron en *flasks* de 75 cm^2 a una densidad de 2×10^6 células y, 48 h después del tratamiento con $CoCl_2$ y con o sin sorafenib, las células se recolectaron. Las células tripsinizadas se centrifugaron a 350 g y 4°C durante 5 min, se lavaron con PBS helado y se centrifugaron nuevamente en las mismas condiciones. Las células se fijaron durante 2 h a 4°C con etanol al 70% en PBS. Para preparar las muestras, se centrifugaron aproximadamente 1×10^6 células fijadas y permeabilizadas por muestra a 850 g durante 5 min y se lavaron con PBS. Tras otra ronda de centrifugación, estas 1×10^6 células se incubaron con 0,5 ml de un tampón de tinción durante 15 min a temperatura ambiente y en condiciones de oscuridad. Dicho tampón está compuesto por el agente intercalante yoduro de propidio (PI, por sus siglas en inglés) y ribonucleasa (RNase, por sus siglas en inglés) (BD Pharmingen™, Franklin Lakes, NJ, EE. UU.). Finalmente, utilizando un citómetro de flujo *FACSCalibur* (Becton Dickinson, San José, CA, EE. UU.) y el *software CellQuest Pro™* (Becton Dickinson), se adquirieron 5.000 eventos para cada muestra y se evaluó el porcentaje de células en fase subG1 mediante el *software* analítico *WEASEL* (Walter y Eliza Hall Institute (WEHI), Melbourne, VIC, Australia).

3.3.3 Evaluación de la expresión proteica

Inmunocitoquímica e inmunofluorescencia (ICC/IF)

Se sembraron las células HepG2, HepG2S1 y HepG2S3 en placas de 24 pocillos que contenían un cubreobjetos, a una densidad de $2,5\times10^4$ células. Los cubreobjetos se pretrataron con gelatina al 0,2% (Sigma-Aldrich) disuelta en H_2O desionizada (diH_2O)

durante 10 min a temperatura ambiente, para favorecer la adhesión de las células al vidrio. Luego, se retiró la solución de gelatina y se dejó secar durante al menos 15 min.

Después del tratamiento con $CoCl_2$ y con o sin sorafenib, las células se fijaron con una solución de formaldehído al 4% (Thermo Fisher Scientific) durante 15 min, se permeabilizaron durante 20 min con saponina al 0,2% (Sigma-Aldrich) y se bloquearon durante 30 min con 1% de albúmina de suero bovino libre de ácidos grasos (FAF-BSA, por sus siglas en inglés) (Sigma-Aldrich) en PBS. Estos pasos se realizaron a temperatura ambiente y con 3 lavados con PBS entre cada uno de ellos. A continuación, las células se incubaron durante la noche a 4°C con los anticuerpos primarios frente a Ki67 (1:200; sc-23900, Santa Cruz Biotechnology), HIF-1α (1:300; ab2185, Abcam, Cambridge, Reino Unido), HIF-2α (1:300; ab199, Abcam) o BNIP3 (1:200; sc-56167, Santa Cruz Biotechnology). Las células se lavaron con PBS y se incubaron durante 1 h a temperatura ambiente con los anticuerpos secundarios inmunoglobulina G (IgG) anti-ratón conjugado con *Alexa Fluor® 488* (1:1.000; ab150113, Abcam) o IgG anti-conejo conjugado con *Alexa Fluor® 647* (1:1.000; ab150079, Abcam). Los cubreobjetos se lavaron con PBS y se montaron en portaobjetos de vidrio con *Fluoroshield™* (Sigma-Aldrich), un medio de montaje fluorescente que contiene 4'6-diamidino-2-fenilindol (DAPI) para la tinción de los núcleos. Los resultados se visualizaron en el microscopio confocal *Zeiss LSM 800* (Zeiss AG, Jena, Alemania) y las imágenes se obtuvieron con el *software ZEN* (Zeiss AG). La cuantificación de la fluorescencia se realizó utilizando el *software ImageJ* (National Institutes of Health (NIH), Bethesda, MD, EE. UU.) aplicando la fórmula de fluorescencia celular total corregida (CTCF) [238,239].

Western blot

Las células se sembraron en placas p60 a una densidad de $7{,}5\times10^5$ células/placa. Se realizaron los tratamientos correspondientes con $CoCl_2$, sorafenib, CHX, MG132, TSA, 5-Aza y/o silenciamiento génico para varios experimentos. Las células se lavaron con PBS y se recogieron en un tampón de homogeneización (sacarosa 0,25 mM, Tris 10 mM y EDTA 1 mM; pH 7,4) suplementado con cócteles inhibidores de proteasas y fosfatasas (Roche Diagnostics, Basilea, Suiza), para evitar la

degradación de las proteínas por acción de estas enzimas. Las células se lisaron mediante sonicación durante 2 pulsos de 20 s a 60% de amplitud utilizando el *UP50H Compact Ultrasonic Processor* (Hielscher-Ultrasound Technology, Teltow, Alemania) y se centrifugaron a 14.000 g durante 10 min. La cuantificación de la concentración de proteína de las muestras se realizó mediante el método de Bradford, usando el reactivo *Coomassie® Brilliant Blue G-205* (Bio-Rad, Hercules, CA, EE. UU.) de acuerdo con las instrucciones del fabricante. Se utilizaron el lector *Synergy™ HT Multi-Mode Microplate Reader* y el *software Gen 5* para medir la absorbancia a una longitud de onda de 595 nm, y una recta patrón de BSA (Sigma-Aldrich).

Las muestras se prepararon con la misma cantidad de proteína y se sometieron a un proceso de desnaturalización agregando 1:4 del tampón de muestra *Laemmli 4x* (Bio-Rad) y calentando a 100°C durante 3 min. Se cargaron junto con el marcador de peso molecular *PageRuler™ Prestained Protein Ladder* (Thermo Fisher Scientific) o el *Precision Plus Protein Dual Color Standards* (Bio-Rad) en geles de poliacrilamida y se sometieron a electroforesis en gel de poliacrilamida con dodecilsulfato sódico (SDS-PAGE, por sus siglas en inglés), que separa las proteínas en función de su peso molecular aplicando un campo eléctrico de 100 V. Los geles resultantes se transfirieron a membranas de difluoruro de polivinilideno (PVDF) (Bio-Rad) empleando el *Trans-Blot® Turbo™ Transfer System* (Bio-Rad). Todo el material utilizado para la elaboración de los geles de poliacrilamida, SDS-PAGE y transferencia se obtuvo de Bio-Rad y se empleó siguiendo las instrucciones del fabricante.

Las membranas de PVDF se bloquearon con leche al 5% disuelta en PBS-*Tween 20* (Bio-Rad) (PBS-T) al 0,05% durante 1 h a temperatura ambiente para evitar uniones inespecíficas. Luego, cada membrana se incubó durante la noche a 4°C con el correspondiente anticuerpo primario **(Tabla 5)**. El antígeno nuclear de células en proliferación (PCNA) se utilizó como control de carga. Al día siguiente, las membranas se incubaron durante 1 h a temperatura ambiente con los anticuerpos secundarios IgG anti-conejo (1:20.000; 31460, Thermo Fisher Scientific) o Ig anti-ratón (1:5.000; P0206, Dako, Glostrup, Alemania), que se encuentran conjugados con la peroxidasa de rábano picante (HRP, por sus siglas en inglés). Entre cada paso, las membranas se lavaron 3

veces con PBS-T. Por último, las membranas se incubaron con el sustrato quimioluminiscente de la HRP *Pierce™ enhanced chemiluminescence (ECL) Western Blotting Substrate* (Thermo Fisher Scientific), según las instrucciones del fabricante. Esto permitió la detección de las proteínas exponiendo las membranas a películas *Amersham Hyperfilm™ ECL* (VWR International, Radnor, PA, EE. UU.) y sumergiendo estas películas en revelador (Rosex Medical, SL., Barcelona, España), H_2O y fijador (Rosex Medical), consecutivamente. La densidad de las bandas proteicas se cuantificó con el *software ImageJ*.

3.3.4 Análisis de ácidos nucleicos

Análisis de expresión génica por microarray

Para realizar el análisis de expresión génica, se sembraron las células HepG2 y HepG2S1 a una densidad de 1×10^6 en *flasks* de 25 cm². Después de 72 h en condiciones de mantenimiento, las células se recolectaron con el reactivo *TRIzol™ reagent* (Invitrogen, Carlsbad, CA, EE. UU.) y se aisló el RNA utilizando el *RNeasy kit* (Qiagen, Chatsworth, CA, EE. UU.) tal y como indica en el protocolo del fabricante. Se evaluó la calidad del RNA mediante el *2100 BioAnalyzer Instrument* (Agilent, Palo Alto, CA, EE. UU.). Se empleó el *GeneChip® Human Gene 1.0 ST Array* (Affymetrix, Santa Clara, CA, EE. UU.) como plataforma para el microarray. Dicho análisis fue llevado a cabo por el grupo de la Universidad KU Leuven (Bélgica) que colabora con nuestro laboratorio.

Reacción en cadena de la polimerasa con retrotranscripción (RT-PCR) y RT-PCR cuantitativa en tiempo real (qRT-PCR)

Las células se sembraron en placas de 6 pocillos a una densidad de $2{,}5\times10^5$ células. Después del tratamiento con $CoCl_2$ y con o sin sorafenib y 5-Aza para diversos experimentos, se aisló el RNA total con el reactivo *TRIzol™ reagent* (Invitrogen) y se cuantificó utilizando el espectrofotómetro *Nanodrop™ ND-1000* (Thermo Fisher Scientific). Se empleó la desoxirribonucleasa (DNase, por sus siglas en inglés) libre de RNase RQ1 (Promega, Madison, WI, EE. UU.) para eliminar el DNA residual y, posteriormente, cantidades iguales de RNA (500 ng) se retrotranscribieron a DNA

complementario (cDNA, por sus siglas en inglés) con el *High-Capacity cDNA Reverse Transcription Kit* (Applied Biosystems, Carlsbad, CA, EE. UU.). Todos los procedimientos se realizaron según lo indicado por las instrucciones del fabricante.

Para el análisis por qRT-PCR, el cDNA se amplificó utilizando el *Power SYBR™ Green PCR Master Mix* (Applied Biosystems) de acuerdo con el protocolo del fabricante y con las siguientes condiciones: desnaturalización inicial durante 10 min a 95°C, y 40 ciclos de desnaturalización durante 15 s a 95°C y anillamiento durante 60 s a 60°C, utilizando el *StepOnePlus™ Real-Time PCR System* y el *software StepOne™* (Applied Biosystems). Los cambios relativos en los niveles de expresión génica se evaluaron mediante el método $2^{-\Delta\Delta CT}$ [244].

Mientras que para la RT-PCR, la amplificación del cDNA se realizó utilizando el *KAPA HiFi HotStart ReadyMix PCR Kit* (Kapa Biosystems, Wilmington, MA, EE. UU.) y el termociclador *MJ Research PTC-200 Thermal Cycler* (Marshall Scientific, Hampton, NH, EE. UU.) bajo las siguientes condiciones: desnaturalización inicial durante 5 min a 95°C; 30 ciclos de desnaturalización durante 30 s a 94°C, anillamiento durante 45 s a 60°C, y extensión durante 30 s a 72°C; y una etapa de extensión final durante 10 min a 72°C. Los productos obtenidos se sometieron a electroforesis en gel de agarosa junto con el marcador *100 base pair (bp) DNA ladder* (Invitrogen). Los geles de agarosa se prepararon disolviendo agarosa al 2% (Biotools, Madrid, España) en 1:50 de tampón Tris-acetato-EDTA (TAE) 50X (Tris 2 M, ácido acético glacial 1 M, EDTA 50 mM) y añadiendo *GelRed® Nuclei Acid Gel Stain* (Biotium, Fremont, CA, EE. UU.), que permite visualizar las bandas utilizando el *ChemiDoc™ XRS Universal Hood II* y el *software Quantity One®* (Bio-Rad).

Los cebadores humanos empleados para qRT-PCR y RT-PCR fueron los detallados a continuación: BNIP3 *forward* 5'-CGCAGACACCACAAGATACC-3' y *reverse* 5'-TCTTCATGACGCTCGTGTTC-3'; 18S *forward* 5'-GGCGCCCCCTCGATGCTCTTAG-3' y *reverse* 5'-GCTCGGGCCTGCTTTGAACACTCT-3'. El RNA ribosómico (rRNA) 18S se utilizó como control endógeno.

PCR específica de metilación (MSP)

Las células se sembraron en placas de 6 pocillos a una densidad de $2,5\times10^5$ células/placa. Después de los tratamientos con $CoCl_2$ y con o sin sorafenib y 5-Aza, se extrajo el DNA usando Fenol:Cloroformo:Alcohol Isoamílico 25:24:1 (Sigma-Aldrich) y se modificó el DNA usando el *bisulfite conversion EZ DNA Methylation™ Kit* (Zymo Research, Irvine, CA, EE. UU.). Ambos procedimientos se realizaron siguiendo las instrucciones del fabricante.

La MSP se llevó a cabo utilizando cebadores específicos para detectar el DNA de BNIP3 metilado (M) y no metilado (U): M-BNIP3 *forward* 5'-TAGGATTCGTTTCGCGTACG-3' and *reverse* 5'-ACCGCGTCGCCCATTAACCGCG-3'; U-BNIP3 *forward* 5'-TAGGATTTGTTTTGTGTATG-3' and *reverse* 5'-ACCACATCACCCATTAACCACA-3'. La amplificación se realizó empleando el *KAPA HiFi HotStart ReadyMix PCR Kit* y el termociclador *MJ Research PTC-200 Thermal Cycler*, y las condiciones empeladas fueron las siguientes: desnaturalización preliminar durante 15 min a 95°C; 35 ciclos de desnaturalización durante 30 s a 94°C, anillamiento durante 50 s a 58°C, y extensión durante 1 min a 72°C; y una extensión final durante 10 min a 72°C. Los productos de la MSP se cargaron en geles de agarosa al 2% junto con un marcador de bp, y se visualizaron con el *ChemiDoc™ XRS Universal Hood II* y el *software Quantity One®*.

3.3.5 Silenciamiento génico

RNAs pequeño de interferencia (siRNAs, por sus siglas en inglés) comerciales contra HIF-1α (sc-35561), EPAS-1 (o HIF-2α) (sc-35316) y BNIP3 (sc-37451), así como un siRNA control que codifica una secuencia no dirigida (sc-36869) se adquirieron en Santa Cruz Biotechnology. Estos siRNAs comerciales están compuestos por varios siRNAs de 19-25 nucleótidos específicos diseñados para anular la expresión del gen de interés. Cada siRNA se introdujo en las células mediante transfección inversa utilizando el reactivo *Lipofectamine® RNAiMAX Reagent* (Invitrogen) de acuerdo con el protocolo del fabricante. Tras preparar los complejos siRNA-lipofectamina dentro de las placas de 6 pocillos, se añadieron células a una densidad de 5×10^5 células/pocillo. 5 h después de la transfección, el medio se reemplazó con medio fresco completo y, 24 h después de

la transfección, las células se trataron con $CoCl_2$ y con o sin sorafenib y 5-Aza para finalmente llevar a cabo MTT y *Western blot*.

3.3.6 Análisis estadístico

Los datos del microarray se obtuvieron a partir de tres experimentos independientes y se analizaron con el paquete *Limma* de *Bioconductor* (http://www.bioconductor.org) [247]. La expresión diferencial de los genes se midió realizando una prueba t-test moderada. Los valores p resultantes se corrigieron con Benjamini-Hochberg para controlar el *false discovery rate* [248]. Para seleccionar genes con expresión diferenciada, se aplicó un *cut-off* de Δlog (^{2}log *fold change* (FC)) >+0,7 o <−0,7 y una p corregida<0,05.

El análisis de ruta, con los análisis de enriquecimiento, el agrupamiento funcional y el mapeo de la ruta *Kyoto Encyclopedia of Genes and Genomes* (KEGG), se realizó con las herramientas bioinformáticas *WEB-based GEne SeT AnaLysis Toolkit* (WebGestalt) (http://webgestalt.org/) [249] y *Database for Annotation, Visualization and Integrated Discovery* (DAVID) (https://david.ncifcrf.gov/) [250] de forma paralela. Estos datos están disponibles en el *National Center for Biotechnology Information* (NCBI), *GEO DataSets*, serie GSE62813 (https://www.ncbi.nlm.nih.gov/geo/query/acc.cgi?acc=GSE62813).

El resto de los resultados se detallaron como valores medios ± desviación estándar (SD, por sus siglas en inglés) de tres experimentos independientes. Los datos se analizaron con el paquete estadístico *GraphPad Prism 6* (GraphPad Software, San Diego, CA, EE. UU.), comprobando la normalidad de los datos mediante el método Kolmogorov-Smirnov. En función de los distintos experimentos, se realización pruebas t-test para datos no apareados, o bien análisis de varianza (ANOVA) *one-way* o *two-way* seguidos del análisis *post-hoc* de Tukey para examinar las diferencias entre los diferentes grupos evaluados. Se consideraron resultados estadísticamente significativos cuando p<0,05.

4 Resultados y discusión

4.1 Valor pronóstico y clínico-patológico de HIF-1α y HIF-2α en el HCC: Revisión sistemática con meta-análisis

La hipoxia es una característica frecuente en los tumores sólidos que surge en respuesta a una vascularización defectuosa y una mayor actividad metabólica [123]. A pesar de que el HCC se caracteriza por ser uno de los tumores más hipervascularizados, las regiones hipóxicas suelen aparecer en este tumor debido a la rápida proliferación de células tumorales y al desarrollo de vasos sanguíneos defectuosos [126,127]. Aunque inicialmente una disminución en el suministro de oxígeno es perjudicial para la supervivencia celular, algunas células tumorales pueden desarrollar cambios adaptativos para sobrevivir en el microambiente hipóxico [128]. Esta respuesta adaptativa es facilitada principalmente por los HIFs, factores de transcripción que modulan un conjunto de genes pro-supervivencia asociados con la agresividad tumoral, la recurrencia, la selección de clones más invasivos, la resistencia a los tratamientos y peores resultados clínicos [123].

El HCC es la tercera causa principal de muerte relacionada con el cáncer y se ha reconocido como un tumor de mal pronóstico [254]. Esto es consecuencia, en gran medida, debido a su difícil detección precoz y su alta tasa de recurrencia. Además, los biomarcadores típicos como la AFP tienen un valor insuficiente para predecir el pronóstico del HCC y la recurrencia [255]. Por tanto, es necesario definir nuevos biomarcadores eficaces para determinar con precisión el pronóstico clínico y la respuesta al tratamiento de los pacientes con HCC. En el presente estudio evaluamos los principales mediadores de la respuesta a la hipoxia, HIF-1α y HIF-2α, como posibles biomarcadores para predecir el pronóstico del HCC. Para examinar la correlación entre la expresión de HIF y el HCC, el presente meta-análisis tuvo como objetivo evaluar la asociación de la sobreexpresión de HIF-1α o HIF-2α con el pronóstico y las características clínico-patológicas de los pacientes con HCC.

4.1.1 Selección y características del estudio

De acuerdo a los términos de búsqueda especificados anteriormente, se identificaron un total de 3.888 estudios potencialmente relevantes a partir de las búsquedas en las bases de datos. Entre ellos, se eliminaron 2.172 registros duplicados. Después de la selección en base a los títulos y resúmenes, se excluyeron otros 1.386 estudios por las siguientes razones: artículos de investigación no originales (revisiones, capítulos de libros o similares), estudios en modelos animales o celulares, y artículos no relacionados con HCC o HIF. Se examinó el texto completo de 330 artículos para determinar su elegibilidad, identificando 24 estudios con texto completo en chino, 264 sin IHC para los HIFs y/o sin análisis de supervivencia o características clínico-patológicas, uno sobre HIF-3α y siete donde no se realizó resección quirúrgica. Por lo tanto, estos 296 artículos también fueron omitidos de nuestro estudio, siendo 34 [198–231] los artículos sometidos a la extracción de datos y evaluación de calidad en la síntesis cualitativa. Cao *y cols.* [231] y Zhou *y cols.* [223] no proporcionaron datos suficientes para estimar el HR y su CI 95% mediante el método de Parmar. Además, Zhou *y cols.* [223] no alcanzó el umbral de calidad de la escala NOS **(Tabla 3)**. Finalmente, 32 publicaciones fueron seleccionadas para el meta-análisis: 25 sobre HIF-1α, seis sobre HIF-2α y una sobre ambos factores **(Figura 17)**.

La **Tabla 3** resume las características básicas de los artículos incluidos en nuestro trabajo, aportando las puntuaciones de calidad. Los 32 estudios finalmente analizados en el estudio cuantitativo se publicaron entre 2004 y 2020, y comprendieron un total de 3.578 (ocho datos se "perdieron" en el análisis de la expresión de HIF-1α) y 1.213 pacientes con HCC para la evaluación de HIF-1α y HIF-2α, respectivamente. Los artículos sobre el estudio de HIF-1α incluyeron un número de pacientes que oscilaba entre 35 y 419, y 1.846 pacientes (51,7%) mostraron sobreexpresión de HIF-1α. En cuantos a los trabajos sobre HIF-2α, registraron entre 84 y 315 pacientes en cada estudio, mostrando un total de 553 pacientes (45,6%) con sobreexpresión de HIF-2α.

En cuanto a los datos necesarios para la evaluación cuantitativa del presente meta-análisis, dentro de los 25 artículos comprendidos para HIF-1α, 18 aportaron datos sobre la OS, ocho sobre DFS/RFS y 23 sobre diversas características clínico-

patológicas; mientras que de los siete estudios sobre HIF-2α, cinco proporcionaron OS, tres DFS/RFS y todos ellos varias características clínico-patológicas. Además, aunque cinco de las investigaciones sobre HIF-1α determinaron el TTR, solo una aportó el HR. Dado que el HR y su CI 95% no se pudieron estimar de acuerdo con el método de Parmar para los estudios restantes, no fue factible incluir el estudio de la asociación entre HIF-1α y el TTR.

Todos los pacientes incluidos fueron sometidos a resección quirúrgica. Sin embargo, algunos de los pacientes incluidos en los estudios de Wada *y cols.* [199] y Dai *y cols.* [201] recibieron terapia antitumoral preoperatoria. Asimismo, en Xiang *y cols.* [206] los pacientes se sometieron a radioterapia como tratamiento adyuvante postoperatorio. El resto de pacientes evaluados no recibió ninguna intervención adicional a la cirugía.

Todos los pacientes involucrados procedían de Asia: un estudio de Japón (1,3%) [199], otro de Singapur (3,8%) [213] y el resto de China (94,9%). En cuanto a la etiología, 21 de los 32 artículos evaluaron el número de pacientes con hepatitis B [198–200,202–208,210,212,213,215,219–221,226–228,230], nueve los pacientes con hepatitis C [199,203,205,210,212,213,226–228], y solo uno los pacientes alcohólicos [213]. Esto se correlaciona con el hecho de que todos los estudios se realizaron en población asiática, donde la hepatitis B es el principal factor etiológico [1]. Además, 20 de los artículos examinaron el número de pacientes con HCC derivado de cirrosis [198–203,205,208,210,212,213,215,217,219–221,225–228]. Con estos datos, determinamos que el 78,2% de los pacientes incluidos en el presente metaanálisis tenían hepatitis B, 6,6% hepatitis C y 66,1% cirrosis.

4.1.2 Correlación de la expresión proteica de HIF-1α y HIF-2α con el pronóstico

Para iniciar la síntesis cuantitativa del meta-análisis, evaluamos la asociación entre cada HIF y los parámetros relacionados con la supervivencia. Como se muestra en la **Figura 18A**, la sobreexpresión de HIF-1α mostró una fuerte correlación con la OS (HR, 1,73; CI 95%, 1,54-1,94; p=0,00) y la DFS/RFS (HR, 1,64; CI 95%, 1,36-1,99; p=0,00) en pacientes con HCC, sin mostrar heterogeneidad significativa. Estos resultados

indican que HIF-1α podría ser utilizado como biomarcador fiable para de pronóstico y recurrencia para pacientes con HCC.

Además, los resultados indicaron que no hubo una asociación significativa entre la sobreexpresión de HIF-2α y la OS en pacientes con HCC (HR, 1,25; CI 95%, 0,68-2,32; p=0,48), y que se obtuvo una heterogeneidad elevada entre los estudios (I^2=91,46%, Q-test p=0,00). Por el contrario, la expresión elevada de HIF-2α se correlacionó con la DFS/RFS (HR, 1,37; CI 95%, 1,05-1,79; p=0,02) y no reveló heterogeneidad **(Figura 18B)**. Sin embargo, tras el análisis de subgrupos, observamos que si existía una relación con la OS utilizando como moderadores el tamaño de la muestra (n<200: HR, 1,83; CI 95%, 1,18-2,84; p=0,01) y el tiempo de seguimiento (seguimiento>72: HR, 2,47; CI 95%, 2,02-3,03; p=0,00), que además resolvieron la heterogeneidad encontrada inicialmente (n<200: I^2=0,00; Q-test p=0,93) (seguimiento>72: I^2=11,74, Q-test p=0,29) **(Tabla 6)**. Todo ello sugiere que, al igual que HIF-1α, HIF-2α podría emplearse como biomarcador en HCC.

Dos meta-análisis realizados previamente por Zheng *y cols.* [126] y Cao *y cols.* [125], que incluyeron 7 y 8 artículos respectivamente, también examinaron el papel de la expresión de HIF-1α en individuos con HCC. En concordancia con nuestros resultados, ambos estudios también describieron una relación entre la sobreexpresión de HIF-1α y la DFS, y Zheng *y cols.* [126] además encontraron una asociación con la OS. Varias investigaciones realizadas en cáncer de mama [256], cáncer de pulmón [257], cáncer gástrico [258], RCC [259], cáncer de páncreas [260], tumor óseo [261], carcinoma de esófago [262], cáncer colorrectal [263], cáncer de cabeza y cuello [264,265], cáncer de endometrio [266], cáncer epitelial de ovario [267], y carcinoma oral de células escamosas [268], también mostraron una relación significativa entre el mal pronóstico y la sobreexpresión de HIF-1α. Además, los niveles altos de HIF-1α se han correlacionado con un peor pronóstico en pacientes con cáncer avanzado sometidos a quimioterapia o radioterapia [269]. Por lo tanto, además de un biomarcador útil, el diseño de terapias dirigidas contra HIF-1α podría ser un enfoque prometedor para mejorar los tratamientos para pacientes con cáncer avanzado.

En cuanto a HIF-2α, un meta-análisis previo de Yao *y cols.* [127] y otro de Luo *y cols.* [128] evaluaron el papel de HIF-2α en el HCC y en varios tipos de cáncer, respectivamente. Así Luo *y cols.* [128] observaron una asociación entre la OS y la sobreexpresión de HIF-2α en pacientes con HCC después de estratificar por tipo de tumor. Del mismo modo, este meta-análisis determinó que la elevada expresión de HIF-2α también da como resultado una peor OS en otros tumores, como cáncer de pulmón, mama, colorrectal, de cabeza y cuello, y sarcomas [128]. Por el contrario, Yao *y cols.* [127] no encontraron una relación significativa entre la OS y la expresión de HIF-2α, lo que se explica debido a que nuestro trabajo incluyó los artículos más recientes y excluyó aquellos con texto completo en chino [127]. Cabe señalar que ninguna investigación previa ha analizado antes el efecto de este factor de transcripción sobre la DFS o la RFS. Otros trabajos han detectado la correlación entre la sobreexpresión de HIF-2α y un peor pronóstico en otros tumores, incluido el RCC [259], cáncer colorrectal [263,270], cáncer de cabeza y cuello [264], cáncer de pulmón [271], carcinoma oral de células escamosas [272], y cáncer gástrico [273].

De manera similar, un reciente estudio paralelo al nuestro realizado por Ding *y cols*. [274] evaluó el papel de la expresión de ambos factores, HIF-1α y HIF-2α, en pacientes con HCC. A pesar de que este estudio solo incluyó 25 artículos sobre HIF, de acuerdo con nuestros resultados, sus datos también indicaron que la sobreexpresión de HIF-1α en el HCC se asoció con peores OS y DFS. Por el contrario, este trabajo no mostró ninguna relación significativa con la expresión de HIF-2α, diferencia que podría explicarse por el menor número de artículos incluidos y la ausencia de análisis de subgrupos [274].

4.1.3 Correlación de la expresión proteica de HIF-1α y HIF-2α con características clínico-patológicas

Para investigar más a fondo el papel de los HIFs en el HCC, analizamos su posible correlación con varias características clínicas y patológicas.

Por un lado, diversos parámetros mostraron una asociación positiva con la expresión elevada de HIF-1α, incluyendo BCLC (OR, 2,49; CI 95%, 1,56-3,98; p=0,00), infiltración capsular (OR, 2,48; CI 95%, 1,29-4,77; p=0,01), metástasis intrahepática

(OR, 2,90; CI 95%, 1,62-5,20; p=0,00), metástasis a los nódulos linfáticos (OR, 3,74; CI 95%, 1,73-8,07; p=0,00), clasificación tumor-nódulo-metástasis (TNM) (I, II-III) (OR, 1,59; CI 95% CI, 1,21-2,09; p=0,00), TNM (I-II, III) (OR, 2,62; CI 95%, 1,69-4,08; p=0,00), TNM (I-II, III-IV) (OR, 2,23; CI 95%, 1,37-3,64; p=0,00), diferenciación tumoral (OR, 1,78; CI 95%, 1,07-2,96; p=0,03), número de tumores o nódulos (OR, 1,50; CI 95%, 1,15-1,96; p=0,00), tamaño del tumor (*cut-off* 3 cm) (OR, 3,70; CI 95%, 1,29-10,63; p=0,02), invasión vascular (OR, 2,61; CI 95%, 1,82-3,75; p=0,00), y mimetismo vasculogénico (OR, 2,61; CI 95%, 1,67-4,09; p=0,00) **(Figuras 19 y 20)**. De ellas, se observó una marcada heterogeneidad para la diferenciación tumoral (I^2=66,79%, Q-test p=0,00) y la invasión vascular (I^2=69,59%, Q-test p=0,00) **(Figura 20)**.

Por otro lado, no se encontró una relación significativa entre la sobreexpresión de HIF-1α y otras características: niveles de AFP (*cut-off* 20 y 400 ng/ml), edad (*cut-off* 50 y 60 años), niveles de albúmina (*cut-off* 35 U/L), niveles de alanina aminotransferasa (ALT) (*cut-off* 40 y 80 U/L), niveles de bilirrubina (*cut-off* 1 µmol/L), formación de cápsulas, puntuación Child-Pugh, cirrosis, metástasis a distancia, clasificación de Edmondson, género, hepatitis B o C, grado histológico, y tamaño del tumor (*cut-off* 5 cm) **(Figuras 21 y 22)**. Se obtuvo una heterogeneidad sustancial en niveles de AFP (20 ng/ml) (I^2=54,11%, Q-test p=0,05), AFP (400 ng/ml) (I^2=73,88%, Q-test p=0,01), edad (50 años) (I^2=47,38%, Q-test p=0,07), niveles de albúmina (35 U/L) (I^2=51,97%, Q-test p=0,13), cirrosis (I^2=44,47%, Q-test p=0,03), metástasis a distancia (I^2=82,75%, Q-test p=0,02), grado histológico (I^2=49,79%, Q-test p=0,09), y tamaño del tumor (5 cm) (I^2=85,08%, Q-test p=0,00) **(Figura 22)**.

De acuerdo a los análisis de subgrupos, se consiguió resolver la heterogeneidad para todos los parámetros que inicialmente fueron heterogéneos para el estudio sobre HIF-1α. Además, se detectó a mayores una asociación entre la elevada expresión de dicho factor con niveles de AFP (20 ng/ml), cirrosis, grado histológico y tamaño del tumor (5 cm) **(Tabla 6)**. La relación de HIF-1α con todas estas características permitiría establecer un pronóstico aún más preciso para los pacientes con HCC.

Todos los estudios sobre HIF-2α se incorporaron para el meta-análisis de las características clínico-patológicas. Sin embargo, los resultados no mostraron una

relación significativa entre la sobreexpresión de HIF-2α y ningún parámetro evaluado: niveles de AFP (*cut-off* 400 ng/ml) (OR, 0,88; CI 95%, 0,60-1,30; p=0,52), edad (*cut-off* 50 años) (OR, 1,17; CI 95%, 0,79-1,73; p=0,44), formación de cápsulas (OR, 1,31; CI 95%, 0,93-1,83; p=0,12), infiltración capsular (OR, 1,82; CI 95%, 0,54-6,13; p=0,33), cirrosis (OR, 1,22; CI 95%, 0,91-1,64; p=0,19), clasificación de Edmondson (OR, 11,05; CI 95%, 0,02-6.167,72; p=0,46), género (OR, 0,95; CI 95%, 0,68-1,35; p=0,79), hepatitis B (OR, 1,03; CI 95%, 0,76-1,39; p=0,86), grado histológico (OR, 0,93; CI 95%, 0,43-1,99; p=0,85), necrosis (OR, 1,32; CI 95%, 0,25-6,98; p=0,74), estadificación TNM (I-II, III-IV) (OR, 1,12; CI 95%, 0,40-3,10; p=0,83), número de tumores (OR, 1,44; CI 95%, 0,92-2,27; p=0,11), tamaño del tumor (*cut-off* 5 cm) (OR, 1,20; CI 95%, 0,36-3,99; p=0,77) e invasión vascular (OR, 1,16; CI 95%, 0,67-2,00; p=0,60) **(Figuras 23 y 24)**. Además, la heterogeneidad fue sustancial para infiltración capsular (I^2=77,06%, Q-test p=0,03), clasificación de Edmondson (I^2=94,64%, Q-test p=0,00), necrosis (I^2=89,88%, Q-test p=0,00), estadificación TNM (I-II, III-IV) (I^2=56,26%, Q-test p=0,13), tamaño del tumor (5 cm) (I^2=94,27%, Q-test p=0,00) e invasión vascular (I^2=62,18%, Q-test p=0,02) **(Figura 24)**.

De acuerdo al análisis de subgrupos, la heterogeneidad fue resuelta para todos los parámetros, excepto para el tamaño del tumor. Además, la infiltración capsular mostró estar correlacionada con la sobreexpresión de HIF-2α cuando se utilizó la edad media como moderador (años≥50: OR, 2,71; CI 95%, 1,55-4,73; p = 0,00) **(Tabla 6)**.

Los dos meta-análisis previos sobre HIF-1α también mostraron que la sobreexpresión de este factor de transcripción estaba relacionada con la invasión vascular [125,126]; sin embargo, Cao *y cols.* [125] no encontraron una relación significativa con la formación de cápsulas, cirrosis, diferenciación tumoral o tamaño tumoral. Este desacuerdo puede explicarse por el menor número de estudios, y por lo tanto de pacientes con HCC, incluidos en dicho meta-análisis, así como por la falta de análisis de subgrupos [125]. Con respecto a HIF-2α, Yao *y cols.* [127] también encontraron una asociación positiva con la infiltración capsular y, al igual que en nuestro trabajo, no vieron correlación de HIF-2α con cirrosis, necrosis y tamaño

tumoral. Sin embargo, ellos sí mostraron una relación de los niveles de esta proteína con la invasión y el grado histológico [127].

En concordancia con nuestro trabajo, el estudio paralelo de Ding *y cols*. [274] encontró que la sobreexpresión de HIF-1α se asoció con el número de tumores, el tamaño del tumor y la invasión vascular. Por el contrario, este estudio no observó una relación con la formación de cápsulas, la cirrosis o la diferenciación tumoral para HIF-1α, ni ninguna correlación significativa con la expresión de HIF-2α [274]. Como ya se indicó anteriormente, esto se debe a que Ding *y cols.* [274] emplearon un menor número de artículos y no realizaron análisis de subgrupos.

La hipoxia, a través de la inducción de factores angiogénicos, constituye el principal estímulo fisiológico que promueve la angiogénesis en el HCC. El VEGF, un factor pro-angiogénico regulado transcripcionalmente por ambos HIF, es clave para el desarrollo de los vasos sanguíneos al inducir el crecimiento y la migración de las células endoteliales [103,275]. Algunos estudios incluidos en nuestro meta-análisis mostraron que una alta expresión de VEGF se asoció con angiogénesis, mimetismo vasculogénico, densidad vascular y peor pronóstico; mostrando una relación positiva entre VEGF y HIF-1α [198,199,203,214,218]. Otros factores pro-angiogénicos regulados por los HIFs también están involucrados en la angiogénesis en el HCC, como la expresión de la angiopoyetina-2 (ANG-2) y la proteína morfogenética ósea 4 (BMP4) mediada por HIF-1α [103,199], la expresión del factor de células madre (SCF) y del inhibidor del activador del plasminógeno-1 (PAI-1) inducida por HIF-2α, y la expresión de la eritropoyetina (EPO) y PDGF regulada por ambos HIFs [103,275]. Definitivamente, la hipoxia y más precisamente los HIFs contribuyen a la angiogénesis en el HCC, lo que se confirma con nuestros resultados que asocian la sobreexpresión de HIF-1α con una mayor invasión vascular y mimetismo vasculogénico.

Además, la EMT y la metástasis pueden promoverse en condiciones hipóxicas en el HCC [106]. De acuerdo con ello, varios estudios incluidos en nuestro análisis mostraron que el aumento de la capacidad invasiva y el mal pronóstico en pacientes con HCC están asociados con la expresión de proteínas como metaloproteinasas (MMPs), E-cadherina o interleuquina-8 (IL-8), también controladas por los HIFs

[201,203,209,212,213]. En estudios preclínicos, se describieron resultados comparables que relacionan la alta invasividad y metástasis con la expresión mediada por HIF-1α de Snail, la quimioquina 6 de motivo C-X-C (CXCL6) y la proteína 4 que interactúa con la familia Rab11 (Rab11-FIP4) [276–278]; y con la regulación dependiente de HIF-2α de SerpinB3, SCF y de la proteína 1 que contiene el dominio CUB (CDCP1) [279–281]. Estos datos confirman la asociación que encontramos entre ambos HIF y los parámetros clínico-patológicos ligados a la metástasis, como la infiltración capsular y la metástasis intrahepática o a los ganglios linfáticos.

4.1.4 Sesgo de publicación

En análisis del sesgo de publicación identificó una fuerte asimetría en el *funnel plot* de la OS para HIF-1α que evidencia el sesgo de publicación, y que fue confirmado por la prueba de Egger (p=0,00). Por lo tanto, se implementó el método *trim-and-fill*, donde se imputaron siete estudios y se reajustó el tamaño del efecto global (HR, 1,56; CI 95%, 1,41-1,73). Por el contrario, la prueba de Egger no indicó asimetría en DFS/RFS (p=0,06) para HIF-1α, ni en OS (p=0,93) o DFS/RFS (p=0,55) para HIF-2α **(Tabla 7; Figura 25)**.

Entre las características clínico-patológicas de HIF-1α, se detectó asimetría para el género (p=0,03), la diferenciación tumoral (p=0,04) y la invasión vascular (p=0,00). En el género, el análisis *trim-and-fill* imputó cinco estudios y estimó un efecto global corregido (OR, 0,83; CI 95%, 0,69-1,00). De manera similar, se agregaron seis estudios al *funnel plot* de la invasión vascular, corrigiendo el tamaño del efecto combinado (OR, 1,75; CI 95%, 1,12-2,73). Por el contrario, para la diferenciación tumoral, el método *trim-and-fill* no incluyó ningún estudio; por lo tanto, el tamaño del efecto global permaneció intacto **(Tabla 7; Figuras 26 y 27)**. En cuanto a las características clínico-patológicas de HIF-2α, la prueba de Egger solo mostró asimetría para los niveles de AFP (p=0,02). Después del análisis *trim-and-fill*, se imputó un único estudio y se ajustó el efecto global (OR, 1,00; CI 95%, 0,69-1,44) **(Tabla 7; Figura 28)**.

4.1.5 Ventajas y limitaciones del estudio

El presente trabajo es una completa revisión sistemática con meta-análisis que realiza un análisis cuantitativo exhaustivo de las evidencias científicas sobre la relación de HIF-1α y HIF-2α con parámetros relacionados con la supervivencia, incluyendo OS y DFS/RFS, y con características clínico-patológicas en pacientes con HCC. Estos hallazgos sugieren que ambos HIFs podrían ser biomarcadores útiles para predecir el pronóstico y la recurrencia en pacientes con HCC, pudiendo mejorar las decisiones clínicas. Los resultados obtenidos se han representado en la **Figura 40**.

Nuestro trabajo también incluye la evaluación de la heterogeneidad, el análisis de subgrupos y del sesgo de publicación. Los meta-análisis previos que evaluaron la correlación entre los niveles de HIF-1α o HIF-2α y los resultados tumorales, que se describieron a lo largo de la discusión, incluyeron menos artículos y por ende menos pacientes con HCC, y examinaron una menor cantidad de parámetros. Además, la mayoría de estos estudios no evaluaron el sesgo de publicación ni realizaron análisis de subgrupos.

A pesar de todo, existen algunas limitaciones en nuestro meta-análisis que deben tenerse en cuenta. Primero, durante la evaluación de elegibilidad, se omitieron aquellos artículos con texto completo en chino y, en consecuencia, se excluyeron datos relevantes. En segundo lugar, la extracción de datos no fue posible en algunos casos debido a la falta de información necesaria para estimar el HR y su CI 95% según el método de Parmar, como el tiempo de seguimiento o el número de pacientes en cada grupo. En tercer lugar, los estudios incluidos utilizaron anticuerpos variados o no especificados para la detección de HIF, empleando procedimientos de tinción inconsistentes y diferentes *cut-off* para la definición de la sobreexpresión de HIF-α, lo que podría conducir a heterogeneidad. En cuarto lugar, todos los estudios se realizaron con población asiática, principalmente de China, donde la hepatitis B es el principal factor de riesgo [1]. De acuerdo con esto, la mayoría de los artículos evaluaron el efecto de la hepatitis. Por lo tanto, se requieren estudios adicionales para evaluar el papel de la expresión de HIF en otras regiones étnicas o geográficas, como los países occidentales donde prevalecen otros factores etiológicos como NASH [1]. En quinto

lugar, el volumen de información encontrada sobre HIF-2α fue menor y, por lo tanto, el efecto de este factor está subrepresentado en este análisis. Finalmente, se denotó sesgo de publicación en algunos parámetros.

4.2 Papel de la respuesta mediada por hipoxia en la resistencia adquirida a sorafenib: un estudio *in vitro*

Para el HCC avanzado, solo están disponibles los tratamientos paliativos sistémicos [18]. Además, el HCC se ha descrito como uno de los tumores más resistentes a la quimioterapia, lo que dificulta el manejo de los pacientes con HCC [282]. En 2007, se aprobó el tratamiento sistémico con sorafenib para el HCC avanzado; a pesar de que ha demostrado ser eficaz prolongando la supervivencia, el tratamiento a largo plazo con sorafenib permite el desarrollo de células tumorales resistentes. La hipoxia provocada como consecuencia de su actividad anti-angiogénica se ha sugerido como uno de los principales mecanismos responsables de la resistencia adquirida [123]. Para estudiar la implicación de la hipoxia en el fenómeno de la resistencia a sorafenib, se empleó la línea celular de HCC humano HepG2, sensible a dicho fármaco, y dos líneas celulares derivadas de HepG2 con resistencia adquirida a sorafenib, definidas como HepG2S1 y HepG2S3.

4.2.1 Caracterización de la dinámica de crecimiento y la proliferación celular de células resistentes a sorafenib

En primer lugar, caracterizamos la dinámica de crecimiento y la proliferación del fenotipo resistente a sorafenib. Para ello, comparamos dichos procesos entre dos líneas celulares con resistencia adquirida a sorafenib, HepG2S1 y HepG2S3, y la línea celular parental HepG2 tratada o no con sorafenib. El tratamiento con sorafenib redujo la capacidad proliferativa de las células HepG2 en condiciones de normoxia e hipoxia **(Figuras 29A y 30)**. Esta represión de la proliferación por acción del sorafenib también se observó en normoxia con las líneas celulares de HCC humano HepG2, Huh7 y Hep3B [283,284], y en hipoxia en células Hep3B [118]. Además, nuestros resultados mostraron que la hipoxia reprimió de forma marcada el crecimiento celular de HepG2 con respecto a las condiciones normales de oxígeno, dado que la hipoxia representa un estrés para las células **(Figura 29B)**. Por el contrario, Prieto-Domínguez *y cols.* [118] no

encontraron que la hipoxia disminuyese la viabilidad celular en la línea Hep3B. Sin embargo, en este estudio se indujo la hipoxia en las células Hep3B durante solo 48 h [118], mientras que nosotros observamos diferencias significativas en el crecimiento de las células HepG2 a partir del tercer día tras la inducción de la hipoxia **(Figura 29B)**.

En nuestros experimentos, el análisis de crecimiento y la expresión de Ki67 en ambas líneas celulares resistentes a sorafenib mostraron una mayor capacidad de proliferación en comparación con las células HepG2 tratadas con sorafenib e incluso en ausencia de tratamiento **(Figuras 29A y 30)**. Este rápido crecimiento de las células resistentes se corresponde con su mayor potencial invasivo previamente descrito por van Malenstein *y cols*. [88]. Dicha diferencia en la tasa de crecimiento entre las células resistentes y las sensibles a sorafenib aumentó de manera más evidente en hipoxia **(Figura 29A)**. Además, las células HepG2S1 y HepG2S3 mostraron un crecimiento similar entre normoxia e hipoxia, a diferencia de las células HepG2, lo que sugiere que las células resistentes a sorafenib podrían poseer mecanismos adaptativos para hacer frente a las condiciones hipóxicas **(Figura 29B)**. Se ha determinado la influencia de la hipoxia en el desarrollo de células de HCC resistentes después del tratamiento con 5-fluorouracilo (5-FU) [144], doxorrubicina y cisplatino [140]. La resistencia adquirida a sorafenib relacionada con la hipoxia también se ha descrito en otros tipos de cáncer, incluido el RCC [137,138], el cáncer gástrico [285], y la leucemia mieloide aguda [139]. Además, algunos estudios han demostrado que las muestras provenientes de pacientes con HCC resistentes a sorafenib presentan un aumento de la hipoxia intratumoral en contraste con lo que ocurre en pacientes no tratados o sensibles a sorafenib [135].

En conjunto, estos datos sugieren que las líneas celulares resistentes muestran un fenotipo más agresivo que las células sensibles a sorafenib y que, además, parecen tener una mayor capacidad de adaptación frente a la hipoxia.

4.2.2 Evaluación de la expresión proteica y de la regulación de los principales reguladores de la respuesta mediada por hipoxia, HIF-1α y HIF-2α, en líneas celulares resistentes a sorafenib

La hipoxia constituye un estrés celular que promueve una respuesta adaptativa mediante la estabilización de los HIFs [123]. Teniendo en cuenta los datos anteriores, evaluamos cómo las células HepG2S1 y HepG2S3 resistentes a sorafenib responden a la hipoxia mediante el estudio de la expresión de HIF-1α y HIF-2α.

Cabe mencionar que, en cuanto al análisis por *Western blot*, encontramos cambios marcados en los niveles de expresión de β-actina entre las células parentales y las resistentes, concretamente una sobreexpresión en las células HepG2S1 y HepG2S3 **(Figura 31)**. Por lo tanto, dado que las proteínas del citoesqueleto parecían estar alteradas, lo que podría explicarse por la diferente morfología de las células resistentes **(Figura 16)**, decidimos emplear la proteína nuclear PCNA como control *housekeeping* **(Figura 31)**. El empleo de PCNA como referencia interna de expresión ha sido validado en varios estudios de forma satisfactoria [251–253].

Las células HepG2 exhibieron un incremento progresivo en la expresión proteica de HIF-1α debido a la inducción de hipoxia **(Figura 31)**. En esas condiciones de hipoxia, el sorafenib disminuyó los niveles de proteína y la translocación nuclear de HIF-1α en HepG2, mientras que la expresión de HIF-2α fue muy reducida en ausencia o en presencia del fármaco en estas células **(Figuras 31 y 32)**. Estudios anteriores ya demostraron que el sorafenib disminuye los niveles de HIF-1α en las células de HCC al prevenir su síntesis [122,131]. Por el contrario, ambas líneas resistentes mostraron un aumento en la expresión y en la translocación al núcleo de la proteína HIF-1α, destacando la marcada sobreexpresión de este factor de transcripción en HepG2S1 con respecto a HepG2 incluso sin tratamiento con sorafenib **(Figuras 31 y 32)**. Del mismo modo, en muestras de pacientes de HCC resistentes a sorafenib, también se ha encontrado una mayor expresión de HIF-1α en comparación con pacientes sensibles al fármaco o no tratados [135]. Además, ya se había observado que el tratamiento prolongado con sorafenib en modelos de HCC *in vitro* e *in vivo* conducía a una mayor expresión de HIF-1α [135,146,286]. Curiosamente, nuestros resultados indicaron que

los niveles proteicos y la translocación nuclear de HIF-2α también se encontraban significativamente aumentados en las células resistentes a sorafenib **(Figuras 31 y 32)**. De acuerdo con esto, investigaciones previas en modelos *in vitro* de HCC mostraron que una alta expresión de HIF-2α podría estimular la resistencia al sorafenib [149], mientras que la supresión de este factor mejoraba sus efectos anti-tumorales [136]. Se observaron hallazgos similares en células de cáncer de ovario, donde la regulación positiva de HIF-2α mediaba la resistencia a la adriamicina [287]. Por tanto, el incremento en los niveles de proteína y la translocación nuclear de ambos factores HIF-α encontrados en las células resistentes parecen estar relacionados con la adquisición de resistencia a sorafenib.

Un hallazgo interesante fue que las células resistentes revelaron una expresión significativa de HIF-1α y HIF-2α incluso en condiciones de normoxia, donde su expresión es prácticamente nula en las células HepG2 parentales **(Figura 31)**. Este curioso resultado podría deberse a alteraciones en los procesos de síntesis y/o degradación de los HIFs, originadas durante la adquisición de resistencia a sorafenib. Dado que la expresión de HIF-2α es casi indetectable en las células HepG2, comprobamos la posible alteración de estos mecanismos sobre la expresión de HIF-1α. El bloqueo de la degradación proteasomal con MG132, no mostró diferencias en el mecanismo de síntesis proteica entre las líneas celulares examinadas. Sin embargo, el bloqueo de la síntesis usando CHX disminuyó significativamente los niveles de HIF-1α en las células HepG2, mientras que la cantidad de HIF-1α no se vio alterada en las células HepG2S1 y HepG2S3 **(Figura 33)**. De acuerdo con nuestro estudio, la estabilización de HIF-1α al evitar su degradación proteasomal se correlacionó con la quimiorresistencia a la doxorrubicina en el HCC [288]. Además, la promoción de la degradación de HIF-1α dependiente de pVHL se observó que contribuía a mejorar la sensibilidad al sorafenib en el HCC [135].

Estos resultados sugieren que el proceso de degradación proteasomal de HIF-α se encuentra reprimido en las líneas resistentes a sorafenib, lo que puede explicar los altos niveles de HIF-α encontrados tanto en normoxia como en hipoxia y, por tanto, su mayor translocación al núcleo.

4.2.3 Determinación del estado de la muerte celular apoptótica en células resistentes a sorafenib y de la implicación de los HIFs en su capacidad de supervivencia

Junto con la hipoxia, mecanismos como la desregulación del ciclo celular y la evasión de la muerte celular son comunes en la progresión tumoral y el desarrollo de resistencia a los tratamientos [74]. De hecho, la hipoxia en si misma puede promover alteraciones en estos procesos para favorecer la supervivencia de las células tumorales [123]. Por ello, verificamos si nuestro modelo de HCC i*n vitro* de resistencia a sorafenib muestra alguna alteración en el proceso de apoptosis en comparación con las células parentales HepG2.

El porcentaje de población de células subG1, asociado con células apoptóticas, sufrió un incremento pronunciado en las células HepG2 cuando se administró sorafenib en condiciones de hipoxia **(Figura 35)**. Estos hallazgos son consistentes con el efecto del sorafenib mostrado en la distribución del ciclo celular de varias líneas celulares de HCC, incluido en HepG2 [289,290]. Sin embargo, observamos un porcentaje significativamente menor de población subG1 en células HepG2S1 y HepG2S3 que en la línea parental HepG2 también tratada con el fármaco, lo que sugiere una tasa apoptótica reducida en las células resistentes a sorafenib **(Figura 35)**. Este resultado parece estar presente no solo en células de HCC resistentes a sorafenib, sino que también se ha descrito en las células de cáncer de mama MCF-7 resistentes al tamoxifeno [291].

Asimismo, la adición de sorafenib promovió una mayor expresión de la proteína pro-apoptótica Bax y la escisión de la caspasa-3 en HepG2 **(Figura 34)**. De igual modo, en múltiples estudios, el tratamiento con sorafenib también supuso un aumento de las señales pro-apoptóticas [284,289,292,293]. Por el contrario, la expresión de Bax y la escisión de la caspasa-3 se encontraban sustancialmente reprimidas en las líneas resistentes HepG2S1 y HepG2S3 **(Figura 34)**. En concordancia, los datos de la expresión de genes relacionados con la apoptosis, examinados por microarray, también indicaron alteraciones relacionadas con la evasión de la apoptosis, mostrando un enriquecimiento significativo de la vía KEGG para la apoptosis (hsa04210) **(Tabla 8)**.

Otros autores, también empleando dos líneas de HCC resistentes a sorafenib, observaron una mayor expresión de la proteína anti-apoptótica Bcl-2, siendo responsable de una menor inducción de apoptosis [166]. De hecho, se ha indicado que la sobreexpresión del microRNA (miRNA)-34a, un inhibidor de Bcl-2, mejora la sensibilidad al efecto anti-tumoral del sorafenib en células de HCC [294]. Además, la inhibición de la proteína anti-apoptótica Bcl-x_L potenció la apoptosis inducida por sorafenib en estudios tanto *in vitro* como *in vivo* [164,165]. Finalmente, Liang *y cols.* [135] refirieron un índice apoptótico más bajo en muestras resistentes a sorafenib de pacientes con HCC que en las susceptibles.

En conjunto, estos resultados sugieren que las líneas celulares HepG2S1 y HepG2S3 han desarrollado mecanismos para evadir la apoptosis como una estrategia de supervivencia frente al tratamiento con sorafenib.

Por último, los resultados paralelos obtenidos en células resistentes a sorafenib sobre la sobreexpresión de los HIFs y la evasión de la apoptosis, probablemente correlacionados, nos llevaron a analizar el papel de ambos HIFs en su capacidad de supervivencia. Para ello, realizamos un silenciamiento génico tanto para HIF-1α como para HIF-2α en ambas líneas resistentes HepG2S1 y HepG2S3, y evaluamos su impacto sobre la viabilidad. La eficacia del silenciamiento génico se examinó mediante *Western blot*. Los silenciamientos tanto de HIF-1α como de HIF-2α promovieron una disminución significativa en la viabilidad de ambas líneas celulares resistentes a sorafenib **(Figura 36)**. Estos datos destacan el papel clave de ambos HIFs en la capacidad de supervivencia de las células resistentes a sorafenib, lo que sugiere que dirigirse a estos factores de transcripción podría ser un buen enfoque terapéutico para superar la resistencia a sorafenib.

De acuerdo con nuestros resultados, el silenciamiento de HIF-1α indujo la apoptosis mediada por sorafenib en las células de HCC [295] y mejoró la quimiosensibilidad a la temozolomida de las células de glioblastoma y astrocitoma humano, reduciendo su capacidad invasiva [296]. Además, estudios en modelos de HCC *in vitro* e *in vivo* mostraron que los miRNAs dirigidos contra HIF-1α sensibilizan a las células de HCC a la muerte celular mediada por sorafenib [145,286]. También, el

miRNA-18a parece ser capaz de inhibir a HIF-1α evitando la metástasis en el cáncer de mama [297]. Se ha sugerido que la combinación de sorafenib con otras moléculas, como EF24, melatonina o genisteína, mejora los efectos del sorafenib en situaciones de hipoxia mediante la regulación a la baja de HIF-1α [118,135,148]. Con respecto a HIF-2α, se observó que silenciar este factor regula negativamente la vía del factor de crecimiento transformante α (TGF-α)/receptor del factor de crecimiento epidérmico (EGFR) para inducir la apoptosis en el HCC [149]; y también se dirige a la proteína de resistencia al cáncer de mama (BCRP) para mejorar la sensibilidad a la adriamicina en las células de cáncer de ovario resistentes a dicho fármaco [287]. Además, la resistencia al 5-FU y al temsirolimus se superó mediante su combinación con un inhibidor específico de HIF-2α en células de cáncer de colon primario derivadas de pacientes [298]. La metformina reprimió la expresión de HIF-*2α in vitro* y en un modelo de ratón ortotópico, lo que permitió la recuperación de la sensibilidad de las células de HCC a la apoptosis mediada por el sorafenib [152]. Por lo tanto, los tratamientos dirigidos simultáneamente contra HIF-1α y HIF-2α podrían suponer una estrategia interesante; de acuerdo con ello, Ma *y cols.* [122] observaron que la administración de 2-metoxiestradiol suprimía la expresión proteica y la translocación nuclear de HIF-1α y HIF-2α en las células de HCC, actuando de forma sinérgica con el sorafenib para detener la proliferación y promover la apoptosis. Asimismo, el ortovanadato de sodio también disminuyó la expresión y la actividad transcripcional de ambos factores, superando la resistencia al sorafenib en las células de HCC [299]. Nuestros hallazgos junto con los estudios previos enfatizan el papel clave que desempeñan ambos HIF-α en la promoción de la supervivencia celular y la resistencia a los tratamientos.

4.2.4 Análisis de la expresión y la regulación del principal mediador apoptótico en condiciones de hipoxia, BNIP3, en líneas celulares resistentes a sorafenib

Dado el importante papel que ha mostrado la respuesta mediada por hipoxia en la adquisición de resistencia a sorafenib en nuestro modelo, probamos la posible participación de BNIP3. BNIP3 es una proteína mitocondrial responsable de preservar la homeostasis celular durante la hipoxia mediante la regulación de los procesos de apoptosis, necrosis, autofagia y mitofagia [167,168,171,172]. Además, la expresión de

BNIP3 está controlada por HIF-1α, ya que su promotor contiene el HRE. Por lo tanto, esta proteína es un importante regulador de la muerte celular en condiciones de hipoxia [175,181,191].

En cuanto a su expresión, los niveles proteicos y de RNA mensajero (mRNA) de BNIP3 disminuyeron en respuesta a la administración de sorafenib en las células HepG2 y, sorprendentemente, se encontró una reducción aún más significativa de BNIP3 en las células resistentes HepG2S1 y HepG2S3 **(Figura 37)**. En varios estudios, la regulación a la baja de BNIP3 se ha asociado con una peor supervivencia y una mayor proliferación celular en leucemia, cáncer de páncreas, RCC, cáncer colorrectal y HCC [171,180–190]. Además, algunas de estas investigaciones confirmaron una asociación entre la pérdida de expresión de BNIP3 y la adquisición de quimiorresistencia a 5-FU y gemcitabina en el adenocarcinoma ductal pancreático [183], y a oxaliplatino [188] o 5-FU [171,186] en el cáncer colorrectal.

Estos resultados sugieren que la represión de BNIP3 podría estar regulada por un mecanismo aguas arriba. De hecho, se ha establecido una estrecha asociación entre las modificaciones epigéneticas, donde destacan la hipermetilación del DNA y la desacetilación de histonas, con el silenciamiento génico de múltiples genes, lo que está relacionado con efectos patológicos [15,168]. En nuestro trabajo, para determinar la posible desacetilación de histonas de BNIP3, utilizamos TSA como inhibidor de HDACs. Tras la adición de TSA, no encontramos cambios en la expresión de BNIP3, rechazando la desacetilación de histonas como responsable de la represión de BNIP3 en nuestras células resistentes a sorafenib **(Figura 38A)**. Posteriormente, examinamos la metilación por MSP como posible mecanismo de supresión de BNIP3, y observamos la presencia de hipermetilación en el promotor de BNIP3 en ambas líneas celulares resistentes **(Figura 38B)**. Además, la expresión de BNIP3 se restauró después del tratamiento con 5-Aza (inhibidor de DNMTs), tanto a nivel proteico como a nivel de mRNA **(Figuras 38C-E)**. Para aclarar si la represión de BNIP3 por metilación es responsable de la evasión de la muerte celular en células resistentes a sorafenib, evaluamos el efecto del tratamiento con 5-Aza sobre la viabilidad celular, así como su combinación con el silenciamiento génico de BNIP3. La recuperación de la expresión de BNIP3 mediante 5-

Aza redujo la viabilidad de las células HepG2S1 y HepG2S3; mientras que el silenciamiento de BNIP3 favoreció de nuevo la supervivencia de las células resistentes también tratadas con 5-Aza **(Figura 39)**. Por tanto, la resistencia adquirida a sorafenib parece estar relacionada con la metilación aberrante y el consecuente silenciamiento epigenético de BNIP3. Esto sugiere que la estimulación de BNIP3 podría mejorar la quimiosensibilidad de las células de HCC al sorafenib.

En concordancia, estudios previos han asociado el silenciamiento de BNIP3 con la metilación de su promotor como mecanismo adaptativo frente a la muerte celular en leucemia, cáncer de páncreas y cáncer colorrectal [171,180,182,184,185,190,300,301]. La hipermetilación fue promovida por la actividad de DNMT1 en el cáncer de páncreas [182], y por DNMT1/DNMT3B en el cáncer colorrectal [171]. En la mayoría de dichas investigaciones, también se empleó 5-Aza para recuperar la expresión normal de BNIP3, sensibilizando a las células de cáncer de páncreas [182,184,185] y a las células de leucemia mieloide resistentes al busulfán [180] a la apoptosis mediada por hipoxia. Este mecanismo de hipermetilación también se ha estudiado ampliamente en el cáncer colorrectal, donde 5-Aza restauró los niveles de BNIP3 para aumentar la quimiosensibilidad al 5-FU [171], y como tratamiento previo para mejorar la sensibilidad a irinotecán [300]. Además, otros autores han demostrado que la quimioterapia y la radioterapia redujeron la expresión de DNMT1 para inducir BNIP3 y promover la apoptosis dependiente de esta proteína [301]. También, el tratamiento con verticilina A parece ser capaz de restaurar los niveles de BNIP3 de una manera dependiente de la desmetilación del DNA, superando la resistencia a la apoptosis [190].

Por el contrario, otros autores mostraron que el silenciamiento de BNIP3 en las células de cáncer colorrectal fue causado conjuntamente por la metilación del promotor y la desacetilación de histonas, lo que demuestra que tanto 5-Aza como TSA fueron capaces de restaurar la expresión de BNIP3 [187,189], incluso de forma más eficaz cuando ambas moléculas eran coadministradas [187]. Además, Shao *y cols.* [181] evidenciaron que la desacetilación de las histonas, pero no la metilación del promotor, es el principal mecanismo responsable de la represión de BNIP3 en el RCC. Este estudio

utilizó TSA para restaurar el estado de acetilación de BNIP3, bloqueando el crecimiento celular e induciendo la apoptosis dependiente de BNIP3 [181].

4.2.5 Resultados globales

En general, los resultados del presente estudio *in vitro* destacan el papel de la estabilización de los HIFs y el silenciamiento dependiente de metilación de BNIP3 en la adquisición de resistencia a sorafenib en el HCC. Los resultados obtenidos se han representado en la **Figura 41**. Por ello, estrategias dirigidas contra estos mecanismos pro-supervivencia podrían superar la resistencia al sorafenib e implementar los futuros enfoques terapéuticos.

5 Conclusiones

De acuerdo con los hallazgos obtenidos en la presente Tesis Doctoral, se obtuvieron las siguientes conclusiones:

Conclusión primera

La sobreexpresión de ambos factores, HIF-1α y HIF-2α, se correlaciona con una peor OS y DFS/RFS en pacientes con HCC sometidos a resección quirúrgica.

Conclusión segunda

La elevada expresión de HIF-1α está relacionada con una amplia gama de características clínico-patológicas de los pacientes con HCC, incluidas los estadios avanzados de BCLC y TNM, la cirrosis, elevados niveles de AFP, una pobre diferenciación tumoral y grado histológico, un mayor tamaño y número de tumores, la metástasis intrahepática y a los ganglios linfáticos, la infiltración capsular, la invasión vascular y el mimetismo vasculogénico. Por otro lado, los niveles elevados de la proteína HIF-2α solo parecen estar asociados con la infiltración capsular.

Conclusión tercera

Las líneas celulares de HCC con resistencia adquirida a sorafenib muestran tasas de crecimiento y proliferación más agresivas que la línea parental HepG2 sensible al fármaco en ambas condiciones de oxígeno. Además, HepG2S1 y HepG2S3 se ven menos afectadas por la hipoxia que las células parentales, lo que sugiere que estas células resistentes contienen mecanismos adaptativos para hacer frente a la hipoxia.

Conclusión cuarta

Las líneas celulares de HCC resistentes a sorafenib muestran la estabilización de elevados niveles proteicos de HIF-1α y HIF-2α, y un incremento en su posterior translocación nuclear, como consecuencia de una desregulación en su degradación proteasomal, lo que constituye un mecanismo clave en el desarrollo de resistencia a este fármaco.

Conclusión quinta

Las células de HCC resistentes son capaces de evadir la apoptosis mediada por sorafenib como mecanismo de quimiorresistencia, estando la sobreexpresión de HIF-1α y HIF-2α involucrada en esta falta de sensibilidad al sorafenib.

Conclusión sexta

El regulador apoptótico en condiciones de hipoxia, BNIP3, se encuentra silenciado en el fenotipo resistente a sorafenib en respuesta a la hipermetilación de su promotor. Esta regulación a la baja de BNIP3 participa en la resistencia a sorafenib mediada por hipoxia, evitando la muerte celular regulada por BNIP3.

Conclusión general

En conjunto, la respuesta mediada por hipoxia presenta un papel clave en el desarrollo, progresión, recurrencia y resistencia a fármacos en HCC. Concretamente, HIF-1α y HIF-2α muestran una relación con peores resultados en pacientes con HCC y con la resistencia adquirida a sorafenib. Por tanto, estos factores de transcripción podrían constituirse como biomarcadores útiles para predecir el pronóstico y la recurrencia de los pacientes con HCC. Además de la estabilización de los HIFs, el silenciamiento de BNIP3 dependiente de metilación también juega un papel importante en la adquisición de resistencia a sorafenib, lo que sugiere que ambos mecanismos de supervivencia son potenciales dianas terapéuticas para superar la resistencia a sorafenib y para mejorar las estrategias de tratamiento contra el HCC.

Supplemental information

Supplemental Table 1. PRISMA checklist*.

Section/topic	#	Checklist item	Reported on page #
TITLE			
Title	1	Identify the report as a systematic review, meta-analysis, or both.	1
ABSTRACT			
Structured summary	2	Provide a structured summary including, as applicable: background; objectives; data sources; study eligibility criteria, participants, and interventions; study appraisal and synthesis methods; results; limitations; conclusions and implications of key findings; systematic review registration number.	1
INTRODUCTION			
Rationale	3	Describe the rationale for the review in the context of what is already known.	1-2
Objectives	4	Provide an explicit statement of questions being addressed with reference to participants, interventions, comparisons, outcomes, and study design (PICOS).	2
METHODS			
Protocol and registration	5	Indicate if a review protocol exists, if and where it can be accessed (e.g., Web address), and, if available, provide registration information including registration number.	2
Eligibility criteria	6	Specify study characteristics (e.g., PICOS, length of follow-up) and report characteristics (e.g., years considered, language, publication status) used as criteria for eligibility, giving rationale.	2
Information sources	7	Describe all information sources (e.g., databases with dates of coverage, contact with study authors to identify additional studies) in the search and date last searched.	2
Search	8	Present full electronic search strategy for at least one database, including any limits used, such that it could be repeated.	2 and Suppl. Table 2
Study selection	9	State the process for selecting studies (i.e., screening, eligibility, included in systematic review, and, if applicable, included in the meta-analysis).	2 and 5
Data collection process	10	Describe method of data extraction from reports (e.g., piloted forms, independently, in duplicate) and any processes for obtaining and confirming data from investigators.	5

Data items	11	List and define all variables for which data were sought (e.g., PICOS, funding sources) and any assumptions and simplifications made.	5
Risk of bias in individual studies	12	Describe methods used for assessing risk of bias of individual studies (including specification of whether this was done at the study or outcome level), and how this information is to be used in any data synthesis.	5 and Table 1
Summary measures	13	State the principal summary measures (e.g., risk ratio, difference in means).	5
Synthesis of results	14	Describe the methods of handling data and combining results of studies, if done, including measures of consistency (e.g., I^2) for each meta-analysis.	5
Risk of bias across studies	15	Specify any assessment of risk of bias that may affect the cumulative evidence (e.g., publication bias, selective reporting within studies).	5
Additional analyses	16	Describe methods of additional analyses (e.g., sensitivity or subgroup analyses, meta-regression), if done, indicating which were pre-specified.	5
RESULTS			
Study selection	17	Give numbers of studies screened, assessed for eligibility, and included in the review, with reasons for exclusions at each stage, ideally with a flow diagram.	5-6 and Figure 1
Study characteristics	18	For each study, present characteristics for which data were extracted (e.g., study size, PICOS, follow-up period) and provide the citations.	5-6 and Table 1
Risk of bias within studies	19	Present data on risk of bias of each study and, if available, any outcome level assessment (see item 12).	5 and Table 1
Results of individual studies	20	For all outcomes considered (benefits or harms), present, for each study: (a) simple summary data for each intervention group (b) effect estimates and confidence intervals, ideally with a forest plot.	-
Synthesis of results	21	Present results of each meta-analysis done, including confidence intervals and measures of consistency.	7-10 and Figures 2-5
Risk of bias across studies	22	Present results of any assessment of risk of bias across studies (see Item 15).	10, 17, Table 3 and Figures 6-8
Additional analysis	23	Give results of additional analyses, if done (e.g., sensitivity or subgroup analyses, meta-regression [see Item 16]).	10 and Table 2
DISCUSSION			

Summary of evidence	24	Summarize the main findings including the strength of evidence for each main outcome; consider their relevance to key groups (e.g., healthcare providers, users, and policy makers).	17-18, 20 and 23-24
Limitations	25	Discuss limitations at study and outcome level (e.g., risk of bias), and at review-level (e.g., incomplete retrieval of identified research, reporting bias).	24
Conclusions	26	Provide a general interpretation of the results in the context of other evidence, and implications for future research.	24 and Figure 9
FUNDING			
Funding	27	Describe sources of funding for the systematic review and other support (e.g., supply of data); role of funders for the systematic review.	25

*This PRISMA checklist corresponds to the pagination of our published article (https://doi.org/10.1177/1758835920987071), containing the meta-analyzed data of the present PhD Thesis.

Supplemental Table 2. HIF-1α and HIF-2α antibodies and staining procedure employed for IHC of HCC samples.

Study (reference)	Year	HIF-1α antibody	Clone and source reported	Dilution	Incubation conditions
Huang *et al.* [198]	2005	Monoclonal anti-HIF-1α	Clone H1alpha67, Neomarkers, Postsmouth, NH, USA	NR	4°C overnight
Wada *et al.* [199]	2006	Mouse monoclonal anti-HIF-1α	Mouse monoclonal IgG2a, Novus Biologicals, Inc., Littleton, CO	1:50	4°C overnight
Xie *et al.* [200]	2008	Monoclonal anti-HIF-1α	Cayman Chemical, Ann Arbor, MI, USA	1:100	4°C overnight
Dai *et al.* [201]	2009	Rabbit polyclonal anti-HIF-1α	ab65979, Abcam, Cambridge, UK	1:50	NR
Liu *et al.* [202]	2010	Anti-HIF-1α	Sigma-Aldrich, MI, USA	NR	NR
Xiang *et al.* [203]	2011	Mouse monoclonal anti-human anti-HIF-1α	Santa Cruz Biotechnology, CA, USA	NR	4°C overnight
Li *et al.* [204]	2012	Mouse anti-human monoclonal anti-HIF-1α	England NeoMarker Company, England	NR	NR
Xia *et al.* [205]	2012	Anti-HIF-1α	Sigma-Aldrich, MI, USA	NR	4°C overnight
Xiang *et al.* [206]	2012	Mouse monoclonal anti-human anti-HIF-1α	Santa Cruz Biotechnology, CA, USA	NR	4°C overnight
Cui *et al.* [207]	2013	Anti-HIF-1α	Santa Cruz Biotechnology, CA, USA	NR	37°C for 1 h
Ma *et al.* [208]	2013	Rabbit monoclonal anti-human anti-HIF-1α	ab51608, Abcam, American Abcam Company, USA	1:100	NR
Wang *et al.* [209]	2014	Mouse monoclonal anti-human anti-HIF-1α	sc-13515, Santa Cruz Biotechnology, CA, USA	NR	1-2 h
Yang *et al.* [210]	2014	Monoclonal anti-HIF-1α	Clone H1alpha67, Santa Cruz Biotechnology, CA, USA	NR	37°C for 1 h + 4°C overnight

Huang *et al.* [211]	2015	Rabbit monoclonal anti-HIF-1α	Abcam, Cambridge, UK	NR	37°C for 1 h
Li *et al.* [212]	2015	Monoclonal anti-HIF-1α	sc-13515, Santa Cruz Biotechnology, CA, USA	1:200	4°C overnight
Srivastava *et al.* [213]	2015	Mouse monoclonal anti-HIF-1α	Clone H1alpha67, Novus Biological, USA	1:1000	NR
Zhao *et al.* [214]	2015	Anti-HIF-1α	NR	NR	4°C overnight
Tang *et al.* [215]	2016	Rabbit polyclonal anti-HIF-1α	Abcam, Cambridge, UK	NR	NR
Wang *et al.* [216]	2017	Rabbit monoclonal anti-HIF-1α	ZA-0562, USA	NR	4°C overnight
Dai *et al.* [217]	2018	Mouse monoclonal anti-HIF-1α	Clone H1alpha67, Santa Cruz Biotechnology, CA, USA	NR	NR
Tian *et al.* [218]	2018	Rabbit anti-human anti-HIF-1α	Wanjiang Biotechnology Co., Ltd., Shanghai, China	NR	NR
Wang *et al.* [219]	2018	Anti-HIF-1α	Abcam, Cambridge, MA, USA	NR	4°C overnight
Zou *et al.* [220]	2018	Rabbit monoclonal anti-HIF-1α	Boster, PB0245, China	1:200	4°C for 12 h
Gong *et al.* [221]	2019	Anti-HIF-1α	A11945, ABclonal, USA	NR	4°C overnight
Wu *et al.* [222]	2019	Anti-HIF-1α	ab2185, Abcam, Cambridge, MA, USA	NR	4°C overnight
Qian *et al.* [224]	2020	Anti-HIF-1α	GB111339, Wuhan Servicebio, China	1:200	4°C overnight
Study (Reference)	**Year**	**HIF-2α antibody**	**Clone and Source**	**Dilution**	**Incubation conditions**
Bangoura *et al.* [225]	2004	Mouse monoclonal anti-HIF-2α	Anti-HIF-2α/EPAS1 (190b), Dako, Glostrup, Denmark	NR	NR
Bangoura *et al.* [226]	2007	Mouse monoclonal anti-HIF-2α	Anti-HIF-2α/EPAS1 (190b), Santa Cruz Biotechnology, CA, USA	1:80	RT for 1 h

Sun *et al.* [227]	2013	Anti-HIF-2α	ab199, Abcam, Cambridge, MA, USA	1:200	RT for 1 h
Yang *et al.* [210]	2014	Polyclonal anti-HIF-2α	Boster Biological Technology, Wuhan, China	NR	37°C for 1 h + 4°C overnight
Yang *et al.* [228]	2016	Polyclonal anti-HIF-2α	ChIP Grade ab199, Abcam, Cambridge, MA, USA	NR	NR
		Mouse monoclonal anti-HIF-2α	Anti-HIF-2α/EPAS1 (190b), Santa Cruz Biotechnology, CA, USA	NR	NR
Jiang *et al.* [229]	2018	Anti-HIF-2α	ab8365, Abcam, Cambridge, UK	1:150	4°C overnight
Chen *et al.* [230]	2019	Anti-HIF-2α	7096, Cell Signaling Technology	1:300	4°C for 8 h

NR, not reported; RT, room temperature

References

1. Llovet JM, Kelley RK, Villanueva A, Singal AG, Pikarsky E, Roayaie S, et al. Hepatocellular carcinoma. *Nat Rev Dis Primers*. 2021;7(1):6.

2. Bishayee A. The role of inflammation and liver cancer. *Adv Exp Med Biol*. 2014;816:401–35.

3. Alqahtani A, Khan Z, Alloghbi A, Ahmed TSS, Ashraf M, Hammouda DM. Hepatocellular carcinoma: Molecular mechanisms and targeted therapies. *Medicina (Kaunas)*. 2019;55(9):526.

4. Bray F, Ferlay J, Soerjomataram I, Siegel RL, Torre LA, Jemal A. Global cancer statistics 2018: GLOBOCAN estimates of incidence and mortality worldwide for 36 cancers in 185 countries. *CA Cancer J Clin*. 2018;68(6):394–424.

5. Sung H, Ferlay J, Siegel RL, Laversanne M, Soerjomataram I, Jemal A, et al. Global cancer statistics 2020: GLOBOCAN estimates of incidence and mortality worldwide for 36 cancers in 185 countries. *CA Cancer J Clin*. 2021;71(3):209–49.

6. Ferlay J, Colombet M, Soerjomataram I, Dyba T, Randi G, Bettio M, et al. Cancer incidence and mortality patterns in Europe: Estimates for 40 countries and 25 major cancers in 2018. *Eur J Cancer*. 2018;103:356–87.

7. Tu T, Budzinska MA, Maczurek AE, Cheng R, Di Bartolomeo A, Warner FJ, et al. Novel aspects of the liver microenvironment in hepatocellular carcinoma pathogenesis and development. *Int J Mol Sci*. 2014;15(6):9422–58.

8. Dhanasekaran R, Bandoh S, Roberts LR. Molecular pathogenesis of hepatocellular carcinoma and impact of therapeutic advances. *F1000Res*. 2016;5(F1000 Faculty Rev-879):1–15.

9. Ghouri YA, Mian I, Rowe JH. Review of hepatocellular carcinoma: Epidemiology, etiology, and carcinogenesis. *J Carcinog*. 2017;16(1).

10. Nakagawa H, Maeda S. Inflammation- and stress-related signaling pathways in hepatocarcinogenesis. *World J Gastroenterol*. 2012;18(31):4071–81.

11. Yu L-X, Ling Y, Wang H-Y. Role of nonresolving inflammation in hepatocellular carcinoma development and progression. *NPJ Precis Oncol*. 2018;2(1):6.

12. Heindryckx F, Gerwins P. Targeting the tumor stroma in hepatocellular carcinoma. *World J Hepatol*. 2015;7(2):165–76.

13. Piciocchi M, Cardin R, Cillo U, Vitale A, Cappon A, Mescoli C, et al. Differential timing of oxidative DNA damage and telomere shortening in hepatitis C and B virus-related liver carcinogenesis. *Transl Res*. 2016;168:122–33.

14. Llovet JM, Zucman-Rossi J, Pikarsky E, Sangro B, Schwartz M, Sherman M, et al. Hepatocellular carcinoma. *Nat Rev Dis Primers*. 2016;2:16018.

15. Toh TB, Lim JJ, Chow EK. Epigenetics of hepatocellular carcinoma. *Clin Transl Med*. 2019;8(1):13.

16. Janevska D, Chaloska-Ivanova V, Janevski V. Hepatocellular carcinoma: Risk factors, diagnosis and treatment. *Open Access Maced J Med Sci*. 2015;3(4):732–6.

17. Vo Quang E, Shimakawa Y, Nahon P. Epidemiological projections of viral-induced hepatocellular carcinoma in the perspective of WHO global hepatitis elimination. *Liver Int*. 2021;41(5):915–27.

18. Galle PR, Forner A, Llovet JM, Mazzaferro V, Piscaglia F, Raoul J-L, et al. EASL clinical practice guidelines: Management of hepatocellular carcinoma. *J Hepatol*. 2018;69(1):182–236.

19. Mysore KR, Leung DH. Hepatitis B and C. *Clin Liver Dis*. 2018;22(4):703–22.

20. Jindal A, Thadi A, Shailubhai K. Hepatocellular carcinoma: Etiology and current and future drugs. *J Clin Exp Hepatol*. 2019;9(2):221–32.

21. Kucukcakan B, Hayrulai-Musliu Z. Challenging role of dietary aflatoxin B1 exposure and hepatitis B infection on risk of hepatocellular carcinoma. *Open Access Maced J Med Sci*. 2015;3(2):363–9.

22. Sciancalepore D, Zingaro MT, Luglio CV, Sabbà C, Napoli N. Hepatocellular carcinoma: Known and emerging risk factors. *J Cancer Ther*. 2018;9(5):417–37.

23. Brandi G, De Lorenzo S, Candela M, Pantaleo MA, Bellentani S, Tovoli F, et al. Microbiota, NASH, HCC and the potential role of probiotics. *Carcinogenesis*. 2017;38(3):231–40.

24. Dragani TA. Risk of HCC: Genetic heterogeneity and complex genetics. *J Hepatol*. 2010;52(2):252–7.

25. Thylur RP, Roy SK, Shrivastava A, LaVeist TA, Shankar S, Srivastava RK. Assessment of risk factors, and racial and ethnic differences in hepatocellular carcinoma. *JGH Open*. 2020;4(3):351–9.

26. Ayuso C, Rimola J, Vilana R, Burrel M, Darnell A, García-Criado Á, et al. Diagnosis and staging of hepatocellular carcinoma (HCC): Current guidelines. *Eur J Radiol*. 2018;101:72–81.

27. Attwa MH, El-Etreby SA. Guide for diagnosis and treatment of hepatocellular carcinoma. *World J Hepatol*. 2015;7(12):1632–51.

28. Zhou J, Sun H, Wang Z, Cong W, Wang J, Zeng M, et al. Guidelines for the diagnosis and treatment of hepatocellular carcinoma (2019 edition). *Liver Cancer*. 2020;9(6):682–720.

29. Patel M, Shariff MIF, Ladep NG, Thillainayagam AV, Thomas HC, Khan SA, et al. Hepatocellular carcinoma: Diagnostics and screening. *J Eval Clin Pract*. 2012;18(2):335–42.

30. Bellissimo F, Pinzone MR, Cacopardo B, Nunnari G. Diagnostic and therapeutic

management of hepatocellular carcinoma. *World J Gastroenterol*. 2015;21(42):12003–21.

31. Pan Y, Chen H, Yu J. Biomarkers in hepatocellular carcinoma: Current status and future perspectives. *Biomedicines*. 2020;8(12):576.

32. Zacharakis G, Aleid A, Aldossari KK. New and old biomarkers of hepatocellular carcinoma. *Hepatoma Res*. 2018;4(10):65.

33. Di Tommaso L, Spadaccini M, Donadon M, Personeni N, Elamin A, Aghemo A, et al. Role of liver biopsy in hepatocellular carcinoma. *World J Gastroenterol*. 2019;25(40):6041–52.

34. Kinoshita A, Onoda H, Fushiya N, Koike K, Nishino H, Tajiri H. Staging systems for hepatocellular carcinoma: Current status and future perspectives. *World J Hepatol*. 2015;7(3):406–24.

35. Tellapuri S, Sutphin PD, Beg MS, Singal AG, Kalva SP. Staging systems of hepatocellular carcinoma: A review. *Indian J Gastroenterol*. 2018;37(6):481–91.

36. Forner A, Reig M, Bruix J. Hepatocellular carcinoma. *Lancet*. 2018;391(10127):1301–14.

37. Yang JD, Hainaut P, Gores GJ, Amadou A, Plymoth A, Roberts LR. A global view of hepatocellular carcinoma: Trends, risk, prevention and management. *Nat Rev Gastroenterol Hepatol*. 2019;16(10):589–604.

38. Cardarelli-Leite L, Hadjivassiliou A, Klass D, Chung J, Ho SGF, Lim HJ, et al. Current locoregional therapies and treatment strategies in hepatocellular carcinoma. *Curr Oncol*. 2020;27(Suppl 3):S144–51.

39. Dong Y, Liu T-H, Yau T, Hsu C. Novel systemic therapy for hepatocellular carcinoma. *Hepatol Int*. 2020;14(5):638–51.

40. Amaro CP, Tam VC. Management of hepatocellular carcinoma after progression on first-line systemic treatment: Defining the optimal sequencing strategy in second line and beyond. *Curr Oncol*. 2020;27(Suppl 3):S173–80.

41. Javan H, Dayyani F, Abi-Jaoudeh N. Therapy in advanced hepatocellular carcinoma. *Semin Intervent Radiol*. 2020;37(5):466–74.

42. Weinmann A, Galle PR. Role of immunotherapy in the management of hepatocellular carcinoma: Current standards and future directions. *Curr Oncol*. 2020;27(Suppl 3):S152–64.

43. Gauthier A, Ho M. The role of sorafenib in the treatment of advanced hepatocellular carcinoma: An update. *Hepatol Res*. 2013;43(2):147–54.

44. Ibrahim N, Yu Y, Walsh WR, Yang J-L. Molecular targeted therapies for cancer: Sorafenib mono-therapy and its combination with other therapies (review). *Oncol Rep*. 2012;27(5):1303–11.

45. Kane RC, Farrell AT, Saber H, Tang S, Williams G, Jee JM, et al. Sorafenib for the treatment of advanced renal cell carcinoma. *Clin Cancer Res*. 2006;12(24):7271–8.

46. Escudier B, Eisen T, Stadler WM, Szczylik C, Oudard S, Staehler M, et al. Sorafenib for treatment of renal cell carcinoma: Final efficacy and safety results of the phase III treatment approaches in renal cancer global evaluation trial. *J Clin Oncol*. 2009;27(20):3312–8.

47. Heo JH, Park C, Ghosh S, Park S-K, Zivkovic M, Rascati KL. A network meta-analysis of efficacy and safety of first-line and second-line therapies for the management of metastatic renal cell carcinoma. *J Clin Pharm Ther*. 2021;46(1):35–49.

48. McFarland DC, Misiukiewicz KJ. Sorafenib in radioactive iodine-refractory well-differentiated metastatic thyroid cancer. *Onco Targets Ther*. 2014;7:1291–9.

49. Al-Jundi M, Thakur S, Gubbi S, Klubo-Gwiezdzinska J. Novel targeted therapies for metastatic thyroid cancer-A comprehensive review. *Cancers (Basel)*. 2020;12(8):2104.

50. Awada A, Hendlisz A, Gil T, Bartholomeus S, Mano M, De Valeriola D, et al. Phase I safety and pharmacokinetics of BAY 43-9006 administered for 21 days on/7 days off in patients with advanced, refractory solid tumours. *Br J Cancer*. 2005;92(10):1855–61.

51. Strumberg D, Richly H, Hilger RA, Schleucher N, Korfee S, Tewes M, et al. Phase I clinical and pharmacokinetic study of the novel Raf kinase and vascular endothelial growth factor receptor inhibitor BAY 43-9006 in patients with advanced refractory solid tumors. *J Clin Oncol*. 2005;23(5):965–72.

52. Abou-Alfa GK, Schwartz L, Ricci S, Amadori D, Santoro A, Figer A, et al. Phase II study of sorafenib in patients with advanced hepatocellular carcinoma. *J Clin Oncol*. 2006;24(26):4293–300.

53. Connell LC, Harding JJ, Abou-Alfa GK. Advanced hepatocellular cancer: The current state of future research. *Curr Treat Options Oncol*. 2016;17(8):43.

54. Llovet JM, Ricci S, Mazzaferro V, Hilgard P, Gane E, Blanc J-F, et al. Sorafenib in advanced hepatocellular carcinoma. *N Engl J Med*. 2008;359(4):378–90.

55. Cheng A-L, Kang Y-K, Chen Z, Tsao C-J, Qin S, Kim JS, et al. Efficacy and safety of sorafenib in patients in the Asia-Pacific region with advanced hepatocellular carcinoma: A phase III randomised, double-blind, placebo-controlled trial. *Lancet Oncol*. 2009;10(1):25–34.

56. Iavarone M, Cabibbo G, Piscaglia F, Zavaglia C, Grieco A, Villa E, et al. Field-practice study of sorafenib therapy for hepatocellular carcinoma: A prospective multicenter study in Italy. *Hepatology*. 2011;54(6):2055–63.

57. Reig M, Rimola J, Torres F, Darnell A, Rodriguez-Lope C, Forner A, et al. Postprogression survival of patients with advanced hepatocellular carcinoma: Rationale for second-line trial design. *Hepatology*. 2013;58(6):2023–31.

58. Lencioni R, Kudo M, Ye S-L, Bronowicki J-P, Chen X-P, Dagher L, et al. GIDEON (Global Investigation of therapeutic DEcisions in hepatocellular carcinoma and Of its treatment with sorafeNib): Second interim analysis. *Int J Clin Pract*. 2014;68(5):609–17.

59. Ganten TM, Stauber RE, Schott E, Malfertheiner P, Buder R, Galle PR, et al. Sorafenib in patients with hepatocellular carcinoma-Results of the observational INSIGHT study. *Clin Cancer Res*. 2017;23(19):5720–8.

60. Lencioni R, Marrero J, Venook A, Ye S-L, Kudo M. Design and rationale for the non-interventional Global Investigation of therapeutic DEcisions in hepatocellular carcinoma and Of its treatment with sorafeNib (GIDEON) study. *Int J Clin Pract*. 2010;64(8):1034–41.

61. Marrero JA, Kudo M, Venook AP, Ye S-L, Bronowicki J-P, Chen X-P, et al. Observational registry of sorafenib use in clinical practice across Child-Pugh subgroups: The GIDEON study. *J Hepatol*. 2016;65(6):1140–7.

62. Leal CRG, Magalhães C, Barbosa D, Aquino D, Carvalho B, Balbi E, et al. Survival and tolerance to sorafenib in Child-Pugh B patients with hepatocellular carcinoma: A prospective study. *Invest New Drugs*. 2018;36(5):911–8.

63. Suzuki E, Kaneko S, Okusaka T, Ikeda M, Yamaguchi K, Sugimoto R, et al. A multicenter phase II study of sorafenib in Japanese patients with advanced hepatocellular carcinoma and Child Pugh A and B class. *Jpn J Clin Oncol*. 2018;48(4):317–21.

64. Gong L, Giacomini MM, Giacomini C, Maitland ML, Altman RB, Klein TE. PharmGKB summary: Sorafenib pathways. *Pharmacogenet Genomics*. 2017;27(6):240–6.

65. Galati G, Massimo Vainieri AF, Maria Fulgenzi CA, Di Donato S, Silletta M, Gallo P, et al. Current treatment options for HCC: From pharmacokinetics to efficacy and adverse events in liver cirrhosis. *Curr Drug Metab*. 2020;21(11):866–84.

66. Woo HY, Heo J. Sorafenib in liver cancer. *Expert Opin Pharmacother*. 2012;13(7):1059–67.

67. Keating GM. Sorafenib: A review in hepatocellular carcinoma. *Target Oncol*. 2017;12(2):243–53.

68. Walko CM, Grande C. Management of common adverse events in patients treated with sorafenib: Nurse and pharmacist perspective. *Semin Oncol*. 2014;41(Suppl 2):S17–28.

69. Abdel-Rahman O, Lamarca A. Development of sorafenib-related side effects in

patients diagnosed with advanced hepatocellular carcinoma treated with sorafenib: A systematic-review and meta-analysis of the impact on survival. *Expert Rev Gastroenterol Hepatol*. 2017;11(1):75–83.

70. Ara M, Pastushenko E. Antiangiogenic agents and the skin: Cutaneous adverse effects of sorafenib, sunitinib, and bevacizumab. *Actas Dermosifiliogr*. 2014;105(10):900–12.

71. Ai L, Xu Z, Yang B, He Q, Luo P. Sorafenib-associated hand-foot skin reaction: Practical advice on diagnosis, mechanism, prevention, and management. *Expert Rev Clin Pharmacol*. 2019;12(12):1121–7.

72. Zhai B, Sun X-Y. Mechanisms of resistance to sorafenib and the corresponding strategies in hepatocellular carcinoma. *World J Hepatol*. 2013;5(7):345–52.

73. Chen J, Jin R, Zhao J, Liu J, Ying H, Yan H, et al. Potential molecular, cellular and microenvironmental mechanism of sorafenib resistance in hepatocellular carcinoma. *Cancer Lett*. 2015;367(1):1–11.

74. Niu L, Liu L, Yang S, Ren J, Lai PBS, Chen GG. New insights into sorafenib resistance in hepatocellular carcinoma: Responsible mechanisms and promising strategies. *Biochim Biophys Acta Rev Cancer*. 2017;1868(2):564–70.

75. Tang W, Chen Z, Zhang W, Cheng Y, Zhang B, Wu F, et al. The mechanisms of sorafenib resistance in hepatocellular carcinoma: Theoretical basis and therapeutic aspects. *Signal Transduct Target Ther*. 2020;5(1):87.

76. Nishida N, Kitano M, Sakurai T, Kudo M. Molecular mechanism and prediction of sorafenib chemoresistance in human hepatocellular carcinoma. *Dig Dis*. 2015;33(6):771–9.

77. Zhu Y-J, Zheng B, Wang H-Y, Chen L. New knowledge of the mechanisms of sorafenib resistance in liver cancer. *Acta Pharmacol Sin*. 2017;38(5):614–22.

78. Cheng Z, Wei-Qi J, Jin D. New insights on sorafenib resistance in liver cancer with correlation of individualized therapy. *Biochim Biophys Acta Rev Cancer*. 2020;1874(1):188382.

79. Marin JJG, Macias RIR, Monte MJ, Romero MR, Asensio M, Sanchez-Martin A, et al. Molecular bases of drug resistance in hepatocellular carcinoma. *Cancers (Basel)*. 2020;12(6):1663.

80. Xia S, Pan Y, Liang Y, Xu J, Cai X. The microenvironmental and metabolic aspects of sorafenib resistance in hepatocellular carcinoma. *EBioMedicine*. 2020;51:102610.

81. Ezzoukhry Z, Louandre C, Trécherel E, Godin C, Chauffert B, Dupont S, et al. EGFR activation is a potential determinant of primary resistance of hepatocellular carcinoma cells to sorafenib. *Int J Cancer*. 2012;131(12):2961–9.

82. Liang Y, Chen J, Yu Q, Ji T, Zhang B, Xu J, et al. Phosphorylated ERK is a potential

prognostic biomarker for sorafenib response in hepatocellular carcinoma. *Cancer Med*. 2017;6(12):2787–95.

83. Hagiwara S, Kudo M, Nagai T, Inoue T, Ueshima K, Nishida N, et al. Activation of JNK and high expression level of CD133 predict a poor response to sorafenib in hepatocellular carcinoma. *Br J Cancer*. 2012;106(12):1997–2003.

84. Chen W, Xiao W, Zhang K, Yin X, Lai J, Liang L, et al. Activation of c-Jun predicts a poor response to sorafenib in hepatocellular carcinoma: Preliminary clinical evidence. *Sci Rep*. 2016;6:22976.

85. Llovet JM, Peña CEA, Lathia CD, Shan M, Meinhardt G, Bruix J, et al. Plasma biomarkers as predictors of outcome in patients with advanced hepatocellular carcinoma. *Clin Cancer Res*. 2012;18(8):2290–300.

86. Wei L, Wang X, Lv L, Liu J, Xing H, Song Y, et al. The emerging role of microRNAs and long noncoding RNAs in drug resistance of hepatocellular carcinoma. *Mol Cancer*. 2019;18(1):147.

87. Sun T, Liu H, Ming L. Multiple roles of autophagy in the sorafenib resistance of hepatocellular carcinoma. *Cell Physiol Biochem*. 2017;44(2):716–27.

88. van Malenstein H, Dekervel J, Verslype C, Van Cutsem E, Windmolders P, Nevens F, et al. Long-term exposure to sorafenib of liver cancer cells induces resistance with epithelial-to-mesenchymal transition, increased invasion and risk of rebound growth. *Cancer Lett*. 2013;329(1):74–83.

89. Cabral LKD, Tiribelli C, Sukowati CHC. Sorafenib resistance in hepatocellular carcinoma: The relevance of genetic heterogeneity. *Cancers (Basel)*. 2020;12(6):1576.

90. Kudo M, Finn RS, Qin S, Han K-H, Ikeda K, Piscaglia F, et al. Lenvatinib versus sorafenib in first-line treatment of patients with unresectable hepatocellular carcinoma: A randomised phase 3 non-inferiority trial. *Lancet*. 2018;391(10126):1163–73.

91. Finn RS, Qin S, Ikeda M, Galle PR, Ducreux M, Kim T-Y, et al. Atezolizumab plus bevacizumab in unresectable hepatocellular carcinoma. *N Engl J Med*. 2020;382(20):1894–905.

92. Bruix J, Qin S, Merle P, Granito A, Huang Y-H, Bodoky G, et al. Regorafenib for patients with hepatocellular carcinoma who progressed on sorafenib treatment (RESORCE): A randomised, double-blind, placebo-controlled, phase 3 trial. *Lancet*. 2017;389(10064):56–66.

93. El-Khoueiry AB, Sangro B, Yau T, Crocenzi TS, Kudo M, Hsu C, et al. Nivolumab in patients with advanced hepatocellular carcinoma (CheckMate 040): An open-label, non-comparative, phase 1/2 dose escalation and expansion trial. *Lancet*. 2017;389(10088):2492–502.

94. Zhu AX, Finn RS, Edeline J, Cattan S, Ogasawara S, Palmer D, et al. Pembrolizumab in patients with advanced hepatocellular carcinoma previously treated with sorafenib (KEYNOTE-224): A non-randomised, open-label phase 2 trial. *Lancet Oncol*. 2018;19(7):940–52.

95. Abou-Alfa GK, Meyer T, Cheng A-L, El-Khoueiry AB, Rimassa L, Ryoo B-Y, et al. Cabozantinib in patients with advanced and progressing hepatocellular carcinoma. *N Engl J Med*. 2018;379(1):54–63.

96. Zhu AX, Kang Y-K, Yen C-J, Finn RS, Galle PR, Llovet JM, et al. Ramucirumab after sorafenib in patients with advanced hepatocellular carcinoma and increased α-fetoprotein concentrations (REACH-2): A randomised, double-blind, placebo-controlled, phase 3 trial. *Lancet Oncol*. 2019;20(2):282–96.

97. Yau T, Kang Y-K, Kim T-Y, El-Khoueiry AB, Santoro A, Sangro B, et al. Efficacy and safety of nivolumab plus ipilimumab in patients with advanced hepatocellular carcinoma previously treated with sorafenib: The CheckMate 040 randomized clinical trial. *JAMA Oncol*. 2020;6(11):e204564.

98. Masoud GN, Li W. HIF-1α pathway: Role, regulation and intervention for cancer therapy. *Acta Pharm Sin B*. 2015;5(5):378–89.

99. Peerlings J, Van De Voorde L, Mitea C, Larue R, Yaromina A, Sandeleanu S, et al. Hypoxia and hypoxia response-associated molecular markers in esophageal cancer: A systematic review. *Methods*. 2017;130:51–62.

100. Xiong XX, Qiu XY, Hu DX, Chen XQ. Advances in hypoxia-mediated mechanisms in hepatocellular carcinoma. *Mol Pharmacol*. 2017;92(3):246–55.

101. Jing X, Yang F, Shao C, Wei K, Xie M, Shen H, et al. Role of hypoxia in cancer therapy by regulating the tumor microenvironment. *Mol Cancer*. 2019;18(1):157.

102. Wong CC-L, Kai AK-L, Ng IO-L. The impact of hypoxia in hepatocellular carcinoma metastasis. *Front Med*. 2014;8(1):33–41.

103. Chen C, Lou T. Hypoxia inducible factors in hepatocellular carcinoma. *Oncotarget*. 2017;8(28):46691–703.

104. Lin D, Wu J. Hypoxia inducible factor in hepatocellular carcinoma: A therapeutic target. *World J Gastroenterol*. 2015;21(42):12171–8.

105. Gaete D, Rodriguez D, Watts D, Sormendi S, Chavakis T, Wielockx B. HIF-prolyl hydroxylase domain proteins (PHDs) in cancer-Potential targets for anti-tumor therapy? *Cancers (Basel)*. 2021;13(5):988.

106. Ju C, Colgan SP, Eltzschig HK. Hypoxia-inducible factors as molecular targets for liver diseases. *J Mol Med (Berl)*. 2016;94(6):613–27.

107. Wigerup C, Påhlman S, Bexell D. Therapeutic targeting of hypoxia and hypoxia-inducible factors in cancer. *Pharmacol Ther*. 2016;164:152–69.

108. Guo Y, Xiao Z, Yang L, Gao Y, Zhu Q, Hu L, et al. Hypoxia-inducible factors in hepatocellular carcinoma (Review). *Oncol Rep*. 2020;43(1):3–15.

109. Serocki M, Bartoszewska S, Janaszak-Jasiecka A, Ochocka RJ, Collawn JF, Bartoszewski R. miRNAs regulate the HIF switch during hypoxia: A novel therapeutic target. *Angiogenesis*. 2018;21(2):183–202.

110. Nordgren IK, Tavassoli A. Targeting tumour angiogenesis with small molecule inhibitors of hypoxia inducible factor. *Chem Soc Rev*. 2011;40(8):4307–17.

111. Suzuki N, Gradin K, Poellinger L, Yamamoto M. Regulation of hypoxia-inducible gene expression after HIF activation. *Exp Cell Res*. 2017;356(2):182–6.

112. Ravenna L, Salvatori L, Russo MA. HIF3α: The little we know. *FEBS J*. 2016;283(6):993–1003.

113. Araos J, Sleeman JP, Garvalov BK. The role of hypoxic signalling in metastasis: Towards translating knowledge of basic biology into novel anti-tumour strategies. *Clin Exp Metastasis*. 2018;35(7):563–99.

114. Semenza GL. Pharmacologic targeting of hypoxia-inducible factors. *Annu Rev Pharmacol Toxicol*. 2019;59:379–403.

115. Luo D, Wang Z, Wu J, Jiang C, Wu J. The role of hypoxia inducible factor-1 in hepatocellular carcinoma. *Biomed Res Int*. 2014;2014:409272.

116. Wilson GK, Tennant DA, McKeating JA. Hypoxia inducible factors in liver disease and hepatocellular carcinoma: Current understanding and future directions. *J Hepatol*. 2014;61(6):1397–406.

117. Choueiri TK, Kaelin Jr WG. Targeting the HIF2-VEGF axis in renal cell carcinoma. *Nat Med*. 2020;26(10):1519–30.

118. Prieto-Domínguez N, Méndez-Blanco C, Carbajo-Pescador S, Fondevila F, García-Palomo A, González-Gallego J, et al. Melatonin enhances sorafenib actions in human hepatocarcinoma cells by inhibiting mTORC1/p70S6K/HIF-1α and hypoxia-mediated mitophagy. *Oncotarget*. 2017;8(53):91402–14.

119. Toschi A, Lee E, Gadir N, Ohh M, Foster DA. Differential dependence of hypoxia-inducible factors 1α and 2α on mTORC1 and mTORC2. *J Biol Chem*. 2008;283(50):34495–9.

120. Barth DA, Prinz F, Teppan J, Jonas K, Klec C, Pichler M. Long-noncoding RNA (lncRNA) in the regulation of hypoxia-inducible factor (HIF) in cancer. *Non-coding RNA*. 2020;6(3):27.

121. Zhao J, Du F, Shen G, Zheng F, Xu B. The role of hypoxia-inducible factor-2 in digestive system cancers. *Cell Death Dis*. 2015;6(1):e1600.

122. Ma L, Li G, Zhu H, Dong X, Zhao D, Jiang X, et al. 2-Methoxyestradiol synergizes with sorafenib to suppress hepatocellular carcinoma by simultaneously

dysregulating hypoxia-inducible factor-1 and-2. *Cancer Lett*. 2014;355(1):96–105.

123. Méndez-Blanco C, Fondevila F, García-Palomo A, González-Gallego J, Mauriz JL. Sorafenib resistance in hepatocarcinoma: Role of hypoxia-inducible factors. *Exp Mol Med*. 2018;50(10):1–9.

124. Menrad H, Werno C, Schmid T, Copanaki E, Deller T, Dehne N, et al. Roles of hypoxia-inducible factor-1α (HIF-1α) versus HIF-2α in the survival of hepatocellular tumor spheroids. *Hepatology*. 2010;51(6):2183–92.

125. Cao S, Yang S, Wu C, Wang Y, Jiang J, Lu Z. Protein expression of hypoxia-inducible factor-1 alpha and hepatocellular carcinoma: A systematic review with meta-analysis. *Clin Res Hepatol Gastroenterol*. 2014;38(5):598–603.

126. Zheng S-S, Chen X-H, Yin X, Zhang B-H. Prognostic significance of HIF-1α expression in hepatocellular carcinoma: A meta-analysis. *PLoS One*. 2013;8(6):e65753.

127. Yao Q, Lv Y, Pan T, Liu Y, Ma J, Xu G. Prognostic significance and clinicopathological features of hypoxic inducible factor-2alpha expression in hepatocellular carcinoma. *Saudi Med J*. 2015;36(2):170–5.

128. Luo D, Liu H, Lin D, Lian K, Ren H. The clinicopathologic and prognostic value of hypoxia-inducible factor-2α in cancer patients: A systematic review and meta-analysis. *Cancer Epidemiol Biomarkers Prev*. 2019;28(5):857–66.

129. Liu Y, Liu Y, Yan X, Xu Y, Luo F, Ye J, et al. HIFs enhance the migratory and neoplastic capacities of hepatocellular carcinoma cells by promoting EMT. *Tumor Biol*. 2014;35(8):8103–14.

130. Bao X, Zhang J, Huang G, Yan J, Xu C, Dou Z, et al. The crosstalk between HIFs and mitochondrial dysfunctions in cancer development. *Cell Death Dis*. 2021;12(2):215.

131. Liu L-P, Ho RLK, Chen GG, Lai PBS. Sorafenib inhibits hypoxia-inducible factor-1α synthesis: Implications for antiangiogenic activity in hepatocellular carcinoma. *Clin Cancer Res*. 2012;18(20):5662–71.

132. Carbajo-Pescador S, Ordoñez R, Benet M, Jover R, García-Palomo A, Mauriz JL, et al. Inhibition of VEGF expression through blockade of Hif1α and STAT3 signalling mediates the anti-angiogenic effect of melatonin in HepG2 liver cancer cells. *Br J Cancer*. 2013;109(1):83–91.

133. Xu M, Xie X-H, Xie X-Y, Xu Z-F, Liu G-J, Zheng Y-L, et al. Sorafenib suppresses the rapid progress of hepatocellular carcinoma after insufficient radiofrequency ablation therapy: An experiment in vivo. *Acta radiol*. 2013;54(2):199–204.

134. Xu M, Zheng Y-L, Xie X-Y, Liang J-Y, Pan F-S, Zheng S-G, et al. Sorafenib blocks the HIF-1α/VEGFA pathway, inhibits tumor invasion, and induces apoptosis in

hepatoma cells. *DNA Cell Biol*. 2014;33(5):275–81.

135. Liang Y, Zheng T, Song R, Wang J, Yin D, Wang L, et al. Hypoxia-mediated sorafenib resistance can be overcome by EF24 through von Hippel-Lindau tumor suppressor-dependent HIF-1α inhibition in hepatocellular carcinoma. *Hepatology*. 2013;57(5):1847–57.

136. Liu F, Dong X, Lv H, Xiu P, Li T, Wang F, et al. Targeting hypoxia-inducible factor-2α enhances sorafenib antitumor activity via β-catenin/C-Myc-dependent pathways in hepatocellular carcinoma. *Oncol Lett*. 2015;10(2):778–84.

137. Zhao C-X, Luo C-L, Wu X-H. Hypoxia promotes 786-O cells invasiveness and resistance to sorafenib via HIF-2α/COX-2. *Med Oncol*. 2015;32(1):419.

138. Bielecka ZF, Malinowska A, Brodaczewska KK, Klemba A, Kieda C, Krasowski P, et al. Hypoxic 3D in vitro culture models reveal distinct resistance processes to TKIs in renal cancer cells. *Cell Biosci*. 2017;7:71.

139. van Oosterwijk JG, Buelow DR, Drenberg CD, Vasilyeva A, Li L, Shi L, et al. Hypoxia-induced upregulation of BMX kinase mediates therapeutic resistance in acute myeloid leukemia. *J Clin Invest*. 2018;128(1):369–80.

140. Tak E, Lee S, Lee J, Rashid MA, Kim YW, Park J-H, et al. Human carbonyl reductase 1 upregulated by hypoxia renders resistance to apoptosis in hepatocellular carcinoma cells. *J Hepatol*. 2011;54(2):328–39.

141. Jung EU, Yoon J-H, Lee Y-J, Lee J-H, Kim BH, Yu SJ, et al. Hypoxia and retinoic acid-inducible NDRG1 expression is responsible for doxorubicin and retinoic acid resistance in hepatocellular carcinoma cells. *Cancer Lett*. 2010;298(1):9–15.

142. Daskalow K, Rohwer N, Raskopf E, Dupuy E, Kühl A, Loddenkemper C, et al. Role of hypoxia-inducible transcription factor 1alpha for progression and chemosensitivity of murine hepatocellular carcinoma. *J Mol Med (Berl)*. 2010;88(8):817–27.

143. Dai X-Y, Zhuang L-H, Wang D-D, Zhou T-Y, Chang L-L, Gai R-H, et al. Nuclear translocation and activation of YAP by hypoxia contributes to the chemoresistance of SN38 in hepatocellular carcinoma cells. *Oncotarget*. 2016;7(6):6933–47.

144. Li J-Q, Wu X, Gan L, Yang X-L, Miao Z-H. Hypoxia induces universal but differential drug resistance and impairs anticancer mechanisms of 5-fluorouracil in hepatoma cells. *Acta Pharmacol Sin*. 2017;38(12):1642–54.

145. Xu H, Zhao L, Fang Q, Sun J, Zhang S, Zhan C, et al. MiR-338-3p inhibits hepatocarcinoma cells and sensitizes these cells to sorafenib by targeting hypoxia-induced factor 1α. *PLoS One*. 2014;9(12):e115565.

146. Yeh C-C, Hsu C-H, Shao Y-Y, Ho W-C, Tsai M-H, Feng W-C, et al. Integrated stable isotope labeling by amino acids in cell culture (SILAC) and isobaric tags for

relative and absolute quantitation (iTRAQ) quantitative proteomic analysis identifies galectin-1 as a potential biomarker for predicting sorafenib resistance in liver cancer. *Mol Cell Proteomics*. 2015;14(6):1527–45.

147. Wu F-Q, Fang T, Yu L-X, Lv G-S, Lv H-W, Liang D, et al. ADRB2 signaling promotes HCC progression and sorafenib resistance by inhibiting autophagic degradation of HIF1α. *J Hepatol*. 2016;65(2):314–24.

148. Li S, Li J, Dai W, Zhang Q, Feng J, Wu L, et al. Genistein suppresses aerobic glycolysis and induces hepatocellular carcinoma cell death. *Br J Cancer*. 2017;117(10):1518–28.

149. Zhao D, Zhai B, He C, Tan G, Jiang X, Pan S, et al. Upregulation of HIF-2α induced by sorafenib contributes to the resistance by activating the TGF-α/EGFR pathway in hepatocellular carcinoma cells. *Cell Signal*. 2014;26(5):1030–9.

150. Xu J, Zheng L, Chen J, Sun Y, Lin H, Jin R-A, et al. Increasing AR by HIF-2α inhibitor (PT-2385) overcomes the side-effects of sorafenib by suppressing hepatocellular carcinoma invasion via alteration of pSTAT3, pAKT and pERK signals. *Cell Death Dis*. 2017;8(10):e3095.

151. Zhu B, Lin S-S, Liu P-F, Li Y-F, Gao H-Y, Su Z-Y, et al. Desumoylation of hypoxia inducible factor (HIF)-2α by SENP1 is involved in HPPCn-enhanced sorafenib resistance under hypoxia in hepatocellular carcinoma. *J Hepatol*. 2014;60(Suppl 1):S83–4.

152. You A, Cao M, Guo Z, Zuo B, Gao J, Zhou H, et al. Metformin sensitizes sorafenib to inhibit postoperative recurrence and metastasis of hepatocellular carcinoma in orthotopic mouse models. *J Hematol Oncol*. 2016;9:20.

153. D'Arcy MS. Cell death: A review of the major forms of apoptosis, necrosis and autophagy. *Cell Biol Int*. 2019;43(6):582–92.

154. Jan R, Chaudhry G-E. Understanding apoptosis and apoptotic pathways targeted cancer therapeutics. *Adv Pharm Bull*. 2019;9(2):205–18.

155. Savitskaya MA, Onishchenko GE. Mechanisms of apoptosis. *Biochemistry (Mosc)*. 2015;80(11):1393–405.

156. El-Khattouti A, Selimovic D, Haikel Y, Hassan M. Crosstalk between apoptosis and autophagy: Molecular mechanisms and therapeutic strategies in cancer. *J Cell Death*. 2013;6:37–55.

157. Kiraz Y, Adan A, Kartal Yandim M, Baran Y. Major apoptotic mechanisms and genes involved in apoptosis. *Tumor Biol*. 2016;37(7):8471–86.

158. Goldar S, Khaniani MS, Derakhshan SM, Baradaran B. Molecular mechanisms of apoptosis and roles in cancer development and treatment. *Asian Pac J Cancer Prev*. 2015;16(6):2129–44.

159. Voskoboinik I, Whisstock JC, Trapani JA. Perforin and granzymes: Function,

dysfunction and human pathology. *Nat Rev Immunol*. 2015;15(6):388–400.

160. Bajwa N, Liao C, Nikolovska-Coleska Z. Inhibitors of the anti-apoptotic Bcl-2 proteins: A patent review. *Expert Opin Ther Pat*. 2012;22(1):37–55.

161. Xiong S, Mu T, Wang G, Jiang X. Mitochondria-mediated apoptosis in mammals. *Protein Cell*. 2014;5(10):737–49.

162. Carneiro BA, El-Deiry WS. Targeting apoptosis in cancer therapy. *Nat Rev Clin Oncol*. 2020;17(7):395–417.

163. Mohammad RM, Muqbil I, Lowe L, Yedjou C, Hsu H-Y, Lin L-T, et al. Broad targeting of resistance to apoptosis in cancer. *Semin Cancer Biol*. 2015;35(Suppl 0):S78–103.

164. Hikita H, Takehara T, Shimizu S, Kodama T, Shigekawa M, Iwase K, et al. The Bcl-xL inhibitor, ABT-737, efficiently induces apoptosis and suppresses growth of hepatoma cells in combination with sorafenib. *Hepatology*. 2010;52(4):1310–21.

165. Shimizu S, Takehara T, Hikita H, Kodama T, Miyagi T, Hosui A, et al. The let-7 family of microRNAs inhibits Bcl-xL expression and potentiates sorafenib-induced apoptosis in human hepatocellular carcinoma. *J Hepatol*. 2010;52(5):698–704.

166. Zhai B, Hu F, Jiang X, Xu J, Zhao D, Liu B, et al. Inhibition of Akt reverses the acquired resistance to sorafenib by switching protective autophagy to autophagic cell death in hepatocellular carcinoma. *Mol Cancer Ther*. 2014;13(6):1589–98.

167. Zhang J, Ney PA. Mechanisms and biology of B-cell leukemia/lymphoma 2/adenovirus E1B interacting protein 3 and Nip-like protein X. *Antioxidants Redox Signal*. 2011;14(10):1959–69.

168. Vasagiri N, Kutala VK. Structure, function, and epigenetic regulation of BNIP3: A pathophysiological relevance. *Mol Biol Rep*. 2014;41(11):7705–14.

169. Ney PA. Mitochondrial autophagy: Origins, significance, and role of BNIP3 and NIX. *Biochim Biophys Acta*. 2015;1853(10 Pt B):2775–83.

170. Chang JY, Yi H-S, Kim H-W, Shong M. Dysregulation of mitophagy in carcinogenesis and tumor progression. *Biochim Biophys Acta Bioenerg*. 2017;1858(8):633–40.

171. He J, Pei L, Jiang H, Yang W, Chen J, Liang H. Chemoresistance of colorectal cancer to 5-fluorouracil is associated with silencing of the BNIP3 gene through aberrant methylation. *J Cancer*. 2017;8(7):1187–96.

172. Gorbunova AS, Yapryntseva MA, Denisenko TV, Zhivotovsky B. BNIP3 in lung cancer: To kill or rescue? *Cancers (Basel)*. 2020;12(11):3390.

173. Panigrahi DP, Praharaj PP, Bhol CS, Mahapatra KK, Patra S, Behera BP, et al. The

emerging, multifaceted role of mitophagy in cancer and cancer therapeutics. *Semin Cancer Biol*. 2020;66:45–58.

174. Zhang J, Ney PA. Role of BNIP3 and NIX in cell death, autophagy, and mitophagy. *Cell Death Differ*. 2009;16(7):939–46.

175. Chourasia AH, Boland ML, Macleod KF. Mitophagy and cancer. *Cancer Metab*. 2015;3:4.

176. Chen X, Gong J, Zeng H, Chen N, Huang R, Huang Y, et al. MicroRNA145 targets BNIP3 and suppresses prostate cancer progression. *Cancer Res*. 2010;70(7):2728–38.

177. Giatromanolaki A, Koukourakis MI, Sowter HM, Sivridis E, Gibson S, Gatter KC, et al. BNIP3 expression is linked with hypoxia-regulated protein expression and with poor prognosis in non-small cell lung cancer. *Clin Cancer Res*. 2004;10(16):5566–71.

178. Leo C, Horn L-C, Höckel M. Hypoxia and expression of the proapoptotic regulator BNIP3 in cervical cancer. *Int J Gynecol Cancer*. 2006;16(3):1314–20.

179. Kim J-Y, Jung WH, Koo JS. Expression of autophagy-related proteins according to androgen receptor and HER-2 status in estrogen receptor-negative breast cancer. *PLoS One*. 2014;9(8):e105666.

180. Valdez BC, Li Y, Murray D, Corn P, Champlin RE, Andersson BS. 5-Aza-2'-deoxycytidine sensitizes busulfan-resistant myeloid leukemia cells by regulating expression of genes involved in cell cycle checkpoint and apoptosis. *Leuk Res*. 2010;34(3):364–72.

181. Shao Y, Liu Z, Liu J, Wang H, Huang L, Lin T, et al. Expression and epigenetic regulatory mechanism of BNIP3 in clear cell renal cell carcinoma. *Int J Oncol*. 2019;54(1):348–60.

182. Abe T, Toyota M, Suzuki H, Murai M, Akino K, Ueno M, et al. Upregulation of BNIP3 by 5-aza-2'-deoxycytidine sensitizes pancreatic cancer cells to hypoxia-mediated cell death. *J Gastroenterol*. 2005;40(5):504–10.

183. Erkan M, Kleeff J, Esposito I, Giese T, Ketterer K, Büchler MW, et al. Loss of BNIP3 expression is a late event in pancreatic cancer contributing to chemoresistance and worsened prognosis. *Oncogene*. 2005;24(27):4421–32.

184. An H-J, Lee H, Paik S-G. Silencing of BNIP3 results from promoter methylation by DNA methyltransferase 1 induced by the mitogen-activated protein kinase pathway. *Mol Cells*. 2011;31(6):579–83.

185. Li Y, Zhang X, Yang J, Zhang Y, Zhu D, Zhang L, et al. Methylation of BNIP3 in pancreatic cancer inhibits the induction of mitochondrial-mediated tumor cell apoptosis. *Oncotarget*. 2017;8(38):63208–22.

186. de Angelis PM, Fjell B, Kravik KL, Haug T, Tunheim SH, Reichelt W, et al.

Molecular characterizations of derivatives of HCT116 colorectal cancer cells that are resistant to the chemotherapeutic agent 5-fluorouracil. *Int J Oncol*. 2004;24(5):1279–88.

187. Murai M, Toyota M, Suzuki H, Satoh A, Sasaki Y, Akino K, et al. Aberrant methylation and silencing of the BNIP3 gene in colorectal and gastric cancer. *Clin Cancer Res*. 2005;11(3):1021–7.

188. Tang H, Liu Y-J, Liu M, Li X. Establishment and gene analysis of an oxaliplatin-resistant colon cancer cell line THC8307/L-OHP. *Anticancer Drugs*. 2007;18(6):633–9.

189. Bacon AL, Fox S, Turley H, Harris AL. Selective silencing of the hypoxia-inducible factor 1 target gene BNIP3 by histone deacetylation and methylation in colorectal cancer. *Oncogene*. 2007;26(1):132–41.

190. Liu F, Liu Q, Yang D, Bollag WB, Robertson K, Wu P, et al. Verticilin A overcomes apoptosis resistance in human colon carcinoma through DNA methylation-dependent upregulation of BNIP3. *Cancer Res*. 2011;71(21):6807–16.

191. Chourasia AH, Macleod KF. Tumor suppressor functions of BNIP3 and mitophagy. *Autophagy*. 2015;11(10):1937–8.

192. Haidich AB. Meta-analysis in medical research. *Hippokratia*. 2010;14(Suppl 1):29–37.

193. Arya S, Schwartz TA, Ghaferi AA. Practical guide to meta-analysis. *JAMA Surg*. 2020;155(5):430–1.

194. Moher D, Liberati A, Tetzlaff J, Altman DG, PRISMA Group. Preferred reporting items for systematic reviews and meta-analyses: The PRISMA statement. *PLoS Med*. 2009;6(7):e1000097.

195. Page MJ, McKenzie JE, Bossuyt PM, Boutron I, Hoffmann TC, Mulrow CD, et al. The PRISMA 2020 statement: An updated guideline for reporting systematic reviews. *Syst Rev*. 2021;10(1):89.

196. Wells GA, Shea B, O'Connell D, Peterson J, Welch V, Losos M, et al. The Newcastle-Ottawa Scale (NOS) for assessing the quality of nonrandomised studies in meta-analyses. The Ottawa Hospital Research Institute. 2019 [accesed 5 June 2020]. Available from: http://www.ohri.ca/programs/clinical_epidemiology/oxford.asp

197. Parmar MK, Torri V, Stewart L. Extracting summary statistics to perform meta-analyses of the published literature for survival endpoints. *Stat Med*. 1998;17(24):2815–34.

198. Huang G-W, Yang L-Y, Lu W-Q. Expression of hypoxia-inducible factor 1α and vascular endothelial growth factor in hepatocellular carcinoma: Impact on neovascularization and survival. *World J Gastroenterol*. 2005;11(11):1705–8.

199. Wada H, Nagano H, Yamamoto H, Yang Y, Kondo M, Ota H, et al. Expression pattern of angiogenic factors and prognosis after hepatic resection in hepatocellular carcinoma: Importance of angiopoietin-2 and hypoxia-induced factor-1α. *Liver Int*. 2006;26(4):414–23.

200. Xie H, Song J, Liu K, Ji H, Shen H, Hu S, et al. The expression of hypoxia-inducible factor-1α in hepatitis B virus-related hepatocellular carcinoma: Correlation with patients' prognosis and hepatitis B virus X protein. *Dig Dis Sci*. 2008;53(12):3225–33.

201. Dai C-X, Gao Q, Qiu S-J, Ju M-J, Cai M-Y, Xu Y-F, et al. Hypoxia-inducible factor-1 alpha, in association with inflammation, angiogenesis and MYC, is a critical prognostic factor in patients with HCC after surgery. *BMC Cancer*. 2009;9:418.

202. Liu L, Zhu X-D, Wang W-Q, Shen Y, Qin Y, Ren Z-G, et al. Activation of β-catenin by hypoxia in hepatocellular carcinoma contributes to enhanced metastatic potential and poor prognosis. *Clin Cancer Res*. 2010;16(10):2740–50.

203. Xiang Z-L, Zeng Z-C, Fan J, Tang Z-Y, Zeng H-Y, Gao D-M. Gene expression profiling of fixed tissues identified hypoxia-inducible factor-1α, VEGF, and matrix metalloproteinase-2 as biomarkers of lymph node metastasis in hepatocellular carcinoma. *Clin Cancer Res*. 2011;17(16):5463–72.

204. Li S, Yao D, Dong Z, Qian Y, Yu D, Yao N, et al. Abnormal expression of hypoxia inducible factor-1α and clinical values of molecular-targeted interference in hepatocellular carcinoma. *Chinese-German J Clin Oncol*. 2012;11(3):125–9.

205. Xia L, Mo P, Huang W, Zhang L, Wang Y, Zhu H, et al. The TNF-α/ROS/HIF-1-induced upregulation of FoxMI expression promotes HCC proliferation and resistance to apoptosis. *Carcinogenesis*. 2012;33(11):2250–9.

206. Xiang Z-L, Zeng Z-C, Fan J, Tang Z-Y, He J, Zeng H-Y, et al. The expression of HIF-1α in primary hepatocellular carcinoma and its correlation with radiotherapy response and clinical outcome. *Mol Biol Rep*. 2012;39(2):2021–9.

207. Cui S-Y, Huang J-Y, Chen Y-T, Song H-Z, Huang G-C, De W, et al. The role of Aurora A in hypoxia-inducible factor 1α-promoting malignant phenotypes of hepatocelluar carcinoma. *Cell Cycle*. 2013;12(17):2849–66.

208. Ma X, Li J, Tan B. Expression of HIF-1α in hepatocellular carcinoma and its relationship with vasculogenic mimicry and clinical pathology. *Chinese-German J Clin Oncol*. 2013;12(11):528–31.

209. Wang B, Ding Y-M, Fan P, Wang B, Xu J-H, Wang W-X. Expression and significance of MMP2 and HIF-1α in hepatocellular carcinoma. *Oncol Lett*. 2014;8(2):539–46.

210. Yang S-L, Liu L-P, Jiang J-X, Xiong Z-F, He Q-J, Wu C. The correlation of expression levels of HIF-1 and HIF-2 in hepatocellular carcinoma with capsular invasion, portal vein tumor thrombi and patients' clinical outcome. *Jpn J Clin Oncol*.

2014;44(2):159–67.

211. Huang Z, Xu X, Meng X, Hou Z, Liu F, Hua Q, et al. Correlations between ADC values and molecular markers of Ki-67 and HIF-1α in hepatocellular carcinoma. *Eur J Radiol*. 2015;84(12):2464–9.

212. Li X-P, Yang X-Y, Biskup E, Zhou J, Li H-L, Wu Y-F, et al. Co-expression of CXCL8 and HIF-1α is associated with metastasis and poor prognosis in hepatocellular carcinoma. *Oncotarget*. 2015;6(26):22880–9.

213. Srivastava S, Thakkar B, Yeoh KG, Ho KY, Teh M, Soong R, et al. Expression of proteins associated with hypoxia and Wnt pathway activation is of prognostic significance in hepatocellular carcinoma. *Virchows Arch*. 2015;466(5):541–8.

214. Zhao N, Sun B-C, Zhao X-L, Wang Y, Meng J, Che N, et al. Role of Bcl-2 and its associated miRNAs in vasculogenic mimicry of hepatocellular carcinoma. *Int J Clin Exp Pathol*. 2015;8(12):15759–68.

215. Tang Y, Liu S, Li N, Guo W, Shi J, Yu H, et al. 14-3-3ζ promotes hepatocellular carcinoma venous metastasis by modulating hypoxia-inducible factor-1α. *Oncotarget*. 2016;7(13):15854–67.

216. Wang M, Zhao X, Zhu D, Liu T, Liang X, Liu F, et al. HIF-1α promoted vasculogenic mimicry formation in hepatocellular carcinoma through LOXL2 up-regulation in hypoxic tumor microenvironment. *J Exp Clin Cancer Res*. 2017;36(1):60.

217. Dai X, Pi G, Yang S-L, Chen GG, Liu L-P, Dong H-H. Association of PD-L1 and HIF-1α coexpression with poor prognosis in hepatocellular carcinoma. *Transl Oncol*. 2018;11(2):559–66.

218. Tian Q-G, Wu Y-T, Liu Y, Zhang J, Song Z-Q, Gao W-F, et al. Expressions and correlation analysis of HIF-1α, survivin and VEGF in patients with hepatocarcinoma. *Eur Rev Med Pharmacol Sci*. 2018;22(11):3378–85.

219. Wang D, Zhang X, Lu Y, Wang X, Zhu L. Hypoxia inducible factor 1α in hepatocellular carcinoma with cirrhosis: Association with prognosis. *Pathol Res Pract*. 2018;214(12):1987–92.

220. Zou B, Liu X, Zhang B, Gong Y, Cai C, Li P, et al. The expression of FAP in hepatocellular carcinoma cells is induced by hypoxia and correlates with poor clinical outcomes. *J Cancer*. 2018;9(18):3278–86.

221. Gong Y, Zou B, Peng S, Li P, Zhu G, Chen J, et al. Nuclear GAPDH is vital for hypoxia-induced hepatic stellate cell apoptosis and is indicative of aggressive hepatocellular carcinoma behavior. *Cancer Manag Res*. 2019;11:4947–56.

222. Wu Q, Zhou W, Yin S, Zhou Y, Chen T, Qian J, et al. Blocking triggering receptor expressed on myeloid cells-1-positive tumor-associated macrophages induced by hypoxia reverses immunosuppression and anti-programmed cell death ligand 1 resistance in liver cancer. *Hepatology*. 2019;70(1):198–214.

223. Zhou Y, Dong X, Xiu P, Wang X, Yang J, Li L, et al. Meloxicam, a selective COX-2 inhibitor, mediates hypoxia-inducible factor- (HIF-) 1α signaling in hepatocellular carcinoma. *Oxid Med Cell Longev*. 2020;2020:7079308.

224. Qian Y, Li Y, Zheng C, Lu T, Sun R, Mao Y, et al. High methylation levels of histone H3 lysine 9 associated with activation of hypoxia-inducible factor 1α (HIF-1α) predict patients' worse prognosis in human hepatocellular carcinomas. *Cancer Genet*. 2020;245:17–26.

225. Bangoura G, Yang L-Y, Huang G-W, Wang W. Expression of HIF-2alpha/EPAS1 in hepatocellular carcinoma. *World J Gastroenterol*. 2004;10(4):525–30.

226. Bangoura G, Liu Z-S, Qian Q, Jiang C-Q, Yang G-F, Jing S. Prognostic significance of HIF-2alpha/EPAS1 expression in hepatocellular carcinoma. *World J Gastroenterol*. 2007;13(23):3176–82.

227. Sun H-X, Xu Y, Yang X-R, Wang W-M, Bai H, Shi R-Y, et al. HIF-2α inhibits hepatocellular carcinoma growth through the TFDP3/E2F1-dependent apoptotic pathway. *Hepatology*. 2013;57(3):1088–97.

228. Yang S-L, Liu L-P, Niu L, Sun Y-F, Yang X-R, Fan J, et al. Downregulation and pro-apoptotic effect of hypoxia-inducible factor 2 alpha in hepatocellular carcinoma. *Oncotarget*. 2016;7(23):34571–81.

229. Jiang L, Liu Q-L, Liang Q-L, Zhang H-J, Ou W-T, Yuan G-L. Association of PHD3 and HIF2α gene expression with clinicopathological characteristics in human hepatocellular carcinoma. *Oncol Lett*. 2018;15(1):545–51.

230. Chen J, Chen J, Huang J, Li Z, Gong Y, Zou B, et al. HIF-2α upregulation mediated by hypoxia promotes NAFLD-HCC progression by activating lipid synthesis via the PI3K-AKT-mTOR pathway. *Aging (Albany NY)*. 2019;11(23):10839–60.

231. Cao M-Q, You A-B, Cui W, Zhang S, Guo Z-G, Chen L, et al. Cross talk between oxidative stress and hypoxia via thioredoxin and HIF-2α drives metastasis of hepatocellular carcinoma. *FASEB J*. 2020;34(4):5892–905.

232. Taheem DK, Foyt DA, Loaiza S, Ferreira SA, Ilic D, Auner HW, et al. Differential regulation of human bone marrow mesenchymal stromal cell chondrogenesis by hypoxia inducible factor-1α hydroxylase inhibitors. *Stem Cells*. 2018;36(9):1380–92.

233. Coico R. Gram staining. *Curr Protoc Microbiol*. 2005;Appendix 3:Appendix 3C.

234. Feoktistova M, Geserick P, Leverkus M. Crystal violet assay for determining viability of cultured cells. *Cold Spring Harb Protoc*. 2016;2016(4):343–6.

235. Kumar P, Nagarajan A, Uchil PD. Analysis of cell viability by the MTT assay. *Cold Spring Harb Protoc*. 2018;2018(6):469–71.

236. Kajstura M, Halicka HD, Pryjma J, Darzynkiewicz Z. Discontinuous fragmentation of nuclear DNA during apoptosis revealed by discrete "sub-G1" peaks on DNA

content histograms. *Cytometry A*. 2007;71(3):125–31.

237. Im K, Mareninov S, Diaz MFP, Yong WH. An introduction to performing immunofluorescence staining. *Methods Mol Biol*. 2019;1897:299–311.

238. Gavet O, Pines J. Progressive activation of CyclinB1-Cdk1 coordinates entry to mitosis. *Dev Cell*. 2010;18(4):533–43.

239. Ansari N, Müller S, Stelzer EHK, Pampaloni F. Quantitative 3D cell-based assay performed with cellular spheroids and fluorescence microscopy. *Methods Cell Biol*. 2013;113:295–309.

240. Taylor SC, Posch A. The design of a quantitative western blot experiment. *Biomed Res Int*. 2014;2014:361590.

241. Brunelle JL, Green R. One-dimensional SDS-polyacrylamide gel electrophoresis (1D SDS-PAGE). *Methods Enzymol*. 2014;541:151–9.

242. Jaksik R, Iwanaszko M, Rzeszowska-Wolny J, Kimmel M. Microarray experiments and factors which affect their reliability. *Biol Direct*. 2015;10:46.

243. Bachman J. Reverse-transcription PCR (RT-PCR). *Methods Enzym*. 2013;530:67–74.

244. Livak KJ, Schmittgen TD. Analysis of relative gene expression data using real-time quantitative PCR and the $2^{-\Delta\Delta CT}$ method. *Methods*. 2001;25(4):402–8.

245. Hernández HG, Tse MY, Pang SC, Arboleda H, Forero DA. Optimizing methodologies for PCR-based DNA methylation analysis. *Biotechniques*. 2013;55(4):181–97.

246. Neumeier J, Meister G. siRNA specificity: RNAi mechanisms and strategies to reduce off-target effects. *Front Plant Sci*. 2021;11:526455.

247. Huber W, Carey VJ, Gentleman R, Anders S, Carlson M, Carvalho BS, et al. Orchestrating high-throughput genomic analysis with Bioconductor. *Nat Methods*. 2015;12(2):115–21.

248. Benjamini Y, Drai D, Elmer G, Kafkafi N, Golani I. Controlling the false discovery rate in behavior genetics research. *Behav Brain Res*. 2001;125(1–2):279–84.

249. Wang J, Duncan D, Shi Z, Zhang B. WEB-based GEne SeT AnaLysis Toolkit (WebGestalt): Update 2013. *Nucleic Acids Res*. 2013;41(Web Server issue):W77–83.

250. Huang DW, Sherman BT, Lempicki RA. Systematic and integrative analysis of large gene lists using DAVID bioinformatics resources. *Nat Protoc*. 2009;4(1):44–57.

251. Schiller I, Lu ZH, Vaughan L, Weilenmann R, Koundrioukoff S, Pospischil A. Establishment of proliferative cell nuclear antigen gene as an internal reference

gene for polymerase chain reaction of a wide range of archival and fresh mammalian tissues. *J Vet Diagn Invest*. 2003;15(6):585–8.

252. Jagannathan M, Sakwe AM, Nguyen T, Frappier L. The MCM-associated protein MCM-BP is important for human nuclear morphology. *J Cell Sci*. 2012;125(Pt 1):133–43.

253. Mian OY, Khattab MH, Hedayati M, Coulter J, Abubaker-Sharif B, Schwaninger JM, et al. GSTP1 loss results in accumulation of oxidative DNA base damage and promotes prostate cancer cell survival following exposure to protracted oxidative stress. *Prostate*. 2016;76(2):199–206.

254. Sánchez DI, González-Fernández B, San-Miguel B, de Urbina JO, Crespo I, González-Gallego J, et al. Melatonin prevents deregulation of the sphingosine kinase/sphingosine 1-phosphate signaling pathway in a mouse model of diethylnitrosamine-induced hepatocellular carcinoma. *J Pineal Res*. 2017;62(1).

255. Hsu C-C, Hsieh P-M, Chen Y-S, Lo G-H, Lin H-Y, Dai C-Y, et al. Axl and autophagy LC3 expression in tumors is strongly associated with clinical prognosis of hepatocellular carcinoma patients after curative resection. *Cancer Med*. 2019;8(7):3453–63.

256. Sun G, Wang Y, Hu W. Correlation between HIF-1α expression and breast cancer risk: A meta-analysis. *Breast J*. 2014;20(2):213–5.

257. Wang Q, Hu D-F, Rui Y, Jiang A-B, Liu Z-L, Huang L-N. Prognosis value of HIF-1α expression in patients with non-small cell lung cancer. *Gene*. 2014;541(2):69–74.

258. Chen J, Li T, Liu Q, Jiao H, Yang W, Liu X, et al. Clinical and prognostic significance of HIF-1α, PTEN, CD44v6, and survivin for gastric cancer: A meta-analysis. *PLoS One*. 2014;9(3):e91842.

259. Fan Y, Li H, Ma X, Gao Y, Chen L, Li X, et al. Prognostic significance of hypoxia-inducible factor expression in renal cell carcinoma: A PRISMA-compliant systematic review and meta-analysis. *Medicine (Baltimore)*. 2015;94(38):e1646.

260. Ye L-Y, Zhang Q, Bai X-L, Pankaj P, Hu Q-D, Liang TB. Hypoxia-inducible factor 1α expression and its clinical significance in pancreatic cancer: A meta-analysis. *Pancreatology*. 2014;14(5):391–7.

261. Luo D, Ren H, Zhang W, Xian H, Lian K, Liu H. Clinicopathological and prognostic value of hypoxia-inducible factor-1α in patients with bone tumor: A systematic review and meta-analysis. *J Orthop Surg Res*. 2019;14(1):56.

262. Jing SW, Wang J, Xu Q. Expression of hypoxia inducible factor 1 alpha and its clinical significance in esophageal carcinoma: A meta-analysis. *Tumor Biol*. 2017;39(7):1–12.

263. Chen Z, He X, Xia W, Huang Q, Zhang Z, Ye J, et al. Prognostic value and clinicopathological differences of HIFs in colorectal cancer: Evidence from meta-

analysis. *PLoS One*. 2013;8(12):e80337.

264. Gong L, Zhang W, Zhou J, Lu J, Xiong H, Shi X, et al. Prognostic value of HIFs expression in head and neck cancer: A systematic review. *PLoS One*. 2013;8(9):e75094.

265. Swartz JE, Pothen AJ, Stegeman I, Willems SM, Grolman W. Clinical implications of hypoxia biomarker expression in head and neck squamous cell carcinoma: A systematic review. *Cancer Med*. 2015;4(7):1101–16.

266. Sadlecki P, Bodnar M, Grabiec M, Marszalek A, Walentowicz P, Sokup A, et al. The role of hypoxia-inducible factor-1α , glucose transporter-1, (GLUT-1) and carbon anhydrase IX in endometrial cancer patients. *Biomed Res Int*. 2014;2014:616850.

267. Jin Y, Wang H, Liang X, Ma J, Wang Y. Pathological and prognostic significance of hypoxia-inducible factor 1α expression in epithelial ovarian cancer: A meta-analysis. *Tumor Biol*. 2014;35(8):8149–59.

268. Zhou J, Huang S, Wang L, Yuan X, Dong Q, Zhang D, et al. Clinical and prognostic significance of HIF-1α overexpression in oral squamous cell carcinoma: A meta-analysis. *World J Surg Oncol*. 2017;15(1):104.

269. Han S, Huang T, Hou F, Yao L, Wang X, Wu X. The prognostic value of hypoxia-inducible factor-1α in advanced cancer survivors: A meta-analysis with trial sequential analysis. *Ther Adv Med Oncol*. 2019;11(6):1–21.

270. Han S, Huang T, Li W, Liu S, Yang W, Shi Q, et al. Association between hypoxia-inducible factor-2α (HIF-2α) expression and colorectal cancer and its prognostic role: A systematic analysis. *Cell Physiol Biochem*. 2018;48(2):516–27.

271. Li C, Lu H-J, Na F-F, Deng L, Xue J-X, Wang J-W, et al. Prognostic role of hypoxic inducible factor expression in non-small cell lung cancer: A meta-analysis. *Asian Pac J Cancer Prev*. 2013;14(6):3607–12.

272. Qian J, Wenguang X, Zhiyong W, Yuntao Z, Wei H. Hypoxia inducible factor: A potential prognostic biomarker in oral squamous cell carcinoma. *Tumor Biol*. 2016;37(8):10815–20.

273. Zheng F, Du F, Zhao J. Clinicopathological differences and prognostic value of hypoxia-inducible factor-2α expression for gastric cancer: Evidence from meta-analysis. *Medicine (Baltimore)*. 2016;95(7):e2871.

274. Ding Z-N, Dong Z-R, Chen Z-Q, Yang Y-F, Yan L-J, Li H-C, et al. Effects of hypoxia-inducible factor-1α and hypoxia-inducible factor-2α overexpression on hepatocellular carcinoma survival: A systematic review with meta-analysis. *J Gastroenterol Hepatol*. 2021. doi: 10.1111/jgh.15395

275. Rey S, Semenza GL. Hypoxia-inducible factor-1-dependent mechanisms of vascularization and vascular remodelling. *Cardiovasc Res*. 2010;86(2):236–42.

276. Zhang L, Huang G, Li X, Zhang Y, Jiang Y, Shen J, et al. Hypoxia induces epithelial-mesenchymal transition via activation of SNAI1 by hypoxia-inducible factor-1α in hepatocellular carcinoma. *BMC Cancer*. 2013;13:108.

277. Tian H, Huang P, Zhao Z, Tang W, Xia J. HIF-1α plays a role in the chemotactic migration of hepatocarcinoma cells through the modulation of CXCL6 expression. *Cell Physiol Biochem*. 2014;34(5):1536–46.

278. Hu F, Deng X, Yang X, Jin H, Gu D, Lv X, et al. Hypoxia upregulates Rab11-family interacting protein 4 through HIF-1α to promote the metastasis of hepatocellular carcinoma. *Oncogene*. 2015;34(49):6007–17.

279. Cannito S, Turato C, Paternostro C, Biasiolo A, Colombatto S, Cambieri I, et al. Hypoxia up-regulates SERPINB3 through HIF-2α in human liver cancer cells. *Oncotarget*. 2015;6(4):2206–21.

280. Wang X, Dong J, Jia L, Zhao T, Lang M, Li Z, et al. HIF-2-dependent expression of stem cell factor promotes metastasis in hepatocellular carcinoma. *Cancer Lett*. 2017;393:113–24.

281. Cao M, Gao J, Zhou H, Huang J, You A, Guo Z, et al. HIF-2α regulates CDCP1 to promote PKCδ-mediated migration in hepatocellular carcinoma. *Tumor Biol*. 2016;37(2):1651–62.

282. Sánchez DI, González-Fernández B, Crespo I, San-Miguel B, Álvarez M, González-Gallego J, et al. Melatonin modulates dysregulated circadian clocks in mice with diethylnitrosamine-induced hepatocellular carcinoma. *J Pineal Res*. 2018;65(3):e12506.

283. Prieto-Domínguez N, Ordóñez R, Fernández A, Méndez-Blanco C, Baulies A, Garcia-Ruiz C, et al. Melatonin-induced increase in sensitivity of human hepatocellular carcinoma cells to sorafenib is associated with reactive oxygen species production and mitophagy. *J Pineal Res*. 2016;61(3):396–407.

284. Rodríguez-Hernández MA, González R, de la Rosa ÁJ, Gallego P, Ordóñez R, Navarro-Villarán E, et al. Molecular characterization of autophagic and apoptotic signaling induced by sorafenib in liver cancer cells. *J Cell Physiol*. 2018;234(1):692–708.

285. Chen Y, Sun L, Guo D, Wu Z, Chen W. Co-delivery of hypoxia inducible factor-1α small interfering RNA and 5-fluorouracil to overcome drug resistance in gastric cancer SGC-7901 cells. *J Gene Med*. 2017;19(12).

286. Qiu Y, Shan W, Yang Y, Jin M, Dai Y, Yang H, et al. Reversal of sorafenib resistance in hepatocellular carcinoma: Epigenetically regulated disruption of 14-3-3η/hypoxia-inducible factor-1α. *Cell death Discov*. 2019;5:120.

287. He M, Wu H, Jiang Q, Liu Y, Han L, Yan Y, et al. Hypoxia-inducible factor-2α directly promotes BCRP expression and mediates the resistance of ovarian cancer stem cells to adriamycin. *Mol Oncol*. 2019;13(2):403–21.

288. Wang J, Ma Y, Jiang H, Zhu H, Liu L, Sun B, et al. Overexpression of von Hippel-Lindau protein synergizes with doxorubicin to suppress hepatocellular carcinoma in mice. *J Hepatol*. 2011;55(2):359–68.

289. Liu L, Cao Y, Chen C, Zhang X, McNabola A, Wilkie D, et al. Sorafenib blocks the RAF/MEK/ERK pathway, inhibits tumor angiogenesis, and induces tumor cell apoptosis in hepatocellular carcinoma model PLC/PRF/5. *Cancer Res*. 2006;66(24):11851–8.

290. Zhou T-Y, Zhuang L-H, Hu Y, Zhou Y-L, Lin W-K, Wang D-D, et al. Inactivation of hypoxia-induced YAP by statins overcomes hypoxic resistance tosorafenib in hepatocellular carcinoma cells. *Sci Rep*. 2016;6:30483.

291. Hajigholami S, Veisi Malekshahi Z, Bodaghabadi N, Najafi F, Shirzad H, Sadeghizadeh M. Nano packaged tamoxifen and curcumin; Effective formulation against sensitive and resistant MCF-7 cells. *Iran J Pharm Res*. 2018;17(1):1–10.

292. Fernando J, Sancho P, Fernández-Rodriguez CM, Lledó JL, Caja L, Campbell JS, et al. Sorafenib sensitizes hepatocellular carcinoma cells to physiological apoptotic stimuli. *J Cell Physiol*. 2012;227(4):1319–25.

293. Li X-F, Gong R-Y, Wang M, Yan Z-L, Yuan B, Wang K, et al. Sorafenib down-regulates c-IAP expression post-transcriptionally in hepatic carcinoma cells to suppress apoptosis. *Biochem Biophys Res Commun*. 2012;418(3):531–6.

294. Yang F, Li Q-J, Gong Z-B, Zhou L, You N, Wang S, et al. MicroRNA-34a targets Bcl-2 and sensitizes human hepatocellular carcinoma cells to sorafenib treatment. *Technol Cancer Res Treat*. 2014;13(1):77–86.

295. Long Q, Zou X, Song Y, Duan Z, Liu L. PFKFB3/HIF-1α feedback loop modulates sorafenib resistance in hepatocellular carcinoma cells. *Biochem Biophys Res Commun*. 2019;513(3):642–50.

296. Huang S, Qi P, Zhang T, Li F, He X. The HIF-1α/miR-224-3p/ATG5 axis affects cell mobility and chemosensitivity by regulating hypoxia-induced protective autophagy in glioblastoma and astrocytoma. *Oncol Rep*. 2019;41(3):1759–68.

297. Krutilina R, Sun W, Sethuraman A, Brown M, Seagroves TN, Pfeffer LM, et al. MicroRNA-18a inhibits hypoxia-inducible factor 1α activity and lung metastasis in basal breast cancers. *Breast Cancer Res*. 2014;16(4):R78.

298. Saint-Martin A, Martínez-Ríos J, Castañeda-Patlán MC, Sarabia-Sánchez MA, Tejeda-Muñoz N, Chinney-Herrera A, et al. Functional interaction of hypoxia-inducible factor 2-alpha and autophagy mediates drug resistance in colon cancer cells. *Cancers (Basel)*. 2019;11(6):755.

299. Jiang W, Li G, Li W, Wang P, Xiu P, Jiang X, et al. Sodium orthovanadate overcomes sorafenib resistance of hepatocellular carcinoma cells by inhibiting Na^+/K^+-ATPase activity and hypoxia-inducible pathways. *Sci Rep*. 2018;8(1):9706.

300. Ishiguro M, Iida S, Uetake H, Morita S, Makino H, Kato K, et al. Effect of combined therapy with low-dose 5-aza-2'-deoxycytidine and irinotecan on colon cancer cell line HCT-15. *Ann Surg Oncol*. 2007;14(5):1752–62.

301. Deng Q, Huang C-M, Chen N, Li L, Wang X-D, Zhang W, et al. Chemotherapy and radiotherapy downregulate the activity and expression of DNA methyltransferase and enhance Bcl-2/E1B-19-kDa interacting protein-3-induced apoptosis in human colorectal cancer cells. *Chemotherapy*. 2012;58(6):445–53.